

Dissertation thesis

# Self-association of supramolecular cages based on dynamic imine and $\beta$ -diketone bonds

Michał Kołodziejski

Supervisor: Prof. dr hab. Artur R. Stefankiewicz

The work was carried out in the Laboratory of Functional Nanostructures

Faculty of Chemistry/Center of Advanced Technologies

University of Adam Mickiewicz in Poznań, Poland



Poznań 2025



*„Nothing in life is to be feared, it is only to be understood.  
Now is the time to understand more, so that we may fear less.”*

- Marie Skłodowska-Curie





## Acknowledgments

I would like to express my sincere gratitude to **Professor dr hab. Artur R. Stefankiewicz** for allowing me to complete my doctoral thesis under his watchful eye, for his substantive supervision of the research I conducted, and for his incredibly valuable tips, advice, and experience throughout my doctoral studies.

I would like to express my deepest and sincere gratitude to **Professor Jean-Marie Lehn** (ISIS, Strasbourg, France) who provided me an incredible opportunity to join his team as intern. I am very grateful for insightful comments and for the hard question which incited me to widen my research from various perspectives. I am also very thankful for all life advices that influenced my decisions.

I would like to thank the **entire team of the Functional Nanostructures Laboratory** for several years of cooperation, for daily scientific discussions and interesting conversations inside and outside of the laboratory. I would like to express my special thanks to **Dr Wojciech Drożdż**, with whom I shared a laboratory room for many years of research work.

I would like to thank all our **collaborators from the Institute of Supramolecular Science and Engineering (ISIS)** for their professional and fruitful collaboration.

I would like to express my special thanks to my closest ones: my wonderful **wife Karolina** and my wonderful **sons Gabriel and Florian** for their understanding in the most difficult moments, patience, support in difficult times and constant faith in me.

To my **beloved parents**, for always supporting me.

To my **beloved grandfather**.



## Table of contents

Scientific achievements .....	9
Publications in international journals .....	9
➤ included in the Ph.D. thesis .....	9
➤ not included in the Ph.D. thesis .....	9
Contributions to international conferences .....	10
➤ oral communications .....	10
➤ poster presentations .....	10
Contribution to scientific grants .....	11
Internships .....	12
Abstract .....	13
Streszczenie .....	15
Chapter 1: Introduction .....	17
Molecular recognition and host-guest chemistry .....	20
Self-association, self-organization .....	22
Types of interactions in supramolecular structures .....	25
Metal-ligand coordination .....	25
Chemistry of $\beta$ -diketones .....	28
Synthesis of $\beta$ -diketones .....	30
Application of $\beta$ -diketone compounds .....	30
Dynamic Combinatorial Chemistry (DCC) .....	33
Dynamic imine bond .....	34
Imines in Dynamic Combinatorial Chemistry – application .....	35
Research objectives .....	38
Chapter 2: Chemistry of $\beta$ -diketones .....	40
Synthesis of bpmH and its complexes .....	41
Results .....	42
Charge-neutral metallocycles – self-assembly, aggregation and catalysis .....	46
Synthesis of $H_3L$ and its complexes .....	47
Results and characterization .....	48
Catalytic properties in Suzuki-Miyaura Cross-coupling reaction .....	49
Chapter 3: Dynamic Combinatorial Chemistry – Self-sorting with component selection .....	52
Synthesis and characterization .....	53
Self-sorting experiments .....	54
Cage-to-cage transformation .....	59
Conclusion .....	62
References .....	64
Reprints of publications .....	67

<b>A1. Unsymmetrical bidentate ligands as a basis for construction of ambidentate ligands for functional materials: Properties of 4,4-dimethyl-1-phenylpentane-1,3-dionate .....</b>	<b>68</b>
Supplementary information to <b>A1</b> .....	77
<b>A2. Charge Neutral [Cu<sub>2</sub>L<sub>2</sub>] and [Pd<sub>2</sub>L<sub>2</sub>] Metallocycles: Self-Assembly, Aggregation, and Catalysis .....</b>	<b>84</b>
Supplementary information to <b>A2</b> .....	92
<b>A3. Dynamic polyimine macrobicyclic cryptands – self-sorting with component selection .....</b>	<b>111</b>
Supplementary information to <b>A3</b> .....	120
<b>Declaration letters of co-authors .....</b>	<b>151</b>

# Scientific achievements

## Publications in international journals

### ➤ included in the Ph.D. thesis

**A1.** Michał Kołodziejski, Anna Walczak, Zbigniew Hnatejko, Jack Harrowfield, Artur R. Stefankiewicz\*, *Unsymmetrical bidentate ligands as a basis for construction of ambidentate ligands for functional materials: Properties of 4,4-dimethyl-1-phenylpentane-1,3-dionate*, Polyhedron, **2017**, Volume 137, 270-277.

IF = 2.4

**A2.** Michał Kołodziejski, Aidan J. Brock, Gracjan Kurpiak, Anna Walczak, Feng Li, Jack K. Clegg\*, Artur R. Stefankiewicz\*, *Charge Neutral [Cu<sub>2</sub>L<sub>2</sub>] and [Pd<sub>2</sub>L<sub>2</sub>] Metallocycles: Self-Assembly, Aggregation, and Catalysis*, Inorganic Chemistry, **2021**, 60, 9673-9679.

IF = 4.3

**A3.** Michał Kołodziejski, Artur R. Stefankiewicz\*, Jean-Marie Lehn\*, *Dynamic polyimine macrobicyclic cryptands – self-sorting with component selection*, Chemical Science, **2019**, 10, 1836-1843.

IF = 7.6

### ➤ not included in the Ph.D. thesis

**A4.** Wojciech Drożdż, Michał Kołodziejski, Grzegorz Markiewicz, Anna Jenczak, Artur R. Stefankiewicz\*, *Generation of a Multicomponent Library of Disulfide Donor-Acceptor Architectures Using Dynamic Combinatorial Chemistry*, International Journal of Molecular Sciences, **2015**, 16, 16300-16312.

IF = 4.9

**A5.** Grzegorz Markiewicz, Anna Jenczak, Michał Kołodziejski, Julian J. Holstein, Jeremy K. M. Sanders\*, Artur R. Stefankiewicz\*, *Selective C<sub>70</sub> encapsulation by a robust octameric nanospheroid held together by 48 cooperative hydrogen bonds*, Nature Communications, **2017**, 8, 15109.

IF = 14.7

\* corresponding author

## Contributions to international conferences

### ➤ oral communications

1. M. Kołodziejski, A. R. Stefankiewicz, “*Self-association of supramolecular capsules based on beta-diketonates and dynamic imine bonds*”  
**43<sup>rd</sup> Internaional Conference on Coordination Chemistry**,  
August 2018, Sendai, Japan
2. M. Kołodziejski, A. R. Stefankiewicz, “*Dynamic imine cages – self-sorting with sub-component selection*”  
**Chemistry Beyond Nature**,  
June 2018, Poznań, Poland

### ➤ poster presentations

3. M. Kołodziejski, A. R. Stefankiewicz, “*Self-assembly of supramolecular capsules based on  $\beta$ -diketonates and dynamic imine bonds*”  
**Supramolecular Chemistry @ Work - Supr@Lyon**,  
December 2018, Lyon, France
4. M. Kołodziejski, A. R. Stefankiewicz, “*Self-assembly of supramolecular capsules based on  $\beta$ -diketonates and dynamic imine bonds*”  
**Chemistry Beyond Nature**,  
June 2018, Poznań, Poland
5. M. Kołodziejski, A. R. Stefankiewicz, “*Samoasocjacja kapsuł supramolekularnych na bazie dynamicznych wiązań iminowych i  $\beta$ -diketonowych*”  
**XI Ogólnopolskie Sympozjum Chemii Organicznej OSCO XI**,  
April 2018, Warsaw, Poland
6. M. Kołodziejski, A. R. Stefankiewicz, “*Novel metallosupramolecular grid complexes containing S- and O- coordination bridges with d-electron metal ions: synthesis and characterization*”  
**Assises Franco-Polonaises de Chemie 2015**,  
July 2015, Paris, France

## Contribution to scientific grants

1. **Project leader, principal investigator** in **ETIUDA** UMO-2019/32/T/ST4/0057  
*“Self-association of supramolecular capsules based on dynamic imine and beta-diketone bonds.”*



2. **Project leader, principal investigator** in **PRELUDIUM** UMO-2017/25/N/ST5/00942  
*“Dynamic imine cages - self-sorting with component selection.”*



3. **Investigator** in **IUVENTUS** 0446/IP3/2015/73  
*“Synthesis and Complexing Properties of New Dynamic Disulfide Nanocapsules.”*
4. **Investigator** in **LIDER** 024/391/L-5/13/NCBR/2014  
*“Synthesis, physicochemical properties and applications of dynamic metal-organic frameworks.”*
5. **Investigator** in **HOMING PLUS** 2012-6/14  
*“Multi-stimuli responsive self-assembled supramolecular nanocapsules.”*

## Internships

1. **Institute of Supramolecular Science and Engineering (ISIS)**

Strasbourg, France,  
Jean-Marie Lehn Group  
10/2016-03/2017 (6 months)



2. **Institute of Supramolecular Science and Engineering (ISIS)**

Strasbourg, France,  
Jean-Marie Lehn Group  
10/2019-03/2020 (6 months)





# Abstract

This doctoral dissertation, entitled “Self-Association of Supramolecular Capsules Based on Dynamic Iminium and  $\beta$ -Diketone Bonds”, presents comprehensive research at the interface of materials chemistry and fundamental supramolecular chemistry. The research work was carried out within two main, complementary scientific pillars. The first one focused on the design and synthesis of functional metallosupramolecular materials based on  $\beta$ -diketone ligands, with a focus on their catalytic potential. The second pillar was devoted to the study of fundamental principles of self-assembly and self-sorting of components in the process of creating metal-free, organic cages using the tools of Dynamic Covalent Chemistry.

Within the first research area, the work began with a detailed analysis of the coordination chemistry of a simple, unsymmetrical  $\beta$ -diketone ligand (bpmH). The aim was to understand and overcome potential problems, such as uncontrolled oligomerization and complex isomerism, which could complicate the design of more advanced systems. These studies showed that although the bpmH ligand does not fully prevent oligomerization (as demonstrated for the nickel(II) complex), the intermolecular interactions in its complexes are so weak that the formation of isomers in solution is mainly statistical. These observations, including the complex, temperature-dependent dynamic equilibrium in the case of the zinc(II) complex, provided a key foundation for further work. In the next step, an efficient two-step synthetic strategy was developed using a tritopic ligand ( $H_3L$ ). By precisely controlling the stoichiometry, discrete, dimeric metallacycles of the  $[M_2(HL)_2]$  type with Cu(II) and Pd(II) ions, possessing a free, reactive functional arm, were first obtained. Then, in the reaction with excess metal ions, their controlled polymerization was carried out. While in the case of copper(II), the process led to an insoluble product, the reaction with palladium(II) was successful, giving a fully characterized, soluble metallosupramolecular polymer  $[Pd_3L_2]_n$ . The comparison of the catalytic activity of both palladium complexes in the Suzuki-Miyaura cross-coupling reaction was the culmination of this part of the research. It was proven that the  $[Pd_3L_2]_n$  polymer is a much more efficient catalyst, providing higher yields on average by 10-20% compared to its discrete, cyclic precursor. The improved catalytic properties of the polymer were attributed to the larger number of available active sites and the so-called "local concentration effect".

The second pillar of the thesis is devoted to the study of the fundamental principles governing the self-assembly process using Dynamic Covalent Chemistry (DCC). These works, conducted in metal-free organic systems, focused on the phenomenon of self-sorting during the formation of three-dimensional cages (cryptands) based on reversible imine bonds. In a series of competitive experiments, in which one triamine reacted with a complex mixture of different dialdehydes, an extremely high degree of selectivity was observed. In the vast majority of cases, the system spontaneously selected one, most privileged component to build only one, pure (homoleptic) cage product. Crucially, in none of the studied systems was the formation of mixed (heteroleptic) cages observed. Systematic studies allowed us to establish a strict hierarchy of preferences and formulate structural rules governing this process. It was shown that the outcome of sorting is determined by the molecular features of the "building blocks": the most privileged are rigid, fully conjugated components containing a heteroatom (e.g. nitrogen), while flexibility and disorders in the conjugated system significantly reduce the efficiency of a given component. Moreover, it was proven that the observed preferences result from the system reaching a true thermodynamic equilibrium. Using acid-base control over the reversibility of imine bonds, the

possibility of performing a controlled cage-in-cage transformation was demonstrated, in which a less stable structure, in the presence of more favored components, spontaneously reorganizes into the most thermodynamically stable product.

In summary, the presented doctoral thesis comprehensively combines materials chemistry with fundamental research on self-organization. As part of the completed work, not only new, functional materials with increased catalytic activity were obtained, but also the rules governing the process of selective sorting of components in dynamic combinatorial systems were thoroughly investigated and formulated, contributing to the development of both of these dynamically developing fields of chemistry.

# Streszczenie

Niniejsza, przedłożona rozprawa doktorska pt. „Samoasocjacja kapsuł supramolekularnych w opartych o dynamiczne wiązania iminowe oraz  $\beta$ -diketonowe” przedstawia kompleksowe badania z pogranicza chemii materiałowej oraz fundamentalnej chemii supramolekularnej. Chemia supramolekularna, określana jako „chemia poza cząsteczką”, stanowi jedną z najdynamiczniej rozwijających się dziedzin nauki, czerpiąc inspirację z natury do tworzenia złożonych, funkcjonalnych architektur molekularnych. Jej fundamentem są oddziaływania niekowalencyjne, które dzięki efektowi kooperatywnemu umożliwiają spontaniczne formowanie się złożonych, uporządkowanych, trójwymiarowych struktur w procesie samoorganizacji. Celem badań prowadzonych w trakcie przewodu doktorskiego, a podsumowanych w ramach niniejszej pracy, było na zbadanie dwóch kluczowych aspektów tej dziedziny. Pierwszy cel dotyczył projektowania, syntezy i charakterystyki nowej generacji metalosupramolekularnych kompleksów  $\beta$ -diketonowych o cyklicznej budowie z ukierunkowaniem na ich potencjał katalityczny. Drugi cel badawczy, realizowany w ramach Dynamicznej Chemii Kowalencyjnej (DCC), skupiał się na fundamentalnym zjawisku samosortowania komponentów podczas syntezy dynamicznych klatek poliiminowych, aby zrozumieć, jakie cechy strukturalne bloków budulcowych determinują selektywność w tworzeniu złożonych, trójwymiarowych kapsuł.

W ramach realizacji pierwszego celu badawczego, prace rozpoczęto od szczegółowej analizy chemii koordynacyjnej prostego, niesymetrycznego liganda  $\beta$ -diketonowego (bpmH), aby zrozumieć i przezwyciężyć potencjalne problemy, takie jak niekontrolowana oligomeryzacja i złożona izomeria. Badania te wykazały, że chociaż ligand ten nie zapobiega w pełni oligomeryzacji, to tworzenie izomerów w roztworze ma głównie charakter statystyczny, co stanowiło kluczowy fundament pod dalsze prace nad bardziej złożonymi i zaawansowanymi strukturami. W kolejnym kroku opracowano wydajną, dwuetapową strategię syntezy z wykorzystaniem trójramiennego liganda ( $H_3L$ ). Poprzez precyzyjną kontrolę stechiometrii, w pierwszym etapie otrzymano dimeryczne metalocykle typu  $[M_2(HL)_2]$  z jonami Cu(II) oraz Pd(II), posiadające dodatkowo wolne, reaktywne ramie funkcyjne. Następnie, w reakcji z nadmiarem jonów metalu, przeprowadzono ich kontrolowaną polimeryzację. O ile w przypadku miedzi(II) proces prowadził do nierozpuszczalnego produktu, o tyle reakcja z palladem(II) zakończyła się sukcesem, dając w pełni scharakteryzowany, rozpuszczalny polimer metalosupramolekularny  $[Pd_3L_2]_n$ . Zwieńczeniem tej części badań było porównanie aktywności katalitycznej obu kompleksów palladowych w reakcji sprzęgania Suzuki-Miyaura. Udowodniono, że polimer  $[Pd_3L_2]_n$  jest znacznie wydajniejszym katalizatorem, zapewniając wydajności średnio o 10-20% wyższe w porównaniu do swojego cyklicznego prekursora. Lepsze, efektywniejsze właściwości katalityczne polimeru na podstawie analizy dosępných danych przypisano większej liczbie dostępnych miejsc aktywnych oraz tzw. „efektowi stężenia lokalnego”.

Drugi, równoległy filar rozprawy poświęcony został badaniom fundamentalnych zasad rządzących procesem samoorganizacji z wykorzystaniem Dynamicznej Chemii Kowalencyjnej. Prace te, prowadzone w układach czysto organicznych, skupiły się na zjawisku samosortowania komponentów podczas tworzenia trójwymiarowych poliiminowych klatek (kryptandów). W serii eksperymentów kompetycyjnych, w których jedna triamina reagowała ze złożoną mieszaniną różnych dialdehydów, zaobserwowano niezwykle wysoki stopień

selektywności. W zdecydowanej większości przypadków system spontanicznie wybierał jeden, najbardziej uprzywilejowany, dopasowany komponent, budując wyłącznie jeden, czysty (homoleptyczny) produkt klatkowy. Co ważne, w żadnym z badanych układów nie zaobserwowano tworzenia się klatek mieszanych (heteroleptycznych). Systematyczne badania pozwoliły na ustalenie ścisłej hierarchii preferencji oraz sformułowanie reguł strukturalnych rządzących tym procesem. Wykazano, że o wyniku sortowania decydują cechy molekularne bloków budulcowych: najbardziej uprzywilejowane są sztywne, w pełni sprzężone komponenty zawierające heteroatom, podczas gdy elastyczność oraz zaburzenia w układzie sprzężonym znacząco obniżają wydajność danego komponentu w procesie samosortowania. Ponadto, udowodniono, że obserwowane preferencje wynikają z osiągnięcia przez układ prawdziwej równowagi termodynamicznej, demonstrując możliwość przeprowadzenia kontrolowanej transformacji typu „klatka-w-katkę”, w której mniej stabilna struktura w obecności bardziej faworyzowanych komponentów spontanicznie reorganizuje się poprzez wymianę bloków budulcowych w termodynamicznie najstabilniejszy produkt.

Podsumowując, niniejsza rozprawa doktorska w sposób kompleksowy łączy chemię materiałową z badaniami fundamentalnymi nad samoorganizacją. W ramach zrealizowanych prac nie tylko otrzymano nowe, funkcjonalne materiały o podwyższonej aktywności katalitycznej, ale również dogłębnie zbadano i sformułowano reguły rządzące procesem selektywnego samosortowania komponentów w zaprojektowanych dynamicznych bibliotekach kombinatorycznych, przyczyniając się do rozwoju obu tych dynamicznie rozwijających się dziedzin chemii. Wyniki badań nad kompleksami  $\beta$ -diketonowymi otwierają nowe możliwości w projektowaniu polimerycznych katalizatorów, podczas gdy prace nad klatkami iminowymi stanowią istotny wkład w zrozumienie fundamentalnych zasad sterowania złożonymi procesami samoasocjacji, co jest kluczowe dla tworzenia zaawansowanych materiałów adaptacyjnych i systemów inspirowanych naturą.

# Chapter 1: Introduction

Chemistry, in its classical approach, is the science of the molecule. For decades, its main focus was the nature of the classic covalent bond – the powerful force that holds atoms together into stable molecules. It is covalent synthesis that has enabled the creation of countless and various new functional compounds, from drugs to polymers, revolutionizing our world on almost all its fields of science and living. However, both in nature and in the laboratory, there were phenomena that could not be fully explained only in terms of covalent bonds. Processes as fundamental as protein folding, the formation of the DNA double helix or the action of enzymes are based on interactions that are much more subtle but complex and yet highly specific and crucial to functioning. It was at this fascinating frontier that supramolecular chemistry was born – the chemistry of noncovalent interactions, the chemistry of highly organized molecular associations, and finally as Jean-Marie Lehn, one of creators of supramolecular chemistry said - the chemistry "beyond the molecule".<sup>1-4</sup>

Although the formal birth of supramolecular chemistry dates back to the second half of the 20th century, its beginnings should be sought much earlier. It can be assumed that it was the turn of the 19th and 20th centuries, when Emil Fischer, describing the interaction of an enzyme with a substrate, used the vivid metaphor of "key and lock", intuitively describing the essence of specific molecular recognition. A few years later, Paul Ehrlich joined him and formulated the famous principle "*corpora non agunt nisi fixata*" (compounds do not work unless they are bound), postulating the existence of specific receptors in living organisms that allow other, complex chemical compounds to act properly. These were the first, somewhat prophetic ideas, which, however, had to wait decades for their experimental and theoretical confirmation, which came with the development of science and research methodology.

The breakthrough moment came in 1967, when Charles J. Pedersen, while working in the DuPont laboratories, made an accidental but incredibly important discovery, which was one of the most important milestones in the entire process of creating supramolecular chemistry.<sup>5</sup> While synthesizing derivatives of dibenzo-18-crown-6, he noticed that this cyclic polyether was able to "catch" and "release" potassium ions from salts in organic solvents. Pedersen concluded that the cavity in the center of its macrocycle perfectly matched the size of the  $K^+$  cation, forming a stable complex based on ion-dipole interactions. The discovery of crown ethers was, in a way, the foundation of the newly emerging branch of chemistry.

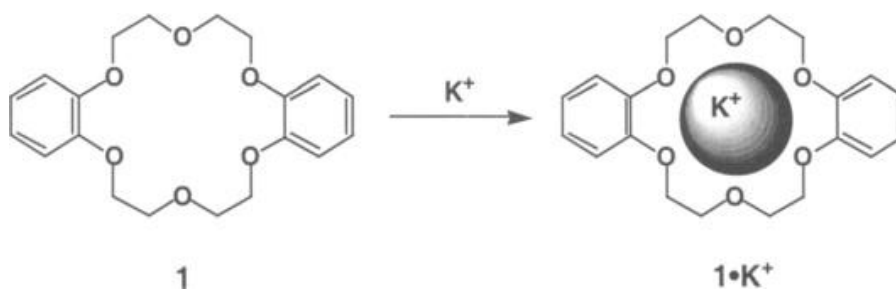


**Figure 1.** Interaction of  $K^+$  with dibenzo-18-crown-6.

Another important moment was the development of Pedersen's work by Donald J. Cram, who introduced the concept of preorganization and guest-host chemistry.<sup>6</sup> According to this, a host with an appropriately designed and rigid structure, complementary to the guest, forms much more stable complexes than its more flexible substitute. Cram's work on spherands and carcerands - molecular "containers" capable of permanently enclosing other molecules inside themselves - brought supramolecular synthesis to a new, advanced level.

The final shape and name of the new discipline were given by Jean-Marie Lehn. It was he who defined supramolecular chemistry in the 1970s as "the chemistry of intermolecular interactions between two or more molecules/aggregates" or "chemistry beyond the molecule". Lehn extended the concept to include three-dimensional cryptands capable of even stronger and more selective ion binding. More importantly, Lehn shifted the focus from simple molecular recognition to the functionality of the structures created. His vision was to create "molecular devices" capable of performing specific tasks, such as ion transport or catalysis.

The culmination of the efforts and work of these three fathers of supramolecular chemistry was awarding them the Nobel Prize in Chemistry in 1987, which was the official recognition of supramolecular chemistry as a mature and extremely promising branch of science. This event contributed to the enormous growth of supramolecular chemistry and, consequently, to the multiplication of the pace of development of this field and research conducted within it. It would certainly not be an exaggeration to say that supramolecular chemistry is currently the driving force of science. This is evidenced, for example, by the pace of growth in the number of scientific publications and articles, but also research projects dealing with the application possibilities of complex, functional supramolecular structures. This is also because it is a branch of science that is very multidisciplinary in nature, because it combines knowledge and issues from the border of chemistry (both organic and inorganic), biology, physics, or modern fields of science, such as nanotechnology.<sup>7-11</sup>

The philosophy of supramolecular chemistry is based on several key pillars. These are: noncovalent interactions (which are the glue of supramolecular chemistry and although these

forces are individually much weaker than covalent bonds, their joint, directed action (the so-called cooperative effect) leads to the formation of stable and highly specific structures). The next pillar is molecular recognition - the ability of one molecule (host) to selectively bind another (guest). The key is geometric complementarity (matching shape and size) and electronic complementarity (matching interactions). As Cram has shown, the better the host is organized for binding before the complexation process itself, the more efficient this process is. Therefore, it is important to consciously design structures before synthesis. And the last pillar, which is self-assembly, i.e. a spontaneous process in which molecules, based on the information encoded in their structure, spontaneously create ordered, complex supramolecular aggregates. This process, ubiquitous in nature, is a powerful tool in the hands of scientists, allowing them to create complex and functional architectures "bottom-up" without the need for tedious, multi-step covalent synthesis.

To better visualize the idea and principles of supramolecular chemistry, scientists sometimes call it “Lego™ chemistry.” This model depicts molecular (covalent) building blocks as individual Lego™ blocks that, through noncovalent interactions, can be assembled together in a variety of reversible ways, resulting in a variety of topologically and functionally diverse supramolecular structures.

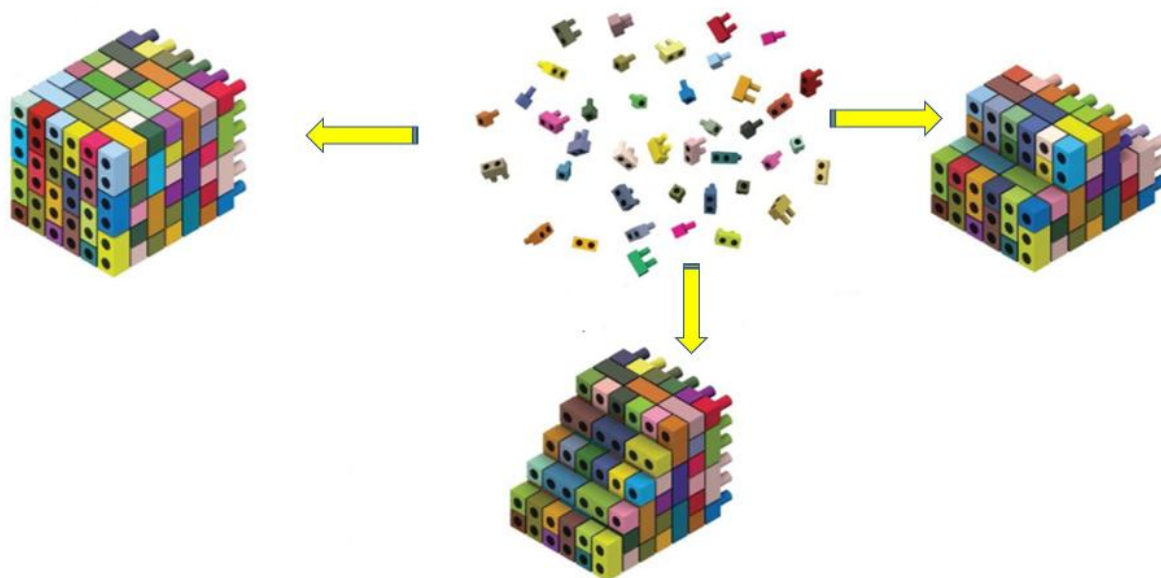


**Figure 2.** A pictorial representation of supramolecular chemistry as “Lego™ chemistry”.<sup>12</sup>

In recent years, these fundamental assumptions have allowed for spectacular achievements. From simple ion-selective sensors based on crown ethers, supramolecular chemistry has evolved towards extremely complex and advanced functional systems. One of

the most exciting and spectacular directions has become molecular machines, which was reflected in the Nobel Prize in 2016 for Jean-Pierre Sauvage, Sir J. Fraser Stoddart and Bernard Feringa. They created molecules (rotaxanes, catenanes, molecular machines) that, under the influence of an external stimulus (light, pH change, redox potential), can perform controlled mechanical movement.<sup>13, 14</sup>

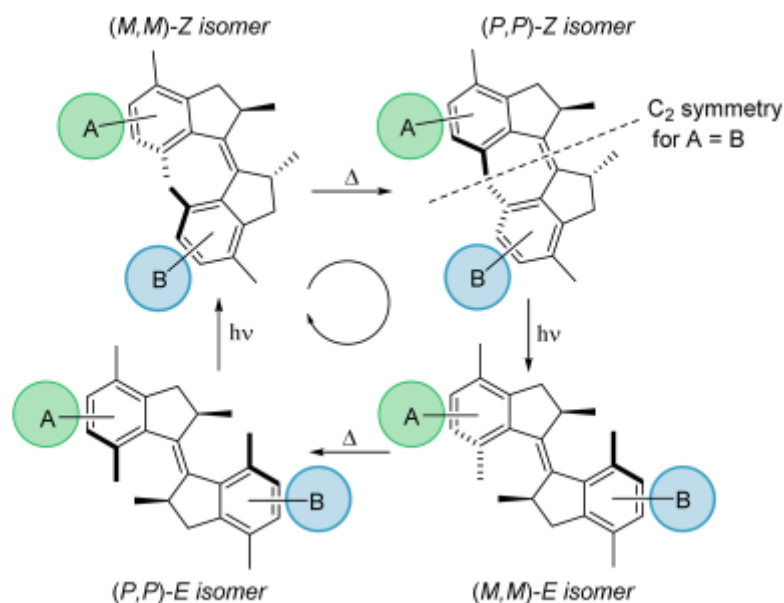


**Figure 3.** Rotary cycle of Molecular Motor.

Supramolecular chemistry, growing out of observations of nature, is now becoming a powerful tool for imitating it and exceeding its capabilities. From the simple act of recognizing single ions, we have reached the stage of designing dynamic, functional systems at the molecular level. This is a field that is still developing dynamically, opening up new, fascinating perspectives. This doctoral dissertation is part of the research trend on phenomena that are the pillars of this branch of chemistry. The aim of the planned work was to design, synthesize and investigate the properties of new supramolecular systems with a cage structure capable of self-sorting, which is a contribution to the further development of this extraordinary "chemistry beyond the molecule".

## Molecular recognition and host-guest chemistry

Molecular recognition<sup>2, 15-17</sup> is one of the most important foundations of supramolecular chemistry. Before this branch of chemistry was officially introduced, molecular recognition, as a phenomenon, was classified as one of the fields of broadly understood guest-host chemistry.<sup>6</sup>



It is a process of binding molecules with the aim of creating a well-defined and, most importantly, stable supramolecular architecture, maintained by intermolecular interactions. In this context, selective interactions between a physically larger host molecule, which in its structure contains the active site, and a smaller guest molecule, which is complementary to it, should be considered.<sup>6</sup> Together, they form a guest-host complex or supramolecule. Professor Lehn defines molecular recognition as "a phenomenon that may contain a specific function, determined by the energy and information contained in the binding and the selection of a substrate or substrates in front of a given molecule, which is the receptor."

Molecular recognition is an important, yet complicated and complex process that requires multi-dimensional complementarity (including geometric, stereochemical, stereoelectronic, toposelectronic, and functional) of the active sites of the host and guest molecules. According to the visual "key and lock" model, the guest molecule interacts with the host molecule like a key with the appropriate lock that it opens. However, this model should be considered very simplified because it does not take into account a series of processes and interactions occurring in solution that affect the entire molecular recognition (e.g. the dynamics of matching the guest molecule to the active site of the host).<sup>15, 18, 19</sup>

Hence the induced fit model was created. The assumption proposed by Daniel Koshland is the basis of a number of processes known from biology – those in which enzymes participate, because they bind substrates in a cooperative manner, by fitting. As a result, in the presence of the appropriate guest molecules, the shape of the host active site changes in such a way that the mutual complementarity of both these molecules is as high as possible. As a result, a more stable molecule with changed properties (enzyme-substrate complex) is formed as a result of the guest-host interaction.

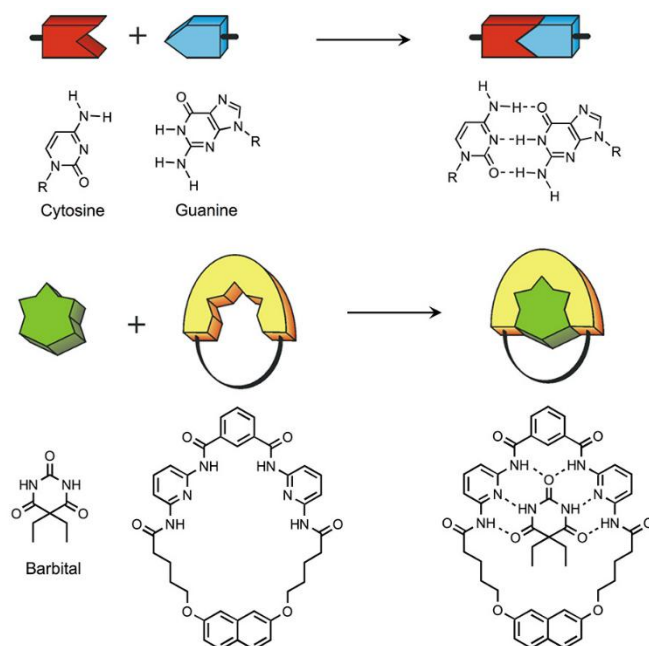


**Figure 4.** Two examples of molecules that are able to recognize each other and associate. In both cases the interaction responsible for the recognition is based on the formation of  $N-H\cdots O$  and  $N-H\cdots N$  hydrogen bonds. For each example, both the chemical formulas and their cartoon representations are shown, from which the spatial complementarity (lock-and-key principle) can be clearly seen.

Molecular recognition between molecules is one of the most fundamental processes in biology, chemistry and medicine. Without this phenomenon, life as we know it would not exist. Enzymes, receptors, antibodies or innovative adaptive materials are examples of incredibly diverse systems whose functioning depends directly on molecular recognition. Although these phenomena have actually developed in the course of evolution for millions of years, understanding them, the ability to control them and properly design structures is crucial for the further development of science, which is why they cannot be ignored.

## Self-association, self-organization

Some of the fundamental processes from the point of view of supramolecular chemistry are spontaneous processes of self-assembly of molecules. We are talking about self-association and self-organization. These twin-like names cover completely different processes that are often confused with each other.

Self-association is the spontaneous formation of relatively small supramolecules from simple, basic building blocks. This is a process that occurs primarily due to non-directional interactions – such as electrostatics or Van der Waals forces. Self-organization is, as it were, the next stage in the hierarchy. This process consists in the combination of small supramolecular molecules into larger assemblies, and consequently into extensive supramolecular structures. In contrast to self-association, self-organization is based on directional interactions (e.g. hydrogen bond, coordination bond). Translating the above information onto the pictorial scale of supramolecular chemistry, we can state that self-association is responsible for the formation of microstructures, in contrast to self-organization, which is responsible for, in a way, the next stage, i.e. the formation of supramolecular macrostructures.<sup>2, 20-22</sup>

Self-organization as a concept is a process that is difficult to define unequivocally. In most sources, it is defined as a process of spontaneous association of two or more molecules or ions into larger supramolecular structures (i.e. complex compounds). Self-organization occurs in accordance with information that is somehow recorded in the structural and electronic structure of the building blocks from which the supramolecular architectures are created. The self-organization process is a phenomenon in itself, because it allows for obtaining a virtually unlimited number of supramolecular structures held by intermolecular interactions, the number of which is limited only by the composition of the initial mixture in which the process takes place - it depends directly on the type and amount of available basic building blocks.<sup>20, 23</sup>

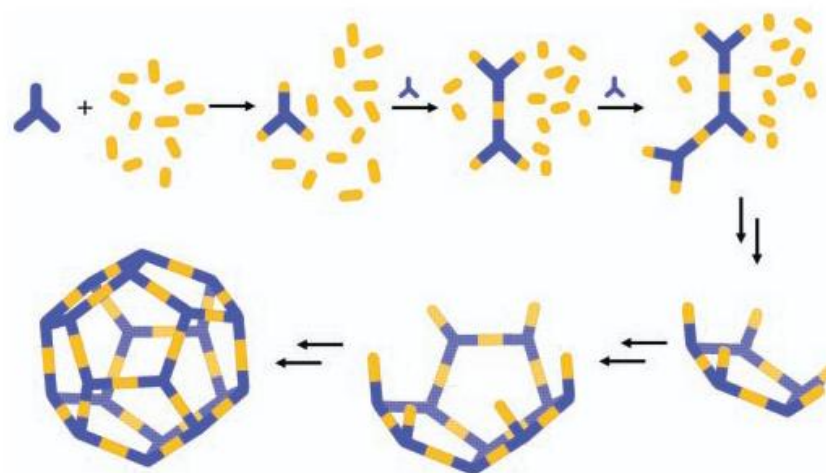


**Figure 5.** Growth of a dodecahedral coordination assembly from 50 components due to self-assembly process.

In the case of metallosupramolecular chemistry, most of the interactions that occur are labile interactions with a high degree of directionality (coordination bond) between the ligand and the metal ion. Self-assembly is a phenomenon that favors the product that is

thermodynamically most stable – it is a selective process towards it. The formation of a supramolecular system must bring a large enough energy gain for the system to overcome entropic effects that tend to maintain the reaction mixture in a maximal degree of disorder.<sup>16, 24</sup>

Obtaining a durable and stable supramolecular structure depends on a number of factors. The basic one is the information contained in the structure of a properly designed ligand, which influences the complementarity of the molecule to the coordination geometry exhibited by the selected metal ion. Factors such as reaction stoichiometry, degree of protonation of functional groups, type of counterion, reaction temperature, type of solvent used or concentration of metal ions also have a significant influence. Often in the case of systems in which self-assembly occurs, the final products are difficult to predict, sometimes even surprising the experimenter, which is one of the greatest challenges for people involved in this field of science. In order to obtain the maximum possible control over the system, the first stages of each research project are crucial - i.e. a thorough analysis of the expected system and the appropriate design, synthesis and characterization of elementary building blocks.

A fascinating example, illustrating how a small change in the structure of basic building blocks (e.g. changing just one atom) has a significant impact on the structure created by self-assembly, is the architecture obtained and described by the research group of Professor Makoto Fujita.<sup>25, 26</sup> In analogous ligand molecules, a sulfur atom was replaced with an oxygen atom, which resulted in molecules with a different bending angle. This small structural difference, together with a change in the mutual stoichiometry of the ligands with respect to each other, led to the formation of two spherical architectures of different sizes.

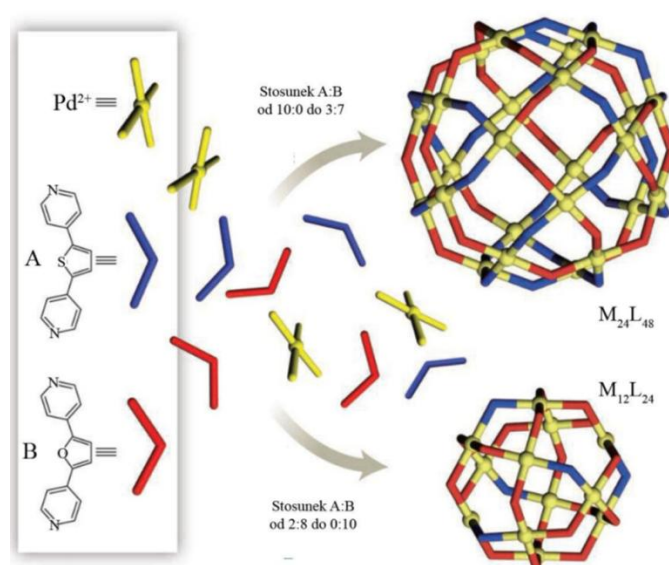


**Figure 6.** Self-assembly of ligands A and B in the presence of palladium(II) ions. Under the given conditions, only one type of coordination polyhedron is formed in solution.

The influence of slight changes in the ligand structure on the type of structures formed spontaneously as a result of the self-assembly process was also observed in the studies described in publication A3, where small changes in the structure of the components forming the cage structures influenced the preferences in the self-sorting process.

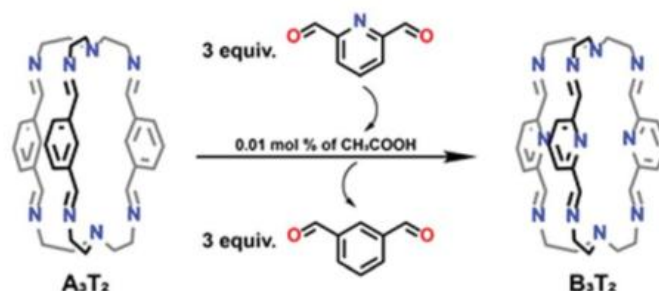


**Figure 7.** The influence of a single atom change in the structure of a building block on the self-assembly and component exchange phenomenon.

## Types of interactions in supramolecular structures

It is still a great challenge to properly design supramolecular architectures with defined structures, but it is more important to understand the interactions responsible for supramolecular synthesis and self-assembly. Understanding the forces that maintain these advanced structures is key to the proper design of substrates, monomers, and ligands, which are then used in subsequent stages of research. The driving forces for supramolecular complex structures are typically recognized as multiple hydrogen bonding, metal-ligand coordination bonds,  $\pi$ - $\pi$  interactions, and other noncovalent interactions such as host-guest interactions or hydrophobic effects. From the point of view of this doctoral thesis, and especially its first part concerning the chemistry of beta-diketone compounds, the most important will be metal-ligand coordination bonds and will be briefly discussed in a moment.

### Metal-ligand coordination

Metal-ligand coordination interactions occupy a unique position in supramolecular chemistry.<sup>1, 27</sup> Combining features of both strong covalent bonds (directivity, predictable geometry) and noncovalent interactions (reversibility, lability), they constitute an extremely

powerful and versatile tool for molecular self-assembly. The use of metal ions as structural "linkers" and organic ligands as the "backbone" has opened the way to the precise, defined design and synthesis of incredibly complex, three-dimensional architectures with predefined and planned topology and function. This approach, often referred to as the "directional bonding" strategy, has transformed and revolutionized the way scientists think about creating complex molecules, shifting the balance from simple covalent synthesis toward efficient, effective self-assembly.

The basic advantage of the coordination bond over other noncovalent interactions is its high directionality and well-defined geometry. Unlike more diffuse and less specific hydrogen bonds or van der Waals forces, the metal–ligand bond is determined by the coordination preferences of a given metal ion, which is a very important factor at the stage of designing complex metallosupramolecular structures. A transition metal ion, such as Pd(II), Pt(II), Cu(I) or Fe(II), imposes a strictly defined geometry on the surrounding ligands – square, tetrahedral or octahedral, respectively. This feature is absolutely crucial, because it allows the chemist to precisely design the structure of the organic ligand with which he or she wants to complex a given metal ion or the entire larger supramolecular structure that will be formed as a result of self-assembly.

The second important factor, which is an advantage of this interaction, is the reversibility (lability) of the bond. The process of complex formation is a dynamic process, remaining in a state of equilibrium. This means that the system has the ability to "correct errors". If a thermodynamically unstable structure (e.g. a strained oligomer) is formed during self-assembly, the labile coordination bonds may be broken and the components may reorganize into the most thermodynamically stable, desired product. This ability to "self-repair" is the secret of the high yields with which complex cages, helicates or molecular knots are often obtained by self-assembly.

Theory and design are reflected in the synthesis of fascinating structures with specific applications. The literature is full of interesting and impressive examples of structures that have emerged as a result of a deliberate process of design and prediction of the function of the target structure.

Helicates,<sup>21, 22, 28, 29</sup> or "intertwined molecular strands", are one of the most classic, but also the most important examples of metal-supramolecular systems. They arise as a result of self-assembly of one or more flexible ligands around metal ions with a preference for tetrahedral (e.g. Cu(I)) or octahedral (e.g. Fe(II)) geometry. The ligands wrap around the axis defined by the metal ions, creating a structure resembling a double (or triple) DNA helix (here we see the

aforementioned inspiration from nature). Due to their inherent chirality, helicates are promising candidates for chiro-optical materials (e.g. for optical switches) and asymmetric catalysts. Their ability to bind to DNA also opens up a number of perspectives in anticancer therapy.

Another great example are molecular squares and cubes, which can be called a kind of precise container or transporter. They use metal ions with square-planar geometry (most often Pd(II) or Pt(II)) and rigid, linear ligands with pyridine groups at the ends (e.g. 4,4'-bipyridine), thanks to which it is possible to obtain (almost with quantitative efficiency) the target structure of the so-called "molecular square" in the self-assembly process. This is a structure in which four metal ions are corners and four ligand molecules - its sides. Such structures are very important from a scientific and practical point of view, because the cavity inside such a molecular square can serve as a nanoreactor, in which, for example, we will carry out chemical reactions in an isolated environment. Additionally, thanks to this, we will often be able to talk about increased selectivity. They can also act as molecular sensors or drug carriers, encapsulating guest molecules, such as anticancer drugs like cisplatin, inside themselves via guest-host chemistry for protection and targeted therapy.<sup>30-32</sup>

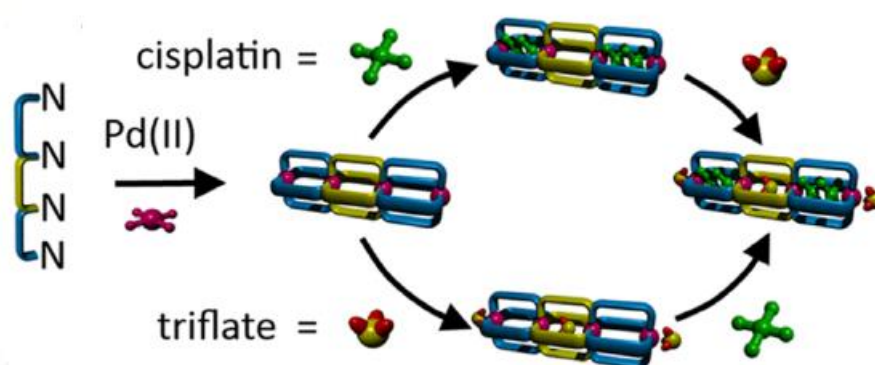


**Figure 8.** Multicavity  $M L$  cage where the two terminal cavities retain the ability to encapsulate cisplatin.

Another example is Coordination Cages (MOCs) – specific molecular reaction vessels. This type of structure provides us with probably one of the most spectacular examples, which is the  $M_{12}L_{24}$  cage, first synthesized by Makoto Fujita's group.<sup>25</sup> It is formed as a result of self-assembly of 12 Pd(II) ions and 24 tridentate, bent triazine ligands. The result is an almost perfectly spherical, highly symmetrical structure with a diameter of several nanometers and a huge internal cavity. Such cages can be excellent nanoreactors. Fujita and co-workers have shown that the  $M_{12}L_{24}$  cage cavity can be used for Diels-Alder reactions or photocycloadditions, which occur in solution with low efficiency or not at all. The cage stabilizes transition states and preorganizes substrates, acting as an artificial enzyme. Moreover, its ability to encapsulate

large biomolecules, such as proteins, makes them promising tools in biotechnology and structural biology, allowing for protein stabilization and facilitating their crystallization for X-ray studies. Another example is the  $M_4L_6$  cages - Tetrahedral cages described by Raymond's group, which are capable of encapsulating a variety of guest molecules. It has been shown that their strongly anionic cavity can stabilize reactive cations, acting as a "molecular flask". This allows the study of reactions that would normally be impossible to carry out.

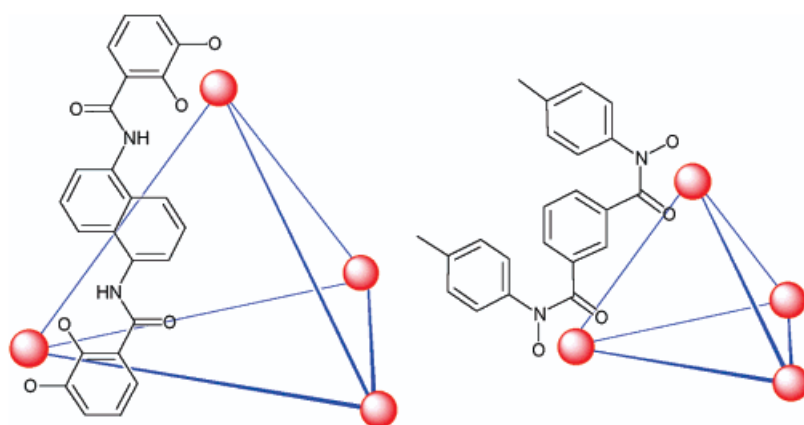


**Figure 9.** Schematic representation of Raymond's  $M_4L_6$  metallocupramolecular cages.

In contrast to the aforementioned cages, coordination polymers are structures extending in one, two, or three dimensions. They are formed when ligands have more than one coordinating group, acting as bridges connecting metal centers in an extensive network. This is the type of structure whose preparation is described in publication A2.

The coordination bond is extremely important for supramolecular chemistry, and also from the point of view of part of the work below, because it is responsible for the binding of metal ions to organic ligands, resulting in the formation of metallocupramolecular complexes. The first segment of the experimental part of this work will concern metallocupramolecular compounds resulting from the formation of a coordination system between the  $\beta$ -diketone system acting as a bond donor and an appropriately selected metal ion.

## Chemistry of $\beta$ -diketones

Metallocupramolecular systems based on  $\beta$ -diketone systems constitute an important class of supramolecular compounds.<sup>29, 33-36</sup> Classical  $\beta$ -diketones have been known and studied for over a century and are undoubtedly the most popular O,O-donating ligands, especially in the coordination chemistry of d- and f-electron elements. Despite the fact that  $\beta$ -diketones represent one of the oldest classes of chelating ligands, their coordination chemistry continues to enjoy great interest (e.g. due to the industrial application of their metallocupramolecular



complexes or the use of diketone derivatives in medicine), and their ability to create rich, interesting and diverse coordination chemistry is well documented.

$\beta$ -Diketone architectures, the most well-known and best-studied representatives of which are pentane-2,4-dione (the simplest of them, acetylacetone, acacH), 1-phenyl-1,3-butanedione (bzacH), 1,3-diphenyl-1,3-propanedione (dbzmH), 2,2,6,6-tetramethyl-3,5-heptanedione (tmhdH), or 1,1,1-trifluoro-2,4-pentanedione (tfacH), due to their structural arrangement - two carbonyl groups separated by one carbon atom (C) - show a number of specific, but at the same time very interesting properties. One of the most important features of this class of compounds is keto-enol tautomerism,<sup>37, 38</sup> i.e. the occurrence of equilibrium between the keto form and the enol form of the  $\beta$ -diketone compound.

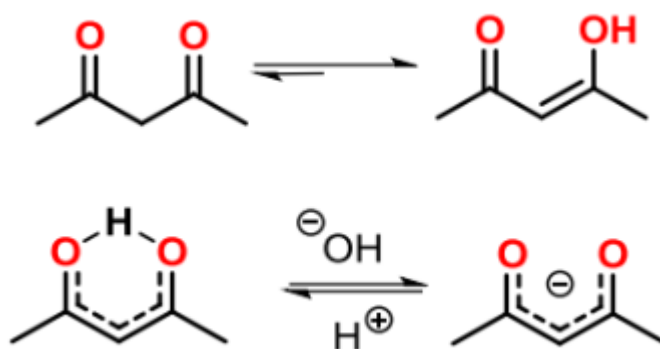


**Figure 10.** Scheme showing keto-enol tautomerism and the sensitivity of the 1,3-diketone group to acid-base changes.

For  $\beta$ -diketones, this equilibrium is strongly shifted towards the enol tautomer. This is due to the formation of a characteristic, stable, transitional six-membered ring (stabilized by an intramolecular hydrogen bond). The equilibrium state between keto-enol tautomers is influenced by many factors, the most important of which are: solvent polarity, the presence of a base in the solution and its type, the nature of the substituents attached to the  $\beta$ -diketone group (terminal and methylene). The occurrence of  $\beta$ -diketone compounds in the enol form has consequences for the chemistry of this type of systems – thanks to this, they are capable of forming durable and stable metallocupramolecular complexes with most metal ions.<sup>35, 39-43</sup>

## Synthesis of $\beta$ -diketones

Classical  $\beta$ -diketones can be obtained by acylation of ketones with esters (Claisen condensation), in the presence of alkali metal hydroxides, ethoxides, hydrides or amides as condensing agents, in order to increase the relatively low reactivity of the ester carbonyl group. However, optimization of the specific reaction conditions can lead to very high and satisfactory values of the final reaction yield. Other, general synthetic methods have been described by Mehrotra.<sup>44</sup> In order to avoid the difficulties encountered in the synthesis via Claisen condensation, such as the formation of regioisomers, competitive O-acylation, proton exchange between the enolate and the final diketone, or generally low yields, new synthetic approaches have been developed, taking into account structural modifications and functionalization of diketones. One of the most important improvements of this type was the reaction of 1-diazo-1-lithioacetone with aldehydes, followed by acid-induced transformation of the resulting  $\alpha$ -diazo- $\beta$ -hydroxyketone into the corresponding  $\beta$ -diketone, in the presence of rhodium(II) acetate as a catalyst.<sup>33, 45, 46</sup>

## Application of $\beta$ -diketone compounds

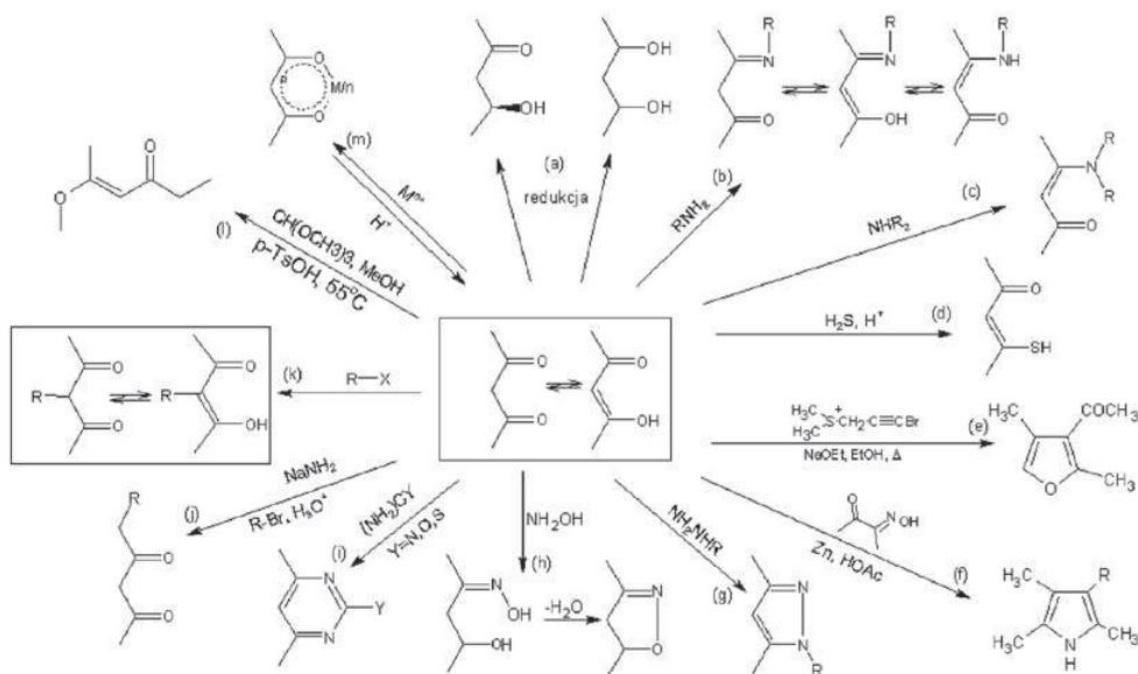


**Figure 11.** Scheme illustrating the application possibilities of  $\beta$ -diketones.

The structural diversity and multitude of supramolecular and metallosupramolecular architectures created by  $\beta$ -diketone compounds are reflected in a whole range of diverse applications they find. The presence of two carbonyl groups in the structure of  $\beta$ -diketones makes this class of compounds one of the very valuable substrates in a number of organic syntheses. They are used, for example, in condensation reactions with amines, leading to the formation of ketimines. The use of  $\beta$ -diketones in the synthesis of heterocyclic compounds allows, among others, the production of pyrimidine derivatives. In addition, the structure of the  $\beta$ -diketone group allows for modifications by introducing a substituent attached to the methylene group (located between the carbonyl groups). Such adaptation of the structure usually does not affect the reactivity of the compound in subsequent reaction steps, but allows the introduction of substituents that can then be modified (e.g. by introducing functional groups via dynamic bonds or polymerizing unsaturated bonds).

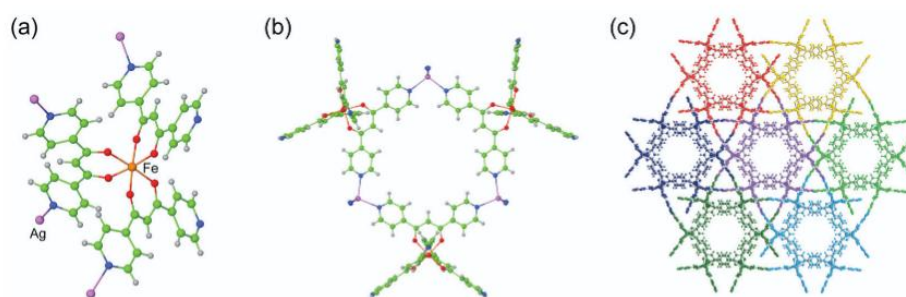


**Figure 12.** Various metallosupramolecular structures based on beta-diketonate ligands described by Warren.

Due to these properties,  $\beta$ -diketone compounds and their supramolecular complexes offer a wide range of applications, both in the world of science and in the chemical and technological industry.  $\beta$ -diketone structures are used, for example, as substrates for the production of catalysts (both homo- and heterogeneous), as substances modifying the properties of polymers (increasing their resistance to physicochemical factors), and their complexes with appropriate metal ions can themselves constitute catalysts used in the polymerization process.  $\beta$ -diketone complexes with transition metal ions are often used in the catalysis of oxidation, epoxidation or oligomerization reactions of olefins.

Several research groups have recognized the potential of  $\beta$ -diketones as extracting and complexing agents for spectrophotometric determination of metal ions in dilute solutions and for chromatographic separation. Lanthanide diketonates have also been found to be useful as NMR shift standards. Due to these properties and their complexing abilities, diketone

compounds are of great importance from the point of view of laboratory analytics. In addition to the examples mentioned above, they are also used, among others, for monitoring air quality.

In the early 1980s, numerous studies on the synthesis of new metal-diketonate derivatives, characterized by appropriate volatility and thermal stability sufficient for their use as molecular precursors in chemical vapor deposition (CVD) techniques,<sup>47-49</sup> appeared. CuI and CuII diketone complexes with supporting Lewis bases are promising precursors for microelectronic devices<sup>50</sup>, and in combination with alkaline earth metal diketonates<sup>51, 52</sup> - for the preparation of new, high-temperature superconducting mixed metal oxides. In addition, many metal-diketone complexes have been investigated as molecular precursors in CVD technique of fluid transport in supercritical state.<sup>53</sup>

After the significant but unexpected discovery of the anticancer properties of cis-platinum, much effort has been put into finding other metal compounds with analogous properties. Several diketonates (including complexes of  $\beta$ -diketones with metal ions Sn, Ti, Zr, or Hf) have been shown to exhibit interesting biological activity in this direction. For example, budotitane ((EtO)<sub>2</sub>Ti(bzac)<sub>2</sub>) was the first non-platinum complex to enter clinical trials as a potential anticancer drug. Considerable progress has also been made in the search for new lanthanide diketone complexes as luminescence sources, which can be used in the production of polymer electroluminescent diodes, and in the production of low-cost, full-color flat-panel displays.<sup>54, 55</sup> Moreover, some complexes seem to be promising chiral NMR reagents for determining enantiomeric purity.<sup>32, 56, 57</sup>

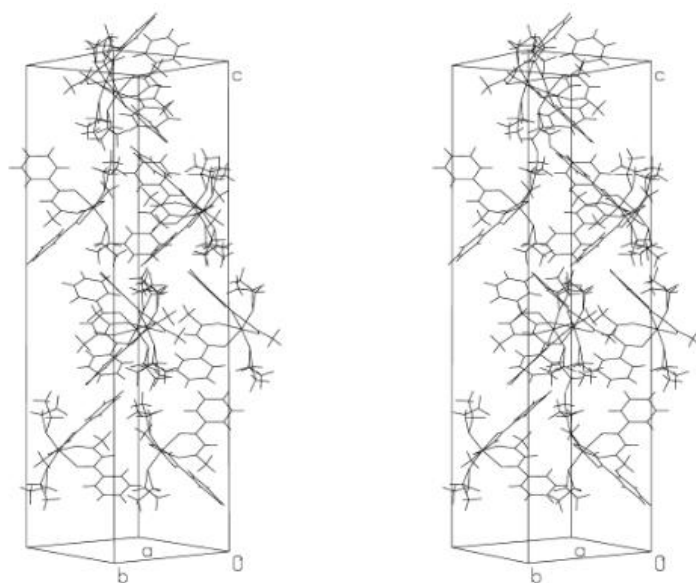


**Figure 13.** Stereo plot of the unit cell of budotitane,  $Ti(bzac)_2(OEt)_2$ .

Another important field of scientific interest in  $\beta$ -diketone compounds is the potential use of metal diketonates as liquid crystal phases. Due to their special magnetic and electronic properties, these metal-containing materials are generally known as "metallomesogens". The vast majority of the literature in this field was devoted to the diketonates Rh(I), Ir(I), Ni(II), Pd(II), Pt(II) and Cu(II), which have linear or planar coordination geometry and therefore mimic conventional liquid crystals. Some lanthanide diketonate adducts containing specific Lewis bases, such as 1-N-alkyl-4-alkyloxy-2-hydroxy-benzaldimine, have also been shown to exhibit interesting mesomorphic properties.<sup>41, 58-60</sup>

Due to the large application potential, it is justified to search for new metallosupramolecular architectures with increasingly better, defined and designable physicochemical properties, and to develop more efficient synthetic routes for expanded metallosupramolecular architectures. For this reason, the first part of the doctoral thesis was devoted to the design and synthesis, and then the characterization of beta-diketone ligands, which then participated in the self-assembly process with appropriately matched metal ions.

## Dynamic Combinatorial Chemistry (DCC)

Dynamic Combinatorial Chemistry (DCC)<sup>61-67</sup> is a method for generating new structures formed by reversible reactions (and bonds) between simple building blocks, under strict thermodynamic control. DCC combines the features of molecular (covalent) and supramolecular chemistry. It is an incredibly useful tool in the hands of scientists, allowing the synthesis of completely new systems, often with a high level of complexity, from simple, but appropriately selected, designed and functionalized building blocks complementary to each other and capable of mutual reactions. The use of dynamic intermolecular connections allows the generation of a specific, specified mixture of compounds, called a Dynamic Combinatorial Library (DCL).<sup>68, 69</sup> All components of such a library are in thermodynamic equilibrium, and their distribution is determined by their thermodynamic stability within this library. The processes occurring in such a reaction mixture are dynamic, which means that the components of a given DCL are constantly being exchanged by breaking and forming appropriate dynamic bonds, with the aim of achieving the lowest energy state. Although it is worth emphasizing here that there are few known examples of libraries of this type created using kinetic control.<sup>62</sup> Among the main dynamic bonds used in Dynamic Combinatorial Chemistry, the following

should be mentioned: disulfide bonds, boronic acid ester bonds, acetylhydrazone bonds, coordination bonds, and extremely important due to the studies described in A3 - imine bonds. For this reason, it will also be briefly described later in the work.

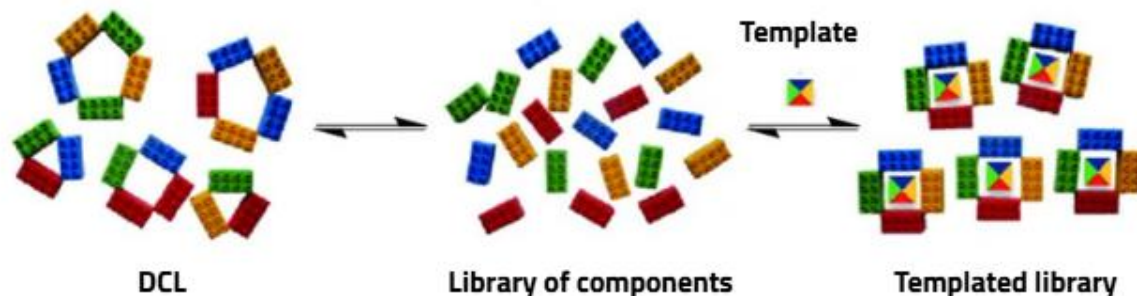


**Figure 14.** Schematic representation of the idea of Dynamic Combinatorial Chemistry (DCC).

The tool of Dynamic Combinatorial Chemistry has enormous application potential, primarily due to the variety of products generated by DCL and the possibility of modifying the composition of libraries. The DCC concept is used, among others, in chemical sciences (chemosensors, receptors, catalysts, transporters, molecular storage systems), in processes such as self-sorting, self-replication, or in biological sciences (use of DCL in selective protein binding). Thanks to continuous research on dynamic systems, the importance of DCC is constantly growing in the world of science, technology, nanotechnology, or the production of adaptive materials. Additionally, this concept gains new tools that allow for the prediction of the composition of DCL libraries, e.g. thanks to computational modeling.<sup>70, 71</sup> One of the stages of this doctoral thesis was conducted using the concept of Dynamic Combinatorial Chemistry, with the use in the synthesis of systems based on reversible imine bonds. This research was initiated during a research internship carried out in the group of Professor Jean-Marie Lehn and was conducted within the framework of two projects financed by the National Science Centre (PRELUDIUM, ETIUDA). Detailed results will be presented in the further part of this work.

## Dynamic imine bond

The imine bond, due to its reversible nature, is of great importance from the point of view of covalent, supramolecular chemistry and the DCC concept. This type of bond has many advantages, among which one should distinguish: numerous, well-described synthetic protocols, enabling the synthesis of imine compounds, a large and diverse library of basic building blocks used for the reaction - amines and carbonyl compounds, which are commercially available. The imine bond is formed as a result of the condensation reaction

between the functional groups - carbonyl and amine - with which the substrates are functionalized. However, this reaction is sensitive to a number of physicochemical conditions, including the pH of the reaction solution, the process temperature, the stoichiometry and concentration, and even the state of matter of the reactants. Usually, the imine formation reaction is favored in solutions with a higher pH value, while the formed imine bond undergoes hydrolysis under acidic conditions. Another factor influencing the course of the imine reaction, in the case of processes occurring in organic solvents, is their polarity (it affects, for example, the reaction time leading to obtaining a thermodynamically stable product). It is worth adding that the factor influencing the acceleration of imine formation in organic solutions is the addition of a catalytic base (e.g. TEA, pyridine) to the system.<sup>23, 72-74</sup>

The imine bond, due to its reversibility and the resulting dynamic character, has been used in the creation of many different complex spatial structures with interesting properties. The nature of imine connections also allows for a high level of error correction (error-checking) at the stage of forming structures within DCL.

## **Imines in Dynamic Combinatorial Chemistry – application**

One of the classic applications of DCC is the discovery of new molecular receptors. In this approach, the target molecule (guest) acts as a template, promoting the synthesis of a macrocycle or cage with a cavity ideally matched to its shape, size, and electronic properties. Davis and colleagues' research group used DCC based on imine chemistry to create water-soluble molecular cages capable of selectively binding neurotransmitters such as acetylcholine over its metabolite, choline. A library consisting of triamine and dialdehyde, in the presence of acetylcholine as a template, rearranged itself, leading to the amplification of the tetrahedral M<sub>4</sub>L<sub>6</sub> cage. This discovery opens the way to the design of sensors for monitoring neurological activity or systems for neutralizing specific signaling molecules.

Imine chemistry is also a key method for the synthesis of highly crystalline, porous materials known as COFs. The ability to “correct errors” resulting from the reversibility of the reaction allows for nearly defect-free, ordered structures. Recent imine-based COFs exhibit record-breaking surface areas and have been successfully used in the catalytic reduction of CO<sub>2</sub>, where the porous structure and active imine sites cooperate to efficiently convert carbon dioxide into useful fuels such as formic acid.

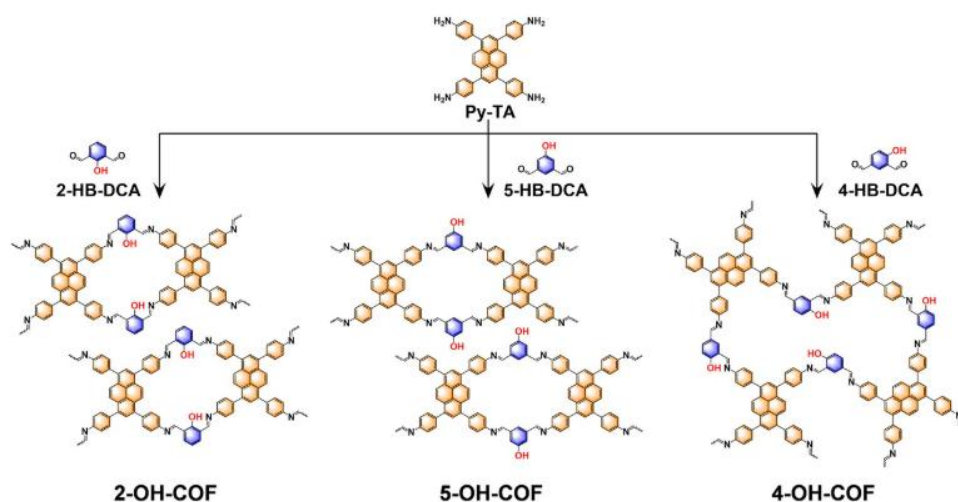


**Figure 15.** Imine COFs built up from different aldehyde building blocks.

DCC also revolutionizes the process of discovering new and innovative drugs by combining the advantages of target-based screening and fragment-based drug design. In this approach, a biological target (e.g. enzyme) is incubated with a dynamic library of small, reactive fragments (amines and aldehydes). The enzyme itself "selects" and "synthesizes" on the surface of its active site the best-matched inhibitor. An example of this are protein kinases, which are key targets in cancer therapy. Using DCC, new, potent inhibitors for several important kinases were identified. A library of simple amines and aldehydes was incubated with the target protein, and LC-MS analysis of the reaction mixture allowed the identification of a newly formed imine molecule that showed many times higher affinity for the enzyme than any single fragment. This is an extremely efficient method for rapid prototyping and optimization of lead structures in medicinal chemistry.<sup>75-81</sup>

DCC allows, due to its characteristics, the study of fundamental principles underlying life, such as self-replication. A replicator molecule, built from two or more components connected by reversible imine bonds, can act as a template for its own synthesis, leading to an exponential increase in its concentration. It is worth mentioning here the research groups of Otto and Lehn, which demonstrated that processes resembling Darwinian evolution can occur in complex dynamic imine libraries. Different replicators can compete for the same, limited resources (building blocks). Adding an external selection factor can lead to "mutations" (e.g. by incorporating a new component into the replicator structure) and the emergence of new species, better adapted to the prevailing conditions. These studies shed light on how molecular complexity could have arisen in the prebiotic world.



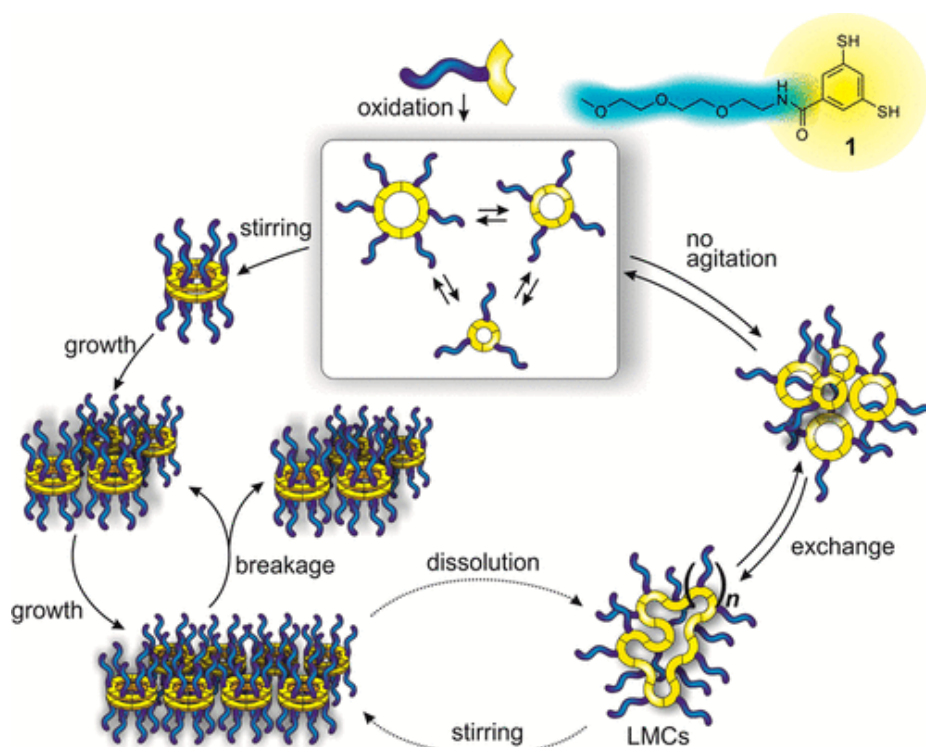


**Figure 16.** Dynamic Combinatorial Library described by Otto and colleagues.<sup>82</sup>

Dynamic Combinatorial Chemistry, driven by the reliability and versatility of imine chemistry, has evolved from a conceptual curiosity into a mature and powerful platform for the discovery and creation of molecular functions. Recent achievements show its enormous potential in the design of receptors, adaptive materials, drugs and models of living systems. The future of this field lies in the creation of even more complex, multicomponent systems operating in conditions far from equilibrium, capable of autonomous action, adaptation and evolution, blurring the boundary between living and non-living matter. For this reason, the second, very important part of this PhD thesis was the research carried out in collaboration with Professor Lehn's group, which was aimed at investigating the phenomenon of self-sorting of components within previously designed combinatorial libraries in order to obtain three-dimensional imine cages, which is described in detail in the publication A3.

## Research objectives

The ultimate scientific goal of the research conducted during the doctoral dissertation entitled "*Self-association of supramolecular capsules based on dynamic imine and  $\beta$ -diketone bonds*" was the design, efficient synthesis, structural and spectroscopic characterization and definition of properties of a new generation of cage-like compounds based on dynamic imine bonds and  $\beta$ -diketone coordination motifs.

The research work was divided into two thematic branches:

- 1) Research on the new generation of  $\beta$ -diketone ligands and their metallosupramolecular complexes. (A1 and A2)
- 2) Research on the new generation of macrocyclic and macrobicyclic three-dimensional polyimine systems according to the concept of Dynamic Combinatorial Chemistry. (A3)

The primary goal of the first part - concerning  $\beta$ -diketones - was to design, synthesize and characterize cage structures of this type. The topic was taken up because, although the chemistry of this class of compounds is very well known, there were few examples of cage structures composed solely of  $\beta$ -diketone ligands, which created a field for the development of research on coordination architectures of this type. An additional aspect of this part of the work was the desire to better learn and understand the self-association processes of metallosupramolecular  $\beta$ -diketone systems containing transition metal ions, and then to study the properties of the obtained structures. Although the main goal for the designed organic ligands was the synthesis of cage structures, in accordance with the idea of "expect the unexpected", the research did not limit itself to this one type of supramolecular architecture. As a result, this led, among others, to obtain complexes with  $\text{Pd}^{2+}$  ions, for which the isomerization processes were investigated and the catalytic properties for metallosupramolecular complexes with different M:L stoichiometry (ratio of metal ions to ligand molecules involved in complex formation) were determined.

The topic of the second part of the doctoral thesis – related to imine systems and Dynamic Combinatorial Chemistry – resulted from a similar motivation. Dynamic cage architectures (both molecular and (metallo-)supramolecular) are constantly gaining importance in the world of science. In this case, scientists, drawing inspiration from nature, are currently paying special attention to biological systems using the self-sorting process to achieve "order over chaos". The research conducted on the dynamics of the formation of imine cages was an innovative approach, because although imine compounds were and still are widely described in

the scientific literature, the issues related to the self-sorting of components towards the formation of polyimine cages were so far somewhat omitted and constituted the primary research goal of this part of the work. The intermediate goals were to design, synthesize, isolate and fully characterize a series of dynamic cages based on imine bonds, which were then to be used for the aforementioned research on the self-sorting of components. An additional goal was to optimize the synthesis conditions using modern techniques.

## Chapter 2: Chemistry of $\beta$ -diketones

### Coordination properties of unsymmetrical $\beta$ -diketonate ligands and their role in functional metallocupramolecular complexes

Supramolecular chemistry is based on the use of labile intermolecular interactions to create complex structures with specific functions. Despite the great diversity in the nature and energy of these labile interactions, an exceptionally useful type is the coordination bond with metal ions. This bond, although not always, is usually labile, and its great advantage is the possibility of changing its state from labile to neutral (inert) by appropriate selection of donor atoms or ligand structure. This can be done even selectively in the coordination sphere of one metal ion, introducing multidentate chelating ligands or, in particular, macrocyclic ligands. In the design of multidentate ligands, a still rarely studied issue, important for the multifunctionality of complexes, is the conscious introduction of ligands with ambidentate coordination sites. In principle, this feature should allow the complex of the appropriate ligand to transition, under the influence of a specific stimulus, between forms with different functions, e.g. with different catalytic activity. Therefore, we undertook a research program focusing on divergent multisite ligands and the analysis of the properties of their isomeric complexes.

During research described in this PhD thesis and to establish background to the possible use of its ambidentate derivatives as stimuli responsive ligands in functional complexes, the basic coordination chemistry of 4,4-dimethyl-1-phenylpentane-1,3-dione (benzoylpivaloylmethane, bpmH) has been re-examined with selected main group and transition metal M(II) and M(III) species. In focus of the research on the possibility of generating ambidentate ligands from a phenyl-substituted 1,3-diketone, appeared to overcome two issues potentially complicating their application: aggregation and isomerism of the complexes. Since the diketone bpmH is a readily available "parent" species for the construction of an ambident ligand, the research work focused on extending in detail the rather limited knowledge of its coordination chemistry with respect to the complications mentioned above. For this purpose, transition metals M(II) and M(III) were used, as well as Al(III) as a representative of the main groups.

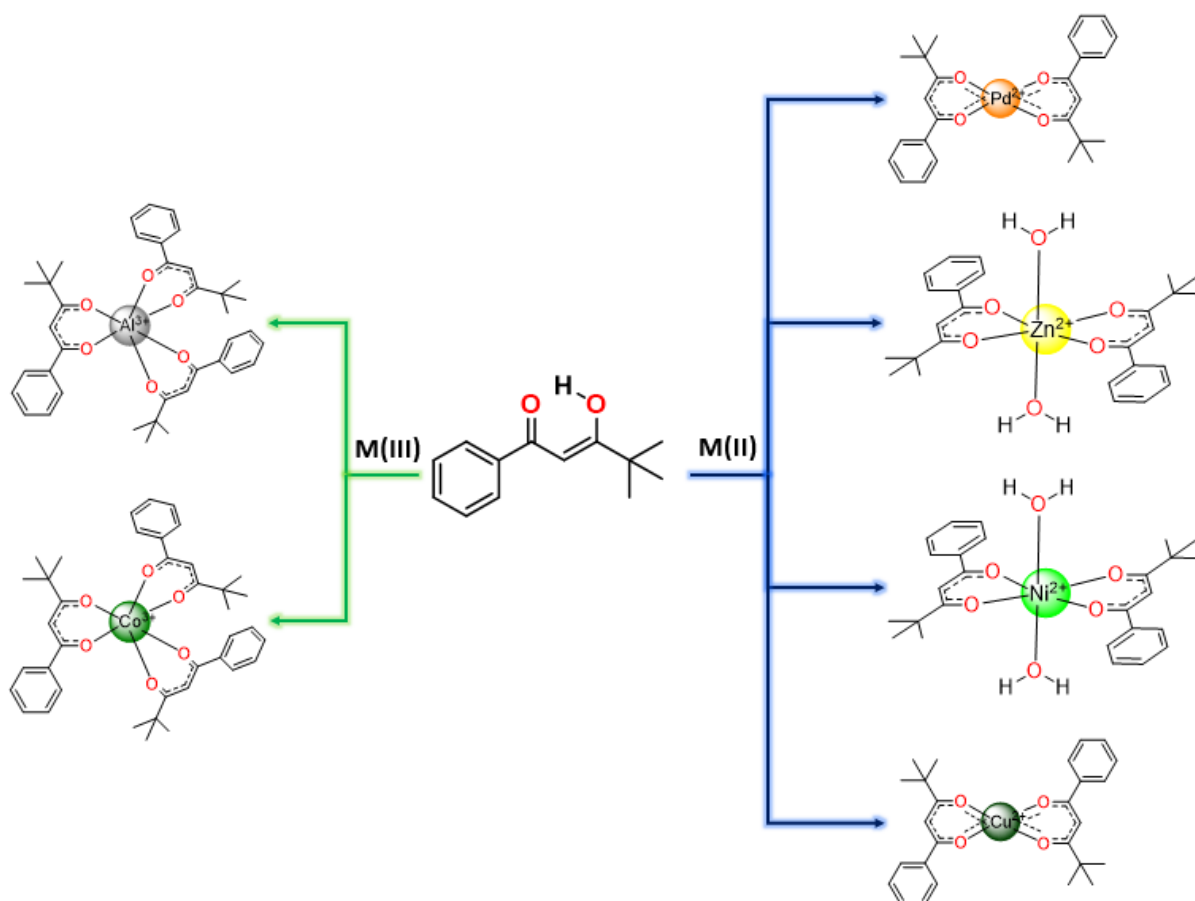


**Figure 17.** Scheme of all the complexes obtained in reactions of 4,4-dimethyl-1-phenylpentane-1,3-dione (*bpmH*) with *M*(II) and *M*(III) ions.

## Synthesis of bpmH and its complexes

The ligand was prepared according to a literature procedure [15], although it is also available commercially. Pinacolone was added to a suspension of NaH in dry THF. After 30 min. of stirring, methyl benzoate was added to the grey-yellow suspension. The mixture was heated at 47 °C for 24 h. Reaction was quenched by the addition of water, followed by aqueous HCl to reduce the pH to ~4. The product was extracted into ethylacetate and the extract evaporated down after drying over Na<sub>2</sub>SO<sub>4</sub>. The crude product was purified by addition of CuCl<sub>2</sub>•2H<sub>2</sub>O, isolation of the solid complex formed and then dissociating the ligand from this by treatment with hot aqueous H<sub>2</sub>SO<sub>4</sub>. Extraction into DCM, drying and evaporation of the extract yielded the desired product as a yellow oil.

The isolated ligand was then implemented in a series of complexation reactions to obtain beta-diketone metallosupramolecular complexes. Both the diketone and diketonate complex

syntheses were based on very familiar literature procedures for the same or closely related species and provided no surprising results. Methanol proved to be a convenient solvent for all the complex ion syntheses, although various other solvents such as ethanol, acetonitrile or tetrahydrofuran could be used with equal success.

## Results

The aim of the conducted studies was to synthesize neutral metal complexes of the  $M(\text{bpm})_n$  type and to investigate their key structural properties: tendency to oligomerization and stereochemistry. The analysis showed that the  $\text{bpm}^-$  ligand does not prevent oligomerization of molecules, which was proven for the nickel(II) complex. It was isolated as a green, octahedral and paramagnetic form  $[\text{Ni}(\text{bpm})_2(\text{OH}_2)_2]$ , which after heating transformed into a structure analogous to the known oligomer  $[\text{Ni}_3(\text{acac})_6]$ . The second part of the studies focused on the analysis of the distribution of *fac* and *mer* isomers in complexes with this asymmetric ligand, using NMR spectroscopy. For aluminum(III) and cobalt(III) complexes, the measured *fac*:*mer* isomer ratio was 1.65. This value is very close to the probability ratio (2:1), suggesting that the formation of individual isomers is a statistical process and not the result of strong intramolecular interactions that would favor a specific form.

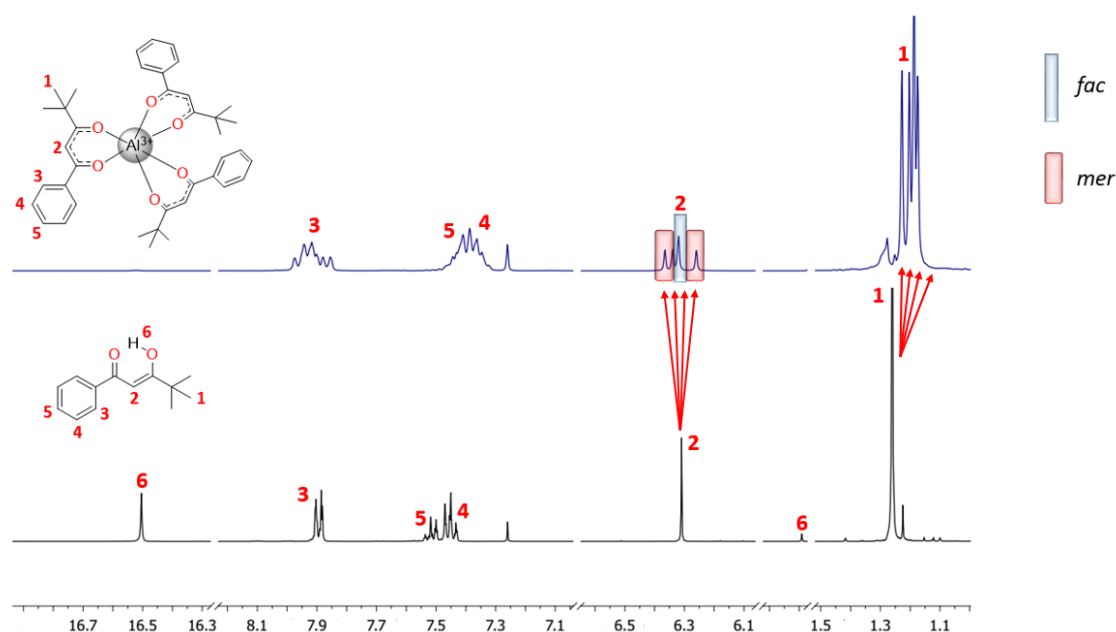


**Figure 18.** Comparison of the  $^1\text{H}$  NMR (300 MHz) spectra of  $\text{bpmH}$  (bottom, black) and the complex  $[\text{Al}(\text{bpm})_3]$  (top, blue) in  $\text{CDCl}_3$  at room temperature.

In the case of the planar, square complex  $[\text{Pd}(\text{bpm})_2]$  cis and trans isomerism is possible. Studies using NMR spectroscopy showed that immediately after dissolving the crystals in solution, only the trans isomer was present, which corresponds to its form in the crystal lattice. However, after an hour, equilibrium was established in the solution, and a mixture of both isomers was observed in the spectrum in a cis to trans ratio of 1:1.66. This result, although it deviates from a purely statistical value (1:1), in combination with earlier observations for the nickel complex leads to the general conclusion that the interactions between the bpm<sup>−</sup> ligands in the complexes are weak. In terms of coordination properties, this places the bpm<sup>−</sup> ligand closer to the simpler acac<sup>−</sup> ligand than to the one with high steric hindrance, i.e. dpm<sup>−</sup>.

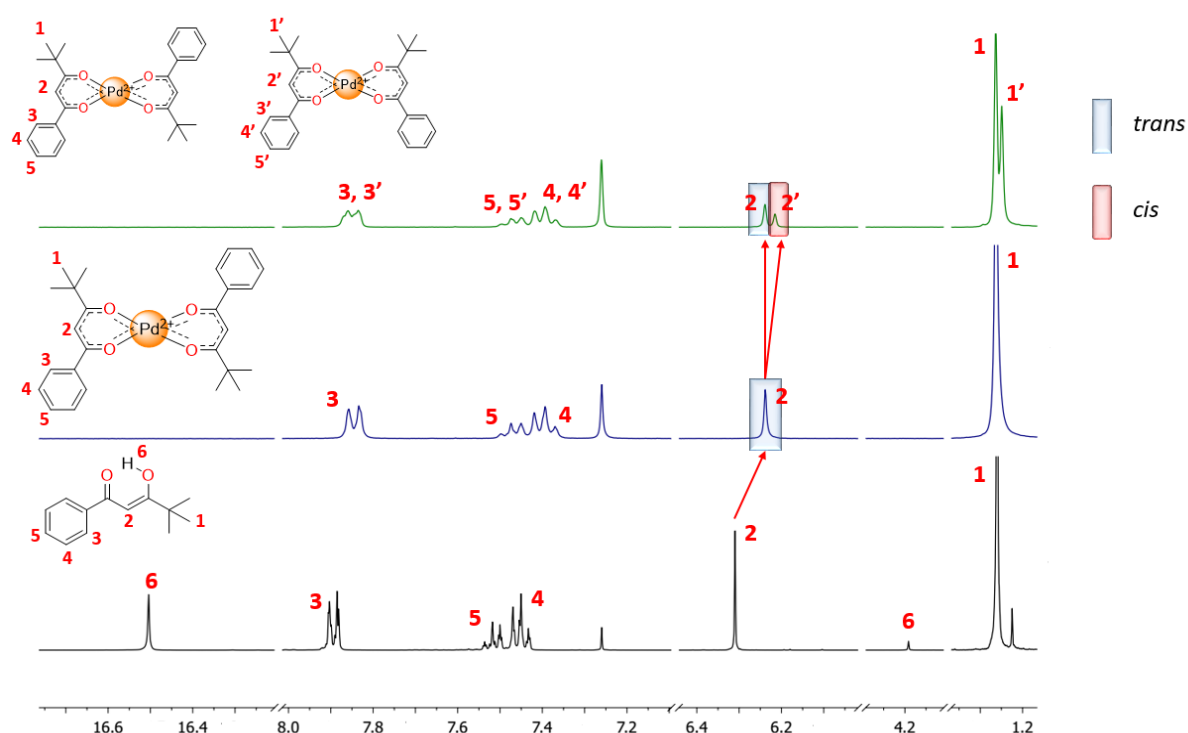


**Figure 19.** Comparison of the  $^1\text{H}$  NMR (300 MHz) spectra of bpmH (bottom, black), the complex  $[\text{Pd}(\text{bpm})_2]$  immediately after preparing the solution (middle, blue) and the complex  $[\text{Pd}(\text{bpm})_2]$  after one hour in solution (top, green) in  $\text{CDCl}_3$  at room temperature.

Elemental analysis of the zinc(II) complex indicated the presence of two water molecules per metal ion, suggesting various possible formulas, such as pentacoordinated  $[\text{Zn}(\text{bpm})_2(\text{OH}_2)] \cdot \text{H}_2\text{O}$  or hexacoordinated  $[\text{Zn}(\text{bpm})_2(\text{OH}_2)_2]$ . In both cases, cis/trans isomerism is possible. NMR spectroscopy confirmed the presence of two different forms in solution, in a ratio of 1:1.5, but their unambiguous assignment to specific isomers is not possible due to overlapping and broadened signals. The key observation is the strong temperature dependence of the NMR spectrum - lowering the temperature causes a shift and significant

broadening of one of the signals. This indicates a more complicated process than simple cis/trans isomerism. This leads to the conclusion that there is a dynamic equilibrium between the pentacoordinated and hexacoordinated forms in solution.

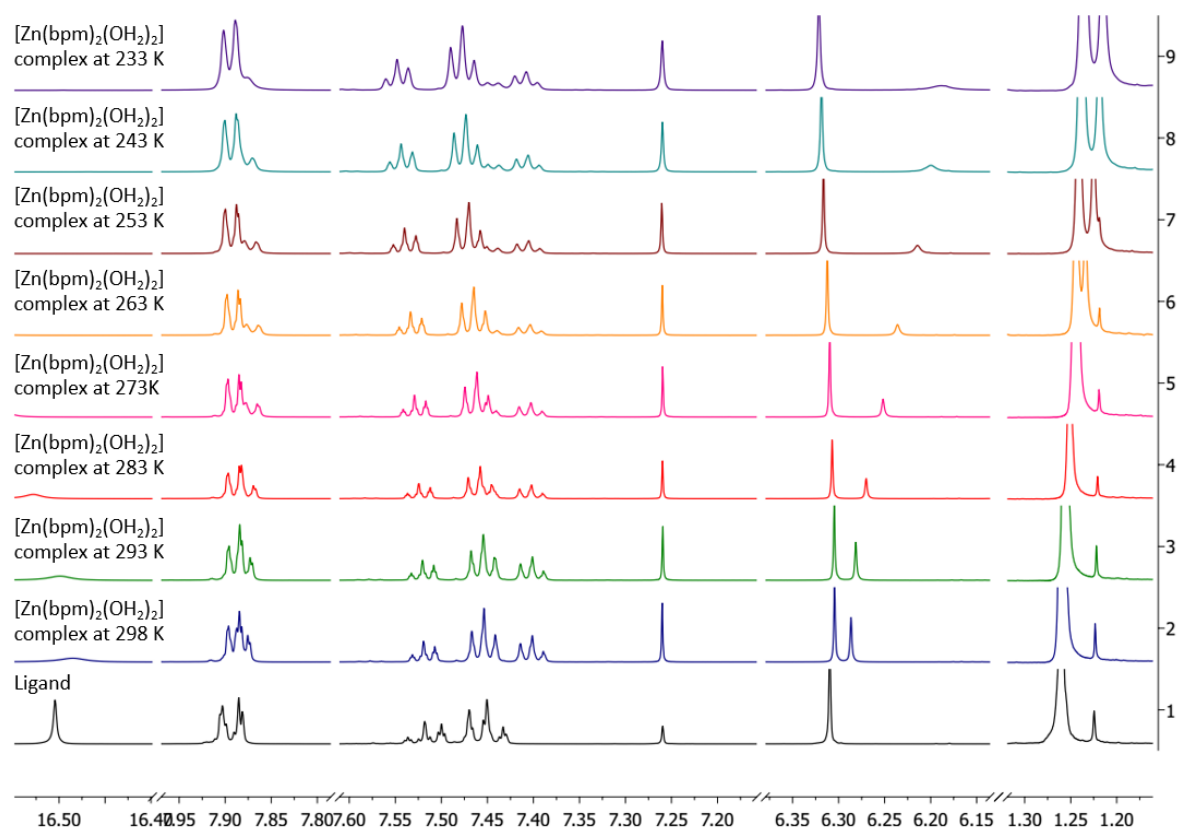


**Figure 20.** Variable Temperature NMR (600 MHz) spectra for  $[\text{Zn}(\text{bpm})_2(\text{OH}_2)_2]$  recorded in  $\text{CDCl}_3$ .

In order to isolate a single, pure form of the compound from the solution, the slow crystallization method was used. This allowed obtaining crystals of the paramagnetic complex  $[\text{Cu}(\text{bpm})_2]$  (by slow evaporation of the solvent) and the diamagnetic  $[\text{Pd}(\text{bpm})_2]$  (by interfacial diffusion method). The structure of both obtained compounds was studied by X-ray crystallography. In the case of the copper complex, this was the only available method to determine its geometry, because its paramagnetism excludes NMR analysis. X-ray analysis showed that both complexes in the solid state adopt a square planar trans geometry.



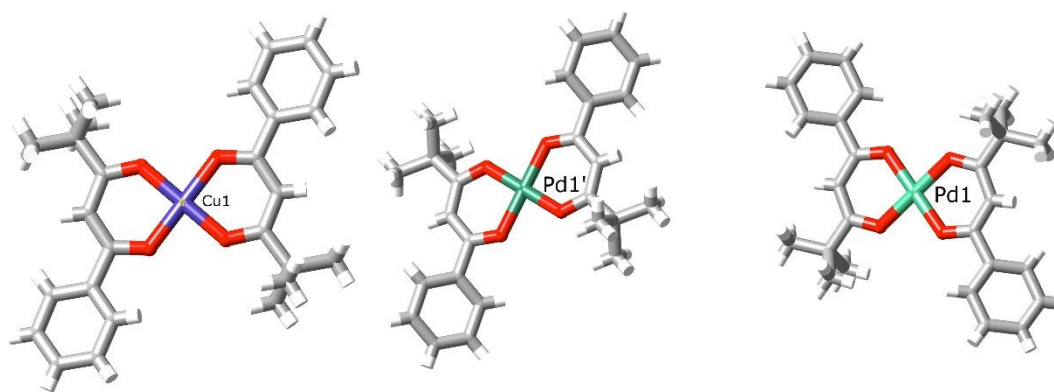


**Figure 21.** Views of (left) the unique molecular unit present in the lattice of  $[\text{Cu}(\text{bpm})_2]$  and (right) the two inequivalent but very similar molecular units present in the lattice of  $[\text{Pd}(\text{bpm})_2]$ .

In this part of the research conducted as part of the doctoral thesis, the focus was on examining the preferences of the ligand in terms of the formation of a specific complex and its isomer. It was proven that simple complexes in solution do not show a strong preference for the formation of one specific isomer, although it is possible to isolate individual isomers in crystalline form. Analysis of the two structures studied showed that the intermolecular interactions for each of them are completely different. This proves that the metal ion has a decisive and unique effect on the external properties of the entire complex. This stage of research was a preparation for the next phase, containing more complex structures that could ultimately be used to synthesize complexes with a cage structure or polymeric ones, which, using an appropriate metal ion, such as palladium(II) ion, could exhibit catalytic properties.

**A full description of the above project is presented in paper A1 and in Supplementary Information A1 which are part of this dissertation.**

Michał Kołodziejski, Anna Walczak, Zbigniew Hnatejko, Jack Harrowfield, Artur R. Stefankiewicz\*, *Unsymmetrical bidentate ligands as a basis for construction of ambidentate ligands for functional materials: Properties of 4,4-dimethyl-1-phenylpentane-1,3-dionate*, Polyhedron, **2017**, Volume 137, 270-277.

The project was carried out in cooperation with prof. Jack Harrowfield from the Institut de Science et d'Ingénierie Supramoléculaires, Université de Strasbourg (France)

## Charge-neutral metallocycles – self-assembly, aggregation and catalysis

The key role in this self-assembly process is played by the design of ligands, the structure of which programs the way components connect. The research described in this doctoral thesis was an introduction to work with more complex structures. The next stage focused on ligands containing multiple  $\beta$ -diketone groups. Their reactions with metal ions allow for the predictable formation of complex systems, such as helicates, tetrahedra, or porous structures.

In the next stage of the doctoral thesis, research was carried out on the tritopic  $\beta$ -diketone ligand ( $H_3L$ ) and its interactions with copper(II) and palladium(II) ions. The main goal was to investigate whether it is possible to obtain  $[M_2(HL)_2]$  type metallocycles under controlled conditions, having free, unreacted  $\beta$ -diketone groups in the side chains. These groups are the starting points for further, controlled oligomerization towards polymeric structures. This arrangement allows for direct comparison of properties, for example catalytic activity, between discrete cycles and their oligomeric counterparts in key palladium(II)-catalyzed cross-coupling reactions. These studies also contribute to the search for new Pd(II)  $\beta$ -diketone complexes with potential anticancer and antibacterial activity.

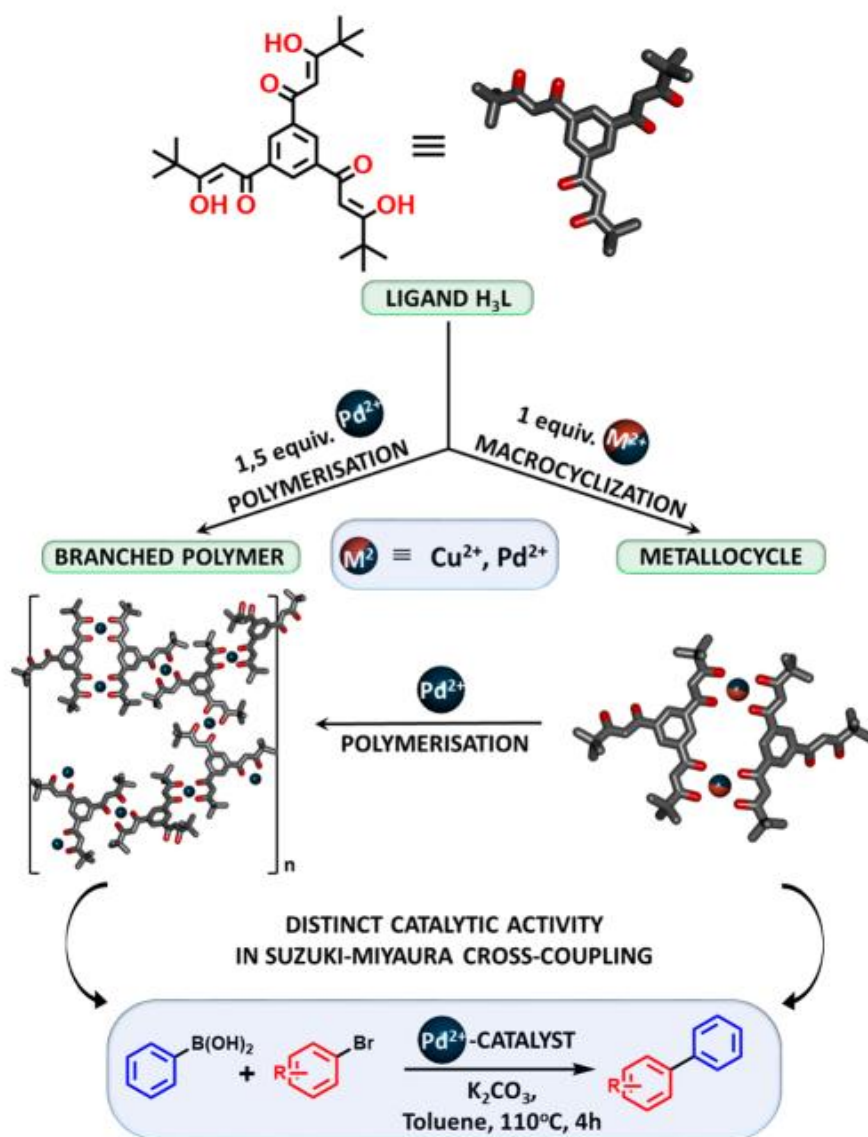


**Figure 22.** Metal-ion induced conversion between tripodal ligand  $H_3L$  and structurally different metallosupramolecular assemblies.

## Synthesis of $H_3L$ and its complexes

The tritopic ligand  $H_3L$  was prepared *via* a Claisen condensation between triethyl benzene-1,3,5-tricarboxylate and pinacolone in the presence of sodium hydride by adapting previously reported procedure. Pinacolone was added to a suspension of NaH in dry THF. After 30 min of stirring, triethyl benzene-1,3,5-tricarboxylate was added to the gray-yellow suspension. The mixture was heated at 47 °C for 24 h. The reaction was then quenched using water and the mixture acidified to pH ~ 4 using HCl. After extraction with  $CHCl_3/H_2O$ , the

organic layer was dried over  $\text{Na}_2\text{SO}_4$  and evaporated to dryness. The crude product was isolated with a good 74% yield as a white solid by recrystallization from ethanol, filtering, washing with EtOH and drying.

The synthesis of  $\text{H}_3\text{L}$  ligand complexes with transition metal ions was carried out by adapting previously used, yet optimized procedures, which were described in detail in paper A2, which is an integral part of this doctoral dissertation. All obtained and isolated compounds were characterized by available spectroscopic methods.

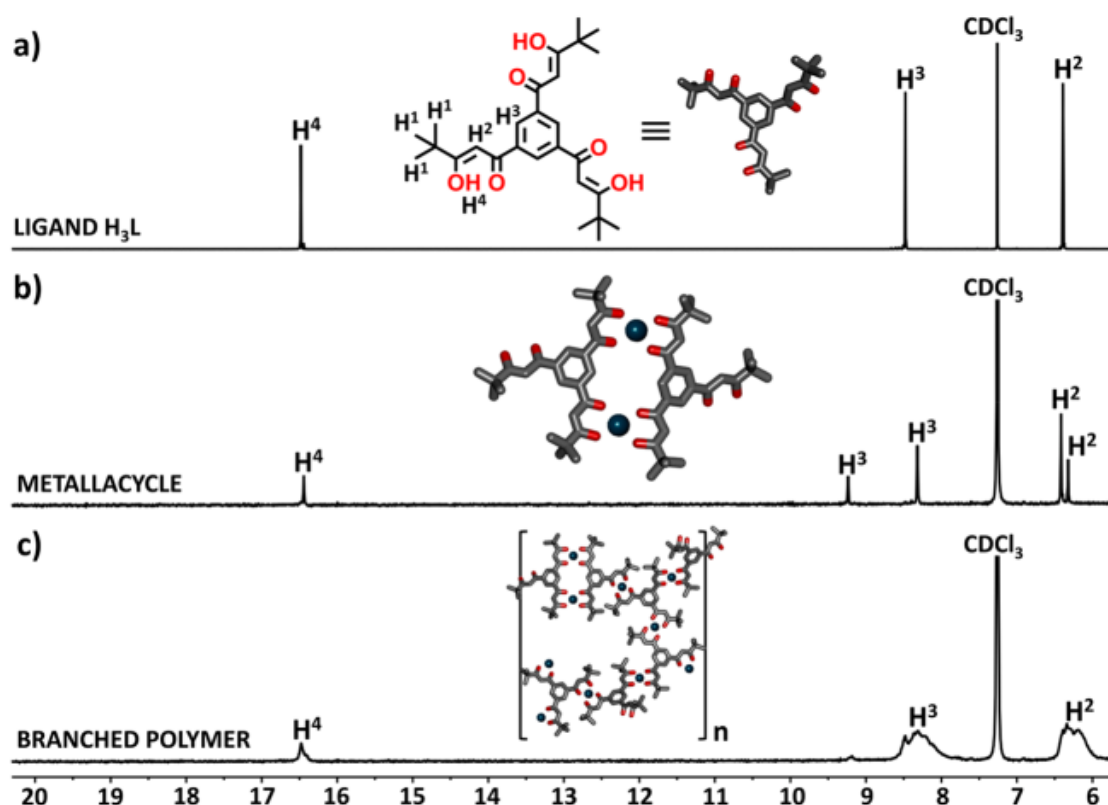


**Figure 23.** Comparison of  $^1\text{H}$  NMR spectra of ligand  $\text{H}_3\text{L}$  (a), metallosupramolecular macrocycle  $[\text{Pd}_2(\text{HL})_2]$  (b), and branched polymer  $[\text{Pd}_3\text{L}_2]_n$  (c) recorded in  $\text{CDCl}_3$  at room temperature. Aliphatic region omitted for clarity.

## Results and characterization

As part of the research, a tritopic ligand ( $\text{H}_3\text{L}$ ) was prepared, which, as confirmed by NMR and X-ray structural methods, occurs mainly in a stable enol form due to internal hydrogen bonds. In the first stage, in the reaction with copper(II) and palladium(II) ions in a 1:1 ratio, dimeric metallocycles of the general formula  $[\text{M}_2(\text{HL})_2]$  were successfully synthesized, in which two arms of the ligand coordinate to metal ions, and the third one remains free. The crystal structure of the copper complex  $[\text{Cu}_2(\text{HL})_2(\text{THF})_2]$  was unequivocally

confirmed by X-ray. In turn, the formation of the palladium dimer was confirmed by NMR, mass spectrometry (MS) and diffusion NMR spectroscopy (DOSY), which showed that this complex is twice as large in solution as a single ligand. Then, an attempt was made to synthesize the polymers by changing the stoichiometry of the reagents (1.5 metal ions per 1 ligand). The reaction with copper(II) led mainly to the formation of an insoluble, difficult to analyze product. In contrast, the analogous reaction with palladium(II) was successful, giving a soluble oligomeric product of the formula  $[\text{Pd}_3\text{L}_2]_n$ . Its formation was proven by: Broadened signals in the NMR spectrum, characteristic of large structures, and data from DOSY analysis, which indicated that the resulting oligomer is about 5 times larger than the free ligand and 3 times larger than the dimeric form. These studies demonstrate that by controlling the reaction conditions and the choice of the metal ion, it is possible to selectively form both simple cycles and more complex soluble polymeric structures based on the same ligand.

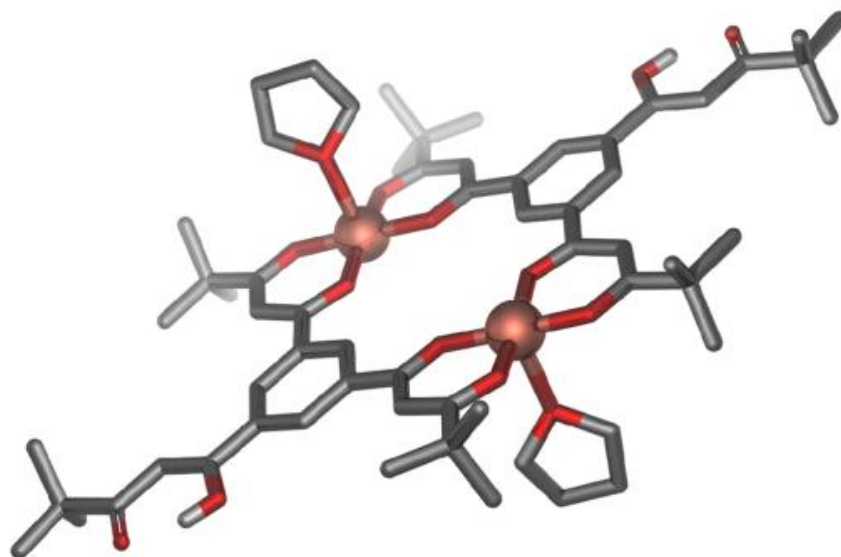


**Figure 24.** X-ray crystal structure of  $[\text{Cu}_2(\text{HL})_2(\text{THF})_2]$ . H atoms (except enol H) have been omitted for clarity.

## Catalytic properties in Suzuki-Miyaura Cross-coupling reaction

Due to differences in structure, the catalytic activity of two previously synthesized palladium(II) complexes was investigated and compared: the dimeric metallocycle  $[\text{Pd}_2(\text{HL})_2]$  and the polymer  $[\text{Pd}_3\text{L}_2]_n$ . Suzuki-Miyaura cross-coupling was chosen as the test reaction. First, the reaction conditions were optimized using the dimer  $[\text{Pd}_2(\text{HL})_2]$  as a catalyst, obtaining

almost 100% product conversion within 4 h under optimal conditions (toluene, 110 °C, K<sub>2</sub>CO<sub>3</sub>). Then, a series of reactions with different substrates was carried out, using both catalysts for direct comparison. The key finding of the study is that the polymer [Pd<sub>3</sub>L<sub>2</sub>]<sub>n</sub> showed significantly higher catalytic activity. The reaction yields using it were very high in most cases (>80%) and on average 10-20% higher than in the case of the dimer. The high polymer efficiency was independent of whether the substrates contained electron-donating or electron-withdrawing groups. Both new catalysts showed activity comparable to the standard catalyst [PdCl<sub>2</sub>(PPh<sub>3</sub>)<sub>2</sub>], which confirms their high potential. The higher polymer efficiency is due to several factors. The polymer molecule contains more palladium ions than the dimer molecule, which means a larger number of catalytic centers. In addition, ICP-MS analysis confirmed a higher mass content of palladium in the polymer (23.6%) compared to the dimer (18.7%). Additionally, it is believed that the accumulation of many active centers in one polymer molecule creates a high local concentration of the catalyst, which significantly increases the reaction efficiency.

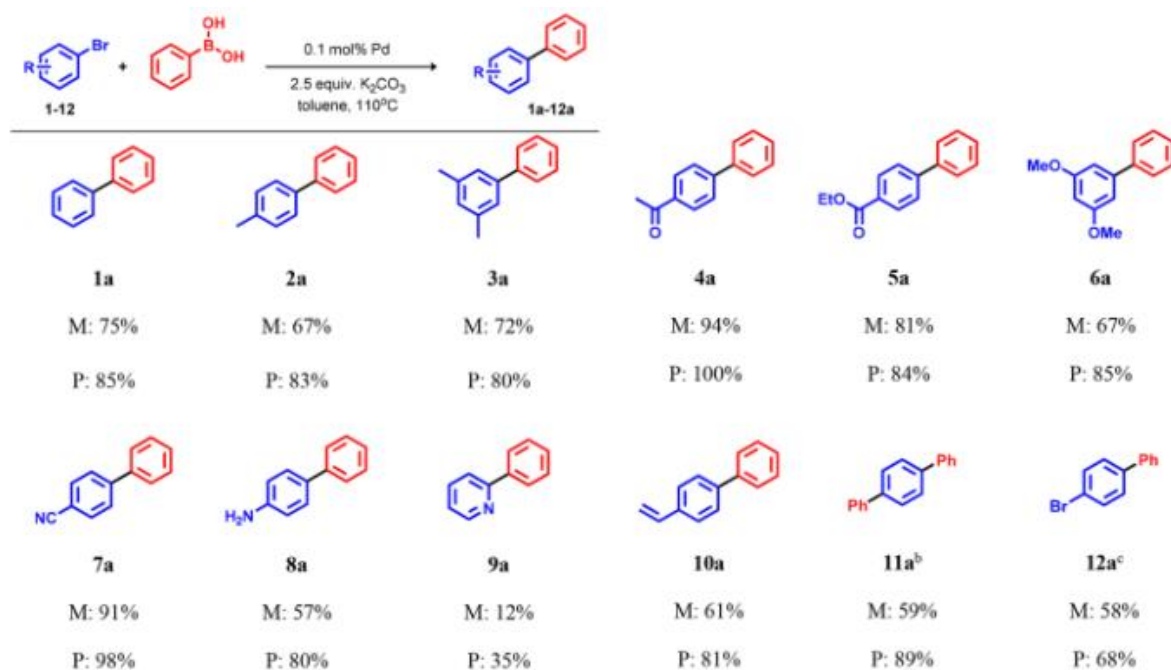


**Figure 25.** Scope of the Suzuki-Miyaura Cross-Coupling Reaction between Aryl Bromides and Phenylboronic Acid

In this part, the synthesis and characterization of a trifunctional  $\beta$ -diketone ligand and its di- and polynuclear complexes with copper(II) and palladium(II) ions are studied and described. The key finding is that a small change in the stoichiometry of the same reactants leads to the formation of completely different materials - from a discrete macrocycle to an

amorphous metal-supramolecular polymer. It was shown that dinuclear macrocycles possess free functional groups, which, upon addition of another portion of metal ions, cause a "structural switch", leading to the formation of complex polymeric systems. The obtained complexes differ not only in structure, but also in catalytic activity in the Suzuki-Miyaura coupling reaction. Importantly, these catalysts are efficient under mild conditions, without requiring the exclusion of water or air from the reaction. The research conducted in this part and its results will be used to more effectively design tritopic ligands for the synthesis of complex, three-dimensional supramolecular structures, e.g. cages.

**A full description of the above project is presented in paper A2 and in Supplementary Information A2 which are part of this dissertation.**

Michał Kołodziejski, Aidan J. Brock, Gracjan Kurpik, Anna Walczak, Feng Li, Jack K. Clegg\*, Artur R. Stefankiewicz\*, *Charge Neutral [Cu<sub>2</sub>L<sub>2</sub>] and [Pd<sub>2</sub>L<sub>2</sub>] Metallocycles: Self-Assembly, Aggregation, and Catalysis*, Inorganic Chemistry, **2021**, 60, 9673-9679.

The project was carried out in cooperation with research group of prof. Jack K. Clegg from the University of Queensland, Australia

## Chapter 3: Dynamic Combinatorial Chemistry – Self-sorting with component selection

The second topic, which is an integral part of this doctoral thesis, is dynamic combinatorial chemistry and the phenomenon of self-sorting of components in the synthesis of dynamic imine cages. This stage of work was initiated during the first internship in the group of Professor Jean-Marie Lehn at the research institute in Strasbourg, and then continued after returning to the parent unit and during the next internship there.

Macrocyclic cage compounds, called cryptands, have long been a fascinating area of supramolecular chemistry due to their unique properties and potential applications in nanotechnology. Their synthesis has traditionally been a complex, multi-step process that is difficult to control. The emergence of Dynamic Covalent Chemistry (DCC) has opened up completely new perspectives, revolutionizing the way we think about the creation of these advanced structures. This strategy is based on the use of reversible covalent reactions, in particular the formation of imine ( $C=N$ ) bonds, which allows for the spontaneous and efficient formation of complex architectures through the process of self-assembly. Due to the reversibility of the bonds, the system automatically tends to achieve the most thermodynamically stable product, effectively "correcting" errors and simplifying the synthesis. Moreover, this approach enables intelligent self-sorting, in which the appropriate "building blocks" are spontaneously selected from a mixture of many different components to build one specific structure. As a result, we obtain not static but adaptive nanostructures, the structure of which can be modified by external stimuli such as changes in pH, temperature or light. This chapter is devoted to the analysis of this powerful tool, which simplifies synthesis and allows the design of advanced materials with great potential in catalysis, sensorics and drug transport.

In this part of the study, the focus was on the influence of structural features of molecular components on the self-sorting phenomenon in the formation of different components of macrobicyclic imine-based cryptand cages. Furthermore, acid-catalyzed exchange processes of components between different cages were investigated. As a preliminary step, different structurally distinct dialdehydes (A–H) were reacted with the triamine "tren" (tris(2-aminoethyl)amine; T) to obtain hexamine cages, thus extending the initial work on such processes. Following the dynamic covalent chemistry approach, dynamic libraries consisting of dialdehyde and triamine components were created to analyze the self-sorting behavior between the aldehydes used. In order to be able to evaluate the influence of structural features



of the components, this part of the study was performed under purely organic conditions, in the absence of metal ions.

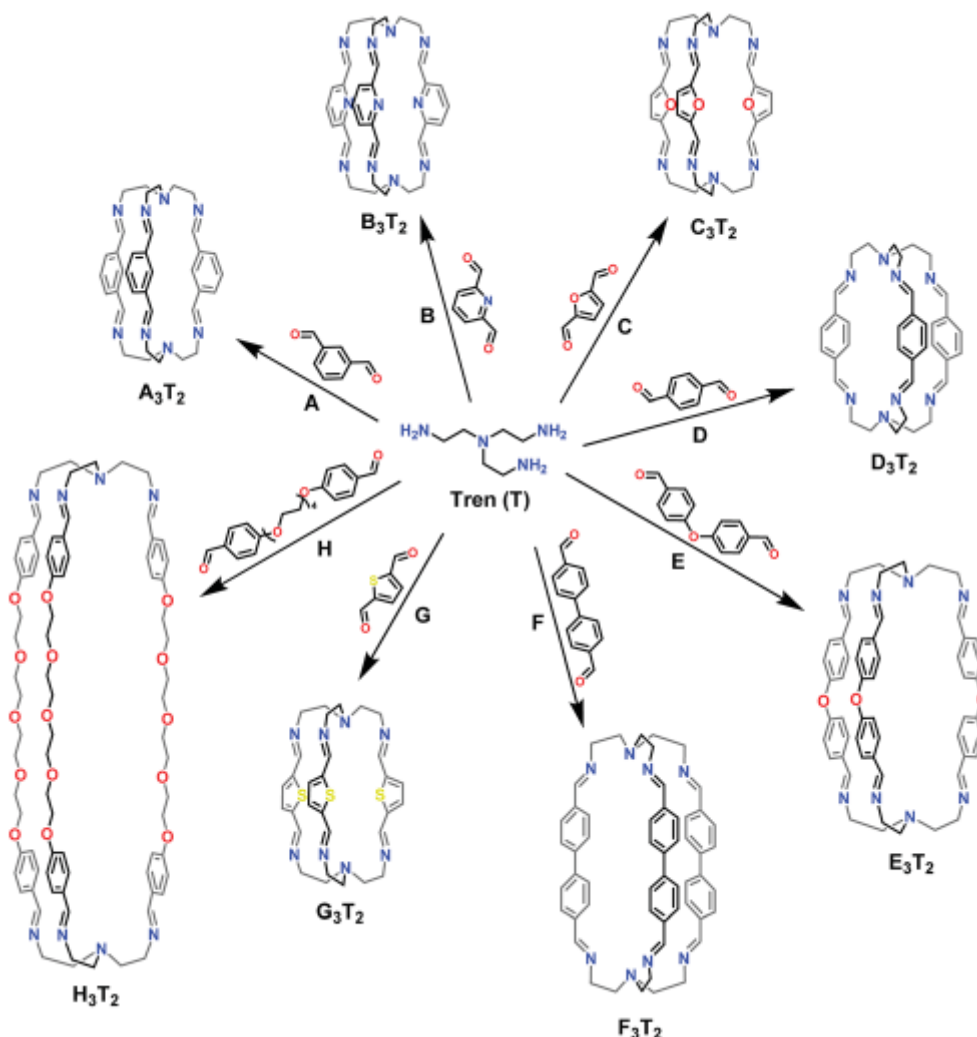


**Figure 26.** Molecular structures of dialdehydes (A–H), the triamine (T) and the generated [3 + 2] homoleptic imine-based organic macrobicyclic cryptand cages.

## Synthesis and characterization

In the course of the studies, a series of reactions of one triamine (T) with eight different aromatic dialdehydes (A–H) were carried out at room temperature. In each case, mixing the reagents led to precipitation in the case of acetonitrile as the solvent, and further analyses confirmed that the desired three-dimensional cage structures with a stoichiometry of 3:2 (dialdehyde to triamine), designated  $X_3T_2$ , were obtained. The identity and high symmetry ( $D_3$ )

of the newly formed compounds were comprehensively confirmed by elemental analysis,  $^1\text{H}$  NMR spectroscopy and mass spectrometry. Key information on the spatial structure was obtained from X-ray structural analysis, which allowed for the detailed characterization of two new cages,  $\text{E}_3\text{T}_2$  and  $\text{F}_3\text{T}_2$ . Both were found to be elongated, chiral capsules of about 15 Å in length. An important conclusion from the analysis of their structures is the fact that they do not enclose solvent molecules inside their interior, which suggests that their interactions with the environment occur mainly on the external surface and not through the inclusion of guests inside the capsule.

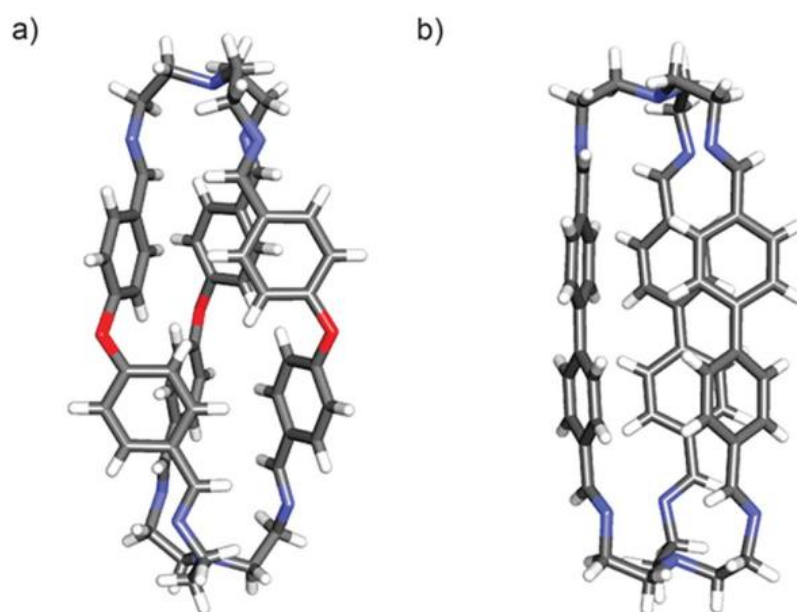


**Figure 27.** Solid state X-ray molecular structures of the cages  $\text{E}_3\text{T}_2$  (left) and  $\text{F}_3\text{T}_2$  (right).

Colour code: red, O; blue, N; grey, C; white, H.

## Self-sorting experiments

In the next stage of the research, after the successful synthesis of single cages, the process of their formation was studied under competitive conditions to observe the phenomenon of self-sorting. For this purpose, triamine (T) was mixed with pairs of different dialdehydes (from the subset A–E and H) under strictly controlled conditions, allowing for reaching the equilibrium state. The composition of the final products was monitored using  $^1\text{H}$  NMR spectroscopy. The results showed an extremely high degree of sorting: in as many as 13 out of 15 systems studied, the presence of only one type of pure (homoleptic) cage was detected at equilibrium. This means that the system selectively chose one, preferred dialdehyde to build the final structure, ignoring the other. Only in two cases (for pairs B/C and D/E) were two types

of pure cages present in the mixture. Most importantly, in none of the experiments was the formation of mixed (heteroleptic) cages, i.e. cages built of different types of dialdehydes, observed.

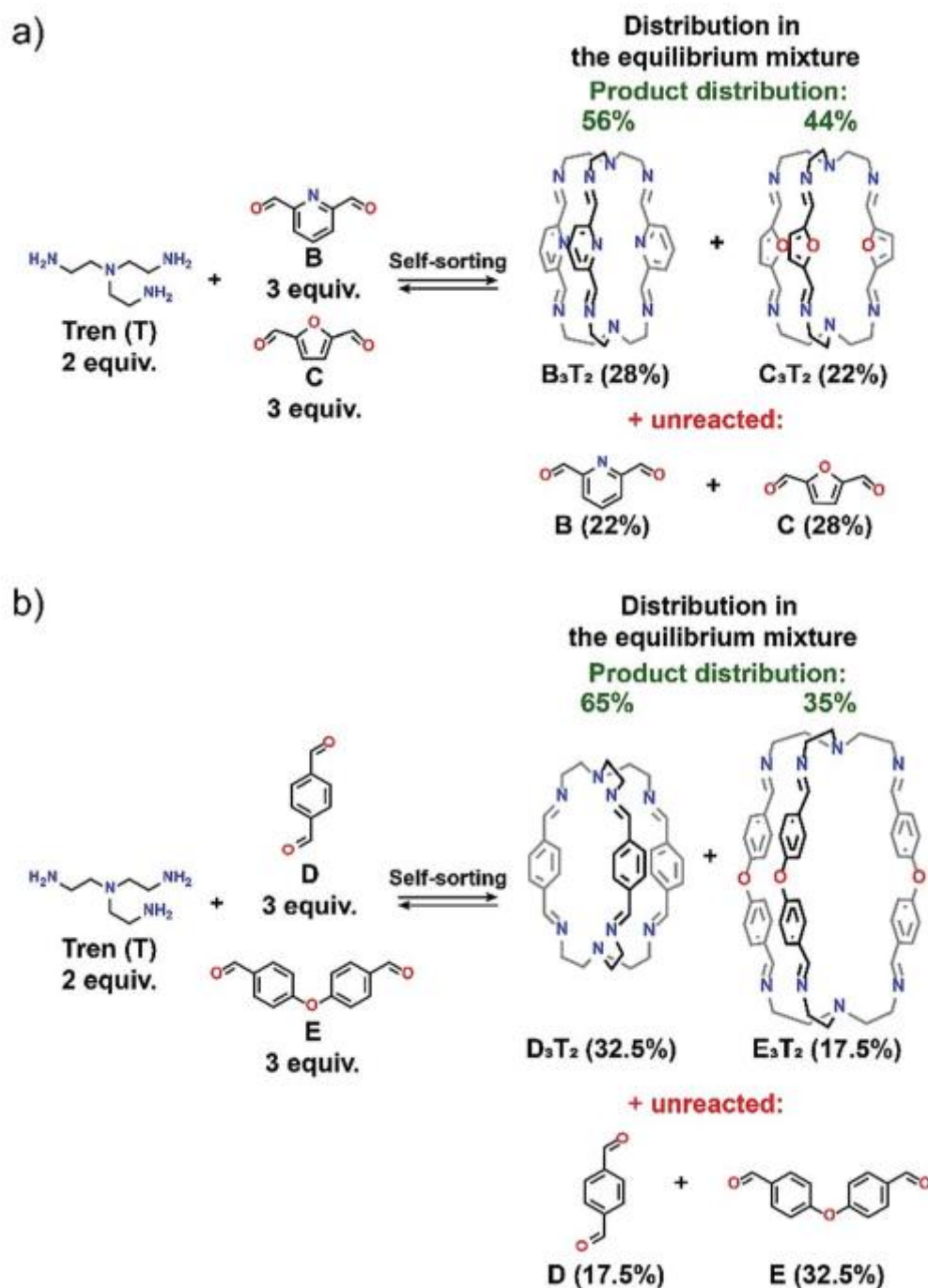


**Figure 28.** General schemes presenting product distribution of an equilibrium mixture for libraries consisting of (a)  $3B + 3C + 2T$  and (b)  $3D + 3E + 2T$ .

The self-sorting process was analyzed in detail with respect to even the smallest structural differences in the structure of the components. In the first experiment, it was investigated how the presence of a heteroatom (nitrogen) affects the self-sorting process. For this purpose, a competitive reaction was carried out between two dialdehydes – A (containing only carbon in the ring) and B (containing nitrogen in the ring) – and triamine T. The result clearly showed that the system selectively chose the dialdehyde with the heteroatom. The  $B_3T_2$  cage, containing nitrogen, was formed with 92% efficiency, while the  $A_3T_2$  cage was not formed at all, and dialdehyde A remained unbound in the mixture. This preference is due to additional, stabilizing intra- and intermolecular interactions, which are only possible in the case of the  $B_3T_2$  cage, making it a favored product both kinetically and thermodynamically.

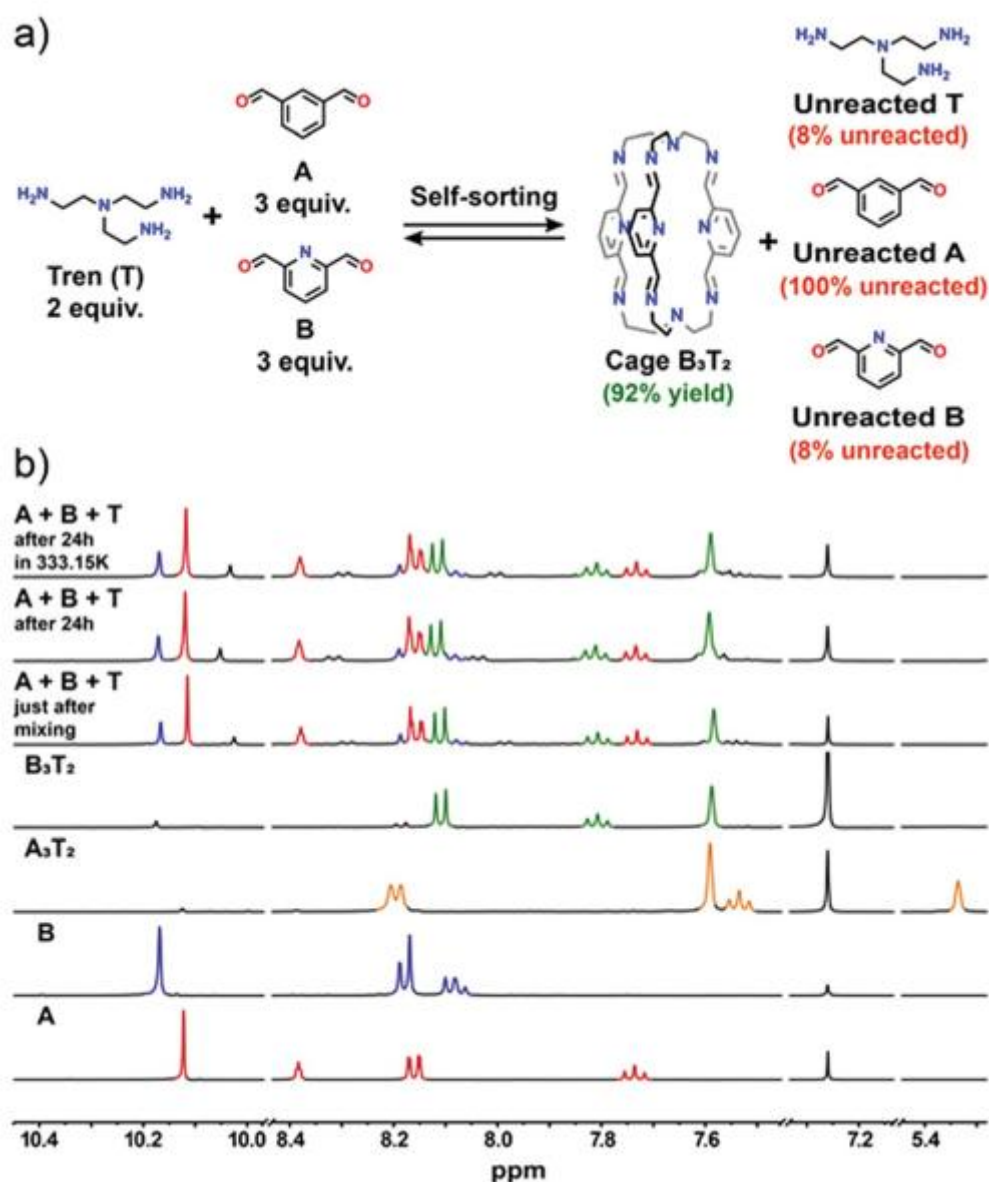


**Figure 29.** General scheme of the self-sorting experiment between components  $A + B + T$  (a); (b) comparison of the  $^1\text{H}$  NMR spectra of all three components recorded over time. The  $^1\text{H}$  NMR spectra of reaction components and isolated cages are also shown for comparison. Low intensity signals observed in the spectra after component mixing may come from trace amounts of intermediate products such as open chain structures. All NMR spectra were recorded in  $\text{CDCl}_3$  at 400 MHz.

Another factor studied was the influence of the flexibility of one of the components on the self-sorting process. A competitive reaction was carried out between the rigid heteroaromatic dialdehyde B and the very flexible dialdehyde H with triamine T. The result was unambiguous: the system selectively chose the rigid component, forming the  $\text{B}_3\text{T}_2$  cage with almost quantitative yield, while the flexible dialdehyde H remained completely in solution. The main reason for this selectivity is the high flexibility of dialdehyde H, which constitutes an entropic barrier, hindering its organization into an ordered cage structure. Additionally, the rigid structure of dialdehyde B favors intramolecular interactions, which preorganize the molecule in a way that favors cyclization (cage formation) instead of polymerization.

In two cases, in contrast to the other experiments, the self-sorting process led to the formation of a mixture of two different cages in solution. In the first case, in the system containing dialdehydes B and C and triamine T, a mixture of cages  $\text{B}_3\text{T}_2$  and  $\text{C}_3\text{T}_2$  was formed in almost equal amounts (in the ratio of 28% to 22%) at equilibrium. Such a similar efficiency results from the fact that both dialdehydes (B and C) are very similar structurally, which means that neither of the resulting cages is significantly favored. In the second case, in the system with dialdehydes D and E, a mixture of two cages was also formed, but this time one of them was clearly favored. The  $\text{D}_3\text{T}_2$  cage was formed in a much larger amount than  $\text{E}_3\text{T}_2$ , and their ratio at equilibrium was 65:35. This selectivity is explained by the difference in the structure of dialdehydes: D is rigid and fully conjugated, while E contains an oxygen atom that breaks the conjugation and gives the molecule greater flexibility, making the resulting cage less stable.

In a key experiment, the self-sorting process was investigated in a complex mixture containing six different dialdehydes (A–E and H) and one triamine (T) simultaneously to see whether the previously established preference hierarchy would be preserved. Triamine was gradually added to the dialdehyde mixture and the progress of the reaction was monitored by NMR. Observations confirmed that the process proceeded in a clear sequence: first, the most favored cages were  $\text{B}_3\text{T}_2$  and  $\text{C}_3\text{T}_2$ , then almost simultaneously  $\text{A}_3\text{T}_2$  and  $\text{D}_3\text{T}_2$ , and finally, as expected,  $\text{E}_3\text{T}_2$  and finally  $\text{H}_3\text{T}_2$ . This experiment allowed us to establish a modified hierarchy

of cage formation efficiency:  $B = C > A = D > E > H$ . Analysis of the results confirmed that selectivity is determined by key features of molecular structure: the most effective are rigid dialdehydes with a heteroatom and full conjugation (B, C), less effective are rigid and conjugated ones but without a heteroatom (A, D), and the least effective are flexible compounds and/or compounds with interrupted conjugation (E, H).

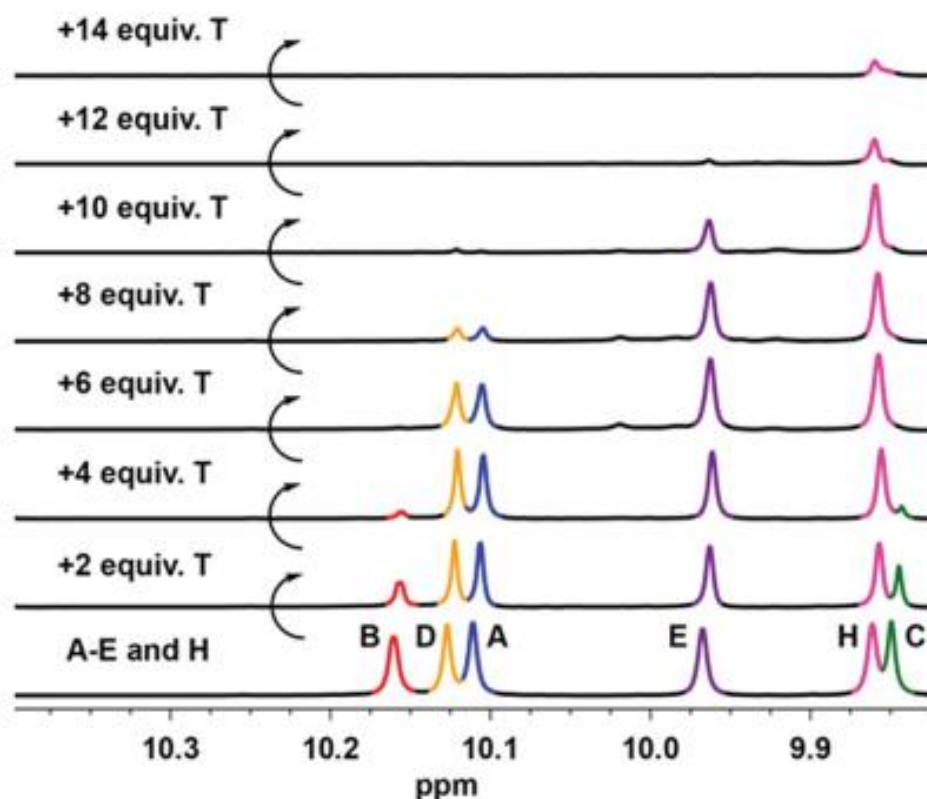


**Figure 30.** Changes in aldehyde proton signals of the  $^1\text{H}$  NMR spectra (400 MHz,  $\text{CDCl}_3$ ) during the self-sorting experiment involving titration of  $3\text{A} + 3\text{B} + 3\text{C} + 3\text{D} + 3\text{E} + 3\text{H}$  with appropriate increasing amounts of T.

In order to investigate in more detail the influence of the size of the conjugated system and flexibility on the sorting process, another experiment was conducted, in which three selected dialdehydes: D, E and F took part in a competitive reaction. NMR analysis clearly showed that dialdehyde D, as the only one forming a fully conjugated and rigid system, reacted the fastest, confirming its privileged position. Dialdehydes E (with a flexible oxygen bridge breaking the conjugation) and F (with a larger but twisted biphenyl system that limits delocalization) reacted slower and at a similar rate. These results confirm that the rigidity and the possibility of full delocalization of electrons in the molecule are key factors favoring a given component in the cage formation process. Importantly, despite the similarity of dialdehydes E and F, once again no mixed (heteroleptic) cages were observed to form.

Also in order to investigate the influence of the heteroatom type on the sorting process, a competitive reaction was carried out in a similar way between three dialdehydes containing different heteroatoms: B (with nitrogen), C (with oxygen) and G (with sulfur) and triamine T. NMR analysis showed a clear sequence of product formation. First, almost simultaneously, B<sub>3</sub>T<sub>2</sub> and C<sub>3</sub>T<sub>2</sub> cages were formed, and only after their complete formation did the G<sub>3</sub>T<sub>2</sub> cage begin to form. The final mixture contained three types of pure cages, without a trace of the formation of mixed structures. This experiment allowed us to establish a hierarchy of preferences in the formation of cages: B > C > G. This order is consistent with the strength of interactions that individual heteroatoms can form. The ability to form hydrogen bonds and electronegativity decrease in the N > O > S series, which directly translates into the stability of the resulting cage and determines the selectivity of the entire process.

## Cage-to-cage transformation

To confirm that the observed sorting processes lead to a true thermodynamic equilibrium, experiments were performed using acid-base control of cage formation and disintegration. In the first test, the less stable A<sub>3</sub>T<sub>2</sub> cage was first disassembled into its components by strong acid and then reconstituted by adding base. When the more favored dialdehyde B was added to this system and the acid-base cycle was re-applied, the system spontaneously reorganized to form only the more stable B<sub>3</sub>T<sub>2</sub> cage. This proves that B<sub>3</sub>T<sub>2</sub> is a true thermodynamic product and demonstrates the possibility of a cage-in-cage transformation. In the second experiment, dialdehyde B was added to the A<sub>3</sub>T<sub>2</sub> cage in the presence of a catalytic amount of acid. A slow but complete transformation was observed, resulting in the formation of only the B<sub>3</sub>T<sub>2</sub> cage, which occurred by direct exchange of components rather than complete disintegration of the structure. Both experiments clearly confirm that the observed cage formation preferences result from the system achieving the most favorable equilibrium state.



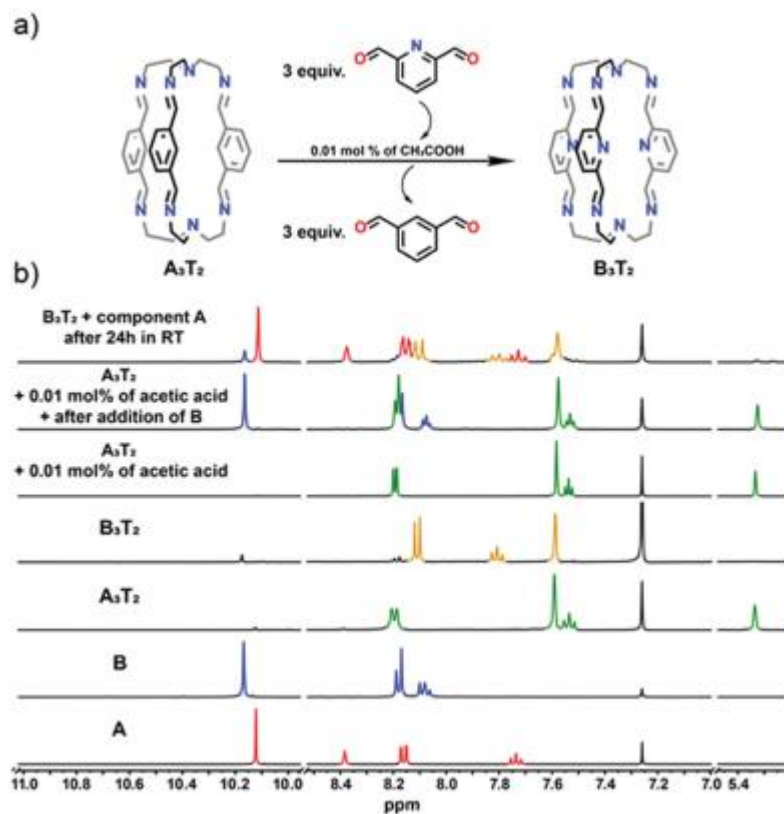


**Figure 31.** General scheme of the exchange experiment ( $A_3T_2 + B / B_3T_2 + A$ ) between components  $A + B + T$  (a); (b)  $^1H$  NMR spectra of acid catalyzed exchange experiment between cage  $A_3T_2$  and component  $B$ . For comparison  $^1H$  NMR spectra of components  $A$  and  $B$  as well as isolated cages  $A_3T_2$  and  $B_3T_2$  are also shown. All NMR spectra were recorded at room temperature in  $CDCl_3$ .

The experiments carried out clearly demonstrate an extremely selective self-sorting process during the formation of organic cages (cryptands) based on imine bonds when triamine reacts with a mixture of different dialdehydes. The final outcome of this process is determined by the molecular structure of the components, which indicates that by properly designing the ligands that will be components of the component library, we can have an indirect effect on the final effect of the process. In the case of the systems studied, the key factors favoring a given component are the presence of a heteroatom in a rigid, aromatic system, which allows for stabilizing hydrogen bonds, favorable electrostatic effects and the formation of a fully conjugated system. In turn, the flexibility of the molecule and any disorders in the conjugated system significantly reduce its efficiency in the sorting process. The studies also showed that although it is possible to "kinetic confine" a less stable structure, the dynamic nature of imine bonds allows for its rearrangement. In the presence of an agent (e.g. acid) that reversibly breaks



these bonds, the system can achieve a state of true equilibrium, leading to the formation of the thermodynamically most stable product.

**A full description of the above project is presented in paper A3 and in Supplementary Information A3 which are part of this dissertation.**

Michał Kołodziejski, Artur R. Stefankiewicz\*, Jean-Marie Lehn\*, *Dynamic polyimine macrobicyclic cryptands – self-sorting with component selection*, Chemical Science, **2019**, 10, 1836-1843.

The project was carried out in cooperation with prof. Jean-Marie Lehn from the Institut de Science et d'Ingénierie Supramoléculaires, Université de Strasbourg (France)

# Conclusion

The presented doctoral thesis focuses on two key yet distinct areas of supramolecular chemistry: on the one hand, the design and synthesis of functional metallosupramolecular materials with catalytic potential, and on the other, the study of fundamental principles of self-assembly and self-sorting in dynamic covalent chemistry.

The first pillar of the research involved work on metal complexes with  $\beta$ -diketone ligands. The starting point was a detailed analysis of the coordination chemistry of a simple, unsymmetrical ligand (bpmH) to understand and overcome potential challenges that could complicate the design of more complex systems, such as oligomerization and isomerism. The studies showed that this ligand does not fully prevent oligomerization, as demonstrated by the nickel(II) complex. It was also found that the formation of isomers in aluminum(III) and cobalt(III) complexes is mainly statistical, indicating weak intramolecular interactions. In the case of the zinc(II) complex, temperature-dependent dynamic equilibrium between five- and six-coordinated forms was observed. These fundamental studies provided the basis for work with more advanced structures.

In the next stage, the focus shifted to a tritopic ligand ( $H_3L$ ) designed to form complex architectures. A key achievement was the development of a two-step synthesis strategy. In the first step, through careful control of stoichiometry, discrete dimeric metallocycles of the type  $[M_2(HL)_2]$  (with Cu(II) and Pd(II) ions) were successfully obtained, each featuring a free, reactive functional arm. Their structures were confirmed by comprehensive methods, including X-ray crystallography and diffusion NMR spectroscopy (DOSY), which quantitatively showed that the dimer is approximately twice the size of the single ligand. In the second step, altering the molar ratio of the reactants enabled the use of the free arms for further polymerization. While the reaction with copper(II) led to the formation of an insoluble product, the reaction with palladium(II) was successful, yielding a fully characterized, soluble metallosupramolecular polymer  $[Pd_3L_2]_n$ . DOSY analysis confirmed its significantly larger size — about five times larger than the ligand and three times larger than the dimer. The most important result of this part of the study was the comparison of the catalytic activity of both palladium complexes in the Suzuki-Miyaura coupling reaction. The  $[Pd_3L_2]_n$  polymer proved to be a significantly more efficient catalyst, providing yields on average 10–20% higher than its discrete, cyclic counterpart. The higher activity was attributed to the larger number of

catalytic centers and the so-called "local concentration effect" resulting from the accumulation of many active sites within a single macromolecule.

The second, parallel pillar of the thesis explored Dynamic Covalent Chemistry (DCC) and the self-sorting phenomenon in metal-free organic systems. The aim was to understand the fundamental principles governing the self-assembly process in complex, multicomponent mixtures. The research focused on the synthesis of organic cages (cryptands) based on reversible imine bonds. An extremely high degree of selectivity was demonstrated. In competitive experiments, where one triamine reacted with a mixture of different dialdehydes, the system formed only one pure (homoleptic) cage product in the vast majority of cases (13 out of 15). Crucially, in none of the experiments was the formation of mixed (heteroleptic) cages observed. This enabled the establishment of a clear hierarchy of preferences, whereby the outcome of sorting is determined by the structural features of the building blocks: the most favored are rigid, fully conjugated components containing a heteroatom (e.g., nitrogen), while flexibility and disruptions in conjugation significantly reduce a component's efficiency. It was also confirmed that the observed preferences result from the system reaching a true thermodynamic equilibrium. Using acid-base control over the reversibility of imine bonds, the possibility of a "cage-in-cage" transformation was demonstrated, in which a less stable structure, in the presence of more favored components, spontaneously reorganizes into the thermodynamically most stable product.

In summary, the presented studies comprehensively combine materials chemistry with fundamental research on self-assembly. This work not only provided new functional materials with enhanced catalytic activity but also led to a thorough understanding and formulation of the principles governing the self-sorting of components within dynamic systems, ultimately enabling the formation of three-dimensional cage structures based on imine bonds.

## References

1. J.-M. Lehn, *Chem. Soc. Rev.*, 2007, **36**, 151-160.
2. J.-M. Lehn, *Angew. Chem. Int. Ed. Engl.*, 1990, **29**, 1304-1319.
3. J.-M. Lehn, *Supramolecular Chemistry: Concepts and Perspectives*, VCH, Weinheim, 1995.
4. C. A. Schalley, A. Lützen and M. Albrecht, *Chem. - Eur. J.*, 2004, **10**, 1072-1080.
5. C. J. Pedersen, *Angew. Chem. Int. Ed. Engl.*, 1988, **27**, 1021-1027.
6. E. P. Kyba, R. C. Helgeson, K. Madan, G. W. Gokel, T. L. Tarnowski, S. S. Moore and D. J. Cram, *J. Am. Chem. Soc.*, 1977, **99**, 2564-2571.
7. D. A. Uhlenheuer, K. Petkau and L. Brunsveld, *Chem. Soc. Rev.*, 2010, **39**, 2817-2826.
8. A. Brzechwa-Chodzyńska, W. Drożdż, J. Harrowfield and A. R. Stefankiewicz, *Coord. Chem. Rev.*, 2021, **434**, 213820.
9. A. Walczak, H. Stachowiak, G. Kurpiak, J. Kaźmierczak, G. Hreczycho and A. R. Stefankiewicz, *J. Catal.*, 2019, **373**, 139-146.
10. W. Drożdż, A. Walczak, Y. Bessin, V. Gervais, X.-Y. Cao, J.-M. Lehn, S. Ulrich and A. R. Stefankiewicz, *Chem. - Eur. J.*, 2018, **24**, 10802-10811.
11. A. J. Brock, H. Al-Fayaad, M. C. Pfrunder and J. K. Clegg, in *Functional Supramolecular Materials: From Surfaces to MOFs*, The Royal Society of Chemistry, 2017, pp. 325-387.
12. Y. Ke, L. L. Ong, W. M. Shih and P. Yin, *Science*, 2012, **338**, 1177-1183.
13. S. A. Nepogodiev and J. F. Stoddart, *Chem. Rev.*, 1998, **98**, 1959-1976.
14. M.-J. Blanco, M. Consuelo Jimenez, J.-C. Chambron, V. Heitz, M. Linke and J.-P. Sauvage, *Chem. Soc. Rev.*, 1999, **28**, 293-305.
15. J. Rebek, *Angew. Chem. Int. Ed. Engl.*, 1990, **29**, 245-255.
16. J.-M. Lehn, *Science*, 2002, **295**, 2400-2403.
17. M. Mammen, S.-K. Choi and G. M. Whitesides, *Angew. Chem., Int. Ed.*, 1998, **37**, 2754-2794.
18. D. Ajami, L. Liu and J. Rebek Jr, *Chem. Soc. Rev.*, 2015, **44**, 490-499.
19. Y.-Y. Zhang, L. Zhang, Y.-J. Lin and G.-X. Jin, *Chem. - Eur. J.*, 2015, **21**, 14893-14900.
20. A. Ulman, *Chem. Rev.*, 1996, **96**, 1533-1554.
21. R. Kramer, J. M. Lehn and A. Marquis-Rigault, *Proc. Natl. Acad. Sci.*, 1993, **90**, 5394-5398.
22. B. Hasenknopf, J. M. Lehn, G. Baum and D. Fenske, *Proc. Natl. Acad. Sci.*, 1996, **93**, 1397-1400.
23. M. Kołodziejski, A. R. Stefankiewicz and J.-M. Lehn, *Chem. Sci.*, 2019, **10**, 1836-1843.
24. G. M. Whitesides and B. Grzybowski, *Science*, 2002, **295**, 2418-2421.
25. Q.-F. Sun, J. Iwasa, D. Ogawa, Y. Ishido, S. Sato, T. Ozeki, Y. Sei, K. Yamaguchi and M. Fujita, *Science*, 2010, **328**, 1144-1147.
26. , !!! INVALID CITATION !!!
27. D. W. Johnson, J. Xu, R. W. Saalfrank and K. N. Raymond, *Angew. Chem., Int. Ed.*, 1999, **38**, 2882-2885.
28. M. Albrecht, *Chem. Rev.*, 2001, **101**, 3457-3498.
29. G. Aromí, P. Gamez and J. Reedijk, *Coord. Chem. Rev.*, 2008, **252**, 964-989.
30. S. Hadizadeh, N. Najafzadeh, M. Mazani, M. Amani, H. Mansouri-Torshizi and A. Niapour, *Biochem. Res. Int.*, 2014, **2014**, 813457.
31. J. E. M. Lewis, E. L. Gavey, S. A. Cameron and J. D. Crowley, *Chem. Sci.*, 2012, **3**, 778-784.

32. G. Sava, S. Zorzet, L. Perissin, G. Mestroni, G. Zassinovich and A. Bontempi, *Inorganica Chim. Acta*, 1987, **137**, 69-71.
33. R. Levine, J. A. Conroy, J. T. Adams and C. R. Hauser, *J. Am. Chem. Soc.*, 1945, **67**, 1510-1512.
34. P. A. Vigato, V. Peruzzo and S. Tamburini, *Coord. Chem. Rev.*, 2009, **253**, 1099-1201.
35. M. Kołodziejski, A. Walczak, Z. Hnatejko, J. Harrowfield and A. R. Stefankiewicz, *Polyhedron*, 2017, **137**, 270-277.
36. A. J. Brock, J. K. Clegg, F. Li and L. F. Lindoy, *Coord. Chem. Rev.*, 2018, **375**, 106-133.
37. J. C. Sloop, C. L. Bumgardner, G. Washington, W. D. Loehle, S. S. Sankar and A. B. Lewis, *J. Fluorine Chem.*, 2006, **127**, 780-786.
38. S. N. Podyachev, S. N. Sudakova, A. K. Galiev, A. R. Mustafina, V. V. Syakaev, R. R. Shagidullin, I. Bauer and A. I. Konovalov, *Russ. Chem. Bull., Int. Ed.*, 2006, **55**, 2000-2007.
39. S. N. Podyachev, S. N. Sudakova, G. S. Gimazetdinova, N. A. Shamsutdinova, V. V. Syakaev, T. A. Barsukova, N. Iki, D. V. Lapaev and A. R. Mustafina, *New J. Chem.*, 2017, **41**, 1526-1537.
40. A. J. Brock, J. C. McMurtrie and J. K. Clegg, *CrystEngComm*, 2019, **21**, 4786-4791.
41. J. Barberá, A. Elduque, R. Giménez, F. J. Lahoz, J. A. López, L. A. Oro, J. L. Serrano, B. Villacampa and J. Villalba, *Inorg. Chem.*, 1999, **38**, 3085-3092.
42. R. W. Saalfrank, H. Maid, A. Scheurer, F. W. Heinemann, R. Puchta, W. Bauer, D. Stern and D. Stalke, *Angew. Chem.*, 2008, **120**, 9073-9077.
43. A. J. Brock, I. Etchells, E. G. Moore and J. K. Clegg, *Dalton Trans*, 2021, **in press**.
44. R. C. Mehrotra, R. Bohra and D. P. Gaur, Metal [beta]-diketonates and allied derivatives, <http://catalog.hathitrust.org/api/volumes/oclc/4667662.html>.
45. J. J. Bloomfield, *J. Org. Chem.*, 1962, **27**, 2742-2746.
46. I. V. Taydakov, Y. M. Kreshchenova and E. P. Dolotova, *Beilstein J Org Chem*, 2018, **14**, 3106-3111.
47. J.-C. Hierso, R. Feurer and P. Kalck, *Coord. Chem. Rev.*, 1998, **178-180**, 1811-1834.
48. P. Doppelt, *Coord. Chem. Rev.*, 1998, **178-180**, 1785-1809.
49. J. Williams, *Chemical Vapor Deposition*, 1995, **1**, 32-33.
50. M. J. Hampden-Smith and T. T. Kodas, *Polyhedron*, 1995, **14**, 699-732.
51. D. J. Otway and W. S. Rees, *Coord. Chem. Rev.*, 2000, **210**, 279-328.
52. F. Marchetti, C. Pettinari, R. Pettinari, A. Cingolani, R. Gobetto, M. R. Chierotti, A. Drozdov and S. I. Troyanov, *Inorg. Chem.*, 2006, **45**, 3074-3085.
53. J. A. Darr and M. Poliakoff, *Chem. Rev.*, 1999, **99**, 495-542.
54. G. F. de Sá, O. L. Malta, C. de Mello Donegá, A. M. Simas, R. L. Longo, P. A. Santa-Cruz and E. F. da Silva, *Coord. Chem. Rev.*, 2000, **196**, 165-195.
55. G. Vicentini, L. B. Zinner, J. Zukerman-Schpector and K. Zinner, *Coord. Chem. Rev.*, 2000, **196**, 353-382.
56. C. Silvestru, *Applied Organometallic Chemistry*, 1994, **8**, 499-500.
57. D. Parker, *Chem. Rev.*, 1991, **91**, 1441-1457.
58. K. Binnemans and K. Lodewyckx, *Angewandte Chemie (International ed. in English)*, 2001, **40**, 242-244.
59. A. M. Giroud-Godquin, *Coord. Chem. Rev.*, 1998, **178-180**, 1485-1499.
60. A.-M. Giroud-Godquin and P. M. Maitlis, *Angew. Chem. Int. Ed. Engl.*, 1991, **30**, 375-402.
61. B. L. Miller, *Dynamic Combinatorial Chemistry*, Wiley, Chichester, 2010.
62. S. O. J. N. H. Reek, *Dynamic Combinatorial Chemistry*, Wiley-VCH, Weinheim, 2010.

63. S. Ladame, *Org. Biomol. Chem.*, 2008, **6**, 219-226.
64. F. B. L. Cougnon and J. K. M. Sanders, *Acc. Chem. Res.*, 2012, **45**, 2211-2221.
65. J.-M. Lehn and A. V. Eliseev, *Science*, 2001, **291**, 2331-2332.
66. J.-M. Lehn, *Chem. - Eur. J.*, 1999, **5**, 2455-2463.
67. Q. Ji, R. C. Lirag and O. Š. Miljanić, *Chem. Soc. Rev.*, 2014, **43**, 1873-1884.
68. A. R. Stefankiewicz and J. K. M. Sanders, *Chem. Commun.*, 2013, **49**, 5820-5822.
69. W. Drożdż, M. Kołodziejski, G. Markiewicz, A. Jenczak and A. Stefankiewicz, *Int. J. Mol. Sci.*, 2015, **16**, 16300.
70. Y. J. Colón and R. Q. Snurr, *Chem. Soc. Rev.*, 2014, **43**, 5735-5749.
71. S. J. Rowan, S. J. Cantrill, G. R. L. Cousins, J. K. M. Sanders and J. F. Stoddart, *Angew. Chem., Int. Ed.*, 2002, **41**, 898-952.
72. M. E. Belowich and J. F. Stoddart, *Chem. Soc. Rev.*, 2012, **41**, 2003-2024.
73. Y. Yu, J. Lin and S. Lei, *RSC Adv.*, 2017, **7**, 11496-11502.
74. A. Chao, I. Negulescu and D. Zhang, *Macromolecules*, 2016, **49**, 6277-6284.
75. R. Huang and I. Leung, *Molecules*, 2016, **21**, 910.
76. M. Mondal and A. K. H. Hirsch, *Chem. Soc. Rev.*, 2015, **44**, 2455-2488.
77. K. Osowska and O. Š. Miljanić, *Synlett*, 2011, **2011**, 1643-1648.
78. P. Howlader and P. S. Mukherjee, *Chem. Sci.*, 2016, **7**, 5893-5899.
79. K. Acharyya and P. S. Mukherjee, *Chem. - Eur. J.*, 2014, **20**, 1646-1657.
80. K. Acharyya, S. Mukherjee and P. S. Mukherjee, *J. Am. Chem. Soc.*, 2013, **135**, 554-557.
81. D. Samanta and P. S. Mukherjee, *Chem. Commun.*, 2013, **49**, 4307-4309.
82. D. Komáromy, M. C. A. Stuart, G. Monreal Santiago, M. Tezcan, V. V. Krasnikov and S. Otto, *J. Am. Chem. Soc.*, 2017, **139**, 6234-6241.

## **Reprints of publications**

**A1.** Unsymmetrical bidentate ligands as a basis for construction of ambidentate ligands for functional materials: Properties of 4,4-dimethyl-1-phenylpentane-1,3-dionate





# Unsymmetrical bidentate ligands as a basis for construction of ambidentate ligands for functional materials: Properties of 4,4-dimethyl-1-phenylpentane-1,3-dionate

Michał Kołodziej<sup>a,b</sup>, Anna Walczak<sup>a,b</sup>, Zbigniew Hnatejko<sup>a</sup>, Jack Harrowfield<sup>c</sup>, Artur R. Stefankiewicz<sup>a,b,\*</sup>

<sup>a</sup> Faculty of Chemistry, Adam Mickiewicz University, Umultowska 89b, 61-614 Poznań, Poland

<sup>b</sup> Centre for Advanced Technologies, Adam Mickiewicz University, Umultowska 89c, 61-614 Poznań, Poland

<sup>c</sup> Institut de Science et d'Ingénierie Supramoléculaires, Université de Strasbourg, 8 allée Gaspard Monge, 67083 Strasbourg Cedex, France

## ARTICLE INFO

### Article history:

Received 26 June 2017

Accepted 17 August 2017

Available online 24 August 2017

### Keywords:

$\beta$ -Diketetonate

Structure

Supramolecular

Isomerism

Self-assembly

## ABSTRACT

To establish a background to the possible use of its ambidentate derivatives as stimulus-responsive ligands in functional complexes, the basic coordination chemistry of the anion derived from 4,4-dimethyl-1-phenylpentane-1,3-dione (benzoylpivaloylmethane, bpmH) has been re-examined with selected main group and transition metal M(II) and M(III) species. There is evidence that the steric bulk of the 1,3-dione substituents is not sufficient to prevent oligomerisation of the Ni(II) complex and equilibrium mixtures of geometric isomers can be detected in solution for at least the Al(III), Co(III) and Pd(III) complexes. Crystal structure determinations on both  $[\text{Cu}(\text{bpm})_2]$  and  $[\text{Pd}(\text{bpm})_2]$  show, however, that a single isomer can be isolated in the solid state.

© 2017 Elsevier Ltd. All rights reserved.

## 1. Introduction

Supramolecular chemistry is based upon the use of labile intermolecular interactions to assemble complex structures with specific functionality [1]. While the nature and energy of these labile interactions are both extremely varied, a particularly useful type of interaction is that involving coordinate bonding to metal ions. A coordinate bond is not necessarily labile but this is commonly the case and one feature of the coordinate bond that greatly enhances its utility is that it can be converted from a labile to an inert state by the appropriate choice of donor atoms and/or ligand structure. This can even be done selectively within the coordination sphere of a single metal ion by the introduction of multidentate chelate or, particularly, macrocyclic ligands [2]. An aspect of multidentate ligand design which has been little explored to date in relation to the multifunctionality of complexes is the deliberate introduction of ambidentate character. In principle, this should allow the complex of an appropriate ligand to switch, under a particular stimulus [3], between forms with various functions such as

different degrees of catalytic activity. Thus, we have begun a programme of research concerned with divergent multitopic ligands and the properties of their isomeric complexes.

An especially versatile and long-studied group of chelate ligands is that based on 1,3-diketones [4–14], acetylacetone (acacH) or pentane-2,4-dione being the best-known of such molecules. While the neutral species can act as O,O'-chelates towards metal ions, provided the carbon atom linking the carbonyl groups has at least one H-substituent, enabling tautomerism with an enol form, these molecules are weak acids and the coordination chemistry of their conjugate-base, delocalised diketonate anion derivatives is far more extensive and includes examples of C-donor bonding as well as O,O' chelation [4–14]. The ease of synthesis of 1,3-diketones, not necessarily directed solely towards metal ion complexation [15], means that an exceptional range of such species is accessible and relatively recent work has provided examples of pyridyl derivatives which could indeed function as ambidentate species [16]. Particularly useful as a means of introducing extra functionality is a phenyl substituent and a variety of derivatives of benzoylpivaloylmethane (bpmH) are known which illustrate this approach [17–19], although the substituents known in this case, with one exception [19], do not provide metal-binding sites competitive with the diketonate unit. A phenyl group or larger aromatic unit can also be employed in the generation of poly-1,3-diketone ligands, such species having been the basis of some

\* Corresponding author at: Faculty of Chemistry, Adam Mickiewicz University, Umultowska 89b, 61-614 Poznań, Poland.

E-mail addresses: [mik.kolodziej1@gmail.com](mailto:mik.kolodziej1@gmail.com) (M. Kołodziej), [anna.jenczak@op.pl](mailto:anna.jenczak@op.pl) (A. Walczak), [zbigniew.hnatejko@amu.edu.pl](mailto:zbigniew.hnatejko@amu.edu.pl) (Z. Hnatejko), [harrowfield@unistra.fr](mailto:harrowfield@unistra.fr) (J. Harrowfield), [ars@amu.edu.pl](mailto:ars@amu.edu.pl) (A.R. Stefankiewicz).

<http://dx.doi.org/10.1016/j.poly.2017.08.022>

0277-5387/© 2017 Elsevier Ltd. All rights reserved.

remarkable recent extensions of diketone coordination chemistry [20–23]. In our focus on the possibility of generating ambidentate ligands from a phenyl-substituted 1,3-diketone, we were confronted with two issues potentially complicating their application: aggregation and isomerism of the complexes. The diketone benzoylpivaloylmethane (bpmH) being a readily available “parent” species for ambidentate ligand construction, we sought to make specific expansions of the rather limited knowledge [17–19,24–26] of the coordination chemistry of the derived diketonate in relation to these potential complications using transition metal M(II) and M(III) species, plus Al(III) as a main group representative (Fig. 1).

## 2. Experimental

### 2.1. Reagents and instrumentation

All reagents were purchased from commercial sources (Sigma, Fluorochem, AlfaAesar). High purity solvents were purchased from POCH and anhydrous THF was dried over molecular sieves under argon. NMR spectra were measured on a Bruker Ultrashield™ 300 + 300 Fourier-Transform spectrometer using deuterated solvents ( $\text{CDCl}_3$ ,  $\text{CD}_3\text{CN}$ ). TOF-MS spectra were measured using chloroform solutions on a BRUKER Impact HD ESI-Q-TOF mass spectrometer. Solution electronic absorption and luminescence spectra were recorded in 1 cm quartz cells at ambient temperature in MeCN on Shimadzu UV-2401 PC and Hitachi F-7000 Fluorescence instruments, respectively. Luminescence spectra were also recorded on the solid complexes.

X-ray diffraction data were obtained on a 4-circle Xcalibur EosS2 diffractometer (Agilent Technologies) equipped with a CCD detector.

### 2.2. Synthesis

#### 2.2.1. 4,4-dimethyl-1-phenylpentane-1,3-dione (benzoylpivaloylmethane), bpmH

The ligand was prepared according to a literature procedure [15], although it is also available commercially. Pinacolone (5.54 g; 0.055 mol) was added to a suspension of NaH (6.65 g; 0.166 mol) in dry THF (50 mL). After 30 min. of stirring, methyl benzoate (3.5 mL; 0.277 mol) was added to the grey-yellow suspension. The mixture was heated at 47 °C for 24 h. Reaction was quenched by the addition of water, followed by aqueous HCl to reduce the pH to ~4. The product was extracted into ethylacetate and the extract evaporated down after drying over  $\text{Na}_2\text{SO}_4$ . The crude product was purified by addition of  $\text{CuCl}_2 \cdot 2\text{H}_2\text{O}$ , isolation of the solid complex formed and then dissociating the ligand from this by treatment with hot aqueous  $\text{H}_2\text{SO}_4$ . Extraction into DCM, drying and evaporation of the extract yielded the desired product as a yellow oil (2.81 g; 50.0% yield).  $^1\text{H}$  NMR (300 MHz,  $\text{CDCl}_3$ )  $\delta$  16.53 (s, 1H, enol-form -OH,  $\text{H}_\text{D}$ ); 7.90, 7.89 (d, 2H,  $\text{H}_\text{A}$ ); 7.54, 7.52, 7.50 (t, 1H,  $\text{H}_\text{E}$ ); 7.47, 7.45, 7.43 (t, 2H,  $\text{H}_\text{A}$ ); 7.26 ( $\text{CDCl}_3$ ), 6.31 (s, 1H, enol-form -CH=,  $\text{H}_\text{D}$ ), 4.19 (s, 2H, keto-form -CH=,  $\text{H}_\text{D}$ ), 1.26 (s, 9H, enol-form -CH<sub>3</sub>,  $\text{H}_\text{I}$ ), 1.23 (s, 9H, keto-form -CH<sub>3</sub>,  $\text{H}_\text{I}$ ) (Signals assigned according to the Fig. S8).  $^{13}\text{C}$  NMR (75 MHz,  $\text{CDCl}_3$ )  $\delta$  202.97 ( $\text{C}_\text{O}$ ), 184.65 ( $\text{C}_\text{O}$ ), 135.59 ( $\text{C}_\text{7}$ ), 132.20 ( $\text{C}_\text{6}$ ), 128.65 ( $\text{C}_\text{5}$ ), 127.05 ( $\text{C}_\text{4}$ ), 92.17 ( $\text{C}_\text{3}$ ), 77.58, 77.16, 76.74 (Solvent,  $\text{CDCl}_3$ ), 39.93 ( $\text{C}_\text{2}$ ), 27.47 ( $\text{C}_\text{1}$ ) (Signals assigned according to the Fig. S9). Absorption spectrum ( $\text{CH}_2\text{CN}$ ):  $\lambda_{\text{max}}$  = 312 nm,  $\epsilon_{\text{max}}$  =  $2.07 \times 10^4 \text{ M}^{-1} \text{ cm}^{-1}$ . Microanalysis: calculated (%) for  $\text{C}_{13}\text{H}_{16}\text{O}_2$ : C 76.44, H 7.90, O 15.66; found: C 76.31, H 8.11, O 15.58.

#### 2.2.2. Tris(4,4-dimethyl-1-phenylpentane-1,3-dionato)aluminium(III), [Al(bpm)<sub>3</sub>]

As for the free diketone, the syntheses of the Al(III) diketonate and of the other complexes described herein were based on litera-

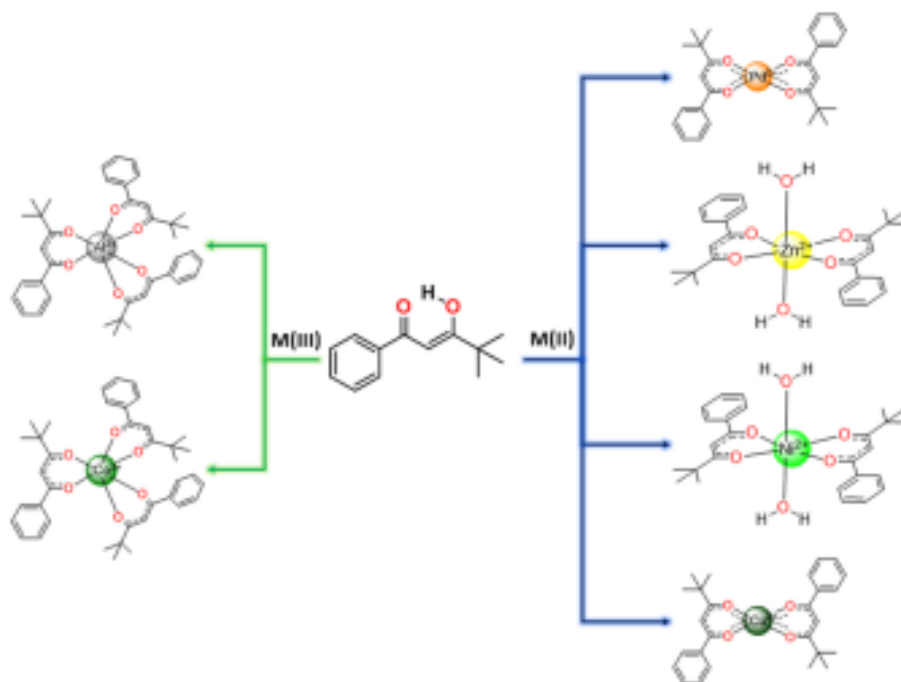


Fig. 1. Complexes obtained in reactions of 4,4-dimethyl-1-phenylpentane-1,3-dione (bpmH) with M(II) and M(III) ions.

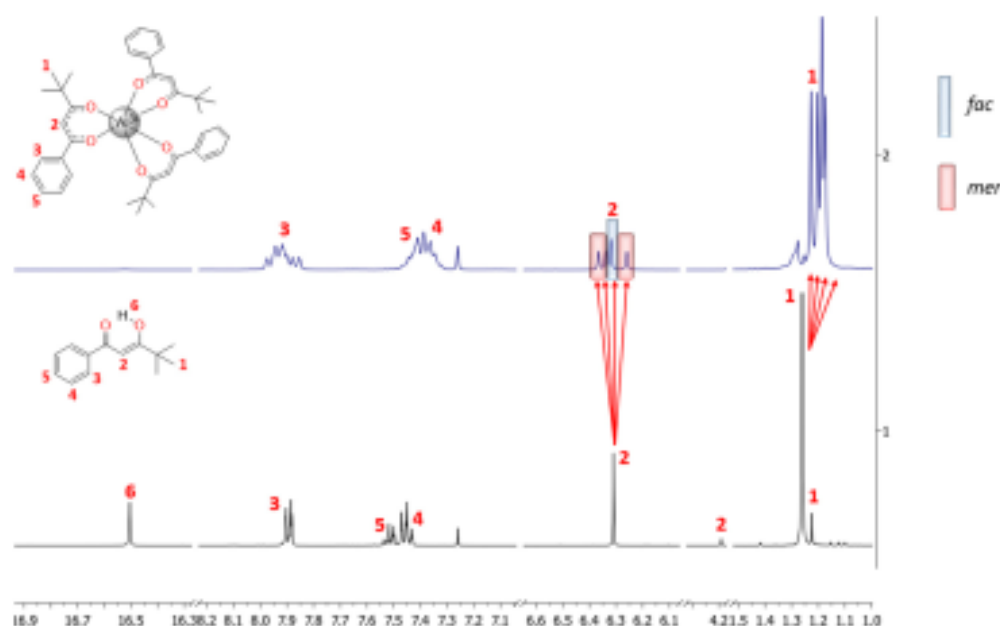


Fig. 2. Comparison of the  $^1\text{H}$  NMR (300 MHz) spectra of bpmH (bottom, black) and the complex  $[\text{Al}(\text{bpm})_3]$  (top, blue) in  $\text{CDCl}_3$  at room temperature.

ture procedures [17,18,24,25]. To a yellow solution of  $\text{Al}(\text{NO}_3)_3 \cdot 9\text{H}_2\text{O}$  (65.2 mg; 0.173 mmol) and bpmH (106.5 mg; 0.521 mmol) in  $\text{MeOH}/\text{H}_2\text{O}$  (1:1, 3 mL),  $\text{NaHCO}_3$  (51.1 mg; 0.608 mmol) was added. The resulting suspension was stirred for 30 min at room temperature. After removal of the solvents under reduced pressure, the residue was extracted with  $\text{CHCl}_3$  ( $2 \times 15$  mL) and washed with water ( $2 \times 15$  mL). The combined organic extracts were dried with  $\text{Na}_2\text{SO}_4$  after which the solvent was removed to give an oily residue. Addition of  $\text{EtOAc}/\text{hexane}$  (1:1, v/v, 5 mL) resulted in the precipitation of a cream solid, which was filtered off and dried in vacuo to give a white powder which was recrystallized from chloroform, yielded white, hairy small crystals (37.1 mg; 33.4% yield).  $^1\text{H}$  NMR (300 MHz,  $\text{CDCl}_3$ )  $\delta$  7.97, 7.94, 7.92, 7.90, 7.88, 7.86 (sext., 6H,  $\text{H}_3$ ); 7.44, 7.43, 7.41, 7.39, 7.36, 7.35, 7.32 (sept., 9H,  $\text{H}_5$ ,  $\text{H}_4$ ); 7.26 ( $\text{CDCl}_3$ ), 6.37, 6.34, 6.32, 6.26 (q, 3H,  $\text{H}_2$ ); 1.23, 1.20, 1.19, 1.17 (q, 27H,  $\text{H}_1$ ) (Signals assigned according to the Fig. 1). TOF-MS:  $m/z = 659.2974$  = calculated for  $\text{C}_{39}\text{H}_{45}\text{AlNaO}_6$  ( $[\text{Al}(\text{bpm})_3]^+$ ); found:  $m/z = 659.2929$ ;  $m/z = 433.1993$  = calculated for  $\text{C}_{26}\text{H}_{30}\text{AlO}_4$  ( $[\text{Al}(\text{bpm})_2]^+$ ); found:  $m/z = 433.1959$ . Absorption spectrum ( $\text{CH}_3\text{CN}$ ):  $\lambda_{\text{max}} = 325$  nm,  $\epsilon_{\text{max}} = 1.76 \times 10^3 \text{ M}^{-1} \text{ cm}^{-1}$ . Microanalysis: calculated (%) for  $\text{C}_{39}\text{H}_{45}\text{AlO}_6$ : C 73.56, H 7.12, O 15.08; found: C 73.72, H 6.98, O 15.23.

### 2.2.3. Tris(4,4-dimethyl-1-phenylpentane-1,3-dionato)cobalt(III), $[\text{Co}(\text{bpm})_3]$

To a solution of bpmH (203 mg; 0.996 mmol) in  $\text{MeOH}$  (2 mL), TEA (143  $\mu\text{L}$ ; 1.03 mmol) was added. After 5 min. of stirring at room temperature, a  $\text{MeOH}$  solution (2 mL) of  $\text{Co}(\text{ClO}_4)_2 \cdot 6\text{H}_2\text{O}$  (121.48 mg; 0.332 mmol) with  $\text{H}_2\text{O}_2$  (11  $\mu\text{L}$ ; 0.365 mmol) was added. The resulting mixture was stirred for 30 min. and then  $\text{H}_2\text{O}$  was added to finish precipitation. The voluminous dark green precipitate was filtered off, washed with water, dried and recrystallized from chloroform, yielded dark green flake-shaped crystals (365 mg; 55% yield).  $^1\text{H}$  NMR (300 MHz,  $\text{CDCl}_3$ )  $\delta$  7.91, 7.88, 7.86, 7.84, 7.81, 7.78 (sext., 6H,  $\text{H}_3$ ); 7.43, 7.41, 7.39, 7.37, 7.34, 7.32, 7.30 (sept., 9H,  $\text{H}_5$ ,  $\text{H}_4$ ); 7.26 ( $\text{CDCl}_3$ ), 6.34, 6.30, 6.28, 6.20 (q, 3H,  $\text{H}_2$ ); 1.26, 1.23, 1.21, 1.19 (q, 27H,  $\text{H}_1$ ) (Signals assigned according to the Fig. S10). TOF-MS:  $m/z = 669.2626$  = calculated for  $\text{C}_{39}\text{H}_{45}\text{CoO}_6$

$\text{CoO}_6$  ( $[\text{Co}(\text{bpm})_3]^+$ ); found:  $m/z = 669.2626$ . Absorption spectrum ( $\text{CH}_3\text{CN}$ ):  $\lambda_{\text{max}} = 595$  nm,  $\epsilon_{\text{max}} = 183.6 \text{ M}^{-1} \text{ cm}^{-1}$  (the visible region absorption due to d-d transitions). Microanalysis: calculated (%) for  $\text{C}_{39}\text{H}_{45}\text{CoO}_6$ : C 70.05, H 6.78, O 14.36; found: C 70.19, H 6.63, O 14.27; calculated (%) for  $\text{C}_{78}\text{H}_{90}\text{Co}_2\text{O}_{12}$ : C 67.09, H 6.50, O 13.75; found: C 66.54, H 6.96, O 13.48 (green paramagnetic species, after dehydration by heating).

### 2.2.4. Diaqua-bis(4,4-dimethyl-1-phenylpentane-1,3-dionato)nickel(II), $[\text{Ni}(\text{bpm})_2(\text{H}_2\text{O})_2]$

To a solution of bpmH (124 mg; 0.608 mmol) in  $\text{MeOH}$  (2 mL), TEA (61  $\mu\text{L}$ ; 0.608 mmol) was added. After 5 min. of stirring at room temperature, a  $\text{MeOH}$  solution (2 mL) of  $\text{Ni}(\text{CH}_3\text{COO})_2 \cdot 4\text{H}_2\text{O}$  (76 mg; 0.304 mmol) was added. The resulting mixture was stirred for 30 min. and then  $\text{H}_2\text{O}$  was added to finish precipitation. The voluminous light green precipitate was filtered off, washed with water, dried and recrystallized from chloroform, yielded small light green cubes (163 mg; 58% yield). TOF-MS:  $m/z = 465.1575$  = calculated for  $\text{C}_{26}\text{H}_{31}\text{NiO}_4$  ( $[\text{Ni}(\text{bpm})_2]^+$ ); found:  $m/z = 465.1563$ . Absorption spectrum ( $\text{CH}_3\text{CN}$ ):  $\lambda_{\text{max}} = 602$  nm,  $\epsilon_{\text{max}} = 255.8 \text{ M}^{-1} \text{ cm}^{-1}$  (the visible region absorption due to d-d transitions). Microanalysis: calculated (%) for  $\text{C}_{26}\text{H}_{34}\text{NiO}_6$ : C 62.30, H 6.94, O 19.15; found: C 62.08, H 7.12, O 18.99.

### 2.2.5. Bis(4,4-dimethyl-1-phenylpentane-1,3-dionato)copper(II), $[\text{Cu}(\text{bpm})_2]$

To a solution of bpmH (199 mg; 0.975 mmol) in THF (5 mL),  $\text{Na}_2\text{CO}_3$  (207 mg; 1.95 mmol) was added. After 5 min. of stirring at room temperature, a THF solution (3 mL) of  $\text{Cu}(\text{BF}_4)_2 \cdot 6\text{H}_2\text{O}$  (77.0 mg; 0.325 mmol) was added. The resulting green mixture was stirred for 24 h at room temperature. A small amount of flocculent material was filtered off and green filtrate taken to dryness in vacuo. The solid obtained was dissolved in  $\text{DCM}/\text{EtOH}$  mixture and left to crystallize by slow solvent evaporation (112 mg; 49% yield). TOF-MS:  $m/z = 470.1553$  = calculated for  $\text{C}_{26}\text{H}_{31}\text{CuO}_4$  ( $[\text{Cu}(\text{bpm})_2]^+$ ); found:  $m/z = 470.1505$ . Absorption spectrum ( $\text{CH}_3\text{CN}$ ):  $\lambda_{\text{max}} = 663$  nm,  $\epsilon_{\text{max}} = 52.6 \text{ M}^{-1} \text{ cm}^{-1}$ ;  $\lambda_{\text{max}} = 538$  nm,  $\epsilon_{\text{max}} = 47 \text{ M}^{-1} \text{ cm}^{-1}$  (the visible region absorption due to d-d trans-



sitions). Microanalysis: calculated (%) for  $C_{26}H_{30}CuO_4$ : C 66.43, H 6.43, O 13.61; found: C 66.68, H 6.29, O 13.49.

### 2.2.6. Hydrated bis(4,4-dimethyl-1-phenylpentane-1,3-dionato)zinc(II), $[Zn(bpm)_2(OH_2)_4]$

To a solution of bpmH (119 mg; 0.583 mmol) in MeOH (2 mL), NaOH (23.4 mg; 0.583 mmol) was added. After stirring the mixture 5 min,  $Zn(CH_3COO)_2 \cdot 2H_2O$  (42.7 mg; 0.194 mmol) was added to give cloudy, yellow solution, which was then stirred for a further 24 h at room temperature. The suspension was filtered and the filtrate taken to dryness to give a yellow solid. This was dissolved in the minimum amount of MeCN and addition of  $Et_2O/n$ -hexane (1:1, v/v, 10 mL) used to precipitate the desired product as yellow solid, recrystallized from dichloromethane/diethyl ether mixture, yielded hairy small white crystals (42.3 mg, 32% yield).  $^1H$  NMR (300 MHz,  $CDCl_3$ )  $\delta$  7.87, 7.85 (d, 4H,  $H_2$ ), 7.57, 7.55, 7.53 (t, 2H,  $H_5$ ), 7.50, 7.48, 7.46 (t, 4H,  $H_4$ ), 7.26 ( $CDCl_3$ ), 6.30, 6.28 (d, 2H,  $H_2$ ), 1.26 (s, 18H,  $H_1$ ) (Signals assigned according to the Fig. 4). TOF-MS:  $m/z = 471.1514$  = calculated for  $C_{26}H_{31}O_4Zn$  ( $[H(Zn(bpm)_2)]^+$ ); found:  $m/z = 471.1508$ . Absorption spectrum ( $CH_2CN$ ):  $\lambda_{max} = 309$  nm,  $\epsilon_{max} = 2.18 \times 10^3$  M $^{-1}$  cm $^{-1}$ . Microanalysis: calculated (%) for  $C_{26}H_{34}ZnO_6$ : C 61.48, H 6.75, O 18.90; found: C 61.31, H 6.96, O 18.68.

### 2.2.7. Bis(4,4-dimethyl-1-phenylpentane-1,3-dionato)palladium(II), $[Pd(bpm)_2]$

To a solution of bpmH (0.156 g; 0.763 mmol) in MeOH (3 mL), NaOH (38.1 mg; 0.953 mmol) was added and the mixture stirred until (1 h) a clear, yellow solution had formed. A solution of  $PdCl_2$  (64.4 mg; 0.363 mmol) in MeOH (5 mL) was added, rapidly producing a green precipitate, and the suspension was stirred for 24 h at r.t. The product was isolated by filtration, washing on the filter with EtOH and  $Et_2O$  and recrystallization from chloroform/diethyl ether system, yielded small yellow-green, needle-shaped crystals (109 mg, 55.2% yield).  $^1H$  NMR (300 MHz,  $CDCl_3$ )  $\delta$  7.86, 7.83 (d, 4H,  $H_2$ ); 7.50, 7.47, 7.45 (t, 2H,  $H_5$ ); 7.42, 7.39, 7.37 (t, 4H,  $H_4$ ); 7.26 ( $CDCl_3$ ); 6.24 (s, 2H,  $H_2$ ); 1.26 (s, 18H,  $H_1$ ) (Signals assigned according to the Fig. 3). TOF-MS:  $m/z = 513.1311$  = calculated for  $C_{26}H_{31}O_4Pd$  ( $[H(Pd(bpm)_2)]^+$ ); found:  $m/z = 513.1257$ .

Absorption spectrum ( $CH_2CN$ ):  $\lambda_{max} = 589$  nm,  $\epsilon_{max} = 90.2$  M $^{-1}$  cm $^{-1}$  (the visible region absorption due to d–d transitions). Microanalysis: calculated (%) for  $C_{26}H_{30}PdO_4$ : C 60.88, H 5.90, O 12.48; found: C 60.75, H 5.74, O 12.69.

### 2.3. Crystallography

Crystals of  $Cu(bpm)_2$  were obtained by slow evaporation of a solution of the complex in a 1:1 dichloromethane/ethanol mixture. Crystals of  $Pd(bpm)_2$  were obtained by diffusion in a two-phase system of the complex in chloroform as the bottom layer and diethyl ether as the top layer in a closed vial. Diffraction data were collected at room temperature using graphite-monochromated MoK $\alpha$  radiation ( $\lambda = 0.71073$  Å) with the  $\omega$ -scan technique. For data reduction, UB-matrix determination and absorption correction, CrysAlisPro [27] software was used.

Using Olex2 [28], the structures were solved by direct methods using SHELX [29] and refined by full-matrix least-squares against  $F^2$  utilizing SHELX. All non-hydrogen atoms were refined anisotropically. Hydrogen atoms were calculated at ideal positions by molecular geometry and refined as rigid groups.  $U_{iso}$  of hydrogen atoms were set as 1.2 (for C-carriers) times  $U_{eq}$  of the corresponding carrier atom. Crystal and refinement data are summarised in Table 1 and selected structural parameters are reported in Tables S1–S4. The data have been deposited in the form of cifs with the Cambridge Crystallographic Data Centre (CCDC), deposition numbers CCDC 1558066 (for  $[Cu(bpm)_2]$ ) and CCDC 1558067 (for  $[Pd(bpm)_2]$ ). These can be obtained free of charge via [www.ccdc.cam.ac.uk/data\\_request/cif](http://www.ccdc.cam.ac.uk/data_request/cif), or by emailing [data\\_request@ccdc.cam.ac.uk](mailto:data_request@ccdc.cam.ac.uk), or by contacting The Cambridge Crystallographic Data Centre, 12, Union Road, Cambridge CB2 1EZ, UK; fax: +44 1223 336033.

### 3. Results and discussion

#### 3.1. Synthesis

Both the diketone and diketonate complex syntheses were based on very familiar literature procedures for the same or closely

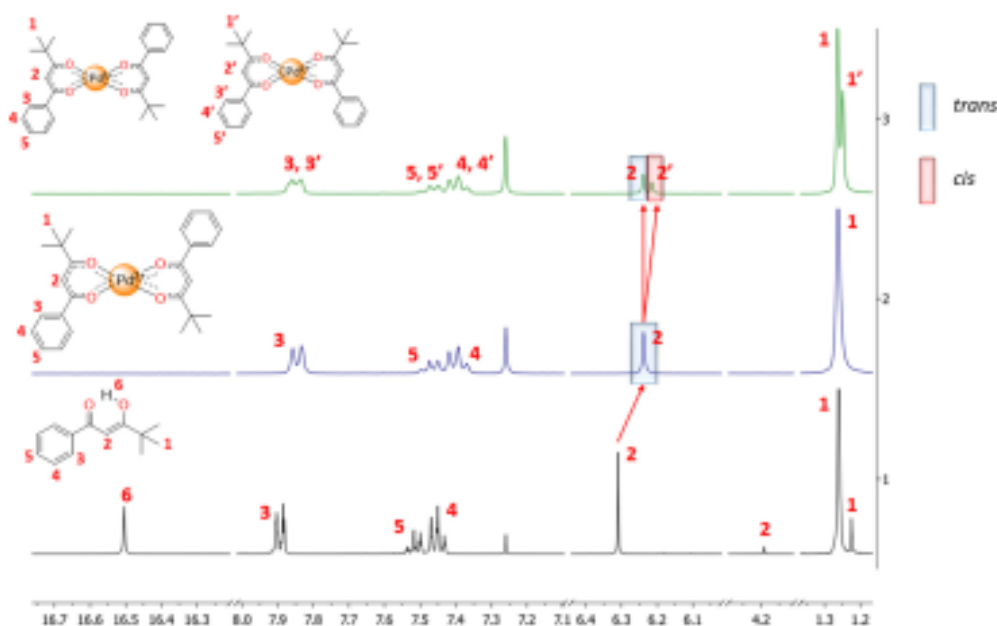


Fig. 3. Comparison of the  $^1H$  NMR (300 MHz) spectra of bpmH (bottom, black), the complex  $[Pd(bpm)_2]$  immediately after preparing the solution (middle, blue) and the complex  $[Pd(bpm)_2]$  after one hour in solution (top, green) in  $CDCl_3$  at room temperature.

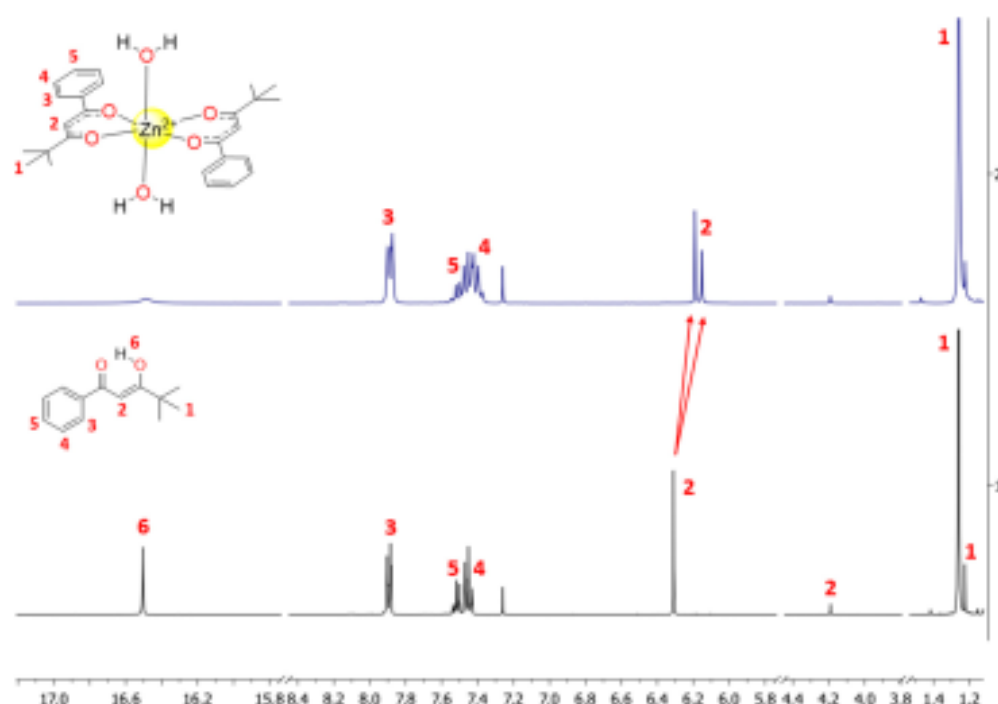


Fig. 4. Comparison of the  $^1\text{H}$  NMR (300 MHz) spectra of bpmH (bottom, black) and the complex  $[\text{Zn}(\text{bpm})_2](\text{OH}_2)_6$  immediately after preparing the solution (top, blue) in  $\text{CDCl}_3$  at room temperature.

Table 1  
Crystal and refinement data.

Complex	$[\text{Cu}(\text{bpm})_2]$	$[\text{Pd}(\text{bpm})_2]$
Empirical formula	$\text{C}_{28}\text{H}_{30}\text{CuO}_4$	$\text{C}_{28}\text{H}_{30}\text{O}_4\text{Pd}$
Formula weight	470.04	512.90
$T$ (K)	293(2)	293(2)
Crystal system	triclinic	monoclinic
Space group	$P\bar{1}$	$P2_1/n$
$a$ (Å)	6.4306(7)	10.6894(2)
$b$ (Å)	9.5411(12)	12.0326(2)
$c$ (Å)	10.3057(9)	18.8931(4)
$\alpha$ (°)	82.414(9)	90
$\beta$ (°)	86.448(8)	97.597(2)
$\gamma$ (°)	72.626(10)	90
$V$ (Å $^3$ )	597.89(12)	2408.72(8)
$Z$	1	4
$\rho_{\text{calc}}$ (g cm $^{-3}$ )	1.305	1.414
$\mu$ (mm $^{-1}$ )	0.941	0.798
$R(000)$	247.0	1056.0
Crystal size (mm $^3$ )	$0.25 \times 0.2 \times 0.02$	$0.2 \times 0.15 \times 0.1$
Radiation	MoK $\alpha$ ( $\lambda = 0.71073$ )	MoK $\alpha$ ( $\lambda = 0.71073$ )
$2\theta$ range for data collection (°)	6.64–48.798	4.158–56.69
Index ranges	$-7 \leq h \leq 7, -11 \leq k \leq 10, -11 \leq l \leq 11$	$-14 \leq h \leq 14, -15 \leq k \leq 15, -24 \leq l \leq 25$
Reflections collected	5575	117908
Independent reflections	1873 [ $R_{\text{int}} = 0.0595, R_{\sigma} = 0.0702$ ]	5768 [ $R_{\text{int}} = 0.0690, R_{\sigma} = 0.0309$ ]
Data/restraints/parameters	1873/0/145	5768/0/289
Goodness-of-fit (GOF) on $F^2$	1.032	1.182
Final $R$ indexes [ $I \geq 2\sigma(I)$ ]	$R_1 = 0.0448, wR_2 = 0.0943$	$R_1 = 0.0454, wR_2 = 0.0819$
Final $R$ indexes [all data]	$R_1 = 0.0665, wR_2 = 0.1027$	$R_1 = 0.0823, wR_2 = 0.0895$
Largest difference peak/hole (e Å $^{-3}$ )	0.22/−0.21	0.39/−0.36

related species and provided no surprising results. Methanol proved to be a convenient solvent for all the complex ion syntheses, although various other solvents such as ethanol, acetonitrile or tetrahydrofuran could be used with equal success.

### 3.2. Composition, structure and stereochemistry of the complexes

Although the syntheses were designed to produce just the neutral, homoleptic species  $\text{M}(\text{bpm})_n$  (possibly as solvates) and were

successful in this regard, it is of course possible that such species could oligomerise [8–10]. Mass spectra of the complexes (see experimental) provided no evidence for the presence of oligomers but the necessary use of ion association to obtain charged species appeared in several cases to result in partial breakdown by dissociation of  $\text{bpm}^-$ , so that depolymerisation of initially weakly associated species cannot be excluded. However, it is known [8–10], [30] that oligomerisation is inhibited by bulky substituents on the diketone unit and complexes of  $\text{Ni(II)}$  [30] are of particular significance in this regard, as the colour (i.e. the absorption spectrum) of diamagnetic square-planar mononuclear species is quite different to that of paramagnetic octahedral oligomers such as formed, for example, by dehydration of octahedral  $\text{trans-[Ni(acac)}_2(\text{OH}_2)_2]$ . While the square-planar form of the  $\text{Ni(II)}$  complex of the symmetrical dipivaloylmethanate ( $\text{dpm}^-$ ) ligand was established long ago by an X-ray structure determination [31] and shown to be maintained in solution [32], there is, however, evidence [17], [24] largely based on solution molecular weight estimates, that benzoylpivaloylmethanate is a less restrictive ligand in regard to oligomerisation. This conclusion is supported by the present observations on the  $\text{Ni(II)}$  complex, which was isolated as the green, octahedral  $[\text{Ni(bpm)}_2(\text{OH}_2)_2]$  complex that, on heating, underwent dehydration to give a green, paramagnetic species analogous to  $[\text{Ni}_2(\text{acac})_4]$  (see experimental).

An alternative index of ligand–ligand interactions within the coordination sphere of a complex can be provided in the case of an unsymmetrical ligand such as  $\text{bpm}^-$  in the distribution of isomeric forms of bis- or tris-ligand complexes. In complexes of sufficient stability and stereochemical rigidity, this isomer distribution can be monitored by NMR spectroscopy. Thus, in the present work

the  $^1\text{H}$  spectra of the diamagnetic complexes  $[\text{Al(bpm)}_3]$ ,  $[\text{Co(bpm)}_3]$ ,  $[\text{Zn(bpm)}_2(\text{OH}_2)_2]$  and  $[\text{Pd(bpm)}_2]$  provided clear evidence for the presence of two species in each case. For the expected octahedral form of the  $\text{Al(III)}$  (Fig. 2) and  $\text{Co(III)}$  (Fig. S10) complexes, the  $C_2$ -symmetric *fac* isomer should give rise to a single peak for the methine and methyl group protons, while the  $C_3$ -symmetric *mer* isomer should show three peaks of equal intensity for each type of proton, enabling ready identification of the separate isomers and therefore a direct establishment of the *fac:mer* ratio (equilibrium constant). For the  $\text{Al(III)}$  and  $\text{Co(III)}$  complexes, this ratio was essentially identical at 1.65, a value little different from that expected for the statistical distribution (2:1 *fac:mer*).

For the expected square-planar form of  $[\text{Pd(bpm)}_2]$ , *cis* and *trans* isomers are possible. On recording the  $^1\text{H}$  NMR spectrum of  $[\text{Pd(bpm)}_2]$  immediately after dissolving crystals of the bulk recrystallized complex, only one methine signal was observed and thus assigned to the *trans* form, given that this is the species found in the crystal lattice. For the same sample after an hour, signals consistent with the presence of a mixture of *cis* and *trans* isomers were observed indicating a *cis:trans* ratio of 1:1.66 (Fig. 3), in this case differing more significantly from the statistical value (of 1:1). In any case, both these spectroscopic results and the nature of the  $\text{Ni(II)}$  complex indicate that ligand–ligand interactions in complexes of  $\text{bpm}^-$  are not strong, making this ligand somewhat closer to  $\text{acac}^-$  than to  $\text{dpm}^-$  (dipivaloylmethanate) in its coordinative properties.

Elemental analyses for the  $\text{Zn(II)}$  complex indicated the presence of two water molecules per  $\text{Zn}$  and thus were consistent with different formulations such as  $[\text{Zn(bpm)}_2(\text{OH}_2)_2] \cdot \text{H}_2\text{O}$  or  $[\text{Zn(bpm)}_2(\text{OH}_2)_4]$ . The former is consistent with the square-pyrami-

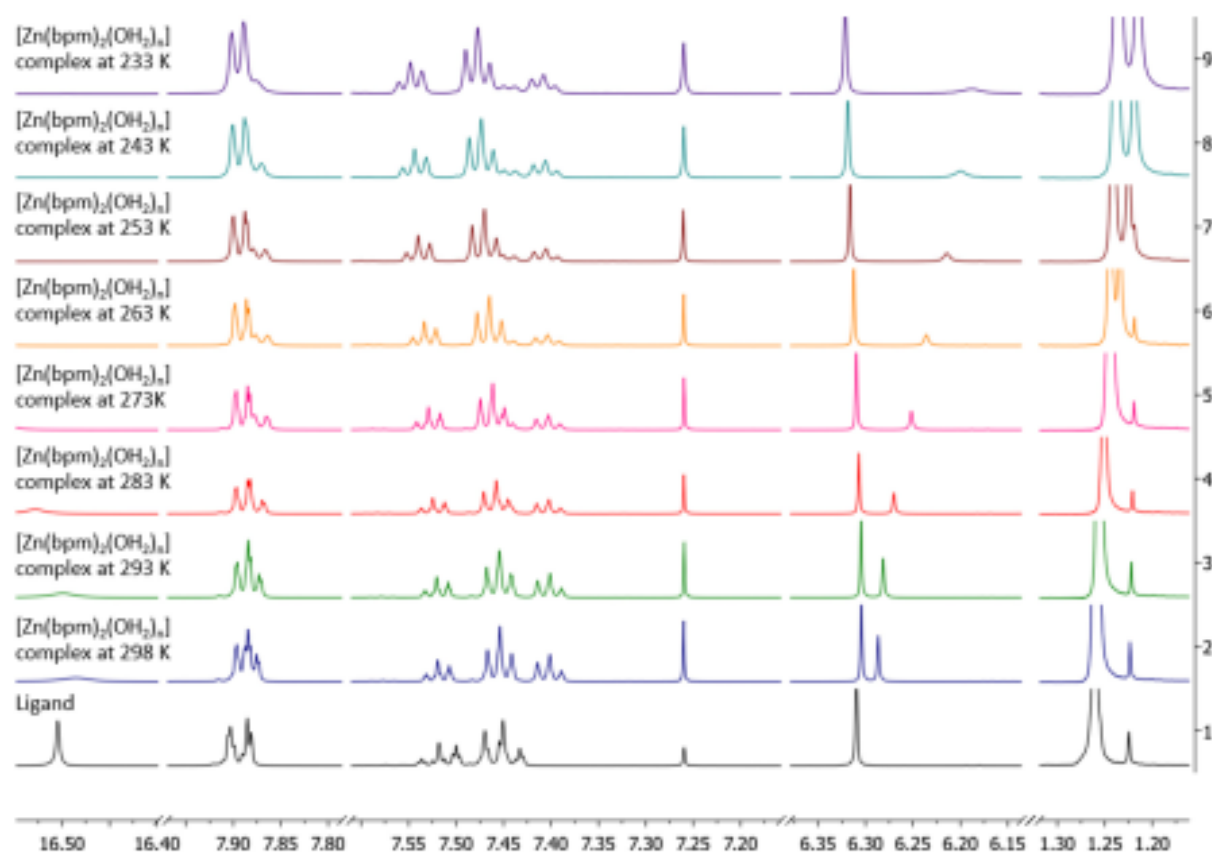


Fig. 5. Variable Temperature NMR (600 MHz) spectra for  $[\text{Zn(bpm)}_2(\text{OH}_2)_2]$  recorded in  $\text{CDCl}_3$ .



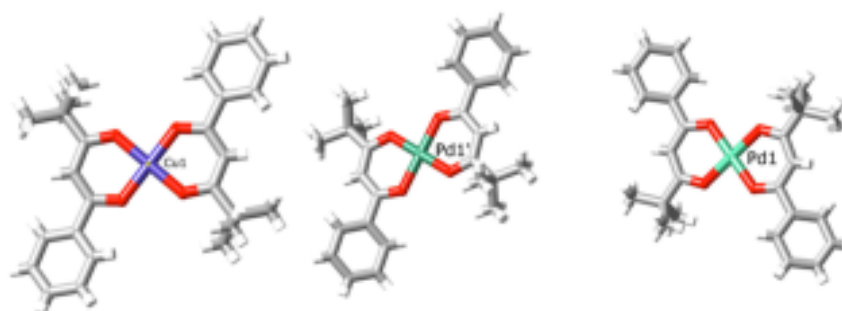


Fig. 6. Views of (left) the unique molecular unit present in the lattice of  $[\text{Cu}(\text{bpm})_2]$  and (right) the two inequivalent but very similar molecular units present in the lattice of  $[\text{Pd}(\text{bpm})_2]$ .

dal structure known for the acetylacetonate analogue [33], but in either case *cis* and *trans* isomeric forms would be possible. At room temperature, the  $^1\text{H}$  NMR spectrum of this complex shows two methine peaks with an intensity ratio of 1:1.5 (Fig. 4) but in this case their assignment to particular isomers is not possible, although the fact that a single methine peak is apparent for each species does not exclude the possibility that any  $[\text{Zn}(\text{bpm})_2(\text{OH}_2)_n]$  species could be a *cis* isomer. The nature of the  $\text{Zn}(\text{II})$  complex in chloroform solution, however, is perhaps, more complicated than expected, as its spectrum shows a significant temperature dependence (Fig. 5) in which the higher-field methine resonance shifts upfield and broadens considerably as the temperature is lowered. This possibly indicative of an equilibrium between five- and six-coordinate species rather than or as well as *cis/trans* isomerism.

While electronic absorption spectra in the visible region of the coloured complexes show d–d absorption bands at positions consistent with O-donor environments (and essentially identical to those in their acetylacetonate analogues [8–10]), these bands are broad and not readily resolved into separate isomer contributions. The much stronger UV absorptions seen in all complexes are also broad and not deconvolutable but they do illustrate the dramatic spectral changes that result from replacement of the acidic ligand proton by a metal ion (Fig. S1).

Given that at least under the conditions of synthesis and crystallisation presently applied, all the metal ions used could be considered to be labile, slow crystallisation was considered as a potential means of isolating a single species from a solution mixture. The paramagnetic  $[\text{Cu}(\text{bpm})_2]$  crystals (reported before by S.V. Borisov et al. [34]) were obtained by slow evaporation of solvent from solution of complex in a 1:1 dichloromethane/ethanol mixture. Crystals of diamagnetic  $[\text{Pd}(\text{bpm})_2]$  were obtained by diffusion in two-phase system of the complex in chloroform as the bottom layer and diethyl ether as the top layer in a closed vial. The X-ray structure of the  $[\text{Cu}(\text{bpm})_2]$  complex was the sole means of establishing its stereochemistry because its paramagnetism excluded the use of  $^1\text{H}$  NMR spectroscopy. Both complexes proved to be the expected bis(diketonate) species and to have a square-planar, *trans* geometry in the solid state [35,36]. X-ray structures of the complex units within their lattices are shown below (Fig. 6) and crystallographic data for both structures are summarised in Table 1.

Unlike their acetylacetonate analogues [37,38],  $[\text{Cu}(\text{bpm})_2]$  and  $[\text{Pd}(\text{bpm})_2]$  are not isomorphous but their lattices are nonetheless quite similar, with stacked columns of  $\text{M}(\text{bpm})_2$  units lying parallel to *a* in both (Figs. S2 and S3). Consideration of the Hirshfeld surfaces [39–41] (Figs. S4 and S5) shows that interactions between the unique  $[\text{Cu}(\text{bpm})_2]$  units do not exceed dispersion forces whereas interactions of the two, inequivalent  $[\text{Pd}(\text{bpm})_2]$  units involve, in addition to dispersion, both aromatic–CH...O and aromatic–C...O interactions that link Pd1 and Pd1' in a reciprocal manner (H5...O2' 2.670(3); C5...O1' 3.141(5) Å) along the *a* direction (Fig. S6), and aliphatic–CH...C (H13E...C3 2.872(6) Å) interactions, again reciprocal (Fig. S6) that link the Pd1 units into a two-dimensional sheet parallel to the (1 0–1) plane (Fig. S7). These differences between the  $\text{Cu}(\text{II})$  and  $\text{Pd}(\text{II})$  complexes must reflect differences in the electronic influence of the two metal ions, although the two Pd units are involved in quite different interactions, indicating that a delicate balance of factors may be operative. An interesting feature of the slipped-stack column in the  $\text{Cu}(\text{II})$  complex lattice is that it places each  $\text{Cu}(\text{II})$  symmetrically in between two phenyl rings, indicating that there may be some axial interaction, even if it does not exceed dispersion, and this could well explain the preference for the *trans* configuration of each complex unit. A similar situation clearly does not apply in the  $\text{Pd}(\text{II})$  complex lattice, where the preference for the *trans* isomer is presumably to be associated with the weak interactions beyond dispersion revealed in the Hirshfeld surface.

matic–C...O interactions that link Pd1 and Pd1' in a reciprocal manner (H5...O2' 2.670(3); C5...O1' 3.141(5) Å) along the *a* direction (Fig. S6), and aliphatic–CH...C (H13E...C3 2.872(6) Å) interactions, again reciprocal (Fig. S6) that link the Pd1 units into a two-dimensional sheet parallel to the (1 0–1) plane (Fig. S7). These differences between the  $\text{Cu}(\text{II})$  and  $\text{Pd}(\text{II})$  complexes must reflect differences in the electronic influence of the two metal ions, although the two Pd units are involved in quite different interactions, indicating that a delicate balance of factors may be operative. An interesting feature of the slipped-stack column in the  $\text{Cu}(\text{II})$  complex lattice is that it places each  $\text{Cu}(\text{II})$  symmetrically in between two phenyl rings, indicating that there may be some axial interaction, even if it does not exceed dispersion, and this could well explain the preference for the *trans* configuration of each complex unit. A similar situation clearly does not apply in the  $\text{Pd}(\text{II})$  complex lattice, where the preference for the *trans* isomer is presumably to be associated with the weak interactions beyond dispersion revealed in the Hirshfeld surface.

#### 4. Conclusions

Despite the relatively bulky nature and different electronic character of the substituents attached to the dionate unit of bpmH, there appears to be little preference in regard to the isomeric form of its homoleptic complexes in solution, although individual species can be isolated in the crystalline state. In the two cases structurally characterised, the solid state interactions associated with the preferred isomeric form are quite different, indicating that the bound metal ion has a significant and unique influence on the peripheral properties of its complex. In relation to the possible use of the phenyl ring of bpm<sup>−</sup> as a site for the introduction of an alternative metal ion binding site, it would seem that the evaluation of the resultant complexes as heterogeneous catalysts containing a single isomeric species is the most obvious starting point.

#### Acknowledgments

We thank the National Centre for Research and Development for funding – LIDER 024/391/L-5/13/NCBR/2014.

#### Conflicts of interests

The authors declare no conflict of interests.

#### Appendix A. Supplementary data

CCDC 1558066 contains the supplementary crystallographic data for  $[\text{Cu}(\text{bpm})_2]$ . CCDC 1558067 contains the supplementary

crystallographic data for [Pd(bpm)<sub>2</sub>]. These data can be obtained free of charge via <http://www.ccdc.cam.ac.uk/conts/retrieving.html>, or from the Cambridge Crystallographic Data Centre, 12 Union Road, Cambridge CB2 1EZ, UK; fax: (+44) 1223-336-033; or e-mail: [deposit@ccdc.cam.ac.uk](mailto:deposit@ccdc.cam.ac.uk). Supplementary data associated with this article can be found, in the online version, at <http://dx.doi.org/10.1016/j.poly.2017.08.022>.

## References

- [1] J.-M. Lehn, *Supramolecular Chemistry: Concepts and Perspectives*, VCH, Weinheim, 1995, <http://dx.doi.org/10.1002/adma.19960081029>.
- [2] B. Dietrich, P. Vioat, J.-M. Lehn, *Macrocyclic Chemistry*, VCH, Weinheim, 1993, <http://dx.doi.org/10.1002/adma.19930051023>.
- [3] A.J. McConnell, C.S. Wood, P.P. Neelakandan, J.R. Nitschke, Stimuli-responsive metal-ligand assemblies, *Chem. Rev.* 115 (2015) 7729, <http://dx.doi.org/10.1021/acs00632f>.
- [4] R.M. Pike, 1,3-Diketone compounds of the non-metallic elements, *Coord. Chem. Rev.* 2 (1967) 163, [http://dx.doi.org/10.1016/S0010-8545\(00\)80087-9](http://dx.doi.org/10.1016/S0010-8545(00)80087-9).
- [5] D.P. Cradock, Divalent transition metal  $\beta$ -keto-enolate complexes as Lewis acids, *Coord. Chem. Rev.* 4 (1969) 1, [http://dx.doi.org/10.1016/S0010-8545\(00\)80090-9](http://dx.doi.org/10.1016/S0010-8545(00)80090-9).
- [6] D. Gibson, Carbon-bonded  $\beta$ -diketone complexes, *Coord. Chem. Rev.* 4 (1969) 225, [http://dx.doi.org/10.1016/S0010-8545\(00\)80087-9](http://dx.doi.org/10.1016/S0010-8545(00)80087-9).
- [7] J.J. Fortman, R.E. Sievers, Optical and geometrical isomerism of  $\beta$ -diketone complexes, *Coord. Chem. Rev.* 6 (1971) 331, [http://dx.doi.org/10.1016/S0010-8545\(00\)80013-2](http://dx.doi.org/10.1016/S0010-8545(00)80013-2).
- [8] S. Kawaguchi, Variety in the Coordination Modes of  $\beta$ -Dicarbonyl Compounds in Metal Complexes, *Coord. Chem. Rev.* 70 (1986) 51, [http://dx.doi.org/10.1016/S0010-8545\(86\)80035-2](http://dx.doi.org/10.1016/S0010-8545(86)80035-2).
- [9] A.R. Seidle, in: W. Kaim, G. McCleverty Jr., G. Gillard (Eds.), *Comprehensive Coordination Chemistry I*, Pergamon Press, Oxford, 1987, vol. 2, Ch. 15.4, 365.
- [10] C. Pettinari, F. Marchetti, A. Donzova, in: W. Kaim, G. McCleverty Jr., G. Gillard (Eds.), *Comprehensive Coordination Chemistry II*, Elsevier, London, 2003, vol. 1, Ch. 1.7, 97.
- [11] P.A. Vigato, V. Peruzzo, S. Tamburini, The evolution of  $\beta$ -diketone or  $\beta$ -diketophenol ligands and related complexes, *Coord. Chem. Rev.* 253 (2009) 1099, <http://dx.doi.org/10.1016/j.ccr.2008.07.013>.
- [12] D.A. Wroblewski, C.S. Day, B.A. Goodman, T.B. Rauchfuss, Synthesis and Characterization of Heterobimetallic Complexes Derived from  $\beta$ -diketone ligands, *J. Am. Chem. Soc.* 106 (1984) 5464, <http://dx.doi.org/10.1021/ja00331a014>.
- [13] D.A. Wroblewski, S.R. Wilson, T.B. Rauchfuss, Synthesis of a mixed-valence copper complex via free-radical additions to a Copper(I) dimer, *Inorg. Chem.* 21 (5) (1982) 2114, <http://dx.doi.org/10.1021/ic00135a086>.
- [14] J.K. Clegg, L.F. Lindoy, J.C. McMurtrie, D. Schiller, Dinuclear bis- $\beta$ -diketonato ligand derivatives of iron(III) and copper(II) and use of the latter as components for the assembly of extended metallo-supramolecular structures, *Dalton Trans.* (2005) 857, <http://dx.doi.org/10.1039/B418870E>.
- [15] A.D. Terent'ev, I.A. Yaramenko, V.A. Vil, L.K. Moiseev, S.A. Kon'kov, V.M. Dembitsky, D.D. Levitsky, G.I. Nikishin, Phenanthrolydic and phosphotungstic acids as efficient catalysts for the synthesis of bridged 1,2,4,5-tetraoxanes from  $\beta$ -diketones and hydrogen peroxide, *Org. Biomol. Chem.* 11 (2013) 2613, <http://dx.doi.org/10.1039/C3OB27239g>, and references therein.
- [16] M. Dudek, J.K. Clegg, C.R.K. Glasson, N. Kelly, K. Gloe, K. Gloe, A. Kelling, H.-J. Buschmann, K.A. Jolliffe, L.F. Lindoy, G.V. Meehan, Interaction of Copper(II) with ditopic pyridyl- $\beta$ -diketone ligands: dimeric, framework and metallogel structures, *Cryst. Growth Des.* 11 (2011) 1697, <http://dx.doi.org/10.1021/cg101629w>.
- [17] E. Kwiakowski, Z. Peprinski, Metal benzoylpivaloylmethanates, Part I. Free ligands and copper(II) chelates, *Transition Met. Chem.* 3 (1978) 305, <http://dx.doi.org/10.1007/BF01393576>.
- [18] E. Kwiakowski, W. Nowicki, Metal Benzoylpivaloylmethanates, Part III. Manganese(III) and Iron(III) Chelates, *Transition Met. Chem.* 12 (1987) 546, <http://dx.doi.org/10.1007/BF01023846>, and references therein.
- [19] T.B. Rauchfuss, S.R. Wilson, D.A. Wroblewski, Synthesis and Structure of a "Dicuprophane", a Dicopper(I) Complex derived from  $\beta$ -diketone ligands, *J. Am. Chem. Soc.* 103 (1981) 6760, <http://dx.doi.org/10.1021/ja00412a050>.
- [20] D.J. Bray, J.K. Clegg, L.F. Lindoy, D. Schiller, Self-assembled metallo-supramolecular systems incorporating  $\beta$ -diketone motifs as structural elements, *Adv. Inorg. Chem.* 59 (2006) 1, [http://dx.doi.org/10.1016/S0898-8838\(06\)50001-4](http://dx.doi.org/10.1016/S0898-8838(06)50001-4).
- [21] G. Aromi, P. Gomez, R. Van Eldik, Poly- $\beta$ -diketonates: prime ligands to generate supramolecular metalloblocks, *Coord. Chem. Rev.* 252 (2008) 964, <http://dx.doi.org/10.1016/j.ccr.2007.07.008>.
- [22] J.K. Clegg, M.J. Hayter, K.A. Jolliffe, L.F. Lindoy, J.C. McMurtrie, G.V. Meehan, S.M. Neville, S. Parsons, P.A. Tasker, P. Turner, F.J. White, New discrete and polymeric supramolecular architectures derived from Cu(II), Ni(II) and Cu(II) complexes of aryl-linked bis- $\beta$ -diketonato ligands and nitrogen bases: synthetic structural and high pressure studies, *Dalton Trans.* 39 (2010) 2804, <http://dx.doi.org/10.1039/B920199H>.
- [23] F. Li, J.K. Clegg, L.F. Lindoy, R.R. Macquart, G.V. Meehan, Metallo-supramolecular Self-assembly of a Universal 3-Ravel, *Nat. Commun.* 2 (2011) 1208, <http://dx.doi.org/10.1038/ncomms1208>.
- [24] G.S. Hammond, D.C. Nonhebel, C.-H. Wu, Chelates of  $\beta$ -diketonates, V. Preparation and properties of chelates containing sterically hindered ligands, *Inorg. Chem.* 2 (1963) 73, <http://dx.doi.org/10.1021/ic50055a021>.
- [25] H.D. Murdoch, D.C. Nonhebel, Acylation of metal chelates. Part IV. Electronic effects in the acylating agent, *J. Chem. Soc.* (1968) 2298, <http://dx.doi.org/10.1039/J9680002298>.
- [26] P. Šimůnek, V. Bertolani, V. Macháček, Diazonium exchange and migration of pivaloyl group upon azo coupling of  $\beta$ -aminones, *Eur. J. Org. Chem.* (2013) 5683, <http://dx.doi.org/10.1002/ejoc.201300534>.
- [27] CrysalisPro: Agilent Technologies, Yarnton, Oxfordshire (2009–2011).
- [28] O.V. Dolomanov, L.J. Bourhis, R.J. Gildea, J.A.K. Howard, H. Puschmann, OLEX2: a complete structure solution, refinement and analysis program, *J. Appl. Crystallogr.* 42 (2009) 339, <http://dx.doi.org/10.1107/S0021889809004726>.
- [29] G. Sheldrick, A short history of SHELX, *Acta Cryst. Sect. A* 64 (2008) 112, <http://dx.doi.org/10.1107/S0108767307043930>.
- [30] A. Döhning, R. Goddard, P.W. Jolly, C. Krüger, V.R. Polyakov, Monomer-Trimer isomerism in 3-substituted Pentane-2,4-dione Derivatives of Nickel(II), *Inorg. Chem.* 36 (1997) 177, <http://dx.doi.org/10.1021/ic960441c>, and references therein.
- [31] F.A. Cotton, J.J. Wise, The crystal and molecular structure of bis(2,2,6,6-tetramethylheptane-3,5-dionato)nickel(II), *Inorg. Chem.* 5 (1966) 1200, <http://dx.doi.org/10.1021/ic50041a028>.
- [32] F.A. Cotton, J.P. Fackler Jr., Molecular association and electronic structures of nickel(II) chelates. I. Complexes of 2,4-pentanedione and 1,5-substituted derivatives, *J. Am. Chem. Soc.* 83 (1961) 2818, <http://dx.doi.org/10.1021/ja01474a008>.
- [33] H. Montgomery, E.C. Lingafelter, The crystal structure of monoacquebis(acetylacetonato)zinc(II), *Acta Cryst.* 16 (1963) 748, <http://dx.doi.org/10.1107/S0365110X6300195X>.
- [34] I.A. Baidina, P.A. Stabnikov, L.K. Igumenov, S.V. Borisov, *Koordinatsionnaya khimiya* 15 (1989) 763.
- [35] J.K. Clegg, K. Gloe, M.J. Hayter, O. Kataeva, Leonard F. Lindoy, L.F. Moubarak, B. McMurtrie, J.C. Murray, K.S. Schiller, New discrete and polymeric supramolecular architectures derived from dinuclear bis- $\beta$ -diketonato)copper(II) metalloblocks, *Dalton Trans.* (2006) 3977, <http://dx.doi.org/10.1039/B606523f>.
- [36] J.W. Seo, M. Niemeyer, trans-Bis(1,1,1,1-tetrakis(4-oxo-3-phenylbut-3-en-2-yl)oxy)copper(II), *Acta Cryst. E* 62 (2006) m1863, <http://dx.doi.org/10.1107/S1600536806027073>.
- [37] P.C. Lebrun, W.D. Lyon, H.A. Kaska, Crystal structure of bis(2,4-pentanedionato)copper(II), *J. Crystallogr. Spectroscop. Res.* 16 (1986) 889, <http://dx.doi.org/10.1007/BF01188194>, and references therein.
- [38] M. Hamid, M. Zeller, A.D. Hunter, M. Mazhar, A.A. Tahir, Redetermination of bis(2,4-pentanedionato)palladium(II), *Acta Cryst. E* 61 (2005) m2181, <http://dx.doi.org/10.1107/S1600536805006902>, and references therein.
- [39] M.A. Spackman, D. Jayatilaka, Hirshfeld surface analysis, *Cryst. Eng. Comm.* 11 (2009) 19, <http://dx.doi.org/10.1039/B818330A>.
- [40] M.A. Spackman, *Molecules in Crystals*, Phys. Scr. 87, (2013), 048103 (12p.).
- [41] S.K. Wolff, D.J. Grimwood, J.J. McKinnon, M.J. Turner, D. Jayatilaka, M.A. Spackman, *CrystalExplorer 3.1*, University of Western Australia, 2012.



## Supplementary information to **A1**

SUPPLEMENTARY MATERIAL

*Unsymmetrical bidentate ligands as a basis for construction of ambidentate ligands for functional materials: Properties of 4,4-dimethyl-1-phenylpentane-1,3-dionate*

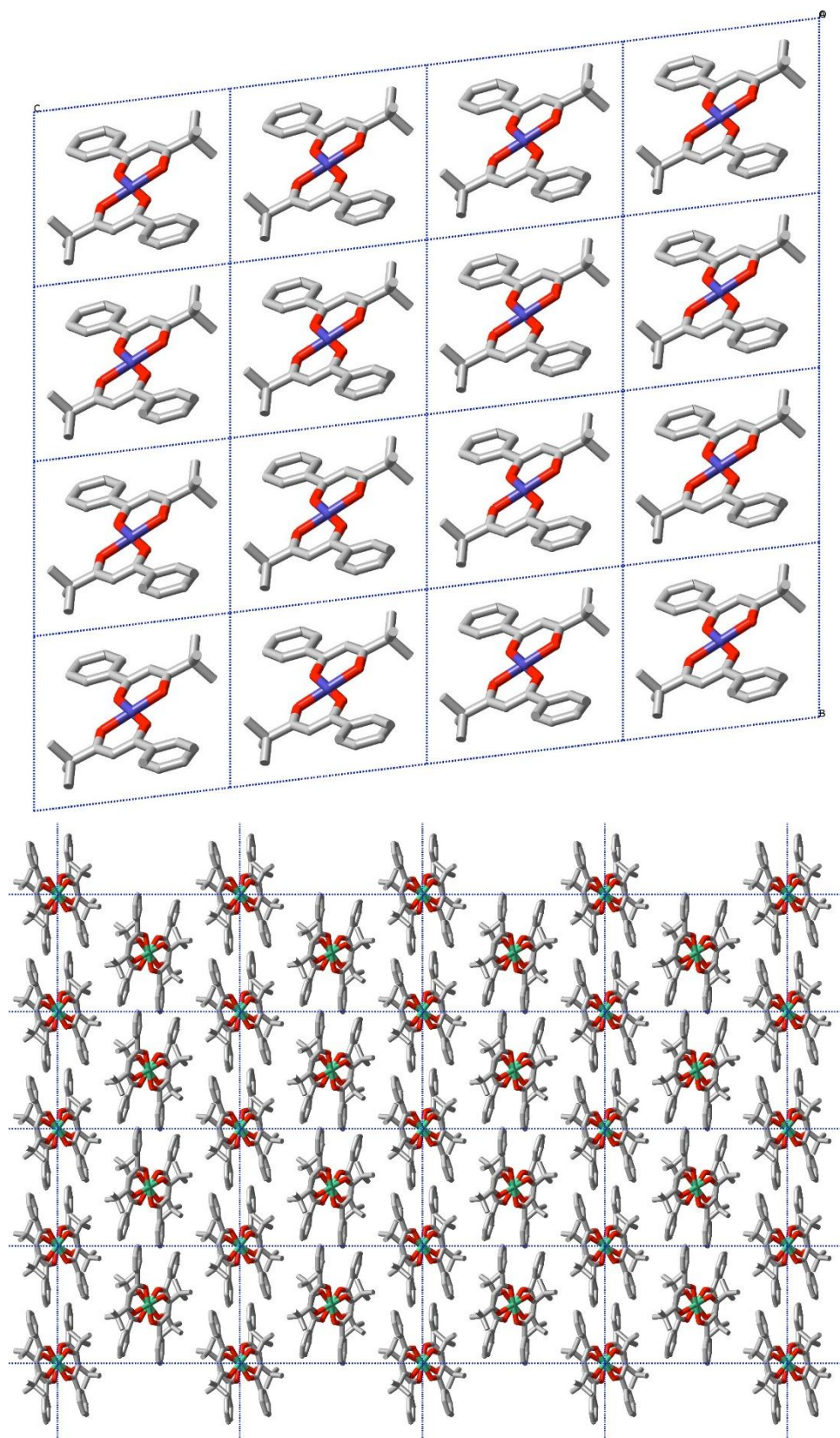


**Figure S1.** Partial views, down *a*, of the lattices of (upper)  $[\text{Cu}(\text{bpm})_2]$  and (lower)  $[\text{Pd}(\text{bpm})_2]$ , H-atoms omitted for clarity. Each complex unit represents the projection of a column of such units lying parallel to the *a* axis. For Pd, two inequivalent units alternate down the columns.

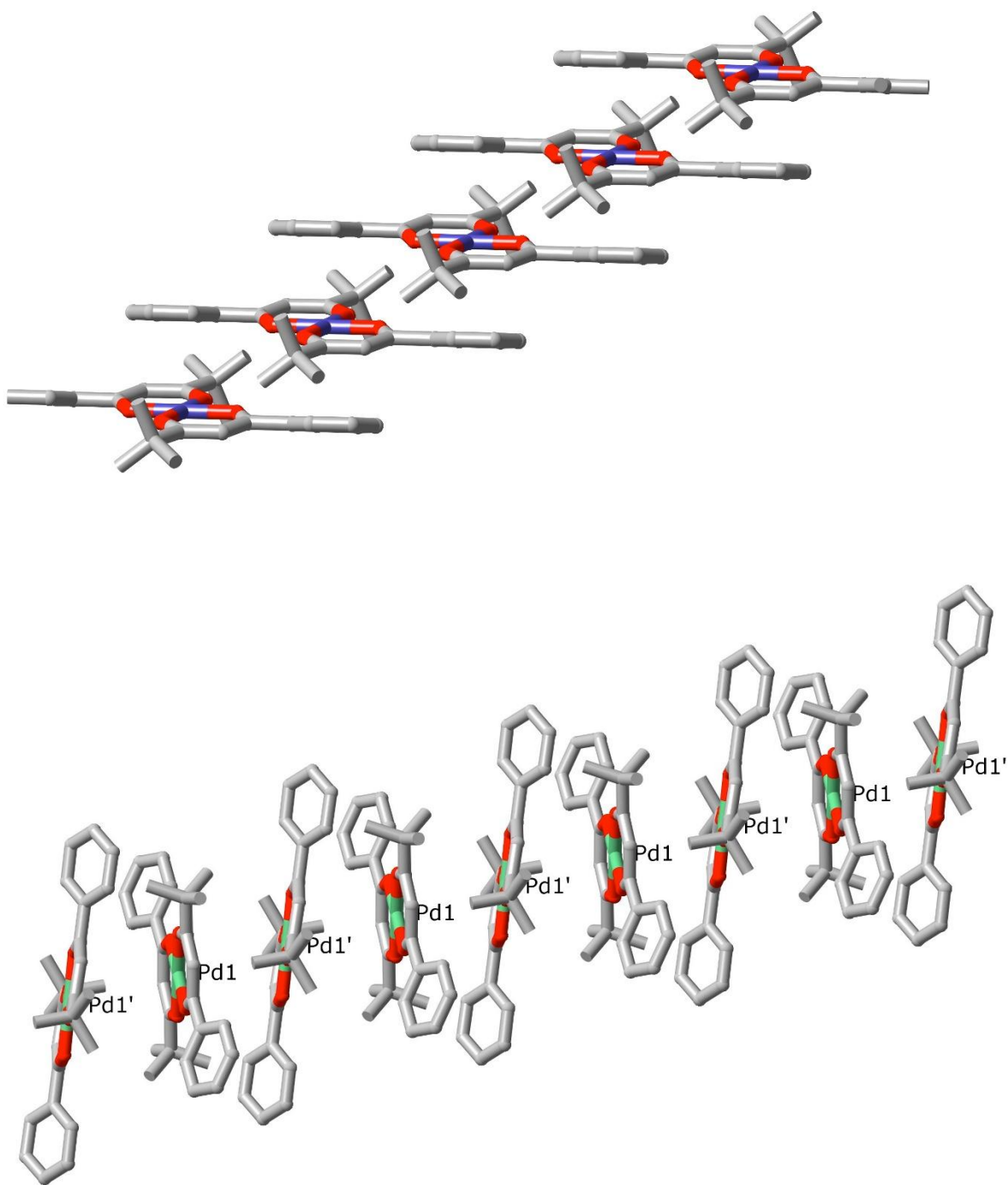


**Figure S2.** Partial perspective views of the slipped-stack columns parallel to *a* in the lattices of (upper)  $[\text{Cu}(\text{bpm})_2]$  and (lower)  $[\text{Pd}(\text{bpm})_2]$ , H-atoms again omitted for clarity.

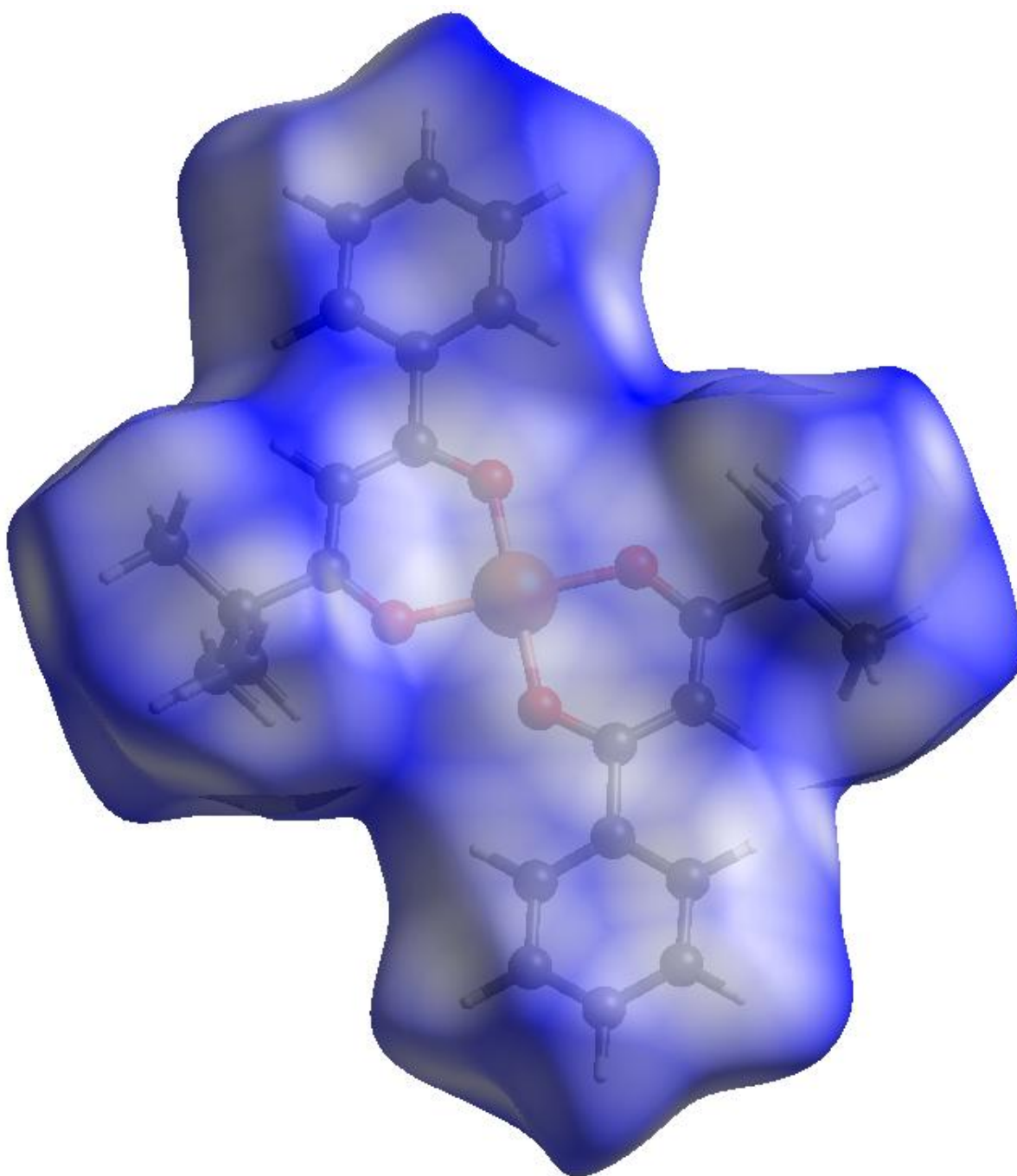


**Figure S3.** The Hirshfeld surface calculated using CrystalExplorer for the  $[\text{Cu}(\text{bpm})_2]$  unit in its crystal lattice

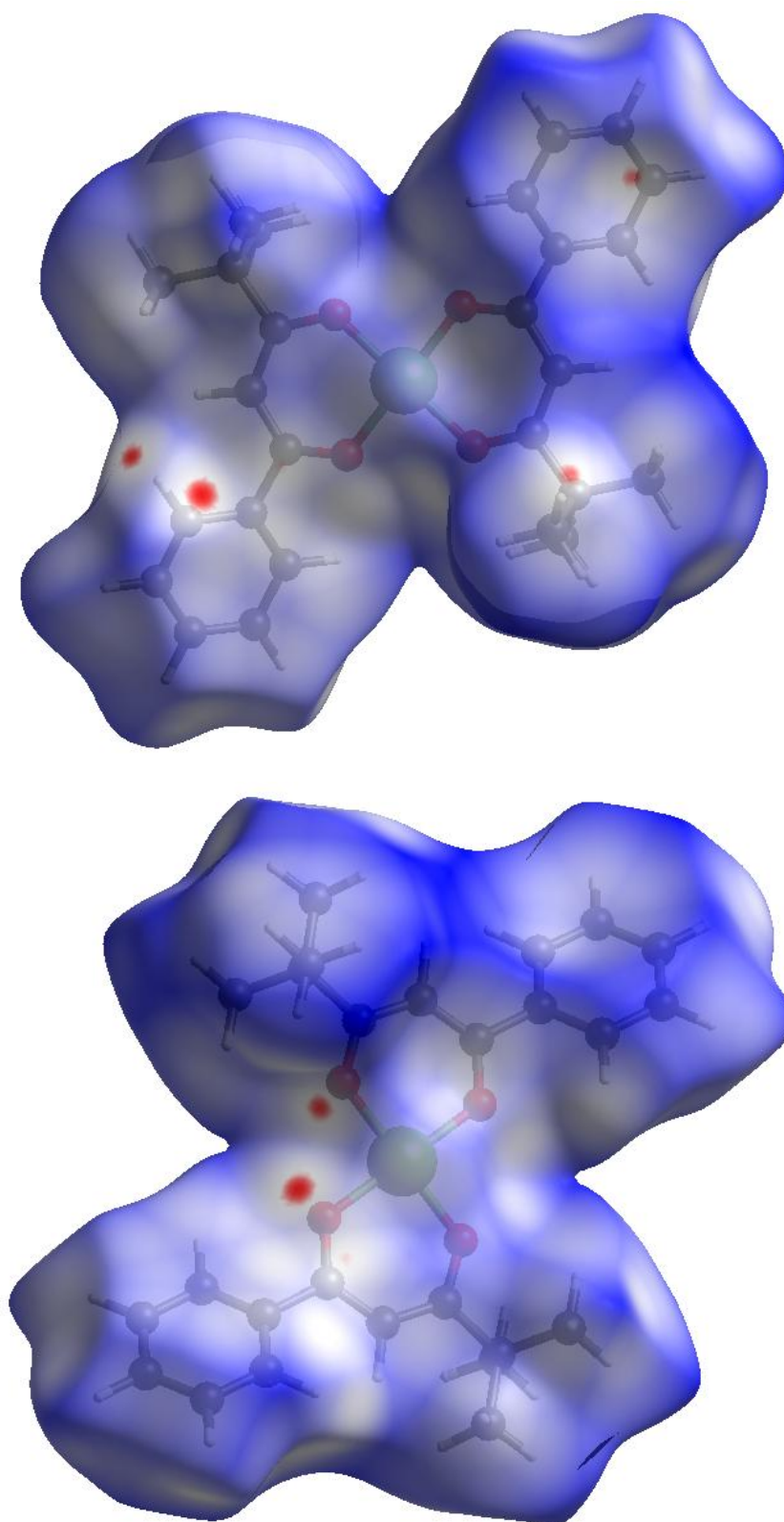


**Figure S4.** Hirshfeld surfaces calculated for the  $[\text{Pd}(\text{bpm})_2]$  units containing (upper) Pd1 and (lower) Pd1'. Red regions indicates points where interactions with atoms of adjacent units exceed those of dispersion.



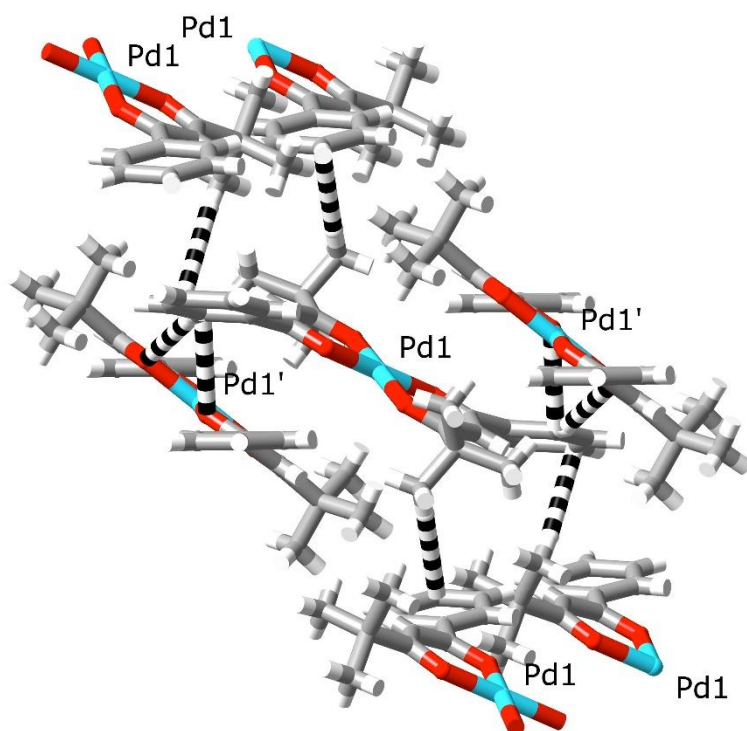


**Figure S5.** View of the aromatic-CH...O, aromatic-C...O and aliphatic-CH...aromatic-C interactions (black and white dashed lines) associated with the columnar and sheet structures found within the lattice of  $[Pd(\text{bpm})_2]$ .

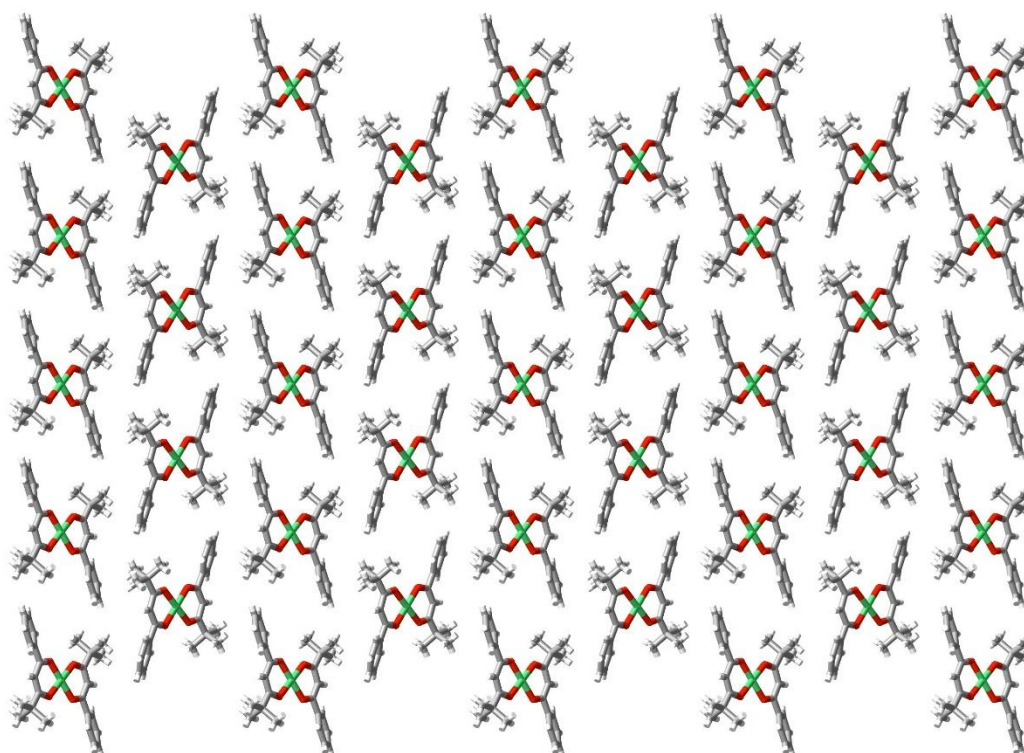


**Figure S6.** Partial view of one sheet of  $[Pd(\text{bpm})_2]$  units incorporating Pd1 lying parallel to the (1 0 -1) plane

## **A2. Charge Neutral $[\text{Cu}_2\text{L}_2]$ and $[\text{Pd}_2\text{L}_2]$ Metallocycles: Self-Assembly, Aggregation, and Catalysis**



Charge Neutral  $[\text{Cu}_2\text{L}_2]$  and  $[\text{Pd}_2\text{L}_2]$  Metalloclusters: Self-Assembly, Aggregation, and Catalysis

Michał Kołodziejewski, Aidan J. Brock, Gracjan Kurpiak, Anna Walczak, Feng Li, Jack K. Clegg,\* and Artur R. Stefankiewicz\*

Cite This: *Inorg. Chem.* 2021, 60, 9673–9679

Read Online

ACCESS |



Metrics &amp; More

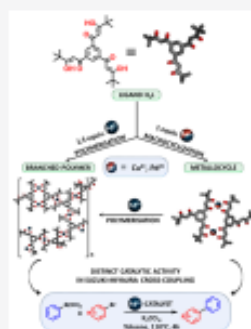


Article Recommendations



Supporting Information

**ABSTRACT:** A range of morphologically distinct metallosupramolecular  $\text{Cu}(\text{II})$  and  $\text{Pd}(\text{II})$  complexes has been constructed, based on the tritopic ligand 1,1',1''-(benzene-1,3,5-triyl)tris(4,4-dimethylpentane-1,3-dione) ( $\text{H}_3\text{L}$ ). By control of the reaction conditions, it is possible to generate distinct coordination assemblies possessing either macrocyclic or polymeric structures and more importantly distinct activity in catalysis of the Suzuki–Miyaura cross-coupling.



## INTRODUCTION

The self-assembly of complex metallosupramolecular architectures from simple metal and organic components<sup>1–4</sup> has yielded a range of interesting and intricate structures with a wide range of applications.<sup>5–13</sup> These structures can be polymeric or discrete and often display unusual topologies and properties that are not present in their constituent building blocks.<sup>14</sup> They have been shown, for example, to display a wide range of guest-binding, catalysis, and storage/separation uses.<sup>12,15–17</sup> The design of the building blocks that are programmed to assemble into these architectures plays a crucial role in determining both the form and function of the resulting metallosupramolecular complexes. It has been shown that ligands incorporating multiple  $\beta$ -diketone groups can be reacted with certain metal ions to form a series of metallosupramolecular structures with a significant degree of predictability.<sup>14,18–28</sup> The resulting structures include helicates,<sup>29,30</sup> tetrahedra,<sup>31–33</sup> and interlocked assemblies,<sup>23,34</sup> as well as stimuli-responsive<sup>24</sup> and exceptionally porous polymeric systems.<sup>35,36</sup>

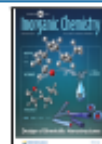
Here, we present an investigation into the tritopic  $\beta$ -diketone ligand  $\text{H}_3\text{L}$  and its interaction with both copper(II) and palladium(II) ions. The coordination of similar ligands with iron(III) and gallium(III) by Saalfrank and Raymond produced charge-neutral  $[\text{M}_4\text{L}_4]$  tetrahedral and  $[\text{M}_6\text{L}_6]$  trigonal antiprismatic assemblies,<sup>37,38</sup> however, no investigations into the use of divalent metals have been previously reported. Along with the synthesis and structural characterization of these systems, we present investigations into the use

of the  $\text{Pd}(\text{II})$  complexes as catalysts in Suzuki–Miyaura cross-coupling.

We anticipated that the reaction of  $\text{H}_3\text{L}$  with divalent metal ions in a 1:1 ratio would lead to the formation of charge-neutral metallosupramolecular complexes of type  $[\text{M}_2(\text{HL})_2]$ , which contain two noncoordinated  $\beta$ -diketone moieties as side chains. These groups could then be used to probe the controlled oligomerization of the metallosupramolecular complexes via hierarchical self-assembly<sup>36</sup> to form complex assemblies of the type  $\{[\text{M}_2(\text{L})_2]\}_n$ <sup>14,19,21</sup> by the reaction with further divalent metal ions, thus allowing, for example, a comparison of the catalytic performance of both the discrete and oligomeric assemblies in palladium(II)<sup>39,40</sup> catalyzed cross-coupling reactions (Figure 1).<sup>41–47</sup> The excellent catalytic properties of palladium and its complexes have been known for many years.<sup>47–49</sup> Palladium creates a number of versatile homo- as well as heterogeneous catalysts that are used in many processes, such as dehydrogenation,<sup>50</sup> hydrogenation,<sup>51</sup> and cross-coupling reactions (e.g., Heck,<sup>52,53</sup> Suzuki–Miyaura,<sup>54</sup> and Negishi–Miyaura<sup>55,56</sup> reactions). Such studies might provide insight into new approaches to boost the reactivity of such catalysts,<sup>52,54,57</sup> especially in nanoenvironments<sup>58</sup> or supramolecular dendrimeric systems.<sup>59</sup>

Received: March 29, 2021

Published: June 11, 2021



ACS Publications

© 2021 American Chemical Society

9673

<https://doi.org/10.1021/acs.inorgchem.1c00967>  
*Inorg. Chem.* 2021, 60, 9673–9679

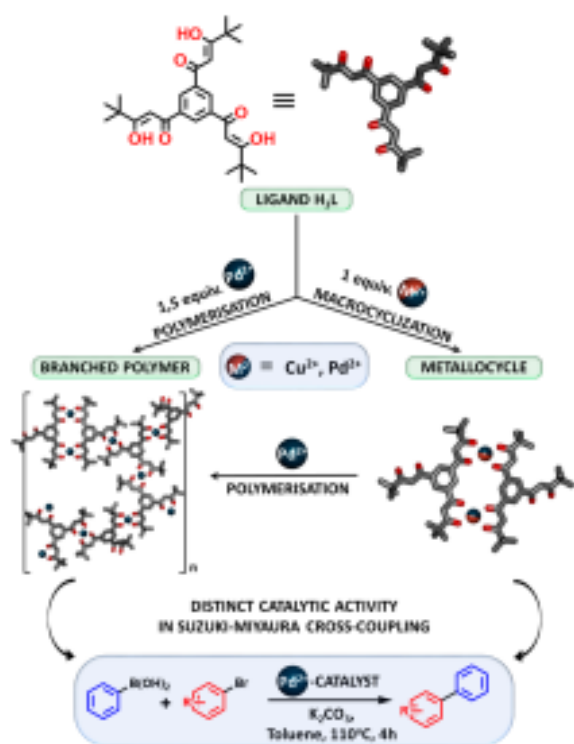


Figure 1. Metal-ion induced conversion between tripodal ligand  $H_3L$  and structurally different metallosupramolecular assemblies.

## RESULTS AND DISCUSSION

The tripodal ligand  $H_3L$  was prepared via a Claisen condensation between triethyl benzene-1,3,5-tricarboxylate and pinacolone in the presence of sodium hydride by adapting a previously reported procedure.<sup>60</sup> The  $^1H$  NMR spectrum in deuterated chloroform ( $CDCl_3$ ) indicated that the ligand

resides predominantly (94%) in its enol form (Figure 2a, see SI, Figure S1). X-ray quality crystals were grown by the slow evaporation of a THF solution, and then the structure was determined (Figure 3 and Figures S8 and S9, Table T1). The

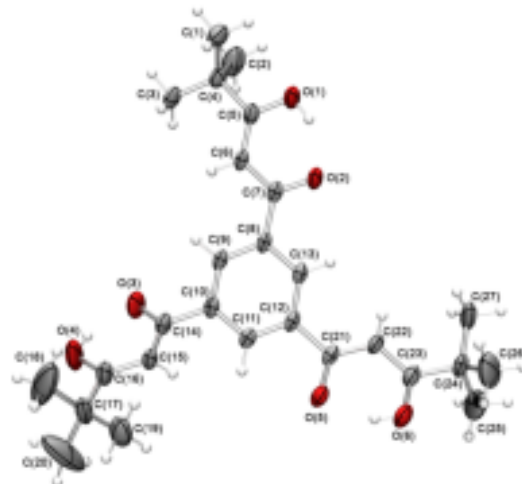


Figure 3. X-ray crystal structure of  $H_3L$  shown with 50% probability ellipsoids. Regions of disorder not shown for clarity.

ligand crystallizes in approximately  $C_3$  symmetry with each of the  $\beta$ -diketone groups in their enol form. The enol hydrogen atom in each case is located between the two oxygen atoms, forming a six-membered intramolecular hydrogen bonding ring, which has been observed in a large number of related structures.<sup>21,40–62</sup> The reaction of one equivalent of  $CuCl_2$  with one equivalent of  $H_3L$  in THF in the presence of solid sodium carbonate followed by filtration produced a dark green solution. Slow evaporation of the reaction solution produced crystals suitable for diffraction studies (Figure 4). The crystal structure confirmed the formation of the desired

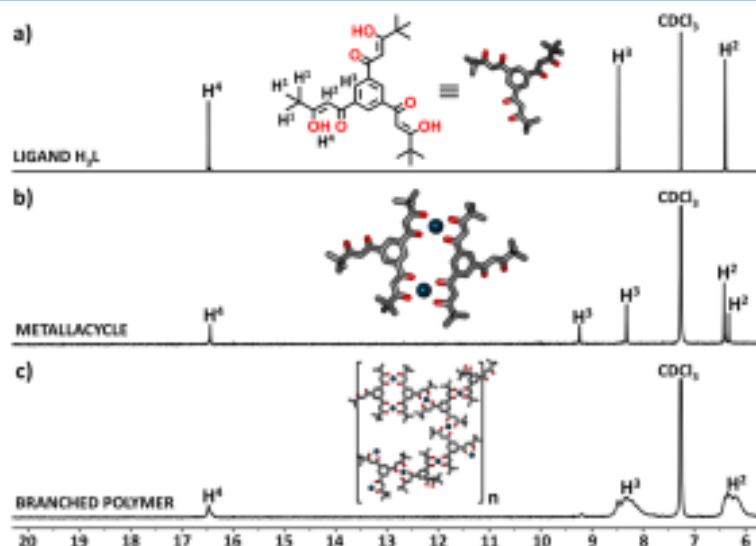


Figure 2. Comparison of  $^1H$  NMR spectra of ligand  $H_3L$  (a), metallosupramolecular macrocycle  $[Pd_2(HL)_2]$  (b), and branched polymer  $[Pd_3L_2]_n$  (c) recorded in  $CDCl_3$  at room temperature. Aliphatic region omitted for clarity.

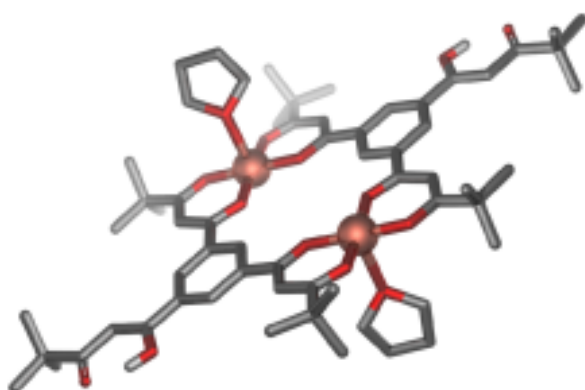


Figure 4. X-ray crystal structure of  $[\text{Cu}_2(\text{HL})_2(\text{THF})_2]$ . H atoms (except enol H) have been omitted for clarity.

$[\text{Cu}_2(\text{HL})_2(\text{THF})_2]$  dimeric metallocycle. The copper(II) centers are positioned between two ligands and adopt a square pyramidal coordination geometry with the  $\beta$ -diketone oxygens occupying the basal plane and a THF solvent molecule bound in the distal apical positions of each of the metal ions. The uncoordinated  $\beta$ -diketone unit is again present in its enol tautomer.

A similar procedure was applied using  $[\text{PdCl}_2(\text{MeCN})_2]$  in place of the copper salt, which led to the isolation of a yellow solid after workup. The  $^1\text{H}$  NMR was consistent with the formation of  $[\text{Pd}_2(\text{HL})_2]$ , with two aromatic proton signals (9.24 and 8.32 ppm) and two methine protons (6.42 and 6.32 ppm; Figure 2b, see SI, Figure S5), both in a 2:1 ratio, as expected for this structure. An enol proton signal at 16.44 ppm confirmed that the third  $\beta$ -diketone arm remains unbound by the metal ion. The formation of the  $[\text{Pd}_2(\text{HL})_2]$  species was also confirmed by TOF-MS analysis, which gave peaks at  $m/z = 1121.27$  for the macrocyclic complex ion  $[\text{Pd}_2(\text{L})(\text{HL})]^-$  and  $m/z = 1157.25$  for its adduct with the chloride anion— $([\text{Pd}_2(\text{HL})_2]\text{Cl})^-$  (see SI, Figures S14–S16). Diffusion ordered spectroscopy experiments (DOSY) were performed on both  $\text{H}_3\text{L}$  and  $[\text{Pd}_2(\text{HL})_2]$  (Table 1, entries 1

Table 1. DOSY NMR Data for Ligand, Metallosupramolecular Complex, and Metallosupramolecular Polymers

entry	compounds	$D$ [ $\text{m}^2 \text{s}^{-1}$ ] <sup>a</sup>	$r_{\text{sd}}$ [Å] <sup>b</sup>	$V_{\text{sp}}$ [Å <sup>3</sup> ] <sup>c</sup>
1	HL	$1.25 \times 10^{-9}$	3.26	144.99
2	$[\text{Pd}_2(\text{HL})_2]$	$6.27 \times 10^{-10}$	6.50	1148.87
3	$[\text{Pd}_3\text{L}_2]_n$	$2.51 \times 10^{-10}$	16.23	17908.20

<sup>a</sup>Diffusion coefficient. <sup>b</sup>Solvodynamic radius. <sup>c</sup>Spherical volume.

and 2). The ligand has a diffusion coefficient of  $D = 1.25 \times 10^{-9} \text{ m}^2 \text{s}^{-1}$ , which corresponds to a solvodynamic radius of 3.26 Å and a volume of 144.99 Å<sup>3</sup> when a spherical structure model is used (see SI, Figure S7). In contrast, experimental values obtained for  $[\text{Pd}_2(\text{HL})_2]$  suggest that the complex is 2 times larger (radius 6.50 Å) than the ligand. These data are fully consistent with the sizes of both  $\text{H}_3\text{L}$  and the  $[\text{Cu}_2(\text{HL})_2(\text{THF})_2]$  complex measured in the solid state by X-ray diffraction.

Next the formation of a polymeric structure was performed by reacting 1.5 equiv of  $\text{CuCl}_2$  with 1 equiv of  $\text{H}_3\text{L}$  under basic conditions. This yielded a mixture of products consisting

mainly of an intractable and insoluble green powder, suggesting the formation of a coordination polymer and a small quantity of the soluble  $[\text{Cu}_2(\text{HL})_2(\text{THF})_2]$  metallocycle. To our delight, similar reactions with Pd(II) produced a soluble product.  $[\text{Pd}_3\text{L}_2]_n$  was formed as a result of a one-step reaction of 1 equiv of a ligand with 1.5 equiv of Pd(II) salt in an alkaline (6 equiv of triethylamine) environment. The  $^1\text{H}$  NMR spectrum of the isolated material recorded in  $\text{CDCl}_3$  showed a broad and highly overlapped set of signals for all of the aromatic and methine protons (around 8.31 and 6.33 ppm, respectively; Figure 2c, see SI, Figure S6). This broadening is characteristic of and consistent with the presence of complex metallosupramolecular assemblies. The spectrum also contained a signal from the enol group of a diketone moiety at  $\delta = 16.46$ , and the low integral of this signal (only 10%) showed that unreacted diketone arms remained at this stage of the self-assembly process, possibly as a result of the creation of a complex branched oligomeric structure. This is supported by DOSY experiments (Table 1, entry 3), which indicated that the oligomeric complex  $[\text{Pd}_3\text{L}_2]_n$  has a radius 5 times larger (16.23 Å) than the uncoordinated ligand  $\text{H}_3\text{L}$  and almost 3 times larger than the metallocycle (Table 1). Thermogravimetric analysis (TGA) showed that the thermal decomposition of the entire polymer structure occurs in a single step, albeit across a relatively wide temperature range (see SI, Figures S19, S20). This indicates that the breakdown of the polymer structure is steady over a given period of time. We also performed TOF-MS analysis for  $[\text{Pd}_3\text{L}_2]_n$  which showed a set of peaks corresponding to the breakdown products of the polymer during the analysis (see SI, Figure S17).

Due to the differences in the structure and composition of the investigated Pd(II) complexes, catalytic studies have been undertaken in order to test and compare their catalytic activity in the Suzuki–Miyaura cross-coupling reaction. First, the use of  $[\text{Pd}_2(\text{HL})_2]$  as catalyst for the coupling between phenylboronic acid and 4-bromoacetophenone was optimized. It was found that the highest GC yields were obtained in toluene at 110 °C using  $\text{K}_2\text{CO}_3$  as a base. Although 0.1 mol % Pd was required, almost 100% conversion was achieved after just 4 h (see Table T2 in the SI). At the next stage, we investigated the scope and limitations of the catalyst. A series of reactions between phenylboronic acid and various functionalized aryl bromides was performed, obtaining moderate to high GC yields for the products 1a–12a (see Table 2). All the reactions were repeated using the polymer  $[\text{Pd}_3\text{L}_2]_n$  as a catalyst under the same conditions. Very high GC yields (>80%) were obtained in most cases and, on average, 10–20% higher than in the corresponding reactions catalyzed by the metallocycle  $[\text{Pd}_2(\text{HL})_2]$ . The high efficiency was observed regardless of the presence of electron donating or electron withdrawing functional groups in the substrate molecules. In contrast, yields of only 12% and 35% for the pyridine derivative 9a revealed a limitation of this procedure. Entry 10a showed that the Suzuki–Miyaura reaction is clearly preferred, since the Heck coupling product, also possible under these conditions, was only observed in trace amounts. We then compared the performance of our catalysts under the same reaction conditions using  $[\text{PdCl}_2(\text{PPh}_3)_2]$ , which illustrates the high catalytic activity of both  $[\text{Pd}_2(\text{HL})_2]$  and  $[\text{Pd}_3\text{L}_2]_n$  (see Table T3 in the SI).

The structural and compositional differences between macrocyclic  $[\text{Pd}_2(\text{HL})_2]$  and polymeric  $[\text{Pd}_3\text{L}_2]_n$  species, incorporating a different quantity of Pd(II) cations per



**Table 2.** Scope of the Suzuki–Miyaura Cross-Coupling Reaction between Aryl Bromides and Phenylboronic Acid<sup>a,d</sup>

M: 75%	M: 67%	M: 72%
P: 85%	P: 83%	P: 80%
M: 94%	M: 81%	M: 67%
P: 100%	P: 84%	P: 85%
M: 91%	M: 57%	M: 12%
P: 98%	P: 80%	P: 35%
M: 61%	M: 59%	M: 58%
P: 81%	P: 89%	P: 68%

<sup>a</sup>Reaction conditions: aryl bromide (0.2 mmol, 1 equiv), phenylboronic acid (0.24 mmol, 1.2 equiv),  $K_2CO_3$  (0.5 mmol, 2.5 equiv), and the Pd(II) complex (0.1 mol % Pd) were stirred in toluene (2 mL) at 110 °C under an air atmosphere over 4 h. <sup>b</sup>1,4-Dibromobenzene (0.1 mmol) used as a substrate. <sup>c</sup>1-Bromo-4-iodobenzene (0.1 mmol) used as a substrate. <sup>d</sup>GC yields determined by GC measurement of aryl bromide decay.

molecule, had a direct impact on the catalyzed reactions and, consequently, on the obtained reaction yields. They revealed similar catalytic activity to  $[PdCl_2(PPh_3)_2]$ , indicating their potential applications in cross-coupling reactions catalyzed by Pd. A number of catalytic sites in a single molecule significantly increased the efficiency of the reactions catalyzed by the polymer  $[Pd_2L_2]_n$  compared with the discrete dinuclear metalocycle  $[Pd_2(HL)_2]$ . The ICP-MS analysis of both metalocycle  $[Pd_2(HL)_2]$  and polymer  $[Pd_2L_2]_n$  allowed determination of the percentage of Pd in both structures, which was equal to 18.7 wt % and 23.6 wt %, respectively, expected for these materials. On the basis of the performed

reactions, a local concentration effect can be observed which explains the differences in GC yields between these Pd(II) complexes.<sup>63–65</sup>

## CONCLUSIONS

In conclusion, we report the synthesis and characterization of a tris- $\beta$ -diketonate ligand based on a 1,3,5-substituted benzene ring and the synthesis and characterization of its binuclear and polynuclear complexes with Cu(II) and Pd(II). In this system, a small change in the stoichiometry of the same reagents leads to completely different materials—in this case a discrete macrocycle and amorphous metallosupramolecular polymer. The soluble binuclear macrocycles have two uncoordinated diketone groups which in the presence of additional portions of metal ions led to the structural switching and ultimately formation of complex coordination assembly. The metallosupramolecular complexes reported in this paper exhibit not only different structural features but also distinct catalytic activity in the Suzuki–Miyaura cross-coupling reaction. Notably, these compounds are efficient under mild conditions, not requiring the exclusion of water or air.

## EXPERIMENTAL SECTION

All reagents were purchased from commercial suppliers (Sigma, Fluorochem, AlfaAesar) and used without further purification. High purity solvents were purchased from VWR, and anhydrous THF was dried over molecular sieves under an argon atmosphere. The triethyl benzene-1,3,5-tricarboxylate was synthesized as previously described.<sup>66</sup> NMR spectra were measured on a Bruker Ultrashield 300 + 300 Fourier-transform spectrometer using deuterated solvents. X-ray diffraction data for  $H_2L$  were obtained on a 4-circle Xcalibur EosS2 diffractometer (Agilent Technologies) equipped with a CCD detector. X-ray diffraction data for  $[Cu_2L_2(THF)_2]$  were collected on an Oxford Diffraction Gemini II ULTRA diffractometer at 173 K operating at Mo K $\alpha$  wavelength. TOF-MS spectra were measured at the Mass Spectrometry Laboratory of the Institute of Organic Chemistry of the Polish Academy of Sciences using dichloromethane solutions on a Waters Synapt GS-2 mass spectrometer. Elemental analysis was done using a FLASH 2000 analyzer. ICP-MS analysis was done using PerkinElmer NexION 300D.

**Synthesis of  $H_2L$ .** Pinacolone (14.3 mL; 114 mmol) was added to a suspension of NaH (9.15 g; 229 mmol) in dry THF (7 mL). After 30 min of stirring, triethyl benzene-1,3,5-tricarboxylate (3.21 g; 12.7 mmol) was added to the gray-yellow suspension. The mixture was heated at 47 °C for 24 h. The reaction was then quenched using water and the mixture acidified to pH ~ 4 using HCl. After extraction with  $CHCl_3/H_2O$ , the organic layer was dried over  $Na_2SO_4$  and evaporated to dryness. The crude product was isolated as a white solid by recrystallization from ethanol, filtering, washing with EtOH and drying (4.30 g; 74% yield). <sup>1</sup>H NMR (300 MHz,  $CDCl_3$ ):  $\delta$  16.48 (s, 3H, H<sub>4</sub>), 8.48 (s, 3H, H<sub>1</sub>), 7.26 (CDCl<sub>3</sub>), 6.39 (s, 3H, H<sub>2</sub>), 4.29 (s, 3H, H<sub>4</sub>), 1.28 (s, 27H, H<sub>1</sub>). <sup>13</sup>C NMR (300 MHz,  $CDCl_3$ ):  $\delta$  203.75 (C<sub>4</sub>), 183.14 (C<sub>3</sub>), 136.88 (C<sub>2</sub>), 128.59 (C<sub>5</sub>), 92.84 (C<sub>6</sub>), 77.16 (t, CDCl<sub>3</sub>), 40.17 (C<sub>2</sub>), 27.52 (C<sub>1</sub>). TOF-MS:  $m/z$  456.2590 calculated for  $C_{27}H_{30}O_6$  (HL). Found:  $m/z$  455.24 (for  $C_{27}H_{30}O_6$ , single deprotonated in negative field). IR: 2920  $cm^{-1}$  ( $\nu$ (OH)<sub>med</sub>); 1620–1500  $cm^{-1}$  ( $\nu$ (C=O)). Anal. Calcd: C, 71.03; H, 7.95%. Found: C, 71.14; H, 8.21%.

**Synthesis of Complex 1  $[Pd_2(HL)_2]$ .** The ligand  $H_2L$  (79.98 mg, 0.175 mmol) was suspended in MeOH, then TEA (73.15  $\mu$ L, 0.525 mmol) was added to give a yellow suspension. After stirring for 10 min, a solution of  $Pd(MeCN)_2Cl_2$  (45.40 mg, 0.175 mmol) in 3 mL of MeOH was added. A clear yellow solution was obtained, with some precipitate observed after about 1 h of stirring. The reaction mixture was allowed to stir for 24 h at room temperature, then filtered. The solid obtained was washed with a large volume of hot EtOH and then dried and recrystallized from DCM. The resulting yellow precipitate

was filtered and dried in vacuo. Yield: 121 mg, 62%.  $^1\text{H}$  NMR (300 MHz,  $\text{CDCl}_3$ ):  $\delta$  16.44 (s, 2H,  $\text{H}_a$ ), 9.24 (s, 1H,  $\text{H}_b$ ), 8.32 (s, 2H,  $\text{H}_c$ ), 6.42 (s, 2H,  $\text{H}_d$ ), 6.32 (s, 1H,  $\text{H}_e$ ), 1.29 (s, 27H,  $\text{H}_{18}$ ). TOF-MS:  $m/z$  1122.2785 calculated for  $\text{C}_{54}\text{H}_{60}\text{O}_{12}\text{Pd}_2$  ( $[\text{Pd}_2(\text{HL})_2]$ ). Found:  $m/z$  1121.2700 (for  $\text{C}_{54}\text{H}_{59}\text{O}_{12}\text{Pd}_2$ , single deprotonated in negative field). Anal. Calcd: C, 51.32, H, 5.42, O, 15.19%. Found: C, 51.41, H, 5.32, O, 15.24%.

**Synthesis of Complex 2**  $[\text{Cu}_2(\text{HL})_2(\text{THF})_2]$ .  $\text{H}_3\text{L}$  (0.1 g, 0.22 mmol) was dissolved in 30 mL of THF. A total of 0.2 g of sodium carbonate was suspended and stirred for 10 min. Then, 0.037 g (0.22 mmol) of  $\text{CuCl}_2 \cdot 2\text{H}_2\text{O}$  was dissolved in 10 mL of THF and added dropwise, with the solution turning dark green within several minutes of addition of the metal salt. The solution was stirred at 40 °C for 12 h before filtering to remove excess sodium carbonate. The complex crystallized as dark green plates upon slow evaporation of the reaction mixture. Yield: 0.083 g, 73%. ESI-MS ( $-ve$ ): 1033  $[\text{M}-\text{H}]^-$ , 516  $[\text{M}-2\text{H}]^{2-}$ . Anal. Calcd: C, 62.59; H, 6.61%. Found: C, 62.74; H, 6.39%.

**Synthesis of Complex 3**  $[\text{Pd}_2\text{L}_2]$  (Metallosupramolecular Branched Polymer). Ligand  $\text{H}_3\text{L}$  (31.03 mg, 0.069 mmol) was suspended in MeOH, then TEA (51.51  $\mu\text{L}$ , 0.407 mmol) was added to give a light yellow suspension.  $\text{Pd}(\text{MeCN})_2\text{Cl}_2$  (26.85 mg, 0.1035 mmol) was dissolved in MeOH and added to the reaction mixture. A clear brown solution was obtained, in which a precipitate formed after 30 min. The mixture was allowed to stir for 2 h, and then precipitation was completed by the addition of 5 mL of  $\text{H}_2\text{O}$ . The brown, cloudy solution was filtered to collect the pale brownish-green precipitate, which was washed with water followed by hot EtOH and Et<sub>2</sub>O, dried, and analyzed by NMR. (In this case, very poor solubility of the precipitate was observed, which after drying in a vacuum had a sticky consistency.)  $^1\text{H}$  NMR (300 MHz,  $\text{CDCl}_3$ ):  $\delta$  16.46 (s, 0.1H,  $\text{H}_a$ ), 8.31 (m, 1H,  $\text{H}_{18}$ ), 6.33 (m, 1H,  $\text{H}_{18}$ ), 1.24 (s, 9H,  $\text{H}_{18}$ ). Anal. Calcd: C, 53.27; H, 5.94%. Found: C, 53.11; H, 5.81%.

## ■ ASSOCIATED CONTENT

### ● Supporting Information

The Supporting Information is available free of charge at <https://pubs.acs.org/doi/10.1021/acs.inorgchem.1c00967>.

Experimental section, NMR spectra, GC-MS spectra, X-ray analysis, IR spectra, thermogravimetric analysis (PDF)

### Accession Codes

CCDC 2070262–2070264 contain the supplementary crystallographic data for this paper. These data can be obtained free of charge via [www.ccdc.cam.ac.uk/data\\_request/cif](http://www.ccdc.cam.ac.uk/data_request/cif), or by emailing [data\\_request@ccdc.cam.ac.uk](mailto:data_request@ccdc.cam.ac.uk), or by contacting The Cambridge Crystallographic Data Centre, 12 Union Road, Cambridge CB2 1EZ, UK; fax: +44 1223 336033.

## ■ AUTHOR INFORMATION

### Corresponding Authors

Jack K. Clegg – School of Chemistry and Molecular Biosciences, The University of Queensland, St Lucia 4072, Queensland, Australia; [j.clegg@uq.edu.au](mailto:j.clegg@uq.edu.au); [orcid.org/0000-0002-7140-5596](https://orcid.org/0000-0002-7140-5596); Email: [j.clegg@uq.edu.au](mailto:j.clegg@uq.edu.au)

Artur R. Stefankiewicz – Faculty of Chemistry, Adam Mickiewicz University in Poznań, 61-614 Poznań, Poland; Centre for Advanced Technologies, Adam Mickiewicz University in Poznań, 61-614 Poznań, Poland; [orcid.org/0000-0002-6177-358X](https://orcid.org/0000-0002-6177-358X); Email: [ars@amu.edu.pl](mailto:ars@amu.edu.pl)

### Authors

Michał Kolodziejewski – Faculty of Chemistry, Adam Mickiewicz University in Poznań, 61-614 Poznań, Poland; Centre for Advanced Technologies, Adam Mickiewicz University in Poznań, 61-614 Poznań, Poland

Aidan J. Brock – School of Chemistry and Molecular Biosciences, The University of Queensland, St Lucia 4072, Queensland, Australia

Gracjan Kurpiak – Faculty of Chemistry, Adam Mickiewicz University in Poznań, 61-614 Poznań, Poland; Centre for Advanced Technologies, Adam Mickiewicz University in Poznań, 61-614 Poznań, Poland

Anna Walczak – Faculty of Chemistry, Adam Mickiewicz University in Poznań, 61-614 Poznań, Poland; Centre for Advanced Technologies, Adam Mickiewicz University in Poznań, 61-614 Poznań, Poland

Feng Li – School of Science, Western Sydney University, Penrith, New South Wales 2751, Australia; [orcid.org/0000-0001-8465-9678](https://orcid.org/0000-0001-8465-9678)

Complete contact information is available at:

<https://pubs.acs.org/doi/10.1021/acs.inorgchem.1c00967>

### Author Contributions

The manuscript was written through contributions of all authors. All authors have given approval to the final version of the manuscript.

### Funding

We thank the National Science Centre (grant SONATA BIS 2018/30/E/ST5/00032) for financial support. The work was supported by grant no. POWR.03.02.00-00-1023/17 cofinanced by the European Union through the European Social Fund under the Operational Program Knowledge Education Development. The authors gratefully acknowledge the support of the Australian Research Council (DP130103157 and FT140100273).

### Notes

The authors declare no competing financial interest.

## ■ REFERENCES

- (1) Lehn, J.-M. *Supramolecular Chemistry: Concepts and Perspectives*; VCH: Weinheim, Germany, 1995.
- (2) McConnell, A. J.; Wood, C. S.; Neelakandan, P. P.; Nitschke, J. R. Stimuli-Responsive Metal–Ligand Assemblies. *Chem. Rev.* 2015, 115 (15), 7729–7793.
- (3) Brzechwa-Chodzyńska, A.; Drożdż, W.; Harrowfield, J.; Stefankiewicz, A. R. Fluorescent sensors: A bright future for cages. *Coord. Chem. Rev.* 2021, 434, 213820.
- (4) Ward, M. D.; Raithby, P. R. Functional behaviour from controlled self-assembly: challenges and prospects. *Chem. Soc. Rev.* 2013, 42 (4), 1619–1636.
- (5) Gorczyński, A.; Harrowfield, J. M.; Patroniak, V.; Stefankiewicz, A. R. Quaterpyridines as Scaffolds for Functional Metallosupramolecular Materials. *Chem. Rev.* 2016, 116 (23), 14620–14674.
- (6) Bocian, A.; Drożdż, W.; Szymańska, M.; Lewandowski, J.; Fik-Jaskółka, M.; Gorczyński, A.; Patroniak, V.; Stefankiewicz, A. R. Complex-decorated surfactant-encapsulated clusters (CD-SECs) as novel multidynamic hybrid materials. *Nanoscale* 2020, 12 (7), 4743–4750.
- (7) Brzechwa-Chodzyńska, A.; Zieliński, M.; Gilski, M.; Harrowfield, J. M.; Stefankiewicz, A. R. Dynamer and Metallosupramolecular Interconversion: An Alternative View to Metal Ion Complexation. *Inorg. Chem.* 2020, 59 (12), 8552–8561.
- (8) Pace, G.; Stefankiewicz, A.; Harrowfield, J.; Lehn, J.-M.; Samori, P. Self-Assembly of Alkoxy-Substituted Bis(hydrazone)-Based Organic Ligands and of a Metallosupramolecular Grid on Graphite. *ChemPhysChem* 2009, 10 (4), 699–705.
- (9) Drożdż, W.; Walczak, A.; Bessin, Y.; Gervais, V.; Cao, X.-Y.; Lehn, J.-M.; Ulrich, S.; Stefankiewicz, A. R. Multivalent Metallosupramolecular Assemblies as Effective DNA Binding Agents. *Chem. - Eur. J.* 2018, 24 (42), 10802–10811.



- (10) Markiewicz, G.; Walczak, A.; Perlitus, F.; Piasecka, M.; Harrowfield, J. M.; Stefankiewicz, A. R. Photoswitchable transition metal complexes with azobenzene-functionalized imine-based ligands: structural and kinetic analysis. *Dalton Trans.* 2018, 47 (40), 14254–14262.
- (11) Markiewicz, G.; Piechocki, M.; Walczak, A.; Polomska, E. A.; Harrowfield, J.; Stefankiewicz, A. R. Generation and transformation of a hemi-iminal-based metal-organic Fe(II) structure obtained via subcomponent self-assembly in water. *Dalton Trans.* 2017, 46 (43), 14826–14830.
- (12) Drożdż, W.; Bessin, Y.; Gervais, V.; Cao, X.-Y.; Lehn, J.-M.; Stefankiewicz, A. R.; Ulrich, S. Switching Multivalent DNA Complexation using Metal-Controlled Cationic Supramolecular Self-Assemblies. *Chem. - Eur. J.* 2018, 24 (7), 1518–1521.
- (13) Stefankiewicz, A. R.; Lehn, J. M. Highly Sensitive Magnetic Effects Induced by Hydrogen-Bonding Interactions in a High-Spin Metallosupramolecular Fe-4(II) [2 × 2] Grid-Type Complex. *Chem. - Eur. J.* 2009, 15 (11), 2500–2503.
- (14) Hooley, R. J. Rings and Things: The Magic of Building Self-Assembled Cages and Macrocycles. *Inorg. Chem.* 2018, 57 (7), 3497–3499.
- (15) Abdine, R. A. A.; Kurpiak, G.; Walczak, A.; Alesh, S. A. A.; Stefankiewicz, A. R.; Monnier, F.; Taillefer, M. Mild Temperature Copper-Catalyzed Amination of Aryl Halides with Aqueous Ammonia in the Presence of Pyridyldiketone Ligands. *J. Catal.* 2019, 376, 119.
- (16) Walczak, A.; Stachowiak, H.; Kurpiak, G.; Kaźmierczak, J.; Hreczycho, G.; Stefankiewicz, A. R. High catalytic activity and selectivity in hydrosilylation of new Pt(II) metallosupramolecular complexes based on ambidentate ligands. *J. Catal.* 2019, 373, 139–146.
- (17) Brock, A. J.; Al-Fayad, H.; Pfunder, M. C.; Clegg, J. K. Chapter 10 Functional Metallo-supramolecular Polyhedral Capsules and Cages. In *Functional Supramolecular Materials: From Surfaces to MOFs*; The Royal Society of Chemistry, 2017; pp 325–387.
- (18) Podtyachev, S. N.; Sudakova, S. N.; Gimazetdinova, G. S.; Shamsutdinova, N. A.; Syakaev, V. V.; Barsukova, T. A.; Iki, N.; Lapaev, D. V.; Mustafina, A. R. Synthesis, metal binding and spectral properties of novel bis-1,3-diketone calix[4]arenes. *New J. Chem.* 2017, 41 (4), 1526–1537.
- (19) van Eldik, R.; Bowman-James, K. Template Effects and Molecular Organization. In *Advance in Inorganic Chemistry*; Elsevier, 2006; Vol. 59.
- (20) Vigato, P. A.; Peruzzo, V.; Tamburini, S. The evolution of  $\beta$ -diketone or  $\beta$ -diketophenol ligands and related complexes. *Coord. Chem. Rev.* 2009, 253 (7), 1099–1201.
- (21) Aromí, G.; Gomez, P.; Reedijk, J. Poly beta-diketones: Prime ligands to generate supramolecular metalloblocks. *Coord. Chem. Rev.* 2008, 252 (8), 964–989.
- (22) Walczak, A.; Stefankiewicz, A. R. pH-Induced Linkage Isomerism of Pd(II) Complexes: A Pathway to Air- and Water-Stable Suzuki–Miyaura-Reaction Catalysts. *Inorg. Chem.* 2018, 57 (1), 471–477.
- (23) Ju, H.; Clegg, J. K.; Park, K.-M.; Lindoy, L. F.; Lee, S. S. Formation of a Dicopper Platform Based Polyrotaxane Whose “String” and “Bead” Are Constructed from the Same Components. *J. Am. Chem. Soc.* 2015, 137 (30), 9535–9538.
- (24) Clegg, J. K.; Brock, A. J.; Jolliffe, K. A.; Lindoy, L. F.; Parsons, S.; Tasker, P. A.; White, F. J. Reversible Pressure-Controlled Depolymerization of a Copper(II)-Containing Coordination Polymer. *Chem. - Eur. J.* 2017, 23 (51), 12480–12483.
- (25) Brock, A. J.; Clegg, J. K.; Li, F.; Lindoy, L. F. Recent developments in the metallo-supramolecular chemistry of oligo- $\beta$ -diketonato ligands. *Coord. Chem. Rev.* 2018, 375, 106–133.
- (26) Brock, A. J.; McMurtrie, J. C.; Clegg, J. K. Self-assembly of bis- $\beta$ -diketonato-based [M<sub>2</sub>L<sub>2</sub>] dinuclear platforms into 2-dimensional coordination polymers. *CrystEngComm* 2019, 21 (32), 4786–4791.
- (27) Pariya, C.; Sparrow, C. R.; Back, C.-K.; Sandi, G.; Fronczek, F. R.; Mavrick, A. W. Copper  $\beta$ -diketonato molecular squares and their host-guest reactions. *Angew. Chem., Int. Ed.* 2007, 46, 6305–6308.
- (28) Brock, A. J.; Etchells, I.; Moore, E. G.; Clegg, J. K. Dinuclear triple stranded phenyl-spaced 1,3-bis- $\beta$ -diketonato lanthanide(III) complexes: synthesis, structures and spectroscopy. *Dalton Trans.* 2021, 50, 4874.
- (29) Grillo, V. A.; Seddon, E. J.; Grant, C. M.; Aromi, G.; Bollinger, J. C.; Fölting, K.; Christou, G. Bis[small beta]-diketonate ligands for the synthesis of bimetallic complexes of Ti(III), VIII, Mn(III) and Fe(III) with a triple-helix structure. *Chem. Commun.* 1997, 16, 1561–1562.
- (30) Clegg, J. K.; Lindoy, L. F.; McMurtrie, J. C.; Schiller, D. Dinuclear bis- $\beta$ -diketonato ligand derivatives of iron(III) and copper(II) and use of the latter as components for the assembly of extended metallo-supramolecular structures. *Dalton Trans.* 2005, 857–864.
- (31) Saalfrank, R. W.; Stark, A.; Peters, K.; von Schnering, H. G. Adamantoid Chelate Complexes 0.1. the 1st Adamantoid Alkaline-Earth Metal Chelate Complex - Synthesis, Structure, and Reactivity. *Angew. Chem., Int. Ed. Engl.* 1988, 27 (6), 851–853.
- (32) Clegg, J. K.; Lindoy, L. F.; Moubarki, B.; Murray, K. S.; McMurtrie, J. C. Triangles and tetrahedra: metal directed self-assembly of metallo-supramolecular structures incorporating bis- $\beta$ -diketonato ligands. *Dalton Trans.* 2004, 2417–2423.
- (33) Clegg, J. K.; Li, F.; Jolliffe, K. A.; Meehan, G. V.; Lindoy, L. F. An Expanded Neutral M<sub>4</sub>L<sub>6</sub> Cage that Encapsulates Four Tetrahydrofuran Molecules. *Chem. Commun.* 2011, 47 (21), 6042–6044.
- (34) Li, F.; Clegg, J. K.; Lindoy, L. F.; MacQuart, R. B.; Meehan, G. V. Metallosupramolecular Self-Assembly of a Universal 3-Ravel. *Nat. Commun.* 2011, 2, 205.
- (35) Walczak, A.; Kurpiak, G.; Stefankiewicz, A. R. Intrinsic Effect of Pyridine-N-Position on Structural Properties of Cu-Based Low-Dimensional Coordination Frameworks. *Int. J. Mol. Sci.* 2020, 21 (17), 6171.
- (36) Clegg, J. K.; Iremonger, S. S.; Hayter, M. J.; Southon, P. D.; MacQuart, R. B.; Duriska, M. B.; Jensen, P.; Turner, P.; Jolliffe, K. A.; Kepert, C. J.; Meehan, G. V.; Lindoy, L. F. Hierarchical Self-Assembly of a Chiral Metal-Organic Framework Displaying Pronounced Porosity. *Angew. Chem., Int. Ed.* 2010, 49, 1075–1078.
- (37) Saalfrank, R. W.; Glaser, H.; Demleitner, B.; Hampel, F.; Chowdhry, M. M.; Schunemann, V.; Trautwein, A. X.; Vaughan, G. B. M.; Yeh, R.; Davis, A. V.; Raymond, K. N. Self-assembly of tetrahedral and trigonal antiprismatic clusters [Fe<sub>4</sub>(L<sub>4</sub>)<sub>4</sub>] and [Fe<sub>6</sub>(L<sub>5</sub>)<sub>6</sub>] on the basis of trigonal tris-bidentate chelators. *Chem. - Eur. J.* 2002, 8 (2), 493–497.
- (38) Johnson, D. W.; Xu, J.; Saalfrank, R. W.; Raymond, K. N. Coordination number incommensurate cluster formation, part 12. Self-assembly of a three-dimensional [Ga<sub>6</sub>(L<sub>2</sub>)<sub>6</sub>] metal-ligand “cylinder”. *Angew. Chem., Int. Ed.* 1999, 38, 2882–2885.
- (39) Miller, M. A.; Askevold, B.; Mikula, H.; Kohler, R. H.; Firovich, D.; Weissleder, R. Nano-palladium is a cellular catalyst for in vivo chemistry. *Nat. Commun.* 2017, 8, 15906.
- (40) Chinchilla, R.; Najera, C. Recent advances in Sonogashira reactions. *Chem. Soc. Rev.* 2011, 40 (10), 5084–5121.
- (41) Samanta, D.; Mukherjee, P. S. Multicomponent self-sorting of a Pd<sup>7</sup> molecular boat and its use in catalytic Knoevenagel condensation. *Chem. Commun.* 2013, 49 (39), 4307–4309.
- (42) Howlader, P.; Mukherjee, P. S. Face and edge directed self-assembly of Pd<sup>12</sup> tetrahedral nano-cages and their self-sorting. *Chem. Sci.* 2016, 7 (9), 5893–5899.
- (43) Zhao, C.-W.; Ma, J.-P.; Lin, Q.-K.; Yu, Y.; Wang, P.; Li, Y.-A.; Wang, K.; Dong, Y.-B. A self-assembled Pd<sub>6</sub>L<sub>8</sub> nanoball for Suzuki–Miyaura coupling reactions in both homogeneous and heterogeneous formats. *Green Chem.* 2013, 15 (11), 3150–3154.
- (44) Pal, S.; Hwang, W.-S.; Lin, I. J. B.; Lee, C.-S. Benzene benzimidazole containing Pd(II) metallacycle: Synthesis, X-ray crystallographic characterization and its use as an efficient Suzuki coupling catalyst. *J. Mol. Catal. A: Chem.* 2007, 269 (1), 197–203.
- (45) de Meijere, A. D. F. *Metal-Catalyzed Cross-Coupling Reactions*; Wiley-VCH: Weinheim, Germany, 2004.

- (46) Le Bras, J.; Muzart, J. Intermolecular Dehydrogenative Heck Reactions. *Chem. Rev.* 2011, 111 (3), 1170–1214.
- (47) Johansson Seechurn, C. C. C.; Kitching, M. O.; Colacot, T. J.; Snieckus, V. Palladium-Catalyzed Cross-Coupling: A Historical Contextual Perspective to the 2010 Nobel Prize. *Angew. Chem., Int. Ed.* 2012, 51 (21), 5062–5085.
- (48) Negishi, E.-i.; Anastasia, L. Palladium-Catalyzed Alkynylation. *Chem. Rev.* 2003, 103 (5), 1979–2018.
- (49) Farina, V. High-Turnover Palladium Catalysts in Cross-Coupling and Heck Chemistry: A Critical Overview. *Adv. Synth. Catal.* 2004, 346 (13–15), 1553–1582.
- (50) Moon, Y.; Kwon, D.; Hong, S. Palladium-Catalyzed Dehydrogenation/Oxidative Cross-Coupling Sequence of  $\beta$ -Heteroatom-Substituted Ketones. *Angew. Chem., Int. Ed.* 2012, 51 (45), 11333–11336.
- (51) Siva Reddy, A.; Kumara Swamy, K. C. Ethanol as a Hydrogenating Agent: Palladium-Catalyzed Stereoselective Hydrogenation of Ynamides To Give Enamides. *Angew. Chem., Int. Ed.* 2017, 56 (24), 6984–6988.
- (52) Beletskaya, I. P.; Chepurkov, A. V. The Heck Reaction as a Sharpening Stone of Palladium Catalysis. *Chem. Rev.* 2000, 100 (8), 3009–3066.
- (53) McMahon, C. M.; Alexanian, E. J. Palladium-Catalyzed Heck-Type Cross-Couplings of Unactivated Alkyl Iodides. *Angew. Chem., Int. Ed.* 2014, 53 (23), 5974–5977.
- (54) Rossi, R.; Bellina, F.; Lessi, M. Selective Palladium-Catalyzed Suzuki–Miyaura Reactions of Polyhalogenated Heteroarenes. *Adv. Synth. Catal.* 2012, 354 (7), 1181–1255.
- (55) Yang, Y.; Mustard, T. J. L.; Cheong, P. H.-Y.; Buchwald, S. L. Palladium-Catalyzed Completely Linear-Selective Negishi Cross-Coupling of Allylzinc Halides with Aryl and Vinyl Electrophiles. *Angew. Chem., Int. Ed.* 2013, 52 (52), 14098–14102.
- (56) Zhou, J.; Fu, G. C. Palladium-Catalyzed Negishi Cross-Coupling Reactions of Unactivated Alkyl Iodides, Bromides, Chlorides, and Tosylates. *J. Am. Chem. Soc.* 2003, 125 (41), 12527–12530.
- (57) Bülis, A.; Centomo, P.; Del Zotto, A.; Zecca, M. Pd Metal Catalysts for Cross-Couplings and Related Reactions in the 21st Century: A Critical Review. *Chem. Rev.* 2018, 118 (4), 2249–2295.
- (58) Jiang, W.-L.; Shen, J.-C.; Peng, Z.; Wu, G.-Y.; Yin, G.-Q.; Shi, X.; Yang, H.-B. Controllable synthesis of ultrasmall Pd nanocatalysts templated by supramolecular coordination cages for highly efficient reductive dehalogenation. *J. Mater. Chem. A* 2020, 8 (24), 12097–12105.
- (59) Ooe, M.; Murata, M.; Mizugaki, T.; Ebitani, K.; Kameda, K. Supramolecular Catalysts by Encapsulating Palladium Complexes within Dendrimers. *J. Am. Chem. Soc.* 2004, 126 (6), 1604–1605.
- (60) Kołodziejewski, M.; Walczak, A.; Hnatejko, Z.; Harrowfield, J.; Stefankiewicz, A. R. Unsymmetrical bidentate ligands as a basis for construction of ambidentate ligands for functional materials: Properties of 4,4-dimethyl-1-phenylpentane-1,3-dione. *Polyhedron* 2017, 137, 270–277.
- (61) Podyachev, S. N.; Sudakova, S. N.; Galiev, A. K.; Mustafina, A. R.; Syakaev, V. V.; Shagidullin, R. R.; Bauer, I.; Kononov, A. I. Synthesis of tris( $\beta$ -diketones) and study of their complexation with some transition metals. *Russ. Chem. Bull.* 2006, 55 (11), 2000–2007.
- (62) Sloop, J. C.; Bumgardner, C. L.; Washington, G.; Loehle, W. D.; Sankar, S. S.; Lewis, A. B. Keto–enol and enol–enol tautomerism in trifluoromethyl- $\beta$ -diketones. *J. Fluorine Chem.* 2006, 127 (6), 780–786.
- (63) Arnby, K.; Törnqvist, A.; Andersson, B.; Skoglundh, M. Investigation of Pt/ $\gamma$ -Al<sub>2</sub>O<sub>3</sub> catalysts with locally high Pt concentrations for oxidation of CO at low temperatures. *J. Catal.* 2004, 221 (1), 252–261.
- (64) Wang, D.; Astruc, D. Dendritic catalysis—Basic concepts and recent trends. *Coord. Chem. Rev.* 2013, 257 (15), 2317–2334.
- (65) Helms, B.; Fréchet, J. M. J. The Dendrimer Effect in Homogeneous Catalysis. *Adv. Synth. Catal.* 2006, 348 (10–11), 1125–1148.
- (66) Baral, M.; Kanungo, B. K.; Moore, P. Synthesis of cis, cis-1,3,5-trisubstituted cyclohexane based chelators with polyfunctional pendant arms. *J. Chem. Res.* 2005, 2005 (1), 43–45.

## Supplementary information to **A2**



Supporting Information for

Charge neutral [Cu<sub>2</sub>L<sub>2</sub>] and [Pd<sub>2</sub>L<sub>2</sub>] metallocycles:  
self-assembly, aggregation and catalysis

*Michał Kołodziejwski<sup>[a],[b]</sup>, Aidan J. Brock<sup>[c]</sup>, Gracjan Kurpik<sup>[a],[b]</sup>, Anna Walczak<sup>[a],[b]</sup>, Feng Li,<sup>[d]</sup> Jack K. Clegg<sup>\*[c]</sup> and Artur R. Stefankiewicz<sup>\*[a],[b]</sup>*

[a] Faculty of Chemistry, Adam Mickiewicz University in Poznań, Uniwersytetu Poznańskiego 8, 61-614 Poznań, Poland. E-mail: ars@amu.edu.pl

[b] Centre for Advanced Technologies, Adam Mickiewicz University in Poznań, Uniwersytetu Poznańskiego 10, 61-614 Poznań, Poland.

[c] School of Chemistry and Molecular Biosciences, The University of Queensland St Lucia 4072, Queensland, Australia. E-mail: j.clegg@uq.edu.au

[d] School of Science, Western Sydney University, Locked Bag 1797, Penrith NSW 2751, Australia.

\*Correspondence: Jack K. Clegg, j.clegg@uq.edu.au; Artur R. Stefankiewicz, ars@amu.edu.pl

## Table of Contents

1. NMR spectra .....	3
1.1. Tripodal ligand $H_3L$ .....	3
1.2. Metallosupramolecular macrocycle $[Pd_2(HL)_2]$ .....	5
1.3. Metallosupramolecular branched polymer $[Pd_3L_2]_n$ .....	6
1.4. DOSY NMR spectra of Pd-based metallosupramolecular structures .....	6
2. X-ray crystallography .....	7
3. InfraRed spectroscopy .....	10
3.1. IR spectrum of the ligand $L$ .....	10
4. ESI-MS analysis .....	10
5.1. ESI-MS analysis of the metallosupramolecular macrocycle $[Pd_2(HL)_2]$ .....	10
5.2. ESI-MS analysis of the metallosupramolecular branched polymer $[Pd_3L_2]_n$ .....	13
5. GC-MS analysis for Suzuki-Miyaura Cross Coupling Reactions .....	14
5.1. Optimization of the conditions of catalytic test reactions .....	14
5.2. Differences in catalytic activity of $[Pd_2(HL)_2]$ , $[Pd_3L_2]_n$ and $[PdCl_2(PPh_3)_2]$ .....	14
6. Thermogravimetric analysis .....	15
7. References .....	16

## 1. NMR spectra

### 1.1. Tripodal ligand H<sub>3</sub>L

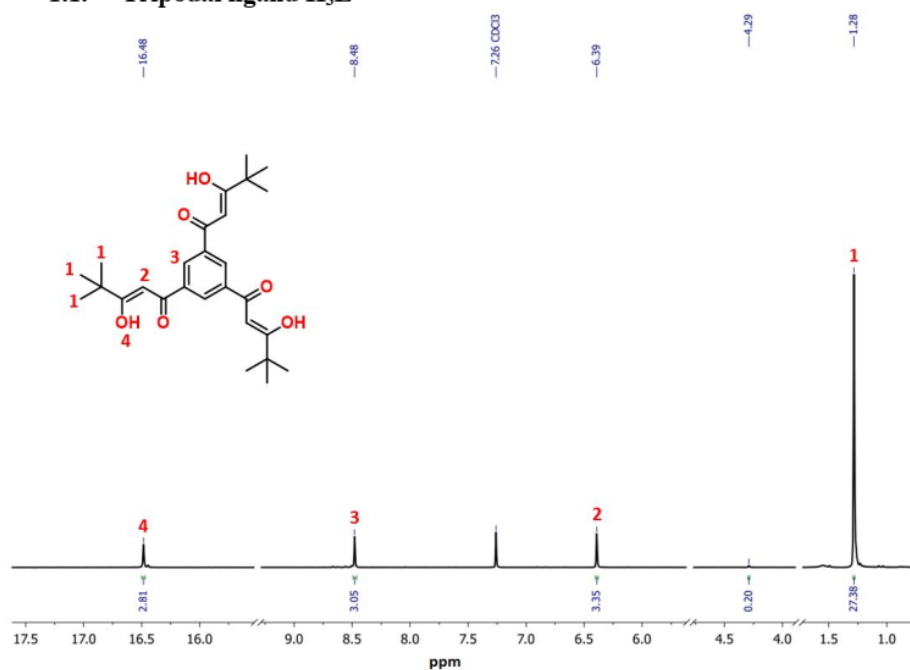


Figure S1. <sup>1</sup>H NMR spectrum of the tripodal ligand H<sub>3</sub>L recorded in CDCl<sub>3</sub> at room temperature.

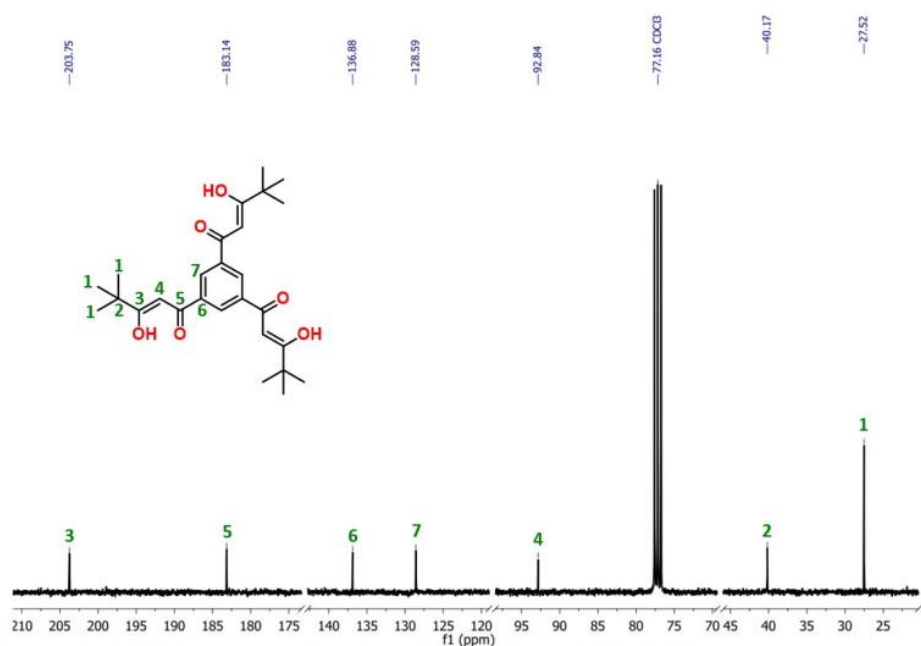


Figure S2.  $^{13}\text{C}$  NMR spectrum of the tripodal ligand  $\text{H}_3\text{L}$  recorded in  $\text{CDCl}_3$  at room temperature.

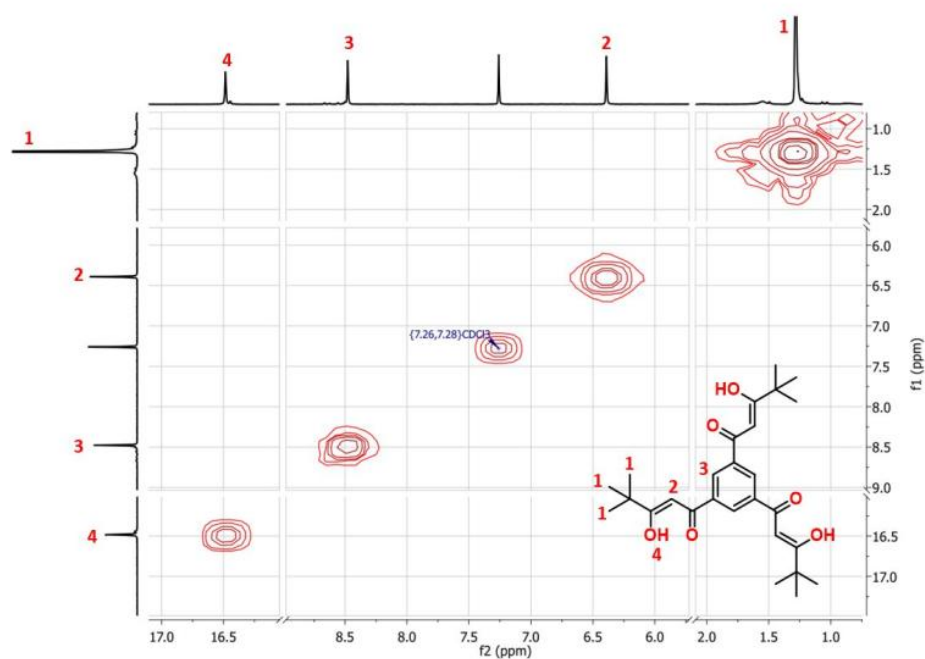
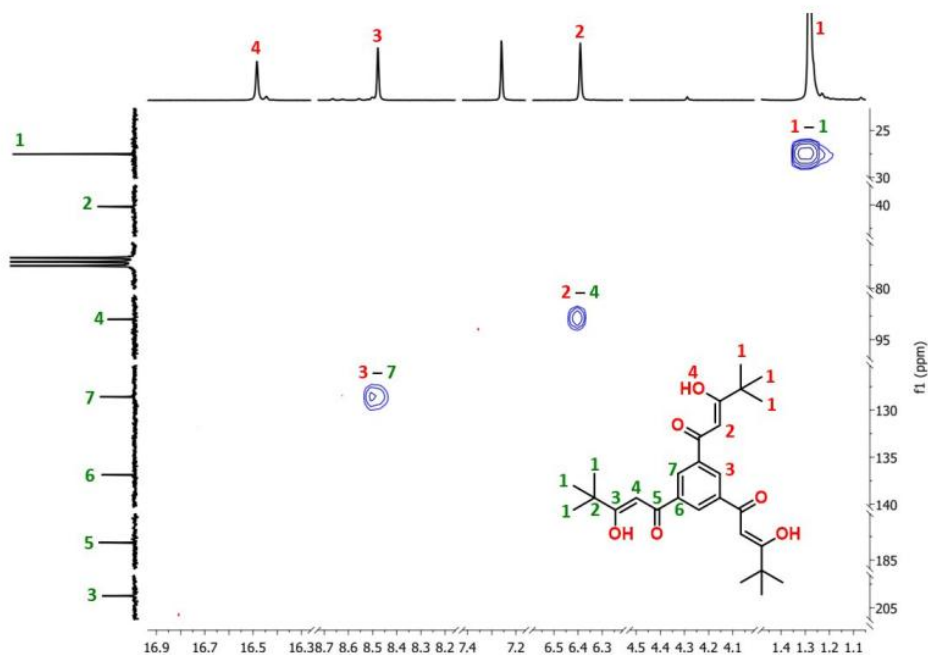
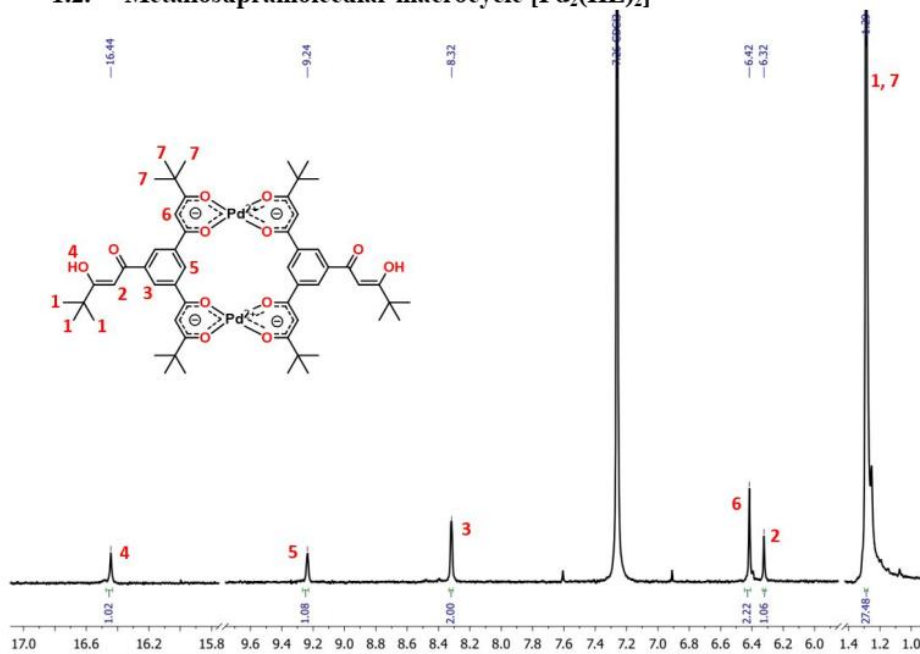


Figure S3. COSY NMR spectrum of the tripodal ligand  $\text{H}_3\text{L}$  recorded in  $\text{CDCl}_3$  at room temperature.



**Figure S4.** HSQC NMR spectrum of the tripodal ligand  $H_3L$  recorded in  $CDCl_3$  at room temperature.

## 1.2. Metallosupramolecular macrocycle $[Pd_2(HL)_2]$



**Figure S5.**  $^1H$  NMR spectrum of macrocyclic metallosupramolecular complex  $[Pd_2(HL)_2]$  recorded in  $CDCl_3$  at room temperature.

### 1.3. Metallocupramolecular branched polymer $[\text{Pd}_3\text{L}_2]_n$

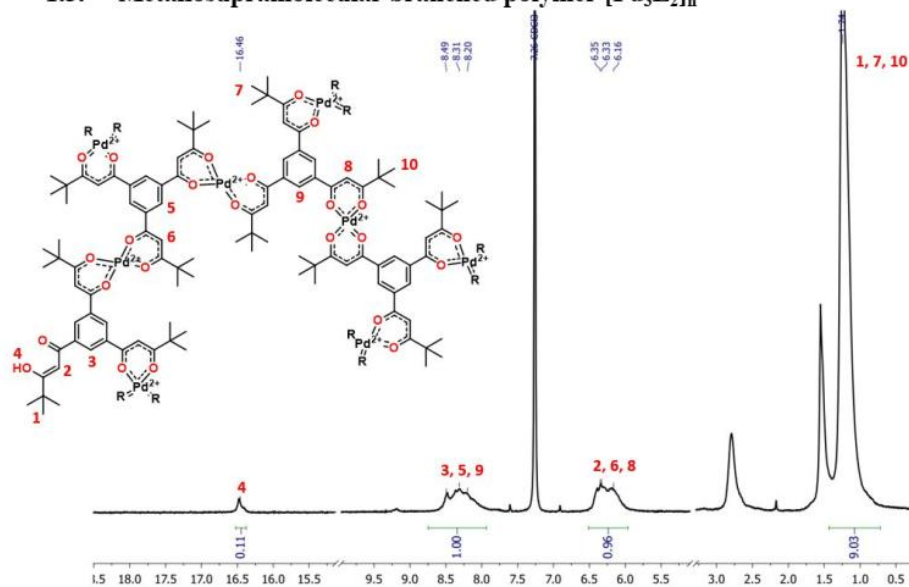


**Figure S6.**  $^1\text{H}$  NMR spectrum of metallocupramolecular polymer  $[\text{Pd}_3\text{L}_2]_n$  recorded in  $\text{CDCl}_3$  at room temperature.

### 1.4. DOSY NMR spectra of Pd-based metallocupramolecular structures

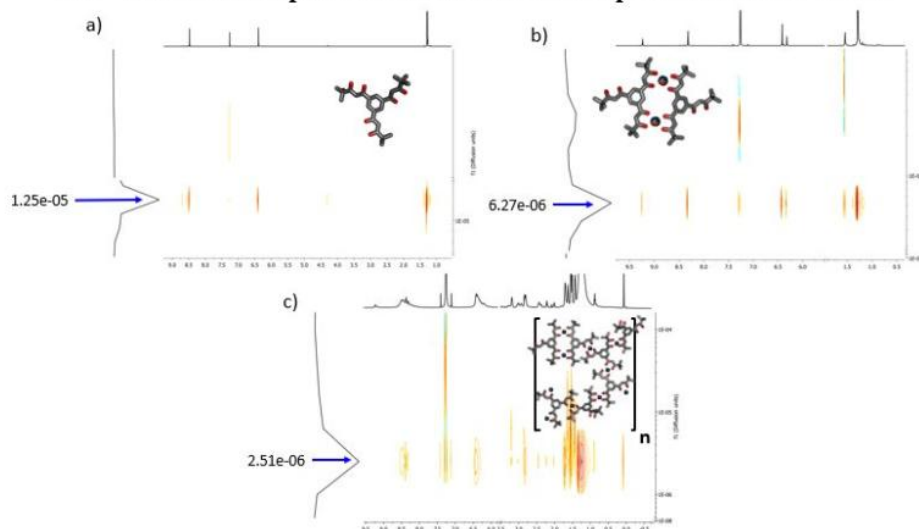


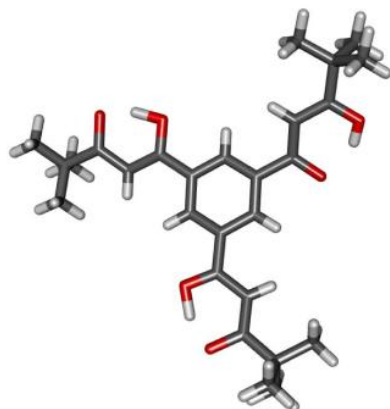
**Figure S7.** DOSY NMR spectra of tripod ligand  $\text{H}_3\text{L}$  (a), metallocupramolecular macrocycle  $[\text{Pd}_2(\text{HL})_2]$  (b), and metallocupramolecular branched polymer  $[\text{Pd}_3\text{L}_2]_n$  (c). All spectra were measured in  $\text{CDCl}_3$  at room temperature.

## 2. X-ray crystallography

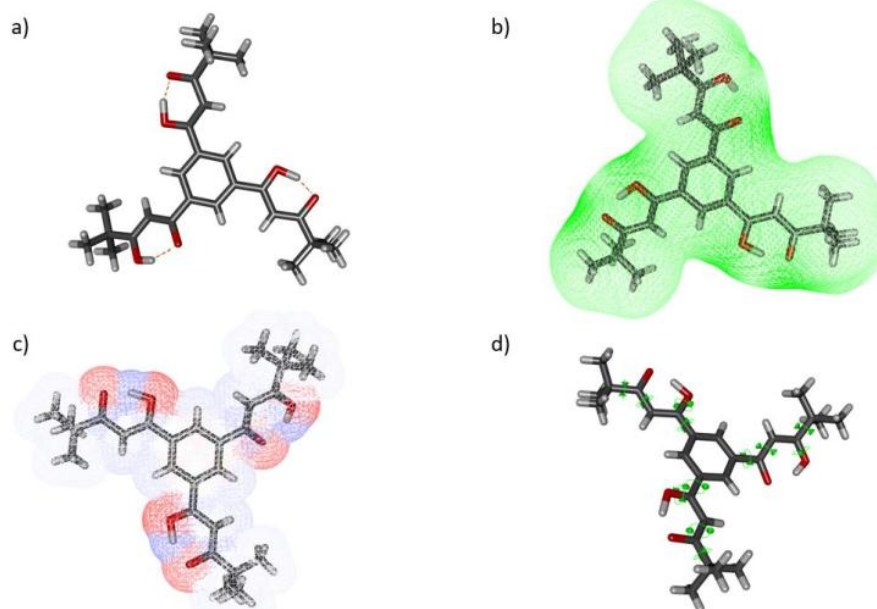
Single-crystal diffraction data were collected using MoK $\alpha$  radiation generated from either a sealed tube or rotating anode using either an Oxford Diffraction Gemini II ULTRA, an Aligent Xcalibur EosS2 or a Bruker APEX-II diffractometer. Data was indexed, integrated and reduced with either CrysAlisPro<sup>1</sup> or SAINT.<sup>2</sup> Processed data was solved using either SIR-97<sup>3</sup> or SHELXT<sup>4</sup>. Solutions were refined *via* a full-matrix least-squares refinement against  $F^2$  using SHELXL<sup>5</sup> through the Olex2<sup>6</sup> graphical interface. Non-hydrogen atoms with occupancies of 50% or greater were refined anisotropically. Where appropriate electron density was identified in the Fourier difference map, hydrogen atoms were explicitly placed. The remainder of the carbon-bound hydrogen atoms were placed in idealised positions and refined using a riding model on the appropriate atom.

Table T1. Crystal data and structure refinement for tripod ligand and complex.

Identification code	H <sub>3</sub> L	H <sub>3</sub> L	[Cu <sub>2</sub> (HL) <sub>2</sub> (THF) <sub>2</sub> ]
Empirical formula	C <sub>27</sub> H <sub>36</sub> O <sub>6</sub>	C <sub>27</sub> H <sub>36</sub> O <sub>6</sub>	C <sub>62</sub> H <sub>64</sub> Cu <sub>2</sub> O <sub>14</sub>
Formula weight	456.56	456.56	1180.37
Temperature/K	293(2)	150(2)	173.00(14)
Crystal system	monoclinic	monoclinic	triclinic
Space group	C2/c	C2/c	P-1
a/Å	31.501(6)	31.171(2)	10.0759(3)
b/Å	6.7598(14)	6.652(1)	10.9995(3)
c/Å	29.7990(6)	29.222(2)	15.4390(3)
$\alpha$ /°	90	90	101.483(2)
$\beta$ /°	119.24(3)	118.116(2)	99.143(2)
$\gamma$ /°	90	90	110.014(2)
Volume/Å <sup>3</sup>	5537.2)	5344.2(10)	1526.94(7)
Z	8	8	1
$\rho_{\text{calc}}/\text{cm}^3$	1.095	1.135	1.284
$\mu/\text{mm}^{-1}$	0.076	0.079	0.758
F(000)	1968.0	1968.0	626.0
Crystal size/mm <sup>3</sup>	0.3 × 0.1 × 0.1	0.31 × 0.07 × 0.02	0.5 x 0.4 x 0.4
Radiation	MoK $\alpha$ ( $\lambda$ = 0.71073)	MoK $\alpha$ ( $\lambda$ = 0.71073)	MoK $\alpha$ ( $\lambda$ = 0.71073)
2 $\theta$ range for data collection/°	6.576 to 51.074	5.576 to 55.1	6.782 to 57.844
Index ranges	-36 ≤ h ≤ 37, -8 ≤ k ≤ 8, -34 ≤ l ≤ 34	-40 ≤ h ≤ 37, -8 ≤ k ≤ 4, -36 ≤ l ≤ 38	-13 ≤ h ≤ 13, -14 ≤ k ≤ 14, -20 ≤ l ≤ 20
Reflections collected	163148	25770	66739
Independent reflections	4842 [R <sub>int</sub> = 0.0697, R <sub>sigma</sub> = 0.0212]	6089 [R <sub>int</sub> = 0.0605, R <sub>sigma</sub> = 0.0618]	7606 [R <sub>int</sub> = 0.0372, R <sub>sigma</sub> = 0.0217]
Data/restraints/parameters	4842/1/358	6089/0/337	7606/6/364
Goodness-of-fit on F <sup>2</sup>	1.144	1.007	1.075
Final R indexes [I > 2 $\sigma$ (I)]	R <sub>1</sub> = 0.0734, wR <sub>2</sub> = 0.1812	R <sub>1</sub> = 0.0659, wR <sub>2</sub> = 0.1627	R <sub>1</sub> = 0.0435, wR <sub>2</sub> = 0.1149
Final R indexes [all data]	R <sub>1</sub> = 0.0925, wR <sub>2</sub> = 0.1902	R <sub>1</sub> = 0.1254, wR <sub>2</sub> = 0.2036	R <sub>1</sub> = 0.0525, wR <sub>2</sub> = 0.1198
Largest diff. peak/hole / e Å <sup>-3</sup>	0.29/-0.17	0.48/-0.53	0.96/-0.42



**Figure S8.** X-ray crystallographic structure of ligand H<sub>3</sub>L.



**Figure S9.** X-ray analysis of tripod ligand H<sub>3</sub>L: (a) intramolecular H-bonds in  $\beta$ -diketonate system; (b) H-bond acceptor sites; (c) atom charge sites and (d) rotatable bonds in ligand structure.



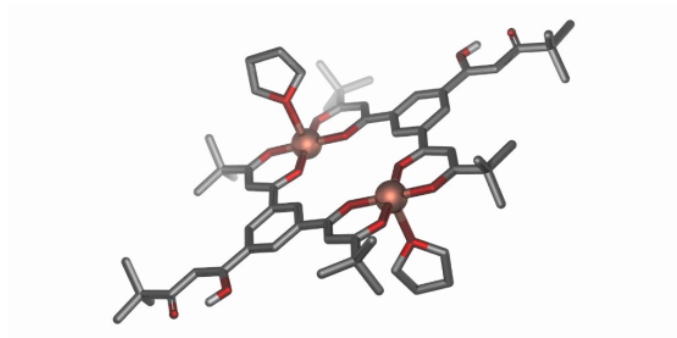


**Figure S10.** Single-crystal X-ray structure of  $[\text{Cu}_2(\text{HL})_2(\text{THF})_2]$ . Hydrogen atoms (except enol hydrogens) have been omitted for clarity. Only a single component of disorder in the THF ligand is shown.

The crystal packing of  $[\text{Cu}_2(\text{HL})_2(\text{THF})_2]$  is dominated by a series of offset  $\pi$ - $\pi$  and CH- $\pi$  stacking interactions (the distance between mean planes of these complexes is 3.74 Å), leading to the propagation of linear chains coincident with the crystallographic *b* axis (Figure S11). The principal interactions appear to occur from stacking of the delocalized  $\pi$  system of a copper(II)-diketonate chelate ring and a non-coordinated  $\beta$ -diketone ring of the adjacent complex (centroid-centroid distance 3.42 Å). Offset interactions between aromatic rings are also observed (4.93 Å centroid-centroid distance, 3.30 Å plane-plane separation), however closer packing of these is precluded by coordinated THF ligands which project above and below the mean plane of the complexes.

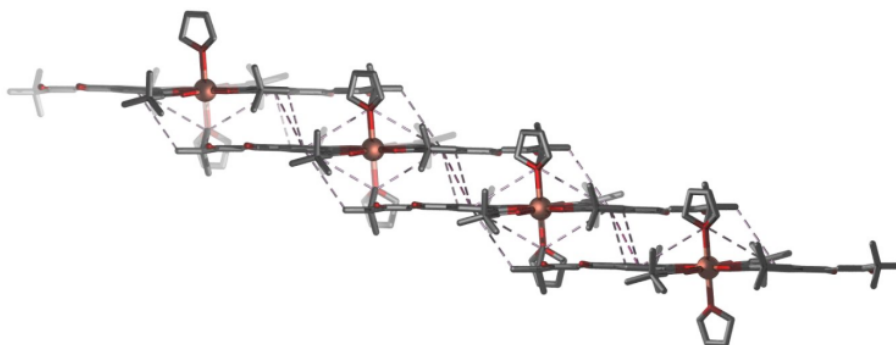


**Figure S11.** One-dimensional stacked chain of complexes in the crystal structure of  $[\text{Cu}_2(\text{HL})_2(\text{THF})_2]$ . Select  $\pi$ - $\pi$  and CH- $\pi$  interactions are shown as dotted lines.

These chains appear mostly isolated and do not display any significant interactions with adjacent chains. The closest interaction is a CH-HC contact (2.39 Å) between tertiary butyl groups and THF ligands of neighbouring complexes (Figure S12). Despite the tight molecular packing, minimal interaction is observed between chains above and below due to the combined steric bulk of the THF ligands and tertiary butyl groups.

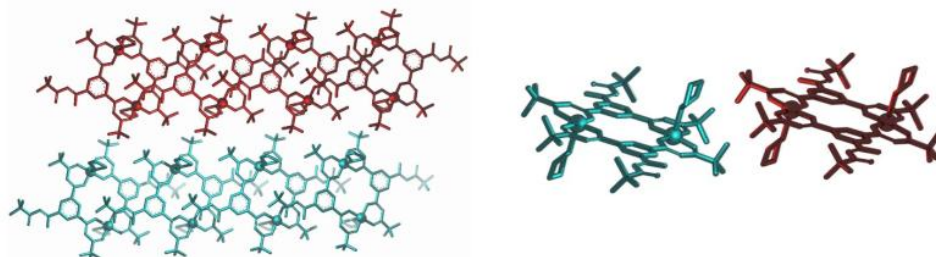


**Figure S12** (Left) Top-down and (right) down-chain view of adjacent stacked chains of [Cu<sub>2</sub>(HL)<sub>2</sub>(THF)<sub>2</sub>]. Chains are coloured in red and cyan respectively for ease of identification.

### 3. InfraRed spectroscopy

#### 3.1. IR spectrum of the ligand L

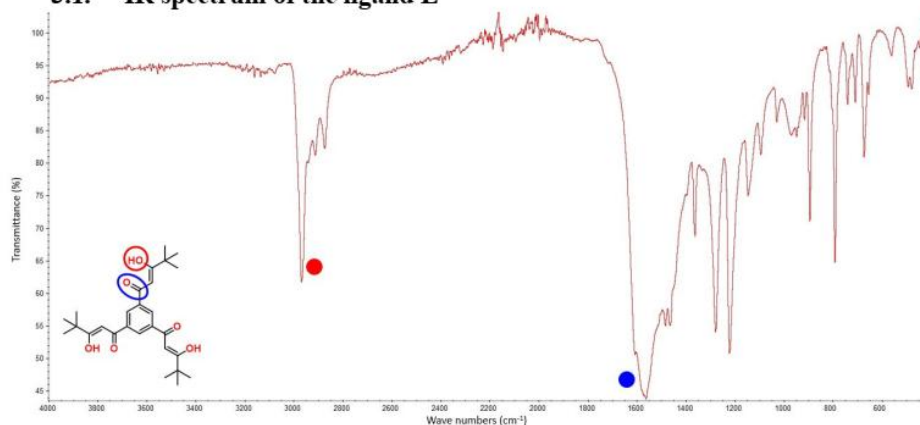


**Figure S13.** IR analysis of tripod ligand H<sub>3</sub>L measured in solid state (from powder).

#### 4. ESI-MS analysis

##### 5.1. ESI-MS analysis of the metallosupramolecular macrocycle $[\text{Pd}_2(\text{HL})_2]$

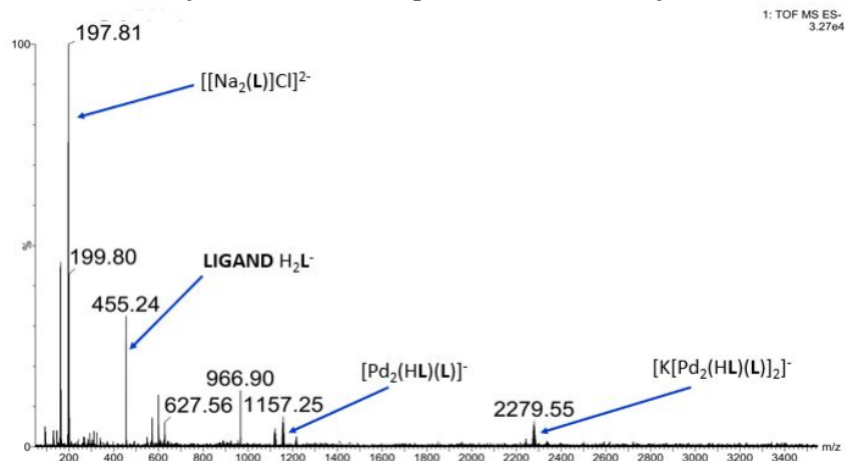


**Figure S14.** Full ESI-MS spectrum of metallosupramolecular macrocyclic complex  $[\text{Pd}_2(\text{HL})_2]$ , measured in negative charge.

MK\_trip\_Pd\_complex

TOF MS ES-

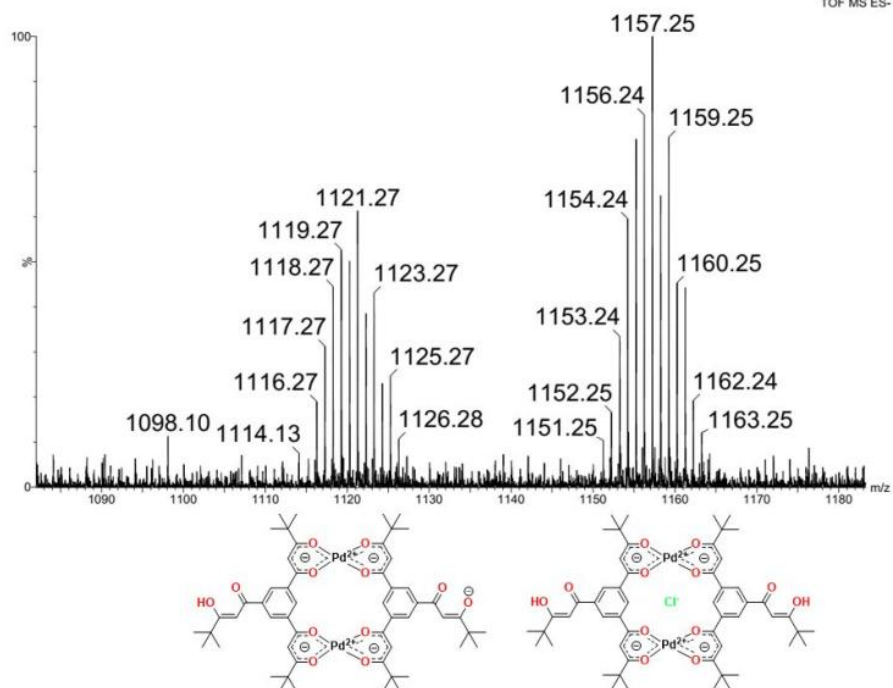


**Figure S15.** Zoom on the ESI-MS peaks of macrocyclic metallosupramolecular complex [Pd<sub>2</sub>(HL)<sub>2</sub>] and its adduct with chloride anion.

S12

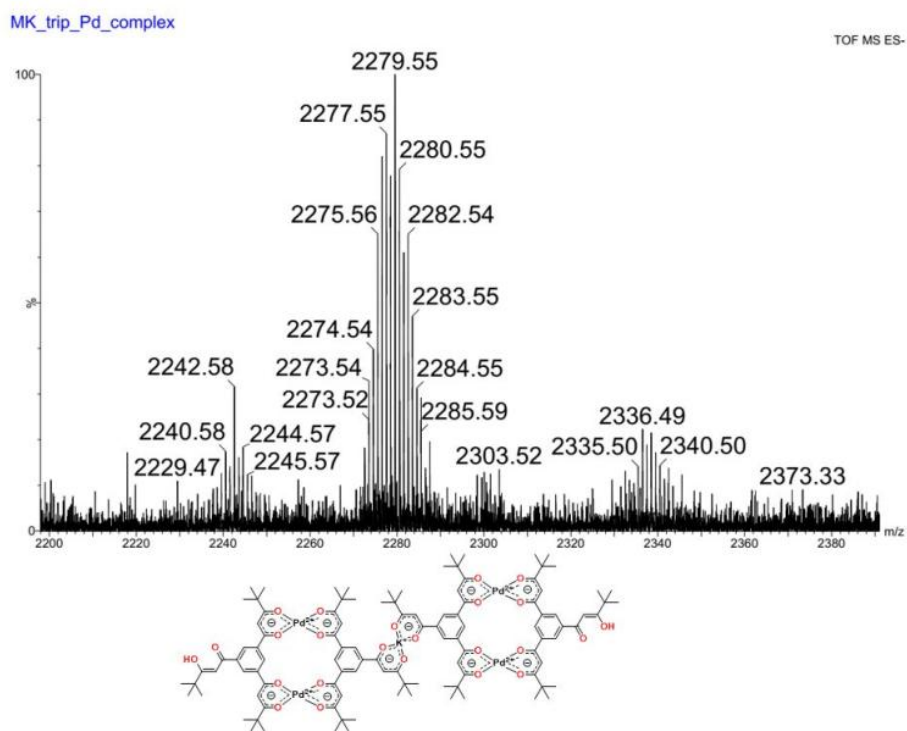


**Figure S16.** Zoom on the ESI-MS peaks of dimer of macrocyclic metallosupramolecular complexes  $[\text{Pd}_2(\text{HL})_2]$  with potassium cation ( $\text{K}^+$ ).

## 5.2. ESI-MS analysis of the metallosupramolecular branched polymer $[\text{Pd}_3\text{L}_2]_n$

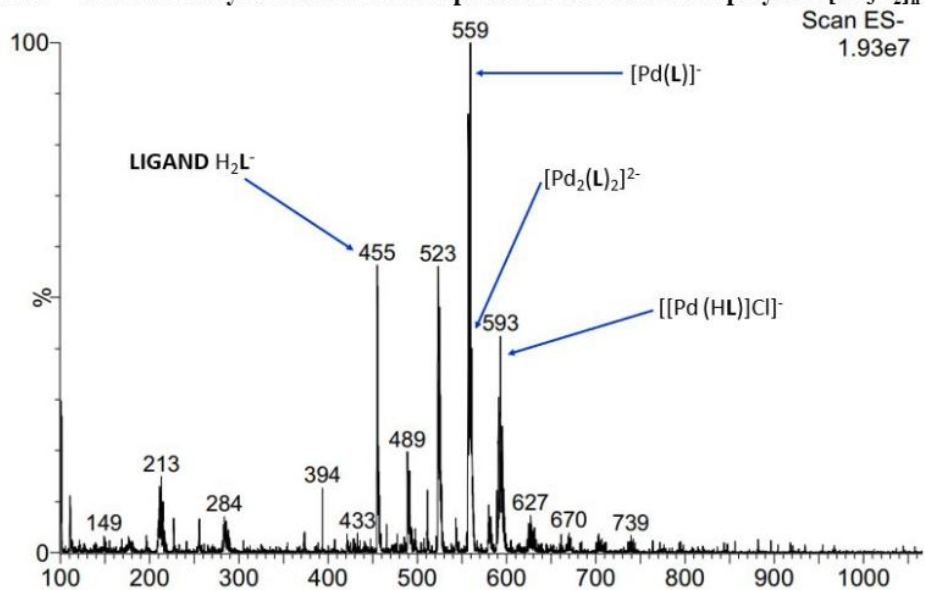


**Figure S17.** ESI-MS spectrum of metallosupramolecular branched polymer  $[\text{Pd}_3\text{L}_2]_n$ , measured in negative charge. Spectrum is presenting breakdown products.

## 5. GC-MS analysis for Suzuki-Miyaura Cross Coupling Reactions

### 5.1. Optimization of the conditions of catalytic test reactions

**Table T2.** Reaction development for the Suzuki-Miyaura cross-coupling between phenylboronic acid and 4'-bromoacetophenone.<sup>a</sup>

	solvent	base	T [°C]	catalyst [mol% Pd]	GC yield [%] <sup>b</sup>	
					2 h	4 h
1	toluene	K <sub>2</sub> CO <sub>3</sub>	80	0.1	51	60
2	toluene	K <sub>3</sub> PO <sub>4</sub>	80	0.1	22	26
3	toluene	Et <sub>3</sub> N	80	0.1	13	16
4	toluene	NaOH	80	0.1	0	1
5	toluene	K <sub>2</sub> CO <sub>3</sub>	60	0.1	26	33
6	toluene	K <sub>2</sub> CO <sub>3</sub>	110	0.1	79	94
7	toluene	K <sub>2</sub> CO <sub>3</sub>	110	0.01	36	48
8	toluene	K <sub>2</sub> CO <sub>3</sub>	110	0.001	21	34
9	DMF	K <sub>2</sub> CO <sub>3</sub>	110	0.1	19	42
10	1,4-dioxane	K <sub>2</sub> CO <sub>3</sub>	110	0.1	66	84
11	THF	K <sub>2</sub> CO <sub>3</sub>	60	0.1	3	8

<sup>a</sup>Reaction conditions: 4'-bromoacetophenone (0.2 mmol, 1 equiv.), phenylboronic acid (0.24 mmol, 1.2 equiv.), base (0.5 mmol, 2.5 equiv.) and the complex [Pd<sub>2</sub>(HL)<sub>2</sub>] were stirred in appropriate solvent (2 mL) at indicated temperature under air atmosphere. <sup>b</sup> Determined by GC measurement of 4'-bromoacetophenone decay.

## 5.2. Differences in catalytic activity of $[\text{Pd}_2(\text{HL})_2]$ , $[\text{Pd}_3\text{L}_2]_n$ and $[\text{PdCl}_2(\text{PPh}_3)_2]$

**Table T3.** GC yields of the Suzuki-Miyaura cross-coupling reactions between aryl bromides and phenylboronic acid catalyzed by  $[\text{PdCl}_2(\text{PPh}_3)_2]$ .<sup>a, b</sup>

<p><b>1a</b> M: 75% P: 85% C: 100%</p>	<p><b>2a</b> M: 67% P: 83% C: 99%</p>
<p><b>3a</b> M: 72% P: 80% C: 93%</p>	<p><b>4a</b> M: 94% P: 100% C: 91%</p>
<p><b>5a</b> M: 81% P: 84% C: 89%</p>	<p><b>6a</b> M: 67% P: 85% C: 81%</p>
<p><b>7a</b> M: 91% P: 98% C: 98%</p>	<p><b>8a</b> M: 57% P: 80% C: 77%</p>

<sup>a</sup> Reaction conditions: aryl bromide (0.2 mmol, 1 equiv.), phenylboronic acid (0.24 mmol, 1.2 equiv.),  $\text{K}_2\text{CO}_3$  (0.5 mmol, 2.5 equiv.) and the catalyst (0.1 mol%), where **M** = metallocycle  $[\text{Pd}_2(\text{HL})_2]$ , **P** = polymer  $[\text{Pd}_3\text{L}_2]_n$  and **C** = complex  $[\text{PdCl}_2(\text{PPh}_3)_2]$ , were stirred in toluene (2 mL) at 110°C under air atmosphere over 4 h. <sup>b</sup> GC yields determined by GC measurement of aryl bromide decay.



## 6. Thermogravimetric analysis

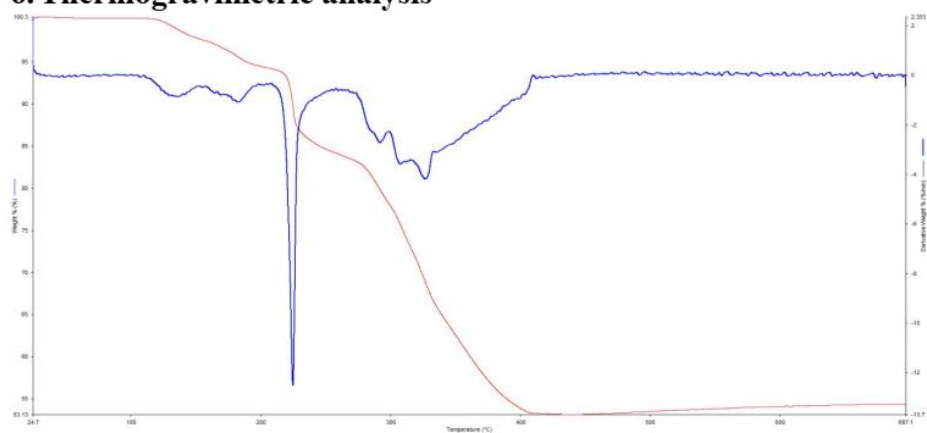


**Figure S18.** TGA (red) and DTG (blue) spectrum measured for metallosupramolecular macrocycle  $[\text{Pd}_2(\text{HL})_2]$ .

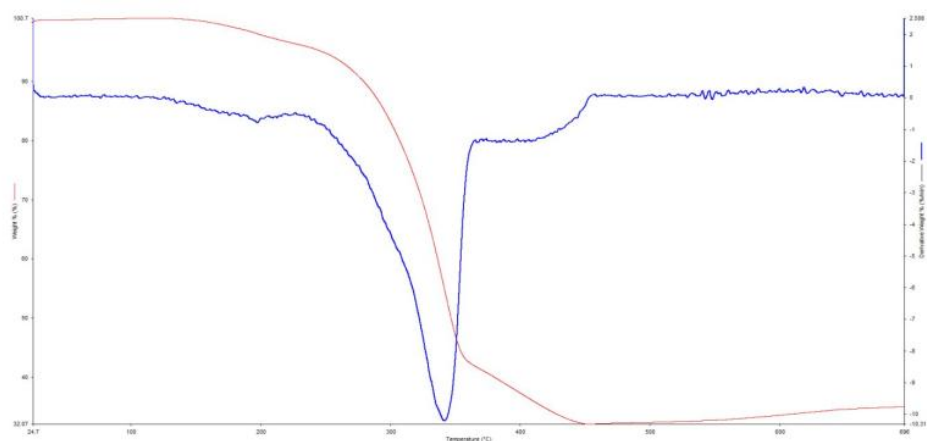


**Figure S19.** TGA (red) and DTG (blue) spectrum measured for metallosupramolecular branched polymer  $[\text{Pd}_3\text{L}_2]_n$ .

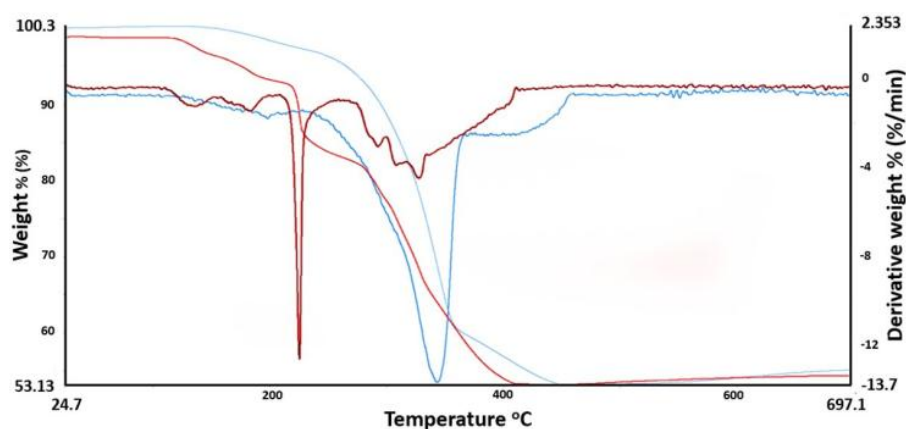


**Figure S20.** Comparison of thermogravimetric analysis of metallocupramolecular macrocycle  $[\text{Pd}_2(\text{HL})_2]$  (red – light (TGA) and dark (DTG)) and  $[\text{Pd}_3\text{L}_2]_n$  polymer (blue – light (TGA) and dark (DTG)) showing decomposition of compounds with temperature.

## 7. References

1. Rigaku Oxford Diffraction, *CrysAlisPro*, 1.171.35.11 Rigaku OD Yarton, Oxfordshire, UK, 2009-2019.
2. Bruker-Nonius *APEX v2.1*, *SAINT v.7* and *XPRED v.6.14*, Bruker AXS Inc., Madison, Wisconsin, USA: Madison Wisconsin, USA, 2003.
3. Altomare, A.; Burla, M. C.; Camalli, M.; Cascarano, G. L.; Giacovazzo, C.; Guagliardi, A.; Moliterni, G. C.; Polidori, G.; Spagna, S., SIR97, A Package for Crystal Structure Solution by Direct Methods and Refinement. *J. Appl. Crystallogr.* **1999**, *32*, 115-119.
4. Sheldrick, G. M., SHELXT - Integrated space-group and crystal-structure determination. *Acta Cryst. A* **2015**, *71*, 3-8.
5. Sheldrick, G. M., A short history of SHELX. *Acta Crystallogr.* **2008**, *64*, 112-122.
6. Dolomanov, O. V.; Bourhis, L. J.; Gildea, R. J.; Howard, J. A. K.; Puschmann, H., OLEX2: a complete structure solution, refinement and analysis program. *J. Appl. Cryst.* **2009**, *42*, 339-341.
7. *CrysAlisPRO*, Oxford Diffraction, Agilent CrysAlis PRO. Agilent Technologies Ltd., Yarnton, Oxfordshire, England, 2014.
8. Sheldrick, G., Crystal structure refinement with SHELXL. *Acta Cryst. C* **2015**, *71* (1), 3-8.
9. Dolomanov, O. V.; Bourhis, L. J.; Gildea, R. J.; Howard, J. A. K.; Puschmann, H., OLEX2: a complete structure solution, refinement and analysis program. *J. Appl. Crystallogr.* **2009**, *42* (2), 339-341.

### **A3. Dynamic polyimine macrobicyclic cryptands – self-sorting with component selection**



Cite this DOI: 10.1039/c8sc04598d

All publication charges for this article have been paid for by the Royal Society of Chemistry

Received 16th October 2018  
Accepted 6th December 2018

DOI: 10.1039/c8sc04598d

rsc.li/chemical-science

## Dynamic polyimine macrobicyclic cryptands – self-sorting with component selection†

Michał Kołodziejewski,<sup>a,b,c</sup> Artur R. Stefankiewicz<sup>b,c</sup> and Jean-Marie Lehn<sup>a,\*</sup>

Self-assembling macrobicyclic cryptand-type organic cages display remarkable self-sorting behavior with efficient component selection. Making use of the dynamic covalent chemistry approach, eight different cages were synthesized by condensation of tris(2-aminopropyl)amine with structurally different dialdehydes. A series of self-sorting experiments were first carried out on simple dynamic covalent libraries. They reveal the influence of different structural features of the aldehyde components on the condensation with two triamine capping units. Subsequently, self-sorting experiments were performed on more complex systems involving several dialdehyde building blocks. Altogether, the results obtained describe the effect of the presence of a heteroatom, of electrostatic interactions, of delocalization and of the flexibility/stiffness of the propensity of a component to undergo formation of a macrobicyclic cage. In the presence of a catalytic amount of acid, the macrobicyclic structure undergoes dynamic component exchange.

## Introduction

Since the first synthesis of the macrobicyclic cryptands and cryptates,<sup>1,2</sup> studies on such compounds have been pursued in numerous laboratories and have represented a fascinating area of investigation in supramolecular chemistry.<sup>3,4</sup> The wide interest in macrobicyclic and, by extension, in macropolycyclic entities resides in the rich set of properties (as molecular receptors, catalysts and carriers) enabled by their structural diversity and specific spatial forms, resulting from the use of a variety of building blocks, as well as in their potential uses in areas such as supramolecular engineering and nanotechnology. Much activity has been displayed in the wide area of cage-type compounds and molecular containers.<sup>5–8</sup>

Cryptands have generally been synthesized by stepwise build-up of the macrobicyclic framework based on covalent bond formation.<sup>9–11</sup> In addition, several such structures have later also been obtained by formation of multiple imine bonds.<sup>12–20</sup> The advent and active development of dynamic covalent chemistry (DCC)<sup>21–26</sup> which rests on the implementation of reversible

covalent reactions (in particular imine formation) in molecular frameworks, prompts to revisit the area of macrobi(poly)cyclic cryptand-type cage compounds in the light of this approach, which opens up new vistas in synthesis, properties and applications of this class of substances.

Dynamic molecules and materials, molecular as well as supramolecular, have attracted increasing interest in the realm of constitutional dynamic chemistry (CDC)<sup>27,28,29</sup> towards the emergence of adaptive chemistry.<sup>30,31</sup> A particular intriguing feature of such constitutional dynamic systems is the ability to perform component selection in the buildup of their constitution through “self-sorting” processes, introduced initially for the case of “self-recognition” (“homo-self-sorting”) in the generation of double and triple stranded helicates.<sup>32</sup> Self-sorting reduces the potential number of combinations of components (thus counteracting entropy) by arranging them into specific organized structures.<sup>33–35</sup> Non-covalent self-sorting in artificial systems, assisted by hydrogen bonds<sup>37</sup> or donor-acceptor interactions<sup>38,39</sup> has been widely explored.<sup>40,41</sup> On the other hand, the initial synthesis and exploration of macrobicyclic cryptand-type molecular cages based on the formation of multiple reversible imine bonds<sup>12,13,15–20</sup> opened the possibility to extend self-sorting processes to the behavior of such dynamic cage architectures. Indeed, the successful high yield generation of these compounds by self-assembly in a single operation based on reversible covalent imine formation, may be considered to involve the operation of “behind-the-scene” dynamic self-sorting. More recently, the chemistry of dynamic covalent cage compounds<sup>42–48</sup> has been subject to inventive developments by several groups based notably on polyimine,<sup>42–44</sup> disulfide<sup>45–47</sup> or orthoester formation.<sup>48–50</sup>

<sup>a</sup>Laboratory of Supramolecular Chemistry, Institut de Science et d'Ingénierie Supramoléculaires (ISIS), UMR 7006, CNRS, Université de Strasbourg, 8 allée Gaspard Monge, 67000 Strasbourg, France. E-mail: lehn@unistra.fr

<sup>b</sup>Faculty of Chemistry, Adam Mickiewicz University, Umultowska 89b, 61-614 Poznań, Poland. E-mail: artur@amu.edu.pl

<sup>c</sup>Center for Advanced Technologies, Adam Mickiewicz University, Umultowska 89c, 61-614 Poznań, Poland

† Electronic supplementary information (ESI) available: Experimental section, characterization of obtained compounds, NMR spectra, CCDC deposition numbers, CCDC 1853998 and 1853999. For ESI and crystallographic data in CIF or other electronic format see DOI: 10.1039/c8sc04598d



Dynamic covalent bond formation is thus clearly a means to generate dynamic cage-type compounds (dynamic cryptands) with various differentiated properties and to enable self-sorting in multicomponent libraries. The reversibility of dynamic covalent bonds, such as C=N of imines, enables removal of undesired intermediates ("errors") and leads to the thermodynamically most stable structures. It also provides a pathway to cage-to-cage transformation in solution – a very useful tool that can be used to change the composition of a dynamic library on purpose.<sup>34</sup>

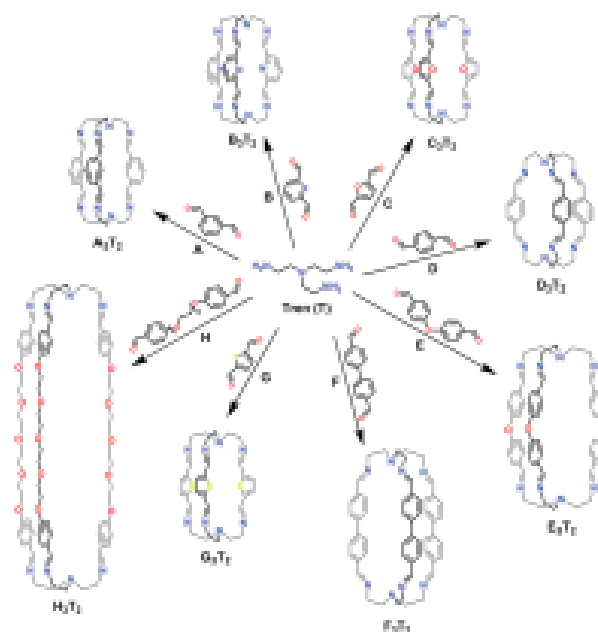
One may thus conclude that organic three-dimensional cage-like architectures can be obtained overall using dynamic covalent bond formation, avoiding complicated, kinetically controlled multistep pathways. Moreover, an important feature of such procedures is the ability to modulate the structural transformations within the component library under the influence of chemical (pH, guest molecule) or physical (temperature, light) stimuli. Such three-dimensional cages suitable for guest inclusion have attracted much attention recently related largely to their use as sensors, drug carriers and catalysts, as well as for storage or isolation of gases.<sup>34,35</sup> However, from the perspective of synthetic self-assembling methodology as well as of functional features, self-sorting protocols add a new dimension to this area and deserve to be closely scrutinized, as they allow for the analysis of the behavior of multicomponent systems.

In the present work, we report the investigation of the effect of structural features of the molecular components on the self-sorting phenomenon in the formation of a variety of imine-based macrobicyclic cryptand-type cage constituents. Moreover, we describe acid-catalysed processes of component exchange between different cages. As a preliminary step, a variety of structurally distinct dialdehydes (A–H; Scheme 1) have been reacted with the triamine "tren" (tris(2-aminoethyl)amine; T) to give hexaimine cages, extending the initial work on such processes.<sup>18–19,36</sup> Following the dynamic covalent chemistry approach, dynamic libraries consisting of dialdehydes and triamine components were set up in order to analyse the self-sorting behaviour between the aldehydes employed. In order to be able to evaluate the effects of the structural features of the components, we have restricted the present work to systems involving just the different dialdehydes A–H and the triamine T in the absence of other agents, such as metal ions.

## Results and discussion

### Synthesis and characterisation of the homoleptic macrobicyclic cages

The reactions examined involved seven aromatic dialdehydes (A–G) of fairly similar type and size as well as one (H) (very different in both size and flexibility) (Scheme 1). Before performing competitive experiments, the dialdehydes (A–H) were separately reacted with triamine T in acetonitrile (MeCN) at room temperature. In all cases, substantial precipitates formed within 24 h and were shown subsequently to be the desired cages involving the bridging of two T units by three dialdehyde



Scheme 1 Molecular structures of dialdehydes (A–H), the triamine (T) and the generated [3 + 2] homoleptic imine-based organic macrobicyclic cryptand cages.

branches by hexa-imine formation, designated as  $X_2T_2$ , with  $X = A-H$ . *ortho*-Phthalaldehyde was also included in the initial list of dialdehydes to be tested but it did not react in the same way with T as the others and did not provide a cage. All the bulk products gave elemental analyses consistent with the 3 : 2 stoichiometry and all showed  $^1H$  NMR spectra (in  $CDCl_3$ ) consistent with the  $D_3$  symmetry expected for the cage where all imine units have the *trans* configuration. The molecular structures of the products also agreed with their ESI-TOF mass spectrometry data. In two cases,  $E_2T_2$  and  $F_2T_2$ , details of their solid-state structures were established by single-crystal X-ray crystallography (Fig. 1a and b, respectively). The crystallographic structures of  $A_2T_2$ ,  $B_2T_2$ ,  $C_2T_2$  and  $D_2T_2$  cages have been previously described in the literature<sup>34,36–38</sup> as well as those of closely related compounds.<sup>36,39</sup> Thus, crystals of  $E_2T_2 \cdot 2CHCl_3$  were obtained as yellow rods by vapour diffusion of diethylether into a chloroform solution. The solid-state molecular structure confirms the structural assignment based on the solution data, showing an extended capsular form with a length of approximately 15 Å, as defined by the distance between the central N atoms of the tren residues, and a twisted chiral shape along this N-to-N axis. The chloroform of crystallisation is not included within the cage, indicating that the lateral dimensions of the cage are unsuited for inclusion, and the lone pairs on the oxygen atoms would appear to be directed out from the cage, indicating that external rather than internal interactions of the cage would be preferred.

Brownish, rod-like crystals of  $F_2T_2$  were obtained by liquid diffusion of diisopropyl ether into a dichloromethane solution at room temperature in a closed vial. The cage unit is again a chiral capsule, though less twisted away from  $D_{3h}$  symmetry



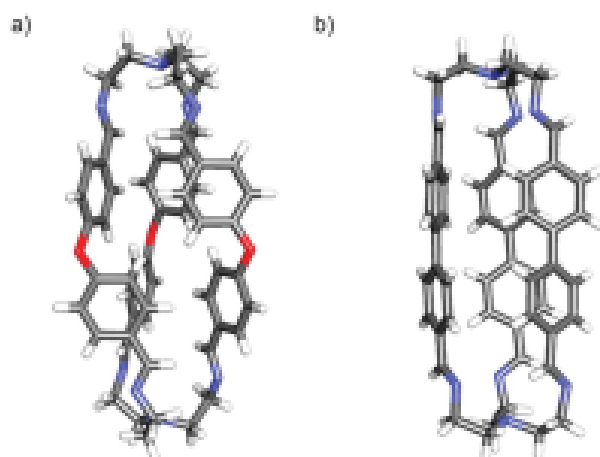


Fig. 1 Solid state X-ray molecular structures of the cages  $E_3T_2 \cdot 2CHCl_3$  (left) and  $F_3T_2 \cdot 2CHCl_3$  (right). Colour code: red, O; blue, N; grey, C; white, H.

than the  $E_3T_2$  cage, and with a separation of the terminal N atoms close to 15 Å. There is no solvent included within the capsule.

### Self-sorting experiments

**General procedure.** After successful synthesis, isolation and characterisation of the eight homoleptic cages  $X_3T_2$  ( $X = A-H$ ), we proceeded to the investigation of the self-sorting process in cage formation between triamine T with all possible twofold mixtures of the subset A-E and H of the dialdehydes in chloroform solution from which the cages do not readily precipitate. Note that the products obtained in solution and on precipitation had the same spectroscopic properties. All these self-sorting experiments were conducted under the same conditions (concentration equal to  $2 \times 10^{-2}$  mol dm $^{-3}$ , CDCl $_3$  as a solvent, 1,4-dioxane as an internal standard, 24 h stirring at room temperature, then 24 h stirring at 318.15 K and again 24 h stirring at room temperature to ensure that equilibrium was reached) and the product distribution was conveniently monitored by  $^1H$  NMR spectroscopy. The results obtained are summarised in Table 1 (all NMR spectra in ESI, Fig. S9–S23†). Remarkably, the  $^1H$  NMR spectra showed that in thirteen of the fifteen simple libraries (i.e. two different dialdehydes and the triamine) only a single homoleptic cage was detectable at equilibrium in every case. A mixture of two homoleptic cages was observed in the two systems involving aldehyde pairs B/C and D/E.

No formation of heteroleptic systems (mixed-aldehyde components cage species) was observed in any of the tested samples, whether at equilibrium or during its attainment. Thus, the species shown in Scheme 1 suffice to describe the formation behaviour in all systems.

**Effect of the presence of a heteroatom on the self-sorting process.** In the first self-sorting experiment on the library consisting on A, B and T (3 : 3 : 2 ratio was applied in all experiments) that was carried out, the influence of a heteroaromatic donor atom was investigated. The dialdehyde components A and B differ only by one atom. The carbon atom in position 2 of isophthalic dicarbaldehyde becomes a nitrogen atom in pyridine-2,6-dicarbaldehyde. Both dialdehydes and their imines contain a fully conjugated system of the aromatic ring and its substituents but only in B are attractive interactions possible between the two imine C–H bonds adjacent to the aromatic ring and the adjacent pyridine N atom of another cage arm.<sup>26</sup> A possible additional factor that works in favour of cage  $B_3T_2$  with respect to cage  $A_3T_2$  are intramolecular interactions that may occur between imine C–H bonds and pyridine N lone pair (see ESI, Fig. S29†). Both cages, however, are stabilized through intramolecular hydrogen bonding interactions between the imine C–H bonds of one arm of the cage and the imine N atom of another.<sup>26</sup> These latter interactions are also responsible for the almost identical position of the imine C–H signal in the  $^1H$  NMR spectra of both cages. Thus, the heteroaromatic cage  $B_3T_2$  appears to be both kinetically and thermodynamically favoured in this self-sorting experiment and was formed in 92% yield. Cage  $A_3T_2$  is not formed and component A remains unreacted in the reaction mixture (Fig. 2). At equilibrium, 8% of unreacted component B and triamine T are also present.

**Effect of the structural flexibility of the components on the self-sorting process.** In the self-sorting experiment between components B, H and T, the homoleptic cage  $B_3T_2$  is also preferentially formed in almost quantitative yield (see ESI, Fig. S17†). The second dialdehyde component – H – remained unreacted in the mixture. Kinetic factors alone may explain the initially preferred formation of  $B_3T_2$  but it is also the thermodynamically preferred species. An obvious disadvantage of dialdehyde H is its flexibility, which must provide an enhanced entropic barrier to both rates and equilibria. Probably more important in explaining the difference in thermodynamic preference for the cage structure (which is but one of many possible cyclic and polymeric imine-containing structures) is the nature of the heteroaromatic unit directly linking the two aldehyde groups of B. The lone pair of the N-atom in B is suitable for interaction with the imine (and aldehyde) CH atoms,

Table 1 Equilibrium distributions observed for competition experiments between two distinct aldehydes (3 equiv. of each) and amine T (2 equiv.)

T	A	B	C	D	E	H
A		$B_3T_2$	$C_3T_2$	$A_3T_2$	$A_3T_2$	$A_3T_2$
B	$B_3T_2$		$B_3T_2 : C_3T_2$ 56 : 44	$B_3T_2$	$B_3T_2$	$B_3T_2$
C	$C_3T_2$	$B_3T_2 : C_3T_2$ 56 : 44		$C_3T_2$	$C_3T_2$	$C_3T_2$
D	$A_3T_2$	$B_3T_2$	$C_3T_2$		$D_3T_2 : E_3T_2$ 65 : 35	$D_3T_2$
E	$A_3T_2$	$B_3T_2$	$C_3T_2$	$D_3T_2 : E_3T_2$ 65 : 35		$E_3T_2$
H	$A_3T_2$	$B_3T_2$	$C_3T_2$	$D_3T_2$	$E_3T_2$	



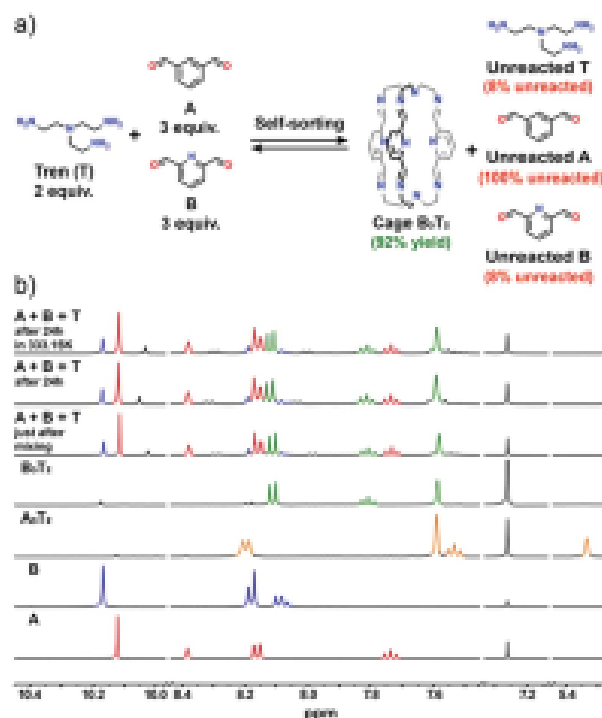


Fig. 2 (a) General scheme of the self-sorting experiment between components A + B + T; (b) comparison of the <sup>1</sup>H NMR spectra of all three components recorded over time. The <sup>1</sup>H NMR spectra of reaction components and isolated cages are also shown for comparison. Low intensity signals observed in the spectra after component mixing may come from trace amounts of intermediate products such as open chain structures. All NMR spectra were recorded in CDCl<sub>3</sub> at 400 MHz.

thus tending to maintain an array better suited to cyclisation than to polymerisation and possibly also providing some activation of the carbonyl centre.

Self-sorting experiments leading to a mixture of two cages. In only two cases (Fig. 3) the competition between two aldehydes for T in cage formation was observed. The <sup>1</sup>H NMR analysis of the library consisting of B, C and T (see ESI, Fig. S14†) revealed initially the preferential formation of cage B<sub>2</sub>T<sub>2</sub> (while at equilibrium both cage species *i.e.* B<sub>2</sub>T<sub>2</sub> and C<sub>2</sub>T<sub>2</sub> were present in almost equal amounts). Integration of the proton NMR signals provided an equilibrium distribution of 28% of B<sub>2</sub>T<sub>2</sub>, 22% of C<sub>2</sub>T<sub>2</sub>, together with unreacted 22% of B and 28% of C (Fig. 3a). Since both aldehydes contain a hetero-aromatic group and form conjugated systems with their substituents, it is unsurprising that there is only a minor difference in their cage formation ability at equilibrium.

In the case of the library comprising component D, E and T a mixture of two cages was again observed, though in this case the formation of D<sub>2</sub>T<sub>2</sub> was favoured by about a factor of 2 at equilibrium, the product ratio D<sub>2</sub>T<sub>2</sub> : E<sub>2</sub>T<sub>2</sub> being 65 : 35 (Fig. 3b). The aldehydes here differ in that the oxygen link in E breaks the conjugation of the two halves and introduces a degree of conformational flexibility that is absent in D (for NMR spectra see ESI, Fig. S21†).

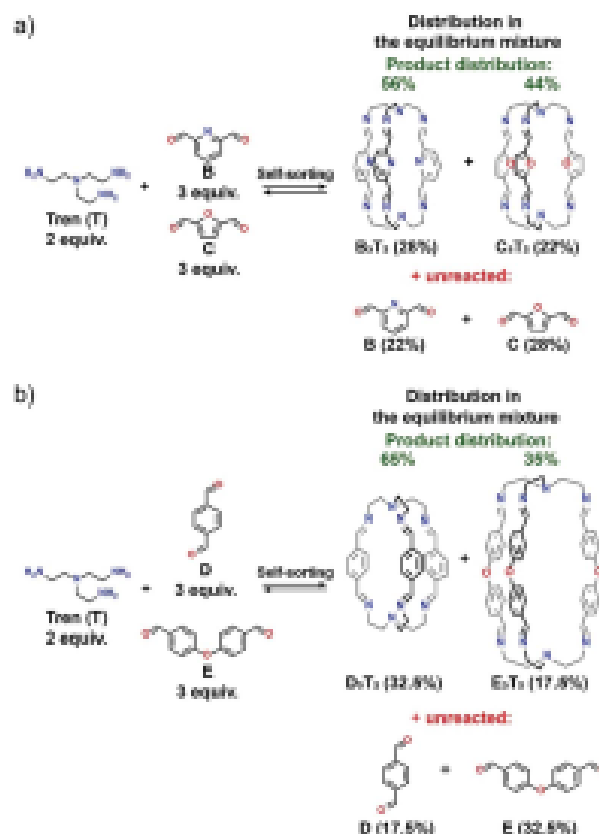


Fig. 3 General schemes presenting product distribution of an equilibrium mixture for libraries consisting of (a) 3B + 3C + 2T and (b) 3D + 3E + 2T.

Self-sorting selectivity in a mixture of six dialdehyde components. The data summarised in Table 1 enable the six aldehydes investigated to be placed in decreasing order of thermodynamic preference in cage formation: B = C > A > D > E > H. To confirm if this order was preserved under conditions where all six aldehydes simultaneously compete for the triamine T, we performed a self-sorting experiment on a library consisting of seven components. The sequence of reactions occurring in this system was clearly revealed by following the changes in the <sup>1</sup>H NMR spectra covering just the region of the reactant aldehyde CHO proton resonances (Fig. 4). Into a mixture of 3 molar amounts of each of the six dialdehydes (A–E and H), six lots of 2 molar amounts of triamine T were titrated progressively. In line with our expectations, after addition of a first dose of T, B<sub>2</sub>T<sub>2</sub> (with a slight advantage) and C<sub>2</sub>T<sub>2</sub> cages began to form almost simultaneously. Addition of another aliquot of T led to nearly complete formation of both cages. With the next dose, it was expected to result in the formation of A<sub>2</sub>T<sub>2</sub> and indeed it was so, but the <sup>1</sup>H NMR spectra showed the simultaneous formation of D<sub>2</sub>T<sub>2</sub> in similar amount. The formation of these cages was complete on addition of another dose of T. The next stages of this experiment went according to our expectations in that another portion of T resulted in formation of E<sub>2</sub>T<sub>2</sub> and in the last step H<sub>2</sub>T<sub>2</sub> (but here a small excess of triamine was required to complete formation).



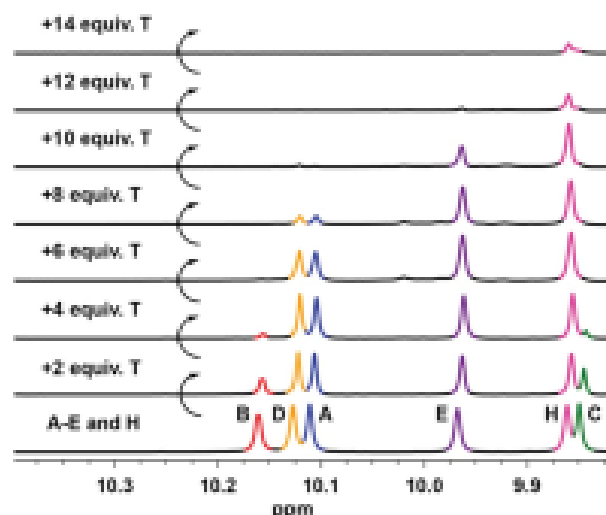


Fig. 4 Changes in aldehyde proton signals of the  $^1\text{H}$  NMR spectra (400 MHz,  $\text{CDCl}_3$ ) during the self-sorting experiment involving titration of  $3\text{A} + 3\text{B} + 3\text{C} + 3\text{D} + 3\text{E} + 3\text{H}$  with appropriate increasing amounts of T. The full spectra of dialdehyde components are shown in ESI†

This experiment led to the slightly modified order of effectiveness in cage formation of  $\text{B} = \text{C} > \text{A} = \text{D} > \text{E} \gg \text{H}$ . Although it is not clear why the behaviour of A and D differs slightly in the full mixture from that in the binary one, the observations confirm that the most effective aldehydes of the chosen group are those (B, C) involving a heteroatom in a simple aromatic unit where there is full conjugation over both imine units. The presence of heteroatoms provides additional possibilities of hydrogen bond formation with the imine C-H, which may further stabilize the cage. Antiparallel orientation of the dipoles of the imine  $-\text{N}=\text{C}-$  groups and the heteroatoms in the aromatic ring may also be a significant electrostatic factor. Next most effective are the aromatic dialdehydes (A, D) lacking a heteroatom in the ring but still enabling full conjugation of the imine units with the rings, while least effective are those (E, H) with some degree of flexibility and an inability to form a conjugated system. Obviously, other factors such as solvation differences may explain some degree of difference but the fact that in all cases it is the cage species that is formed requires that factors controlling the orientation of the imine substituents be considered most important, although here the conformational preferences of the triamine T also require consideration.

**Effect of the number of aromatic rings and rigidity of the dialdehyde component on the self-sorting process.** To explore in greater detail the possible influences of the size of the conjugated unit and the flexibility of the dialdehyde, a further self-sorting titration was conducted with a mixture of just the three dialdehydes D, E and F. The  $^1\text{H}$  NMR spectra obtained during the titration again clearly showed the sequence of equilibria in the region of the formyl proton resonances (Fig. 5a). Aldehyde D, which is capable of forming a fully delocalised diimine unit, reacted the most readily, whereas aldehydes E and F disappeared more slowly but in a similar manner. As seen in the crystal structure of cage  $\text{F}_2\text{T}_2$  (see above) the

biphenyl unit is significantly twisted, indicating that conjugation/delocalisation over the full diimine unit is decreased and it would be expected to be disrupted by the O-bridge in  $\text{E}_2\text{T}_2$ . Despite the similarity of dialdehydes E and F in particular, the observations here confirmed once again the absence of any heteroleptic cages.

**Effect of the type of heteroatom on the self-sorting process.** To get further insights on the effect of the presence of a heteroatom in the dialdehyde components, a titration of a mixture of 3 molar amounts of each of the dialdehydes B, C and G with two-molar doses of T was conducted. Changes in the formyl proton  $^1\text{H}$  NMR signals during the titration are shown in Fig. 5b. Addition of the first portion of triamine T initiated the simultaneous formation of  $\text{B}_2\text{T}_2$  and  $\text{C}_2\text{T}_2$  in the same ratio as in the original self-sorting experiment  $3\text{B} + 3\text{C} + 2\text{T}$  ( $\text{B}_2\text{T}_2 : \text{C}_2\text{T}_2$  as 56 : 44). After addition of 4 molar amounts of triamine in total, these two cages were fully formed. With the final dose of T, the formation of  $\text{G}_2\text{T}_2$  was also completed. At this point, there were three homoleptic cages in solution with once again no evidence of the formation of heteroleptic species, despite the similar equilibrium features shown by the dialdehydes B and C. Given the small advantage of dialdehyde B over C, the affinity of the dialdehydes for the triamine T is:  $\text{B} > \text{C} \gg \text{G}$ . In all three cases, the macrobicyclic cage may be stabilized by H-bonding of the heteroatoms with the imino- $\text{CH}=\text{N}$  hydrogen. The interaction is expected to follow the sequence  $\text{N} > \text{O} > \text{S}$ , which corresponds to the sequence  $\text{B} > \text{C} \gg \text{G}$  observed. In addition, ring size may have an effect when comparing B and C. Furthermore, the difference between C and G may result from the stronger H-bonding to O than to S as well as possibly to the smaller size of O (van der Waals radius = 48 ppm for O and 88 ppm for S) and

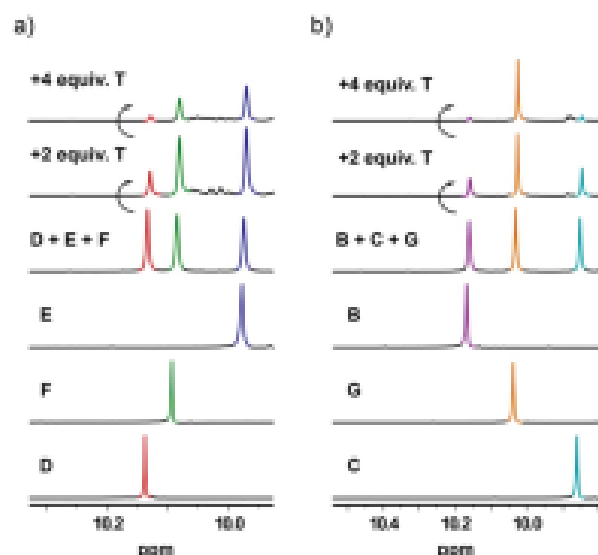


Fig. 5 Comparison of the  $^1\text{H}$  NMR spectra in the range of the dialdehyde signals for self-sorting experiment on libraries consisting in components (a)  $3\text{D} + 3\text{E} + 3\text{F} + 2\text{T}$  and (b)  $3\text{B} + 3\text{C} + 3\text{G} + 2\text{T}$ . The aldehyde proton signal of the dialdehyde components are also shown for comparison. All NMR spectra were recorded at 400 MHz in  $\text{CDCl}_3$  at room temperature.





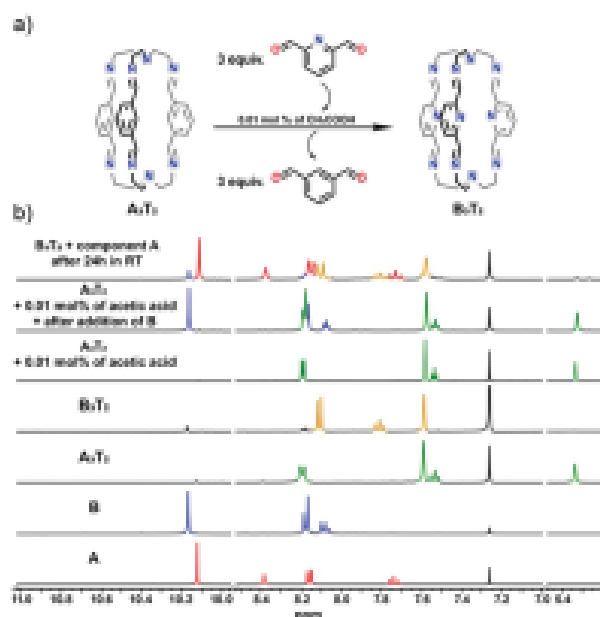


Fig. 6 (a) General scheme of the exchange experiment ( $A_3T_2 + B \rightarrow B_3T_2 + A$ ) between components  $A + B + T$ ; (b)  $^1H$  NMR spectra of acid catalysed exchange experiment between cage  $A_3T_2$  and component B. For comparison  $^1H$  NMR spectra of components A and B as well as isolated cages  $A_3T_2$  and  $B_3T_2$  are also shown. All NMR spectra were recorded at room temperature in  $CDCl_3$ .

to the difference in C=O(S) bond lengths (C=O: 0.136 nm; C=S: 0.182 nm). It would indicate that both the smaller radius of the oxygen atom and the shorter C=O bond length are structurally advantageous for cage formation. In addition, the significant difference in the electronegativity between the O and S heteroatoms may favour a more electronegative oxygen atom, enhancing the effect of antiparallel orientation of the dipoles of the imine  $=CH=N-$  and of the aromatic heterocyclic groups.

Acid/base assisted equilibration and cage-to-cage transformation. As further confirmation that the observations described above apply to true equilibrium systems, the dynamic nature of the imine bonds under acidic conditions<sup>21</sup> was exploited to examine breakage and reformation (after base addition) of cage mixtures. Using methanesulfonic acid (MSA) and triethylamine (TEA) in sequence, experiments were conducted as outlined for the system  $3A + 3B + 2T$  (see ESI, Fig. S27†).

In the first step, the less preferred cage  $A_3T_2$  was broken into its components by the addition of MSA. The cage was then shown to reform rapidly after the addition of TEA. The dialdehyde B, known to form the cage preferentially to A, was then added and the  $^1H$  NMR spectrum of this mixture showed the absence of any perceptible exchange reaction, i.e. the cage  $A_3T_2$  appeared to be stable in the presence of the alternative building block B.

Addition of MSA was once again used to dissociate the cage and this final mixture was thereafter made basic with TEA. The only cage species detectable in this solution was then  $B_3T_2$  as expected. Additionally, these results also demonstrate the possibility to perform cage-to-cage mutation.<sup>44</sup>

These experiments established the lability of the cages in acidic media but involved their complete breakage. As an extension, component exchange from ( $A_3T_2 + B$ ) to ( $B_3T_2 + A$ ) was also investigated using a weak acid at catalytic concentrations to see if exchange of components could be observed in the absence of detectable cage dissociation. While reaction of  $A_3T_2$  with B under such conditions (0.01 mol% catalyst) proved to be slow, cage breakup was not observed other than in that after 24 h reaction, the cage signals in the  $^1H$  NMR spectrum (Fig. 6) were those of  $B_3T_2$  and were accompanied by those of free A. Thus, the strong equilibrium preference for formation of the cage involving B and not A was once more confirmed.

## Conclusions

As demonstrated herein, remarkable self-sorting behavior of high selectivity takes place in the formation of imine-based macrobicyclic cryptand-type organic cages from mixtures of different dialdehyde components reacting with the same capping triamine (see also related processes in ref. 42–53). The structure of the components (their electronic properties, flexibility, presence of a heteroatom, etc.) plays a decisive role in the selective formation of given polyimine cages out of the different structural variations that may be generated from a mixture of very similar dialdehyde building blocks. Structural exploration supports the conclusion that the presence of a heteroatom in a simple aromatic unit favors the cage formation. The results point to the operation of different structural factors comprising attractive H-bonding interactions and electrostatic effects between the imine groups and heteroatomic centers as well as the generation of a conjugated system. Some degree of flexibility and hindrance to optimization of electronic interactions reduce the effectiveness of a component in the self-sorting process. Furthermore, once formed, a given cage may be kinetically trapped, thus forming an out-of-equilibrium mixture. However, in the presence of an agent capable of breaking the imine bonds in the hexaimine structure, exchange of components becomes possible, as expected from the dynamic covalent chemistry of imines, resulting in the generation of the equilibrium state. Developments towards the kinetic behavior of the self-sorting processes, the generation of kinetically trapped out-of-equilibrium states and the encapsulation of substrate molecules may be envisaged.

## Conflicts of interest

There are no conflicts to declare.

## Acknowledgements

The authors acknowledge financial support from the ERC (Advanced Research Grant SUPRADAPT 290585), the ANR DYNAPUN grant No. ANR-15-CE29-0009-01 and the University of Strasbourg. Financial support was also provided by the National Science Centre in Poland (MK, grant PRELUDIUM UMO-2017/25/N/ST5/00942) and the National Centre for Research and Development (ARS, grant LIDER/024/391/L-5/13/NCBR/2014).



We thank Li-Yuan Huang (Strasbourg, Guangzhou) for related work towards polyimine cage compounds. We also thank Prof. Jack Harrowfield for helpful discussions.

## Notes and references

- 1 B. Dietrich, J. M. Lehn and J. P. Sauvage, *Tetrahedron Lett.*, 1969, 10, 2885–2888.
- 2 B. Dietrich, J. M. Lehn, J. P. Sauvage and J. Blanzat, *Tetrahedron*, 1973, 29, 1629–1645.
- 3 J. M. Lehn, *Acc. Chem. Res.*, 1978, 11, 49–57.
- 4 L. Fabbri, *Cryptands and Cryptates*, World Scientific Publishing Company, 2017.
- 5 P. Ballester, M. Fujita and J. Rebek, *Chem. Soc. Rev.*, 2015, 44, 392–393.
- 6 D. S. Kim and J. L. Sessler, *Chem. Soc. Rev.*, 2015, 44, 532–546.
- 7 D. Ajami, L. Liu and J. Rebek Jr, *Chem. Soc. Rev.*, 2015, 44, 490–499.
- 8 S. H. A. M. Leenders, R. Gramage-Doria, B. de Bruin and J. N. H. Reek, *Chem. Soc. Rev.*, 2015, 44, 433–448.
- 9 G. Markiewicz, A. Jenczak, M. Kołodziejewski, J. J. Holstein, J. K. M. Sanders and A. R. Stefankiewicz, *Nat. Commun.*, 2017, 8, 15109.
- 10 J. Jazwinski, J.-M. Lehn, D. Lilienbaum, R. Ziessel, J. Guilhem and C. Pascard, *J. Chem. Soc., Chem. Commun.*, 1987, 1691–1694.
- 11 R. Abidi, F. Arnaud-Neu, M. G. B. Drew, S. Lahely, D. Marrs, J. Nelson and M.-J. Schwing-Weill, *J. Chem. Soc., Perkin Trans. 2*, 1996, 2747–2755.
- 12 D. McDowell and J. Nelson, *Tetrahedron Lett.*, 1988, 29, 385–386.
- 13 D. J. Marrs, V. McKee, J. Nelson, Q. Lu and C. J. Harding, *Inorg. Chim. Acta*, 1993, 211, 195–202.
- 14 Q. Lu, J.-M. Latour, C. J. Harding, N. Martin, D. J. Marrs, V. McKee and J. Nelson, *J. Chem. Soc., Dalton Trans.*, 1994, 1471–1478.
- 15 J.-M. Lehn, J.-P. Vigneron, I. Bkouche-Waksman, J. Guilhem and C. Pascard, *Helv. Chim. Acta*, 1992, 75, 1069–1077.
- 16 D. McDowell, J. Nelson and V. McKee, *Polyhedron*, 1989, 8, 1143–1145.
- 17 O. Koelien, R. J. Mortimer and P. D. Beer, *Tetrahedron Lett.*, 1990, 31, 5069–5072.
- 18 R. Menif, A. E. Martell, P. J. Squattrito and A. Clearfield, *Inorg. Chem.*, 1990, 29, 4723–4729.
- 19 J. de Mendoza, E. Mesa, J.-C. Rodríguez-Ubís, P. Vázquez, F. Vögtle, P.-M. Windschelf, K. Rissanen, J.-M. Lehn, D. Lilienbaum and R. Ziessel, *Angew. Chem., Int. Ed. Engl.*, 1994, 30, 1331–1333.
- 20 V. McKee, J. Nelson and R. M. Town, *Chem. Soc. Rev.*, 2003, 32, 309–325.
- 21 J.-M. Lehn, *Chem.-Eur. J.*, 1999, 5, 2455–2463.
- 22 S. J. Rowan, S. J. Cantrill, G. R. L. Cousins, J. K. M. Sanders and J. F. Stoddart, *Angew. Chem., Int. Ed.*, 2002, 41, 898–952.
- 23 P. T. Corbett, J. Leclaire, L. Vial, K. R. West, J.-L. Wietor, J. K. M. Sanders and S. Otto, *Chem. Rev.*, 2006, 106, 3652–3711.
- 24 S. Ladame, *Org. Biomol. Chem.*, 2008, 6, 219–226.
- 25 S. O. J. N. H. Reek, *Dynamic Combinatorial Chemistry*, Wiley-VCH, Weinheim, 2010.
- 26 B. L. Miller, *Dynamic Combinatorial Chemistry*, Wiley, Chichester, 2010.
- 27 M. E. Belowich and J. F. Stoddart, *Chem. Soc. Rev.*, 2012, 41, 2003–2024.
- 28 Y. Jin, C. Yu, R. J. Denman and W. Zhang, *Chem. Soc. Rev.*, 2013, 42, 6634–6654.
- 29 S. P. Black, J. K. M. Sanders and A. R. Stefankiewicz, *Chem. Soc. Rev.*, 2014, 43, 1861–1872.
- 30 *Dynamic Covalent Chemistry: Principles, Reactions, and Applications*, ed. W. Zhang and J. Yinghua, Wiley-VCH, Weinheim, 2018.
- 31 J.-M. Lehn, in *Constitutional Dynamic Chemistry*, ed. M. Barboiu, Springer Berlin Heidelberg, Berlin, Heidelberg, 2012, pp. 1–32.
- 32 J.-M. Lehn, *Chem. Soc. Rev.*, 2007, 36, 151–160.
- 33 R. Kramer, J. M. Lehn and A. Marquis-Bigault, *Proc. Natl. Acad. Sci. U. S. A.*, 1993, 90, 5394–5398.
- 34 M. M. Safont-Sempere, G. Fernández and F. Würthner, *Chem. Rev.*, 2011, 111, 5784–5814.
- 35 K. Osowska and O. Š. Miljanić, *Synlett*, 2011, 2011, 1643–1648.
- 36 Z. He, W. Jiang and C. A. Schalley, *Chem. Soc. Rev.*, 2015, 44, 779–789.
- 37 A. S. Singh and S.-S. Sun, *Chem. Commun.*, 2012, 48, 7392–7394.
- 38 K. Mahata, M. L. Saha and M. Schmittel, *J. Am. Chem. Soc.*, 2010, 132, 15933–15935.
- 39 W. Drożdż, M. Kołodziejewski, G. Markiewicz, A. Jenczak and A. Stefankiewicz, *Int. J. Mol. Sci.*, 2015, 16, 16300.
- 40 M. A. Squillaci, G. Markiewicz, A. Walczak, A. Ciesielski, A. R. Stefankiewicz and P. Samorl, *Chem. Commun.*, 2017, 53, 9713–9716.
- 41 K. Tahara, T. Fujita, M. Sonoda, M. Shiro and Y. Tobe, *J. Am. Chem. Soc.*, 2008, 130, 14339–14345.
- 42 T. Jiao, G. Wu, L. Chen, C.-Y. Wang and H. Li, *J. Org. Chem.*, 2018, 83, 12404–12410.
- 43 G. Zhu, Y. Liu, L. Flores, Z. R. Lee, C. W. Jones, D. A. Dixon, D. S. Sholl and R. P. Lively, *Chem. Mater.*, 2018, 30, 262–272.
- 44 T. Mitra, K. E. Jelfs, M. Schmidtman, A. Ahmed, S. Y. Chong, D. J. Adams and A. I. Cooper, *Nat. Chem.*, 2013, 5, 276.
- 45 K. Ono and N. Iwasawa, *Chem.-Eur. J.*, 2018, 24, 1–14.
- 46 M. G. B. Drew, V. Felix, V. McKee, G. Morgan and J. Nelson, *Supramol. Chem.*, 1995, 5, 281–287.
- 47 M. G. B. Drew, D. Marrs, J. Hunter and J. Nelson, *J. Chem. Soc., Dalton Trans.*, 1992, 11–18.
- 48 V. McKee, W. T. Robinson, D. McDowell and J. Nelson, *Tetrahedron Lett.*, 1989, 30, 7453–7456.
- 49 N. Giri, C. E. Davidson, G. Melaugh, M. G. Del Pòpolo, J. T. A. Jones, T. Hasell, A. I. Cooper, P. N. Horton, M. B. Hursthouse and S. L. James, *Chem. Sci.*, 2012, 3, 2153–2157.
- 50 G. Zhang and M. Mastalerz, *Chem. Soc. Rev.*, 2014, 43, 1934–1947.



- 51 P. Kleryk, J. Janczak, J. Panek, M. Miklitz and J. Lisowski, *Org. Lett.*, 2016, 18, 12–15.
- 52 X.-Y. Hu, W.-S. Zhang, F. Rominger, I. Wacker, R. R. Schröder and M. Mastalerz, *Chem. Commun.*, 2017, 53, 8616–8619.
- 53 J. C. Lauer, W.-S. Zhang, F. Rominger, R. R. Schröder and M. Mastalerz, *Chem.-Eur. J.*, 2018, 24, 1816–1820.
- 54 K. Acharyya, S. Mukherjee and P. S. Mukherjee, *J. Am. Chem. Soc.*, 2013, 135, 554–557.
- 55 K. Acharyya and P. S. Mukherjee, *Chem.-Eur. J.*, 2014, 20, 1646–1657.
- 56 P. Skowronek, B. Warzajtis, U. Rychlewska and J. Gawronski, *Chem. Commun.*, 2013, 49, 2524–2526.
- 57 P. Skowronek and J. Gawronski, *Org. Lett.*, 2008, 10, 4755–4758.
- 58 D. Beaudoin, F. Rominger and M. Mastalerz, *Angew. Chem., Int. Ed.*, 2017, 56, 1244–1248.
- 59 C. J. Pugh, V. Santolini, R. L. Greenaway, M. A. Little, M. E. Briggs, K. E. Jelfs and A. I. Cooper, *Cryst. Growth Des.*, 2018, 18, 2759–2764.
- 60 T. Hasell, X. Wu, J. T. A. Jones, J. Bacsá, A. Steiner, T. Mitra, A. Trewin, D. J. Adams and A. I. Cooper, *Nat. Chem.*, 2010, 2, 750–755.
- 61 D. Xu and R. Warmuth, *J. Am. Chem. Soc.*, 2008, 130, 7520–7521.
- 62 N. Christinat, R. Scopelliti and K. Severin, *Angew. Chem., Int. Ed.*, 2008, 47, 1848–1852.
- 63 A. R. Stefankiewicz, M. R. Sambrook and J. K. M. Sanders, *Chem. Sci.*, 2012, 3, 2326–2329.
- 64 W. Drożdż, C. Bouillon, C. Kotras, S. Richeter, M. Barboiu, S. Clément, A. R. Stefankiewicz and S. Ulrich, *Chem.-Eur. J.*, 2017, 23, 18010–18018.
- 65 A. R. Stefankiewicz and J. K. M. Sanders, *Chem. Commun.*, 2013, 49, 5820–5822.
- 66 M. von Delius, *Synlett*, 2016, 27, 177–180.
- 67 R.-C. Brachvogel, F. Hampel and M. von Delius, *Nat. Commun.*, 2015, 6, 7129.
- 68 R.-C. Brachvogel and M. von Delius, *Chem. Sci.*, 2015, 6, 1399–1403.
- 69 R.-C. Brachvogel, H. Maid and M. von Delius, *Int. J. Mol. Sci.*, 2015, 16, 20641.
- 70 M. W. Schneider, H.-J. Siegfried Hauswald, R. Stoll and M. Mastalerz, *Chem. Commun.*, 2012, 48, 9861–9863.
- 71 A. Galan and P. Ballester, *Chem. Soc. Rev.*, 2016, 45, 1720–1737.



## Supplementary information to **A3**

Electronic Supplementary Material (ESI) for Chemical Science.  
This journal is © The Royal Society of Chemistry 2018

Supporting Information for

## Dynamic Polyimine Macrobicyclic Cryptands – Self-sorting with Component Selection

Michał Kołodziej<sup>a,b,c</sup>, Artur R. Stefankiewicz<sup>b,c,\*</sup> and Jean-Marie Lehn<sup>a,\*</sup>

<sup>a</sup>Laboratory of Supramolecular Chemistry, Institut de Science et d'Ingénierie Supramoléculaires (ISIS), UMR 7006, CNRS, Université de Strasbourg, 8 allée Gaspard Monge, 67000 Strasbourg, France  
E-mail: lehn@unistra.fr

<sup>b</sup>Faculty of Chemistry, Adam Mickiewicz University, Umultowska 89b, 61-614 Poznań, Poland. E-mail: ars@amu.edu.pl

<sup>c</sup>Center for Advanced Technologies, Adam Mickiewicz University, Umultowska 89c, 61-614 Poznań, Poland

### Table of Contents

1. Experimental .....	3
1.1. Materials and Methods .....	3
1.2. Synthesis and isolation .....	3
1.2.1. A <sub>3</sub> T <sub>2</sub> Cage .....	3
1.2.2. B <sub>3</sub> T <sub>2</sub> Cage.....	4
1.2.3. C <sub>3</sub> T <sub>2</sub> Cage.....	5
1.2.4. D <sub>3</sub> T <sub>2</sub> Cage .....	6
1.2.5. E <sub>3</sub> T <sub>2</sub> Cage.....	7
1.2.6. F <sub>3</sub> T <sub>2</sub> Cage.....	8
1.2.7. G <sub>3</sub> T <sub>2</sub> Cage .....	9
1.2.8. H <sub>3</sub> T <sub>2</sub> Cage .....	10
1.3. Self-sorting experiments .....	11
1.3.1. Self-sorting experiment 3A + 3B + 2T .....	11
1.3.2. Self-sorting experiment 3A + 3C + 2T .....	12
1.3.3. Self-sorting experiment 3A + 3D + 2T .....	13
1.3.4. Self-sorting experiment 3A + 3E + 2T .....	14
1.3.5. Self-sorting experiment 3A + 3H + 2T .....	15
1.3.6. Self-sorting experiment 3B + 3C + 2T .....	16
1.3.7. Self-sorting experiment 3B + 3D + 2T .....	17
1.3.8. Self-sorting experiment 3B + 3E + 2T.....	18
1.3.9. Self-sorting experiment 3B + 3H + 2T .....	19
1.3.10. Self-sorting experiment 3C + 3D + 2T .....	20
1.3.11. Self-sorting experiment 3C + 3E + 2T.....	21

1.3.12.	Self-sorting experiment 3C + 3H + 2T .....	22
1.3.13.	Self-sorting experiment 3D + 3E + 2T .....	23
1.3.14.	Self-sorting experiment 3D + 3H + 2T .....	24
1.3.15.	Self-sorting experiment 3E + 3H + 2T .....	25
1.4.	Complex self-sorting experiments .....	26
1.4.1.	Self-sorting experiment 3A + 3B + 3C + 3D + 3E + 3H + n2T .....	26
1.4.2.	Self-sorting experiment 3D + 3E + 3F + n2T.....	27
1.4.3.	Self-sorting experiment 3B + 3C + 3G + n2T .....	28
1.5.	NMR spectra of an acid/base assisted equilibration .....	29
1.6.	NMR spectra of an exchange experiment $A_3T_2 + 3B \rightarrow 3A + B_3T_2$ .....	29
1.7.	Schematic representation of a self-sorting experiment 3A + 3B + 2T .....	30
2.	Crystallography.....	30
3.	References.....	30

## 1. Experimental

### 1.1. Materials and Methods

All chemicals and solvents were purchased from commercially available sources and were used without further purification. Aldehydes **B** and **H** were synthesised according to reported procedures<sup>1,2</sup>. <sup>1</sup>H and <sup>13</sup>C NMR spectra for the characterization of the products were recorded on a Bruker Ultrashield™ 300 + 300 Fourier-Transform spectrometer. <sup>1</sup>H NMR spectra for characterization of dynamic libraries of components were recorded in CDCl<sub>3</sub> on a Bruker 400 MHz spectrometer, using 1,4-dioxane as an internal standard. In <sup>1</sup>H NMR spectra chemical shift (δ) values are reported relative to TMS (δ = 0.00 ppm) and were measured in CDCl<sub>3</sub> stored over the anhydrous potassium carbonate (K<sub>2</sub>CO<sub>3</sub>). TOF-MS spectra were measured using chloroform solutions on a BRUKER Impact HD ESI-Q-TOF mass spectrometer. X-Ray diffraction data were obtained on a 4-circle Xcalibur EosS2 diffractometer (Agilent Technologies) equipped with a CCD detector.

### 1.2. Synthesis and isolation

#### 1.2.1. A<sub>3</sub>T<sub>2</sub> Cage

**Synthesis of cage A<sub>3</sub>T<sub>2</sub> Tren** [N(CH<sub>2</sub>CH<sub>2</sub>NH<sub>2</sub>)<sub>3</sub>] (64.42 mg; 0.44 mmol) was dissolved in MeCN (1 mL), then isophthalic dialdehyde (88.52 mg; 0.66 mmol) in MeCN (14 mL) was added dropwise over 15 min. The resulting clear, colourless solution was stirred for 3 h at room temperature. The cloudy, greenish-yellow supernatant was filtered off from the yellow precipitate formed, which was washed on the filter with MeCN (10 mL), then dried under vacuum. Yield: 211 mg (75%). <sup>1</sup>H NMR (300 MHz, CDCl<sub>3</sub>) δ 8.21, 8.19 (d, 6H, H<sub>4</sub>), 7.59 (s, 6H, imine, H<sub>3</sub>), 7.53 (t, 3H, H<sub>5</sub>), 5.34 (s, 3H, H<sub>6</sub>), 3.78-3.25 (dt, 12H, H<sub>2</sub>), 2.98-2.67 (dt, 12H, H<sub>1</sub>). Melting point = 419-423 K. TOF-MS: m/z = 587.3611 – calculated for C<sub>36</sub>H<sub>43</sub>N<sub>9</sub> (cage); found m/z = 587.3566 [M+H]<sup>+</sup>. Microanalysis: calculated (%) for C<sub>36</sub>H<sub>42</sub>N<sub>9</sub>: C 73.69, H 7.21, N 19.10 %; found: C 73.58, H 7.32, N 19.16 %.

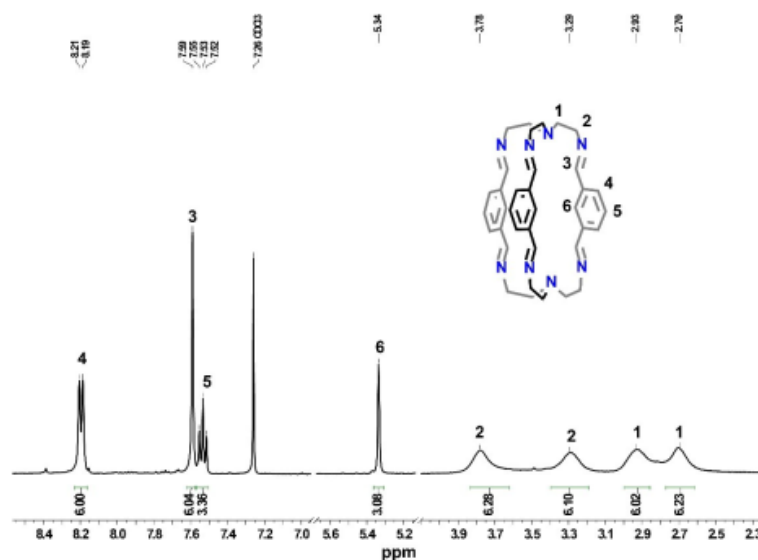


Figure S1. <sup>1</sup>H NMR spectra (300 MHz, CDCl<sub>3</sub>) of synthesized and isolated A<sub>3</sub>T<sub>2</sub> cage, recorded at RT.



### 1.2.2. B<sub>3</sub>T<sub>2</sub> Cage

**Synthesis of cage B<sub>3</sub>T<sub>2</sub>** To the solution of tren [N(CH<sub>2</sub>CH<sub>2</sub>NH<sub>2</sub>)<sub>3</sub>] (205,1 µL; 1,37 mmol) in 3 mL of MeCN was added dropwise to the solution of pyridine-2,6-dicarbaldehyde (277,67 mg; 2,05 mmol) in 12 mL of MeCN during 20 minutes. Before mixing both solutions were clear. After addition of first 5 portions (1 mL each), the reaction mixture became white-greenish suspension for a while. After 6th dose solution became white suspension permanently. The reaction mixture was left for stirring overnight. The yellow suspension was filtered off and dark yellow precipitate was washed with MeCN (10 mL) and dried in vacuum. The dark yellow precipitate was found as a desired cage (231.1 mg; 82% yield). <sup>1</sup>H NMR (300 MHz, CDCl<sub>3</sub>) δ 8.12, 8.10 (d, 6H, H<sub>4</sub>), 7.81 (t, 3H, H<sub>5</sub>), 7.59 (s, 6H, imine, H<sub>3</sub>), 3.59 (t, 12H, H<sub>2</sub>), 2.88 (t, 12H, H<sub>1</sub>). Melting point = 429-433 K. TOF-MS: m/z = 590.3468 – calculated for C<sub>33</sub>H<sub>40</sub>N<sub>11</sub> (cage); found m/z = 590.3471 [M+H]<sup>+</sup>. Microanalysis: calculated (%) for C<sub>33</sub>H<sub>39</sub>N<sub>11</sub>: C 67.21, H 6.67, N 26.13; found: C 67.33, H 6.59, N 26.08 %.

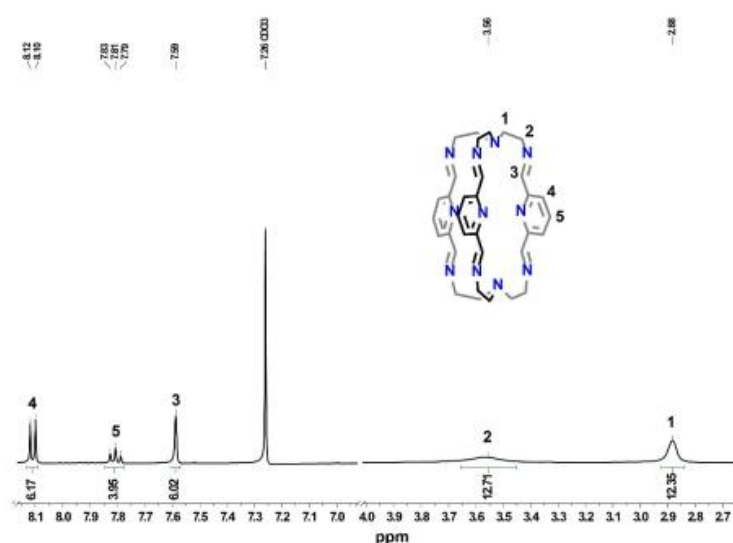


Figure S2. <sup>1</sup>H NMR spectra (300 MHz, CDCl<sub>3</sub>) of synthesized and isolated B<sub>3</sub>T<sub>2</sub> cage, recorded at RT.

### 1.2.3. C<sub>3</sub>T<sub>2</sub> Cage

**Synthesis of cage C<sub>3</sub>T<sub>2</sub>** The tren [N(CH<sub>2</sub>CH<sub>2</sub>NH<sub>2</sub>)<sub>3</sub>] (28.79 mg; 0.197 mmol) was dissolved in 1 mL of MeCN and then 2,5-furandicarbaldehyde (36.65 mg; 0.295 mmol) solution in 10 mL of MeCN was added dropwise during 15 minutes. A clear, yellow-brown solution was left for stirring overnight. The yellow-brownish suspension was filtered off and washed with MeCN (10 mL) and dried in vacuum. The light brown precipitate was found as a desired cage (94.27 mg; 73% yield). <sup>1</sup>H NMR (300 MHz, CDCl<sub>3</sub>) δ 7.72 (s, 6H, imine, H<sub>3</sub>), 7.08 (s, 6H, H<sub>4</sub>), 3.52 (t, 12H, H<sub>2</sub>), 2.76 (t, 12H, H<sub>1</sub>). Melting point = 427-430 K. TOF-MS: m/z = 557.2989 – calculated for C<sub>30</sub>H<sub>37</sub>N<sub>3</sub>O<sub>3</sub> (cage); found m/z = 557.3013 [M+H]<sup>+</sup>. Microanalysis: calculated (%) for C<sub>30</sub>H<sub>36</sub>N<sub>3</sub>O<sub>3</sub>: C 64.73, H 6.52, N 20.13; found: C 64.70, H 6.58, N 20.23 %.

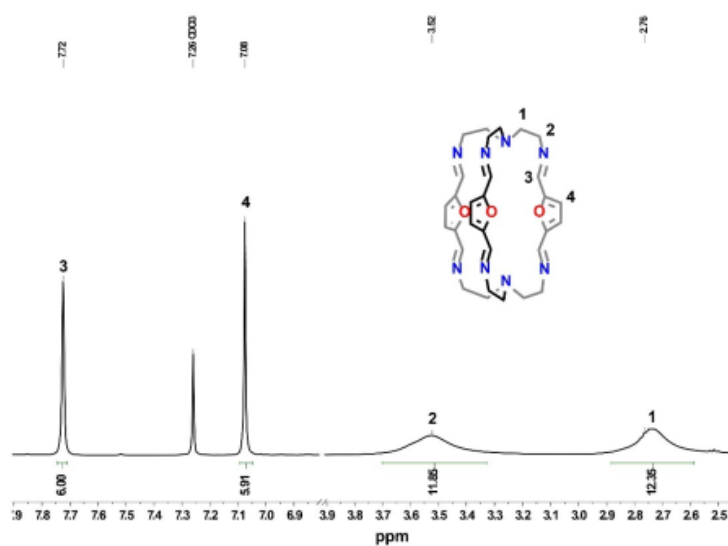


Figure S3. <sup>1</sup>H NMR spectra (300 MHz, CDCl<sub>3</sub>) of synthesized and isolated C<sub>3</sub>T<sub>2</sub> cage, recorded at RT.

#### 1.2.4. D<sub>3</sub>T<sub>2</sub> Cage

**Synthesis of cage D<sub>3</sub>T<sub>2</sub>** The tren [N(CH<sub>2</sub>CH<sub>2</sub>NH<sub>2</sub>)<sub>3</sub>] (56.03 mg; 0.383 mmol) was dissolved in 1 mL of MeCN and then terephthal dialdehyde (77.07 mg; 0.575 mmol) in 10 mL of MeCN was added dropwise during 15 minutes. The resulting clear, colourless solution was left for stirring in 3h in room temperature. Then cloudy, white-cream solution was filtered off and creamy / light yellow precipitate was washed using MeCN (15 mL) and dried in vacuum. The precipitate was found as desired cage compound (262.99 mg; 78% yield). <sup>1</sup>H NMR (300 MHz, CDCl<sub>3</sub>) δ 8.17 (s, 6H, imine, H<sub>3</sub>), 7.17 (s, 12H, H<sub>4</sub>), 3.77 (t, 12H, H<sub>2</sub>), 2.77 (t, 12H, H<sub>1</sub>). Melting point = 418-422 K. TOF-MS: m/z = 587.3611 – calculated for C<sub>38</sub>H<sub>43</sub>N<sub>8</sub> (cage); found m/z = 587.3548 [M+H]<sup>+</sup>. Microanalysis: calculated (%) for C<sub>38</sub>H<sub>43</sub>N<sub>8</sub>: C 73.69, H 7.21, N 19.10; found: C 73.58, H 7.30, N 19.12 %.

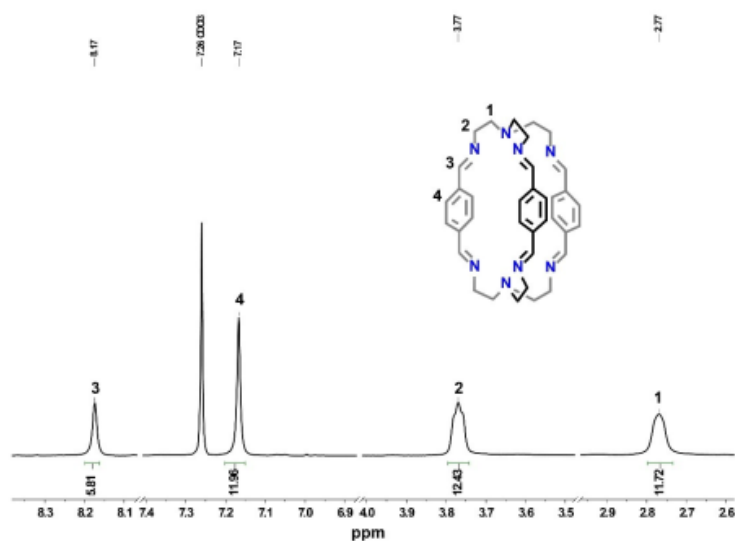


Figure S4. <sup>1</sup>H NMR spectra (300 MHz, CDCl<sub>3</sub>) of synthesized and isolated D<sub>3</sub>T<sub>2</sub> cage, recorded at RT.

### 1.2.5. E<sub>3</sub>T<sub>2</sub> Cage

**Synthesis of cage E<sub>3</sub>T<sub>2</sub>** The tren [N(CH<sub>2</sub>CH<sub>2</sub>NH<sub>2</sub>)<sub>3</sub>] (41.61 mg; 0.284 mmol) was dissolved in 1 mL of MeCN and then 4-(4-formylphenoxy)-benzaldehyde (96.54 mg; 0.427 mmol) dissolved in 10 mL of MeCN was added dropwise during 15 minutes. The clear, colourless solution was left for stirring overnight. Then the yellowish precipitate was filtered off and washed with MeCN (15 mL) and dried in vacuum. The yellowish precipitate was found as a desired compound (298.31 mg; 81% yield). <sup>1</sup>H NMR (300 MHz, CDCl<sub>3</sub>) δ 7.68 (s, 6H, imine, H<sub>3</sub>), 7.12-7.10 (d, 12H, H<sub>4</sub>), 7.03-7.01 (d, 12H, H<sub>5</sub>), 3.57 (t, 12H, H<sub>2</sub>), 2.83 (t, 12H, H<sub>1</sub>). Melting point = 422-426 K. TOF-MS: m/z = 863.4397 – calculated for C<sub>54</sub>H<sub>35</sub>N<sub>9</sub>O<sub>3</sub> (cage); found m/z = 863.4438 [M+H]<sup>+</sup>. Microanalysis: calculated (%) for C<sub>54</sub>H<sub>34</sub>N<sub>9</sub>O<sub>3</sub>: C 75.15, H 6.31, N 12.98; found: C 75.21, H 6.37, N 12.94 %.

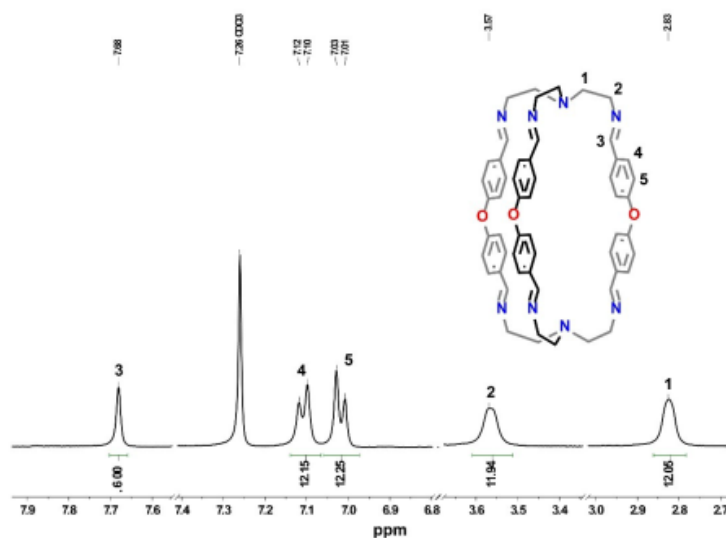
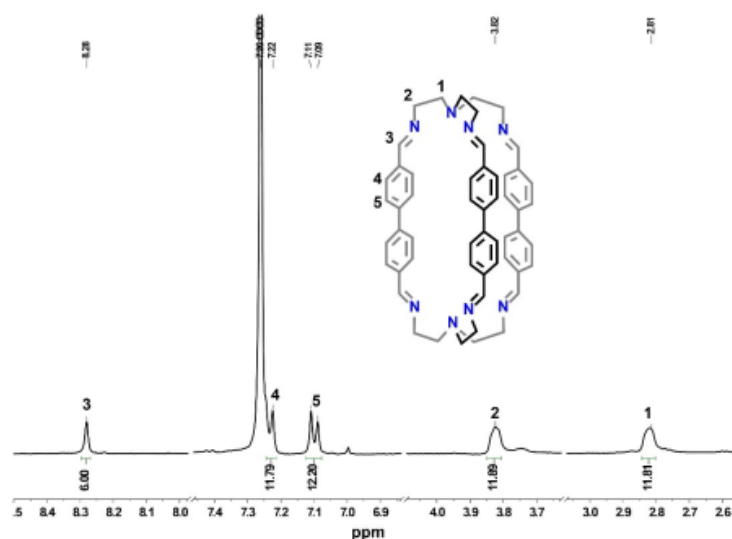


Figure S5. <sup>1</sup>H NMR spectra (300 MHz, CDCl<sub>3</sub>) of synthesized and isolated E<sub>3</sub>T<sub>2</sub> cage, recorded at RT.

### 1.2.6. F<sub>3</sub>T<sub>2</sub> Cage

**Synthesis of cage F<sub>3</sub>T<sub>2</sub>** The tren [N(CH<sub>2</sub>CH<sub>2</sub>NH<sub>2</sub>)<sub>3</sub>] (42.28 mg; 0.289 mmol) was dissolved in 1 mL of MeCN and then 4,4'-biphenyldicarboxaldehyde (91.17 mg; 0.434 mmol) dissolved in 10 mL of MeCN was added dropwise during 15 minutes. The clear, colorless solution was left for stirring overnight. Then the yellow precipitate was filtered off and washed with MeCN (10 mL) and dried in vacuum. The yellow precipitate was found as a desired compound (198 mg; 77.9% yield). <sup>1</sup>H NMR (300 MHz, CDCl<sub>3</sub>) δ 8.28 (s, 6H, imine, H<sub>3</sub>), 7.25-7.22 (d, 12H, H<sub>3</sub>), 7.11-7.09 (d, 12H, H<sub>4</sub>), 3.82 (t, 12H, H<sub>2</sub>), 2.81 (t, 12H, H<sub>2</sub>). Melting point = 414-419 K. TOF-MS: m/z = 815.0820 – calculated for C<sub>54</sub>H<sub>34</sub>N<sub>8</sub> (cage); found m/z = 815.4471. Microanalysis: calculated (%) for C<sub>54</sub>H<sub>34</sub>N<sub>8</sub>: C 79.57, H 6.68, N 13.75; found: C 79.63, H 6.74, N 13.63 %.



**Figure S6.** <sup>1</sup>H NMR spectra (300 MHz, CDCl<sub>3</sub>) of synthesized and isolated F<sub>3</sub>T<sub>2</sub> cage, recorded at RT. A trace amount of intermediate products, most likely open chain species (visible as broad peaks adjacent to that assigned as 1 and 2) was also observed in solution.

### 1.2.7. G<sub>3</sub>T<sub>2</sub> Cage

**Synthesis of cage G<sub>3</sub>T<sub>2</sub>** The tren [N(CH<sub>2</sub>CH<sub>2</sub>NH<sub>2</sub>)<sub>3</sub>] (65.73 mg; 0.449 mmol) was dissolved in 1 mL of MeCN and then 2,5-thiophenedicarboxaldehyde (94.49 mg; 0.674 mmol) dissolved in 10 mL of MeCN was added dropwise during 15 minutes. The clear, colorless solution was left for stirring overnight. Then brownish precipitate was filtered off and washed with MeCN (15 mL) and dried in vacuum. The brownish precipitate was found as a desired compound (112,21 mg; 84.5% yield). <sup>1</sup>H NMR (300 MHz, CDCl<sub>3</sub>) δ 8.03 (s, 6H, imine, H<sub>3</sub>), 7.42 (s, 6H, H<sub>4</sub>), 3.64 (t, 12H, H<sub>2</sub>), 2.72 (t, 12H, H<sub>1</sub>). Melting point = 425-428 K. TOF-MS: m/z = 604.2225 – calculated for C<sub>30</sub>H<sub>36</sub>N<sub>8</sub>S<sub>3</sub> (cage); found m/z = 604.2259. Microanalysis: calculated (%) for C<sub>30</sub>H<sub>36</sub>N<sub>8</sub>S<sub>3</sub>: C 59.57, H 6.00, N 18.53; found: C 59.62, H 6.07, N 18.56 %.

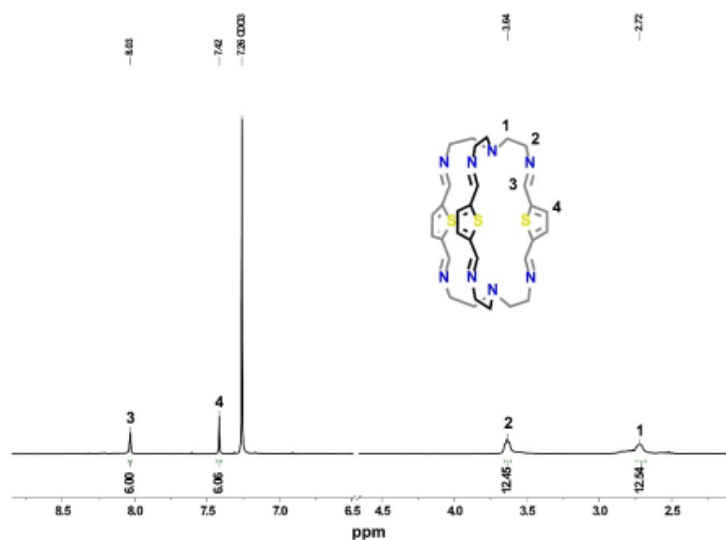


**Figure S7.** <sup>1</sup>H NMR spectra (300 MHz, CDCl<sub>3</sub>) of synthesized and isolated G<sub>3</sub>T<sub>2</sub> cage, recorded at RT. A trace amount of intermediate products, most likely open chain species (visible as broad peaks adjacent to that assigned as 1 and 2) was also observed in solution.

Chemical structure of compound **1** is shown above the <sup>1</sup>H NMR spectrum. The structure is a macrocyclic cage-like molecule with four phenyl rings and four nitrogen atoms. Protons are numbered 1 through 9. The <sup>1</sup>H NMR spectrum (CDCl<sub>3</sub>) shows peaks corresponding to these protons: 1 (13.03 ppm), 2 (3.60 ppm), 3 (7.96 and 7.04 ppm), 4 (7.28 ppm), 5 (6.78 ppm), 6 (4.10 ppm), 7 (3.96 ppm), 8,9 (3.72 ppm), and 10 (2.81 ppm). Solvent peaks for CDCl<sub>3</sub> are at 7.26, 7.26, and 4.76 ppm.

\$10



### 1.3. Self-sorting experiments

#### 1.3.1. Self-sorting experiment 3A + 3B + 2T

In a NMR tube, isophthalic dialdehyde (**A**) (4.08 mg; 0.0304 mmol) and pyridine-2,6-dicarbaldehyde (**B**) (4.18 mg; 0.0304 mmol) were dissolved in 250  $\mu$ L of deuterated chloroform ( $\text{CDCl}_3$ ). Then a deuterated chloroform solution (300  $\mu$ L) containing tris(2-aminoethyl)amine (**T**) (2.97 mg; 0.0203 mmol) was added in two portions. The resulting solution mixture was stirred at room temperature for 24h, then in 318.15 K for another 24h and then again for 24h in RT. The clear solution of the library was checked by  $^1\text{H}$  NMR spectroscopy ( $\text{CDCl}_3$ ) just after mixing the components and after each 24h of stirring (RT/318.15 K/RT).

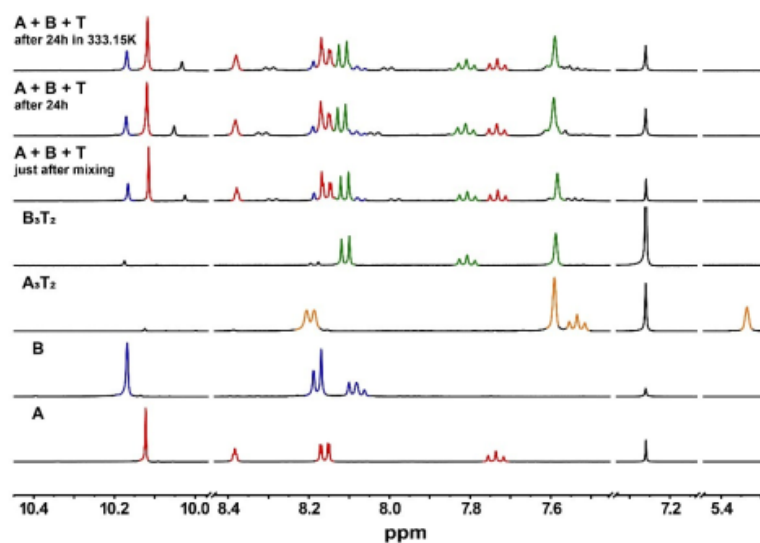


Figure S9. Comparison of  $^1\text{H}$  NMR (400 MHz) spectra for self-sorting experiment 3A + 3B + 2T depending on the time. The spectra of components and pure, isolated cages are also shown for comparison. All NMR spectra were recorded in  $\text{CDCl}_3$  at room temperature.

### 1.3.2. Self-sorting experiment 3A + 3C + 2T

In a NMR tube, isophthalic dicarbaldehyde (A) (5.06 mg; 0.0377 mmol) and furan-2,5-dicarbaldehyde (C) (4.68 mg; 0.0377 mmol) were dissolved in 250  $\mu$ L of deuterated chloroform ( $\text{CDCl}_3$ ). Then a deuterated chloroform solution (300  $\mu$ L) containing tris(2-aminoethyl)amine (T) (3.67 mg; 0.0251 mmol) was added in two portions. The resulting solution mixture was stirred at room temperature for 24h, then in 318.15 K for another 24h and then again for 24h in RT. The clear solution of library was checked by  $^1\text{H}$  NMR spectroscopy ( $\text{CDCl}_3$ ) just after mixing the components and after each 24h of stirring (RT/318.15 K/RT).

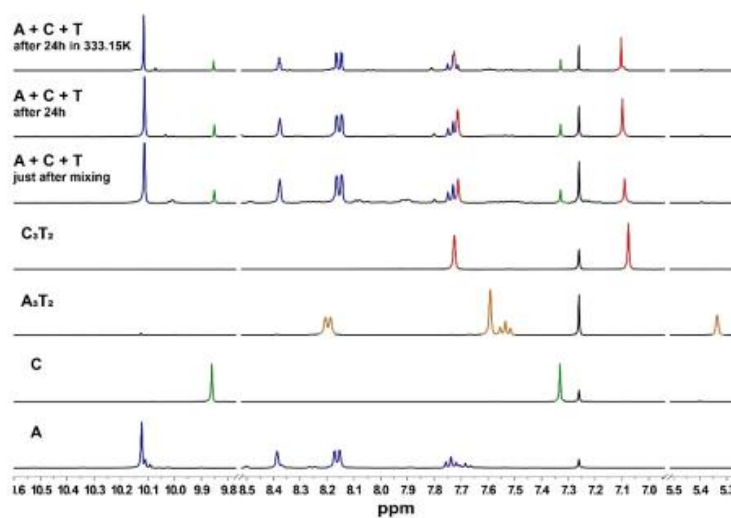


Figure S10. Comparison of  $^1\text{H}$  NMR (400 MHz) spectra for self-sorting experiment 3A + 3C + 2T depending on the time. The spectra of components and pure, isolated cages are also shown for comparison. All NMR spectra were recorded in  $\text{CDCl}_3$  at room temperature.

### 1.3.3. Self-sorting experiment 3A + 3D + 2T

In a NMR tube, isophthalic dicarbaldehyde (A) (3.79 mg; 0.0283 mmol) and terephthalaldehyde (D) (3.79 mg; 0.0283 mmol) were dissolved in 250  $\mu$ L of deuterated chloroform ( $\text{CDCl}_3$ ). Then a deuterated chloroform solution (300  $\mu$ L) containing tris(2-aminoethyl)amine (T) (2.75 mg; 0.0188 mmol) was added in two portions. The resulting solution mixture was stirred at room temperature for 24h, then in 318.15 K for another 24h and then again for 24h in RT. The clear solution of library was checked by  $^1\text{H}$  NMR spectroscopy ( $\text{CDCl}_3$ ) just after mixing the components and after each 24h of stirring (RT/318.15 K/RT).

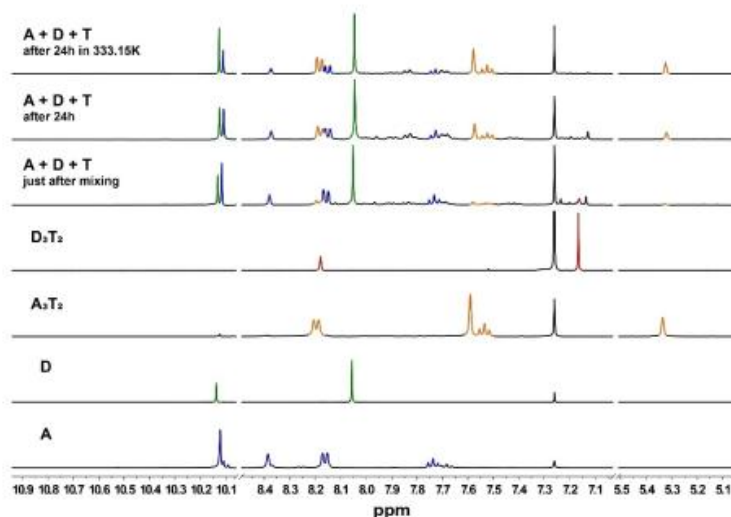


Figure S11. Comparison of  $^1\text{H}$  NMR (400 MHz) spectra for self-sorting experiment 3A + 3D + 2T depending on the time. The spectra of components and pure, isolated cages are also shown for comparison. All NMR spectra were recorded in  $\text{CDCl}_3$  at room temperature.

### 1.3.4. Self-sorting experiment 3A + 3E + 2T

In a NMR tube, isophthalic dialdehyde (A) (3.57 mg; 0.0266 mmol) and 4-(4-formylphenoxy)benzaldehyde (E) (6.02 mg; 0.0266 mmol) were dissolved in 250  $\mu$ L of deuterated chloroform ( $\text{CDCl}_3$ ). Then a deuterated chloroform solution (300  $\mu$ L) containing tris(2-aminoethyl)amine (T) (2.59 mg; 0.0177 mmol) was added in two portions. The resulting solution mixture was stirred at room temperature for 24h, then in 318.15 K for another 24h and then again for 24h in RT. The clear solution of library was checked by  $^1\text{H}$  NMR spectroscopy ( $\text{CDCl}_3$ ) just after mixing the components and after each 24h of stirring (RT/318.15 K/RT).

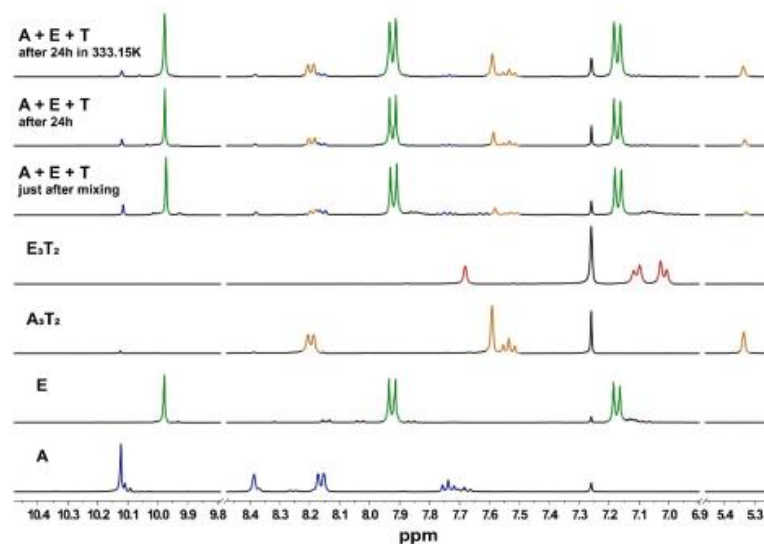


Figure S12. Comparison of  $^1\text{H}$  NMR (400 MHz) spectra for self-sorting experiment 3A + 3E + 2T depending on the time. The spectra of components and pure, isolated cages are also shown for comparison. All NMR spectra were recorded in  $\text{CDCl}_3$  at room temperature.

### 1.3.5. Self-sorting experiment 3A + 3H + 2T

In a NMR tube, isophthalic dialdehyde (A) (0.86 mg; 0.0064 mmol) and 4,4'-(((oxybis(ethane-2,1-diyl))bis(oxy))bis(ethane-2,1-diyl))bis(oxy))dibenzaldehyde (H) (2.58 mg; 0.0064 mmol) were dissolved in 250  $\mu$ L of deuterated chloroform ( $\text{CDCl}_3$ ). Then a deuterated chloroform solution (300  $\mu$ L) containing tris(2-aminoethyl)amine (T) (0.62 mg; 0.0043 mmol) was added in two portions. The resulting solution mixture was stirred at room temperature for 24h, then in 318.15 K for another 24h and then again for 24h in RT. The clear solution of library was checked by  $^1\text{H}$  NMR spectroscopy ( $\text{CDCl}_3$ ) just after mixing the components and after each 24h of stirring (RT/318.15 K/RT).

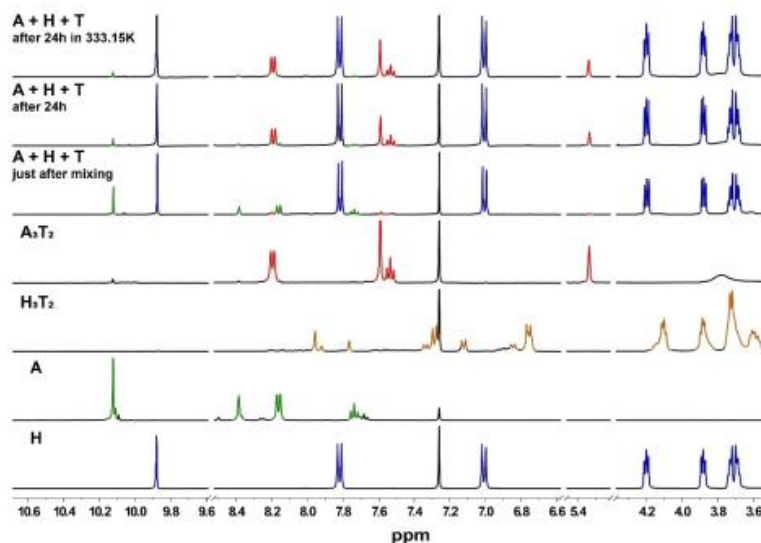


Figure S13. Comparison of  $^1\text{H}$  NMR (400 MHz) spectra for self-sorting experiment 3A + 3H + 2T depending on the time. The spectra of components and pure, isolated cages are also shown for comparison. All NMR spectra were recorded in  $\text{CDCl}_3$  at room temperature.

### 1.3.6. Self-sorting experiment 3B + 3C + 2T

In a NMR tube, pyridine-2,6-dicarbaldehyde (**B**) (3.21 mg; 0.0238 mmol) and furan-2,5-dicarbaldehyde (**C**) (2.96 mg; 0.0238 mmol) were dissolved in 250  $\mu$ L of deuterated chloroform ( $\text{CDCl}_3$ ). Then a deuterated chloroform solution (300  $\mu$ L) containing tris(2-aminoethyl)amine (**T**) (2.32 mg; 0.0159 mmol) was added in two portions. The resulting solution mixture was stirred at room temperature for 24h, then in 318.15 K for another 24h and then again for 24h in RT. The clear solution of library was checked by  $^1\text{H}$  NMR spectroscopy ( $\text{CDCl}_3$ ) just after mixing the components and after each 24h of stirring (RT/318.15 K/RT).

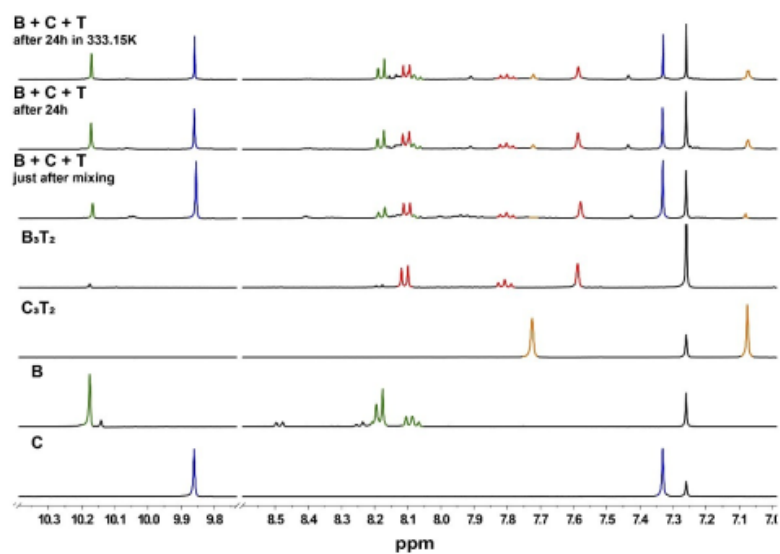


Figure S14. Comparison of  $^1\text{H}$  NMR (400 MHz) spectra for self-sorting experiment **3B** + **3C** + **2T** depending on the time. The spectra of components and pure, isolated cages are also shown for comparison. All NMR spectra were recorded in  $\text{CDCl}_3$  at room temperature.

### 1.3.7. Self-sorting experiment 3B + 3D + 2T

In a NMR tube, pyridine-2,6-dicarbaldehyde (**B**) (3.50 mg; 0.0259 mmol) and terephthalaldehyde (**D**) (3.47 mg; 0.0259 mmol) were dissolved in 250  $\mu$ L of deuterated chloroform ( $\text{CDCl}_3$ ). Then a deuterated chloroform solution (300  $\mu$ L) containing tris(2-aminoethyl)amine (**T**) (2.52 mg; 0.0173 mmol) was added in two portions. The resulting solution mixture was stirred at room temperature for 24h, then in 318.15 K for another 24h and then again for 24h in RT. The clear solution of library was checked by  $^1\text{H}$  NMR spectroscopy ( $\text{CDCl}_3$ ) just after mixing the components and after each 24h of stirring (RT/318.15 K/RT).

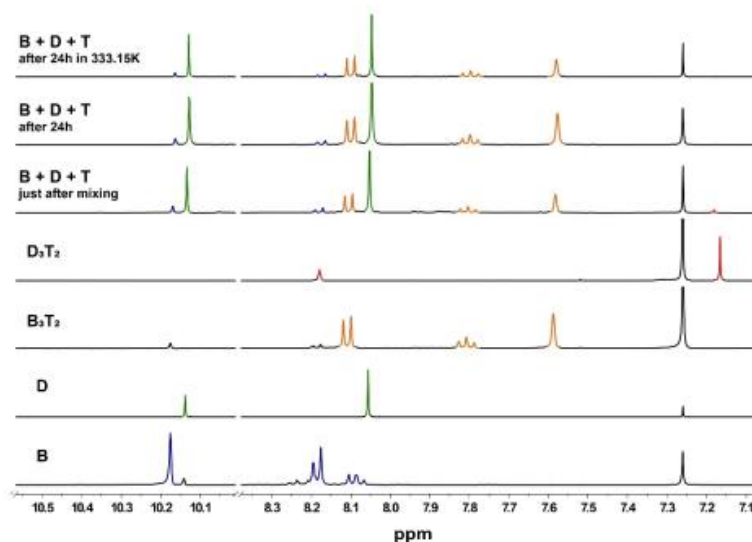


Figure S15. Comparison of  $^1\text{H}$  NMR (400 MHz) spectra for self-sorting experiment **3B + 3D + 2T** depending on the time. The spectra of components and pure, isolated cages are also shown for comparison. All NMR spectra were recorded in  $\text{CDCl}_3$  at room temperature.

### 1.3.8. Self-sorting experiment 3B + 3E + 2T

In a NMR tube, pyridine-2,6-dicarbaldehyde (**B**) (2.80 mg; 0.0207 mmol) and 4-(4-formylphenoxy)benzaldehyde (**E**) (4.68 mg; 0.0207 mmol) were dissolved in 250  $\mu$ L of deuterated chloroform ( $\text{CDCl}_3$ ). Then a deuterated chloroform solution (300  $\mu$ L) containing tris(2-aminoethyl)amine (**T**) (2.02 mg; 0.0138 mmol) was added in two portions. The resulting solution mixture was stirred at room temperature for 24h, then in 318.15 K for another 24h and then again for 24h in RT. The clear solution of library was checked by  $^1\text{H}$  NMR spectroscopy ( $\text{CDCl}_3$ ) just after mixing the components and after each 24h of stirring (RT/318.15 K/RT).

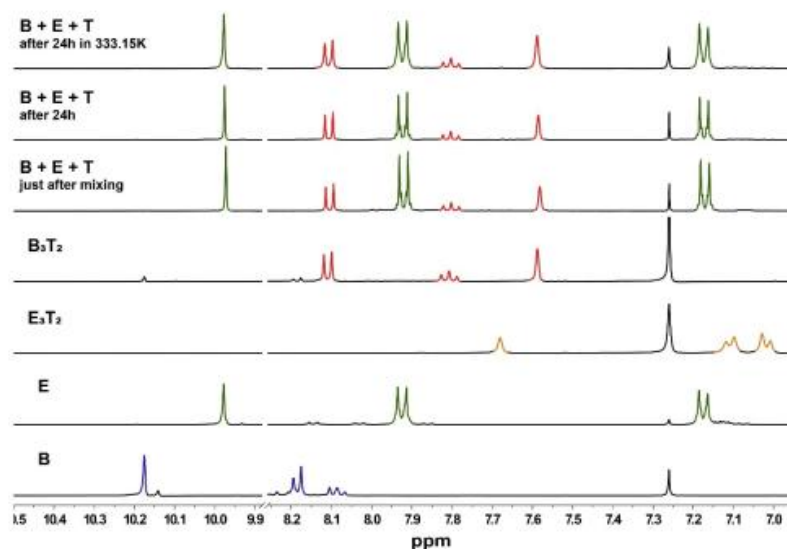


Figure S16. Comparison of  $^1\text{H}$  NMR (400 MHz) spectra for self-sorting experiment 3B + 3E + 2T depending on the time. The spectra of components and pure, isolated cages are also shown for comparison. All NMR spectra were recorded in  $\text{CDCl}_3$  at room temperature.



### 1.3.9. Self-sorting experiment 3B + 3H + 2T

In a NMR tube, pyridine-2,6-dicarbaldehyde (**B**) (1.21 mg; 0.0089 mmol) and 4,4'-(((oxybis(ethane-2,1-diyl))bis(oxy))bis(ethane-2,1-diyl))bis(oxy))dibenzaldehyde (**H**) (3.62 mg; 0.0089 mmol) were dissolved in 250  $\mu$ L of deuterated chloroform ( $\text{CDCl}_3$ ). Then a deuterated chloroform solution (300  $\mu$ L) containing tris(2-aminoethyl)amine (**T**) (0.88 mg; 0.0059 mmol) was added in two portions. The resulting solution mixture was stirred at room temperature for 24h, then in 318.15 K for another 24h and then again for 24h in RT. The clear solution of library was checked by  $^1\text{H}$  NMR spectroscopy ( $\text{CDCl}_3$ ) just after mixing the components and after each 24h of stirring (RT/318.15 K/RT).

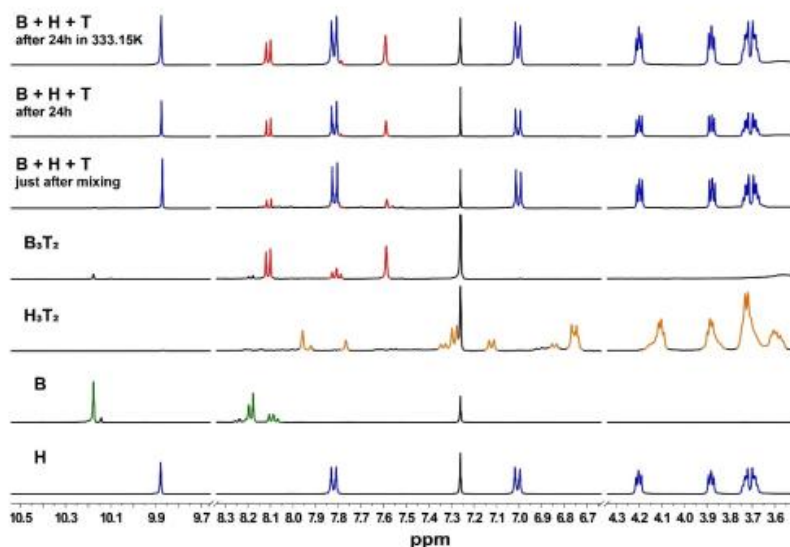
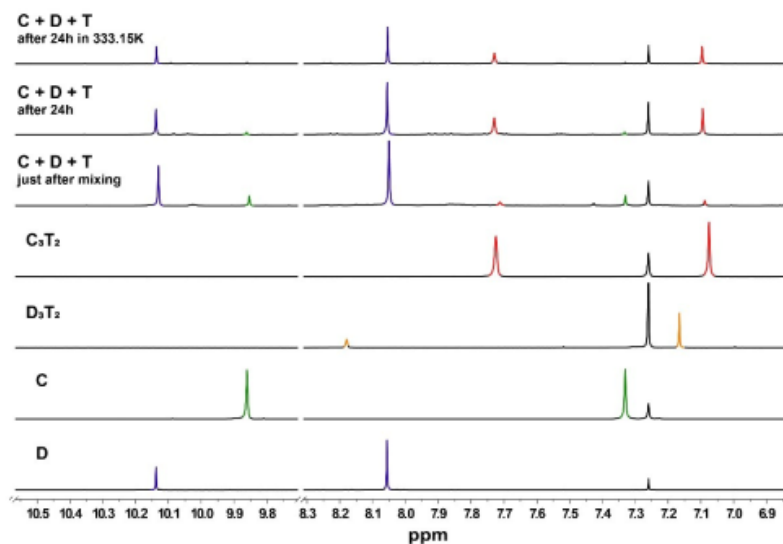


Figure S17. Comparison of  $^1\text{H}$  NMR (400 MHz) spectra for self-sorting experiment 3B + 3H + 2T depending on the time. The spectra of components and pure, isolated cages are also shown for comparison. All NMR spectra were recorded in  $\text{CDCl}_3$  at room temperature.

### 1.3.10. Self-sorting experiment 3C + 3D + 2T

In a NMR tube, furan-2,5-dicarbaldehyde (C) (3.16 mg; 0.0255 mmol) and terephthalaldehyde (D) (3.42 mg; 0.0255 mmol) were dissolved in 250  $\mu$ L of deuterated chloroform ( $\text{CDCl}_3$ ). Then a deuterated chloroform solution (300  $\mu$ L) containing tris(2-aminoethyl)amine (T) (2.49 mg; 0.0171 mmol) was added in two portions. The resulting solution mixture was stirred at room temperature for 24h, then in 318.15 K for another 24h and then again for 24h in RT. The clear solution of library was checked by  $^1\text{H}$  NMR spectroscopy ( $\text{CDCl}_3$ ) just after mixing the components and after each 24h of stirring (RT/318.15 K/RT).



**Figure S18.** Comparison of  $^1\text{H}$  NMR (400 MHz) spectra for self-sorting experiment 3C + 3D + 2T depending on the time. The spectra of components and pure, isolated cages are also shown for comparison. All NMR spectra were recorded in  $\text{CDCl}_3$  at room temperature.

### 1.3.11. Self-sorting experiment 3C + 3E + 2T

In a NMR tube, furan-2,5-dicarbaldehyde (C) (3.80 mg; 0.0306 mmol) and 4-(4-formylphenoxy)benzaldehyde (E) (6.92 mg; 0.0306 mmol) were dissolved in 250  $\mu$ L of deuterated chloroform ( $\text{CDCl}_3$ ). Then a deuterated chloroform solution (300  $\mu$ L) containing tris(2-aminoethyl)amine (T) (2.98 mg; 0.0204 mmol) was added in two portions. The resulting solution mixture was stirred at room temperature for 24h, then in 318.15 K for another 24h and then again for 24h in RT. The clear solution of library was checked by  $^1\text{H}$  NMR spectroscopy ( $\text{CDCl}_3$ ) just after mixing the components and after each 24h of stirring (RT/318.15 K/RT).

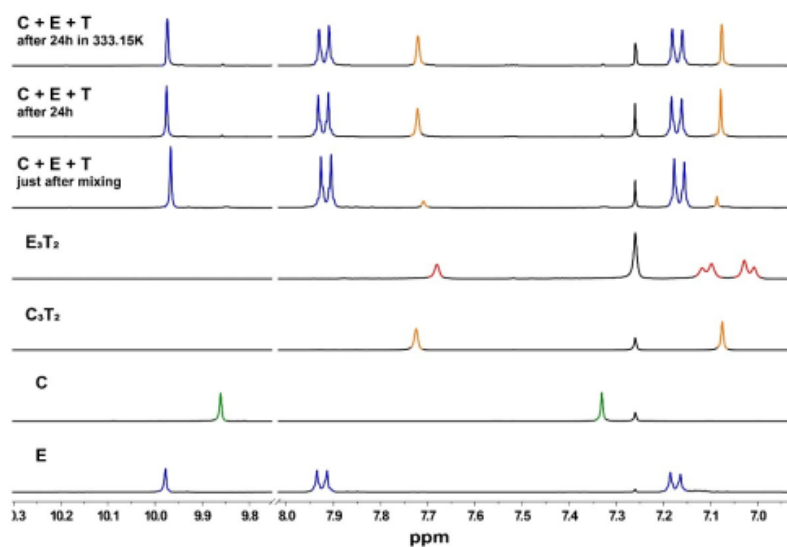


**Figure S19.** Comparison of  $^1\text{H}$  NMR (400 MHz) spectra for self-sorting experiment 3C + 3E + 2T depending on the time. The spectra of components and pure, isolated cages are also shown for comparison. All NMR spectra were recorded in  $\text{CDCl}_3$  at room temperature.

### 1.3.12. Self-sorting experiment 3C + 3H + 2T

In a NMR tube, furan-2,5-dicarbaldehyde (C) (2.51 mg; 0.0202 mmol) and 4,4'-((((oxybis(ethane-2,1-diyl))bis(oxy))bis(ethane-2,1-diyl))bis(oxy))dibenzaldehyde (H) (8.17 mg; 0.0202 mmol) were dissolved in 250  $\mu$ L of deuterated chloroform ( $\text{CDCl}_3$ ). Then a deuterated chloroform solution (300  $\mu$ L) containing tris(2-aminoethyl)amine (T) (1.97 mg; 0.0135 mmol) was added in two portions. The resulting solution mixture was stirred at room temperature for 24h, then in 318.15 K for another 24h and then again for 24h in RT. The clear solution of library was checked by  $^1\text{H}$  NMR spectroscopy ( $\text{CDCl}_3$ ) just after mixing the components and after each 24h of stirring (RT/318.15 K/RT).

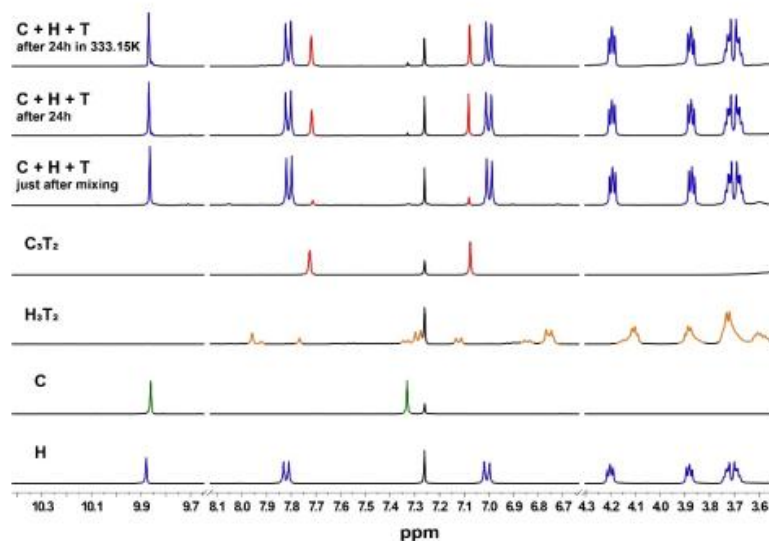
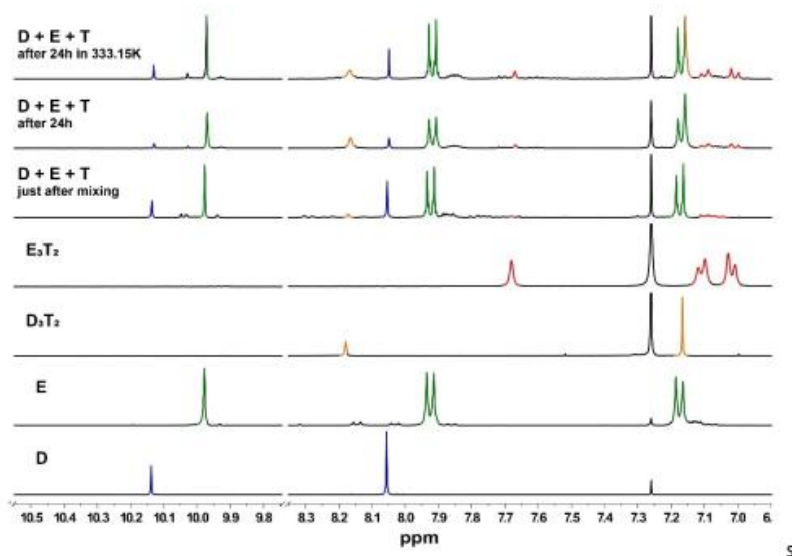


Figure S20. Comparison of  $^1\text{H}$  NMR (400 MHz) spectra for self-sorting experiment 3C + 3H + 2T depending on the time. The spectra of components and pure, isolated cages are also shown for comparison. All NMR spectra were recorded in  $\text{CDCl}_3$  at room temperature.

### 1.3.13. Self-sorting experiment 3D + 3E + 2T

In a NMR tube, terephthalaldehyde (D) (1.91 mg; 0.0143 mmol) and 4-(4-formylphenoxy)benzaldehyde (E) (3.23 mg; 0.0143 mmol) were dissolved in 250  $\mu$ L of deuterated chloroform ( $\text{CDCl}_3$ ). Then a deuterated chloroform solution (300  $\mu$ L) containing tris(2-aminoethyl)amine (T) (1.39 mg; 0.0095 mmol) was added in two portions. The resulting solution mixture was stirred at room temperature for 24h, then in 318.15 K for another 24h and then again for 24h in RT. The clear solution of library was checked by  $^1\text{H}$  NMR spectroscopy ( $\text{CDCl}_3$ ) just after mixing the components and after each 24h of stirring (RT/318.15 K/RT).



**Figure S21.** Comparison of  $^1\text{H}$  NMR (400 MHz) spectra for self-sorting experiment 3D + 3E + 2T depending on the time. The spectra of components and pure, isolated cages are also shown for comparison. All NMR spectra were recorded in  $\text{CDCl}_3$  at room temperature.

### 1.3.14. Self-sorting experiment 3D + 3H + 2T

In a NMR tube, terephthalaldehyde (D) (0.95 mg; 0.0071 mmol) and 4,4'-((((oxybis(ethane-2,1-diyl))bis(oxy))bis(ethane-2,1-diyl))bis(oxy))dibenzaldehyde (H) (2.85 mg; 0.0071 mmol) were dissolved in 250  $\mu$ L of deuterated chloroform ( $\text{CDCl}_3$ ). Then a deuterated chloroform solution (300  $\mu$ L) containing tris(2-aminoethyl)amine (T) (0.69 mg; 0.0047 mmol) was added in two portions. The resulting solution mixture was stirred at room temperature for 24h, then in 318.15 K for another 24h and then again for 24h in RT. The clear solution of library was checked by  $^1\text{H}$  NMR spectroscopy ( $\text{CDCl}_3$ ) just after mixing the components and after each 24h of stirring (RT/318.15 K/RT).

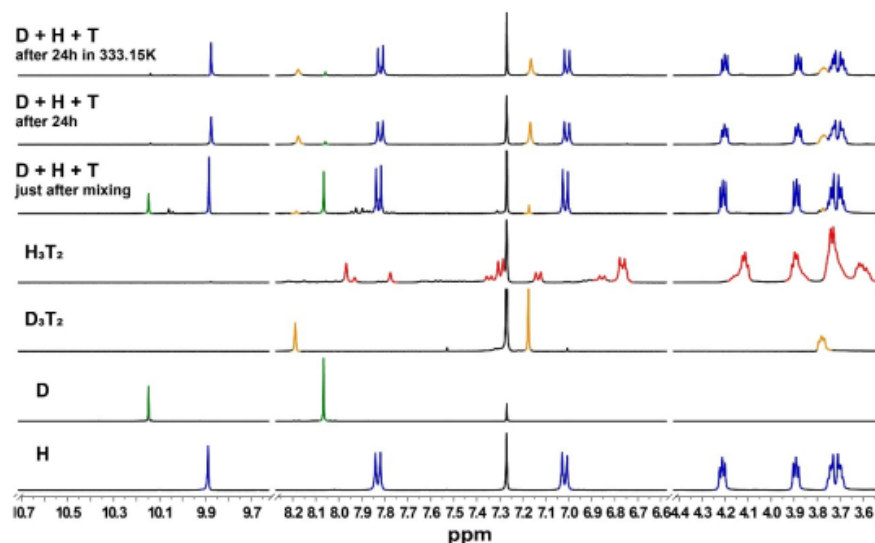
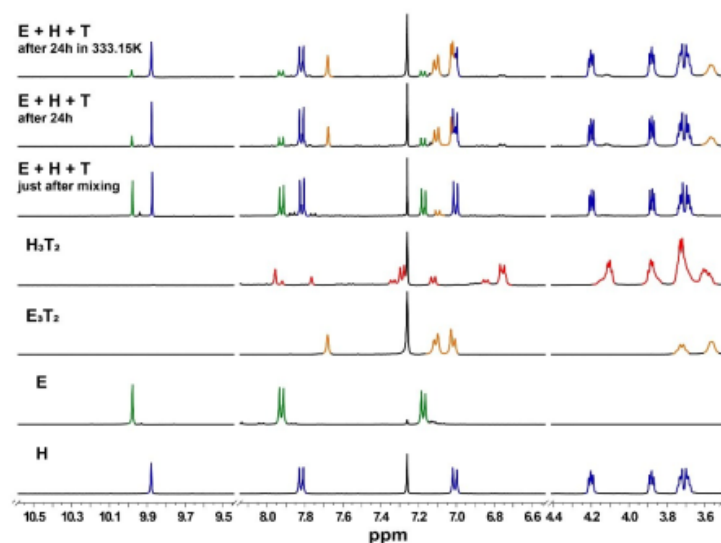


Figure S22. Comparison of  $^1\text{H}$  NMR (400 MHz) spectra for self-sorting experiment 3D + 3H + 2T depending on the time. The spectra of components and pure, isolated cages are also shown for comparison. All NMR spectra were recorded in  $\text{CDCl}_3$  at room temperature.

### 1.3.15. Self-sorting experiment 3E + 3H + 2T

In a NMR tube, 4-(4-formylphenoxy)benzaldehyde (E) (1.35 mg; 0.0059 mmol) and 4,4'-((((oxybis(ethane-2,1-diyl))bis(oxy))bis(ethane-2,1-diyl))bis(oxy))dibenzaldehyde (H) (2.40 mg; 0.0059 mmol) were dissolved in 250  $\mu$ L of deuterated chloroform ( $\text{CDCl}_3$ ). Then a deuterated chloroform solution (300  $\mu$ L) containing tris(2-aminoethyl)amine (T) (0.58 mg; 0.0039 mmol) was added in two portions. The resulting solution mixture was stirred at room temperature for 24h, then in 318.15 K for another 24h and then again for 24h in RT. The clear solution of library was checked by  $^1\text{H}$  NMR spectroscopy ( $\text{CDCl}_3$ ) just after mixing the components and after each 24h of stirring (RT/318.15 K/RT).



**Figure S23.** Comparison of  $^1\text{H}$  NMR (400 MHz) spectra for self-sorting experiment 3E + 3H + 2T depending on the time. The spectra of components and pure, isolated cages are also shown for comparison. All NMR spectra were recorded in  $\text{CDCl}_3$  at room temperature.

#### 1.4. Complex self-sorting experiments

##### 1.4.1. Self-sorting experiment 3A + 3B + 3C + 3D + 3E + 3H + nT

In a NMR tube, isophthalic dialdehyde (A) (1.71 mg; 0.0127 mmol), pyridine-2,6-dicarbaldehyde (B) (1.72 mg; 0.0127 mmol), furan-2,5-dicarbaldehyde (C) (1.58 mg; 0.0127 mmol), terephthal aldehyde (D) (1.71 mg; 0.0127 mmol), 4-(4-formylphenoxy)benzaldehyde (E) (2.88 mg; 0.0127 mmol) and 4,4'-(((oxybis(ethane-2,1-diyl))bis(oxy))bis(ethane-2,1-diyl))bis(oxy))dibenzaldehyde (H) (5.12 mg; 0.0127 mmol) were dissolved in 450  $\mu$ L of deuterated chloroform ( $\text{CDCl}_3$ ). Then a titration was performed with deuterated chloroform stock solution containing tris(2-aminoethyl)amine (T) (1.24 mg; 0.0085 mmol). The resulting solution mixture was stirred at room temperature for 24h after addition of each portion. The clear solution of library was checked by  $^1\text{H}$  NMR spectroscopy ( $\text{CDCl}_3$ ) after mixing the components and after each 24h of stirring (RT/318.15 K/RT).

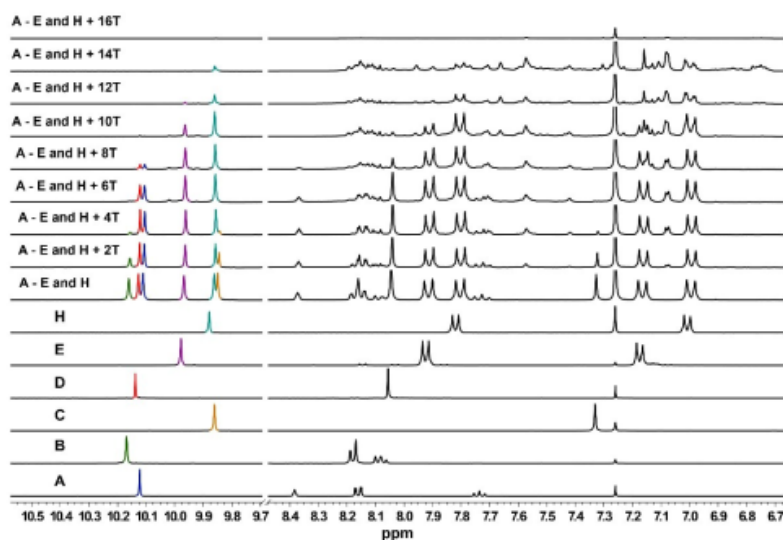


Figure S24. Comparison of  $^1\text{H}$  NMR (400 MHz) spectra for self-sorting experiment involving titration of 3A + 3B + 3C + 3D + 3E + 3H with doses of 2T. The spectra of components are also shown for comparison. All NMR spectra were recorded in  $\text{CDCl}_3$  at room temperature.



#### 1.4.2. Self-sorting experiment 3D + 3E + 3F + n2T

In a NMR tube, terephthalaldehyde (D) (2.99 mg; 0.0223 mmol), 4-(4-formylphenoxy)benzaldehyde (E) (5.04 mg; 0.0223 mmol) and 4,4'-biphenyldicarboxaldehyde (F) (4.68 mg; 0.0223 mmol) were dissolved in 450  $\mu$ L of deuterated chloroform ( $\text{CDCl}_3$ ). Then a titration was performed with deuterated chloroform stock solution containing tris(2-aminoethyl)amine (T) (2.17 mg; 0.0148 mmol). The resulting solution mixture was stirred at room temperature for 24h after addition of each portion. The clear solution of library was checked by  $^1\text{H}$  NMR spectroscopy ( $\text{CDCl}_3$ ) after mixing the components and after each 24h of stirring (RT/318.15 K/RT).

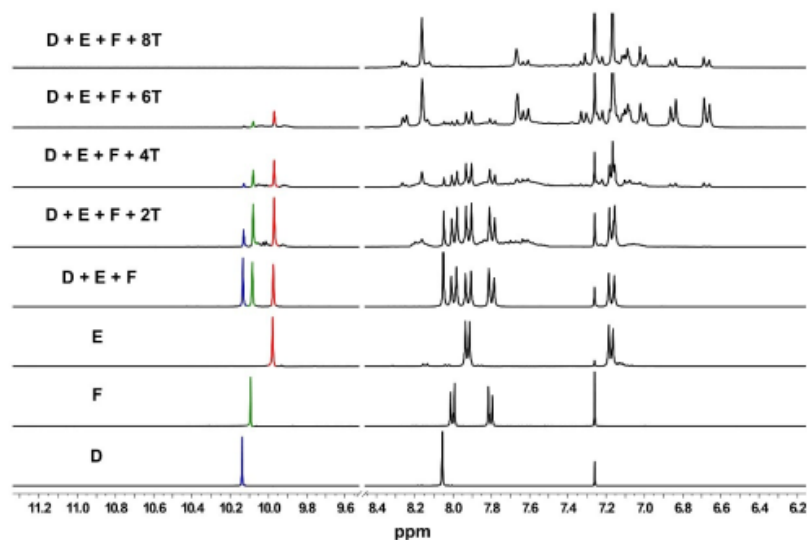


Figure S25. Comparison of  $^1\text{H}$  NMR (400 MHz) spectra for self-sorting experiment involving titration of 3D + 3E + 3F with doses of 2T. The spectra of components are also shown for comparison. All NMR spectra were recorded in  $\text{CDCl}_3$  at room temperature.

### 1.4.3. Self-sorting experiment 3B + 3C + 3G + n2T

In a NMR tube, pyridine-2,6-dicarbaldehyde (B) (5.54 mg; 0.041 mmol), furan-2,5-dicarbaldehyde (C) (5.09 mg; 0.041 mmol) and 2,5-thiophenedicarbaldehyde (G) (5.75 mg; 0.041 mmol) were dissolved in 450  $\mu$ L of deuterated chloroform ( $\text{CDCl}_3$ ). Then a titration was performed with deuterated chloroform stock solution containing tris(2-aminoethyl)amine (T) (4.00 mg; 0.0273 mmol). The resulting solution mixture was stirred at room temperature for 24h after addition of each portion. The clear solution of library was checked by  $^1\text{H}$  NMR spectroscopy ( $\text{CDCl}_3$ ) after mixing the components and after each 24h of stirring (RT/318.15 K/RT).

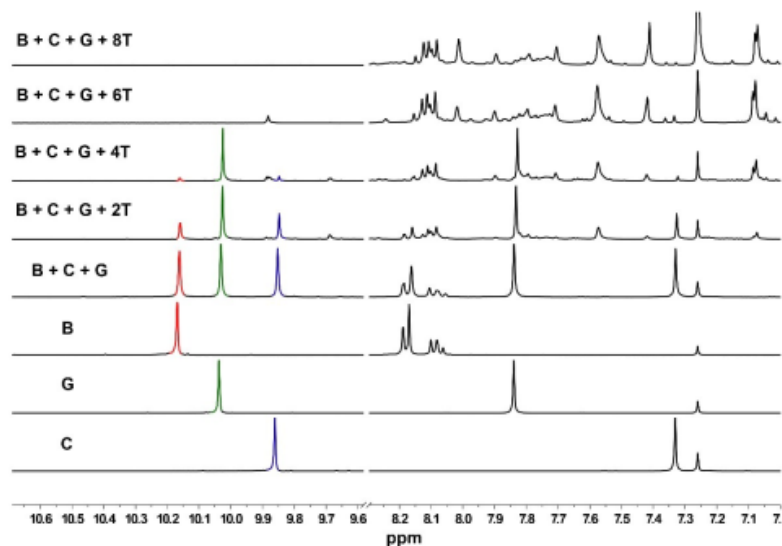


Figure S26. Comparison of  $^1\text{H}$  NMR (400 MHz) spectra for self-sorting experiment involving titration of 3B + 3C + 3G with doses of 2T. The spectra of components are also shown for comparison. All NMR spectra were recorded in  $\text{CDCl}_3$  at room temperature.

### 1.5. NMR spectra of an acid/base assisted equilibration

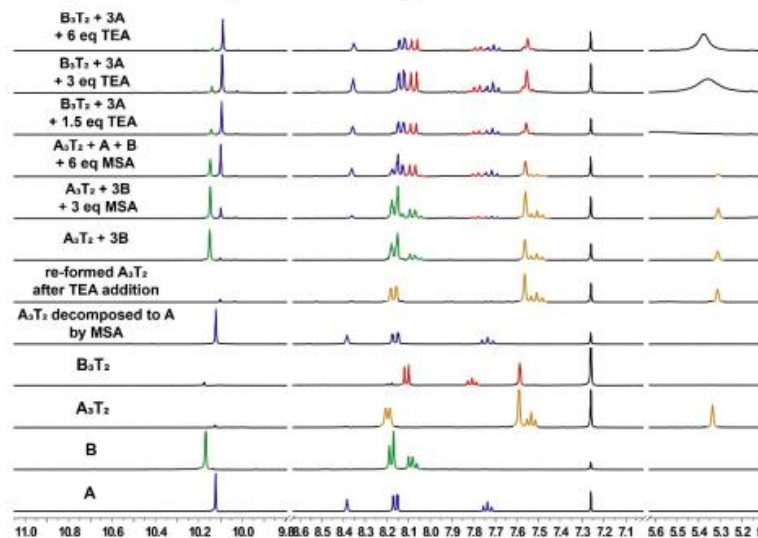


Figure S27.  $^1\text{H}$  NMR (400 MHz) spectra of an acid/base (MSA/TEA) assisted equilibration experiment on  $\text{A}_3\text{T}_2 + 3\text{B} \rightarrow 3\text{A} + \text{B}_3\text{T}_2$  system. Stacked with spectra of components **A** and **B** and isolated cages  $\text{A}_3\text{T}_2$  and  $\text{B}_3\text{T}_2$ . All NMR spectra were recorded at room temperature in  $\text{CDCl}_3$

### 1.6. NMR spectra of an exchange experiment $\text{A}_3\text{T}_2 + 3\text{B} \rightarrow 3\text{A} + \text{B}_3\text{T}_2$

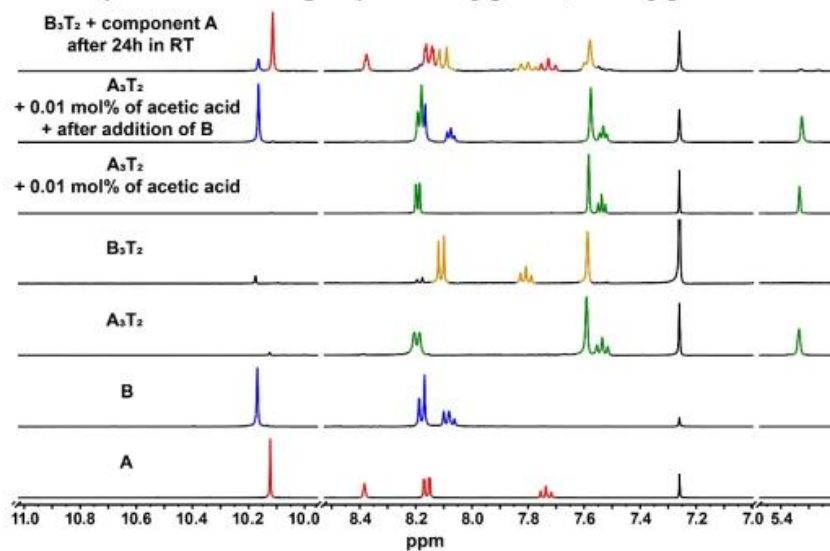
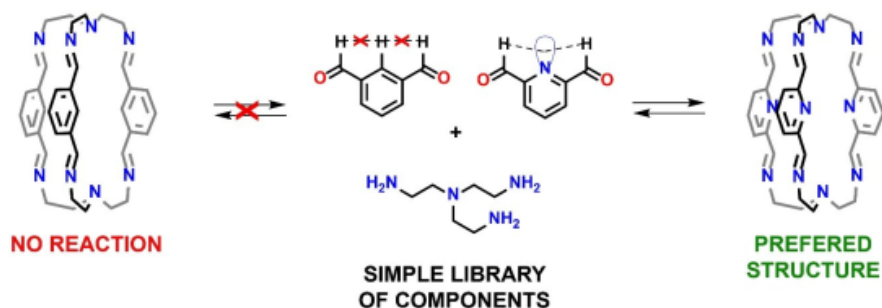


Figure S28.  $^1\text{H}$  NMR (400 MHz) spectra of an exchange experiment  $\text{A}_3\text{T}_2 + 3\text{B} \rightarrow 3\text{A} + \text{B}_3\text{T}_2$ . Stacked with spectra of components **A** and **B** and isolated cages  $\text{A}_3\text{T}_2$  and  $\text{B}_3\text{T}_2$ . All NMR spectra were recorded at room temperature in  $\text{CDCl}_3$

### 1.7. Schematic representation of a self-sorting experiment 3A + 3B + 2T



**Figure S29.** Schematic representation of a self-sorting experiment in a simple library composed of **3A** + **3B** + **2T**. Both dialdehydes (**A** and **B**) and their imines (**A<sub>3</sub>T<sub>2</sub>** and **B<sub>3</sub>T<sub>2</sub>**, respectively) contain a fully conjugated system of the aromatic ring and its substituents but only in **B** are attractive interactions possible between the two imine C-H bonds adjacent to the aromatic ring and the adjacent pyridine nitrogen atom of the another cage arm.<sup>3</sup> A possible additional factor that works in favour of cage **B<sub>3</sub>T<sub>2</sub>** with respect to cage **A<sub>3</sub>T<sub>2</sub>** are intramolecular interactions that may occur between C-H bonds and the N lone pair. Both cages, however, are stabilized through intramolecular hydrogen bonding interactions between imine protons of one arm of the cage and imine nitrogen atom of another.<sup>3</sup>

## 2. Crystallography

Diffraction data were collected at room temperature using graphite-monochromated MoK $\alpha$  radiation ( $\lambda = 0.71073$  Å) with the  $\omega$ -scan technique. For data reduction, UB-matrix determination and absorption correction CrysAlisPro software was used.

Using Olex2<sup>4</sup>, the structures were solved by direct methods using SHELXL<sup>5</sup> and refined by full-matrix least-squares against F<sup>2</sup> utilizing SHELXL. All non-hydrogen atoms were refined anisotropically. Hydrogen atoms were located in idealized positions by molecular 3+3 geometry and refined as rigid groups. Uiso of hydrogen atoms were set as 1.2 (for C-carriers) and 1.5 (for O-carriers) times Ueq of the corresponding carrier atom. Crystal and refinement data are summarised in Table. The data have been deposited in the form of cifs with the Cambridge Crystallographic Data Centre (CCDC), deposition number CCDC 1853998 and 1853999. These can be obtained free of charge via [www.ccdc.cam.ac.uk/data\\_request/cif](http://www.ccdc.cam.ac.uk/data_request/cif), or by emailing [data\\_request@ccdc.cam.ac.uk](mailto:data_request@ccdc.cam.ac.uk), or by contacting The Cambridge Crystallographic Data Centre, 12, Union Road, Cambridge CB2 1EZ, UK; fax: +44 1223 336033.

## 3. References

1. A. Abebayehu, R. Dutta and C. H. Lee, *Chem. - Eur. J.*, 2016, **22**, 13850-13856.
2. A. R. Katritzky, S. A. Belyakov, O. V. Denisko, U. Maran and N. S. Dalal, *J. Chem. Soc., Perkin Trans. 2*, 1998, 611-616.
3. M. G. B. Drew, V. Felix, V. McKee, G. Morgan and J. Nelson, *Supramol. Chem.*, 1995, **5**, 281-287.
4. O. V. Dolomanov, L. J. Bourhis, R. J. Gildea, J. A. K. Howard and H. Puschmann, *J. Appl. Crystallogr.*, 2009, **42**, 339-341.
5. G. Sheldrick, *Acta Crystallogr.*, 2008, **64**, 112-122.

## **Declaration letters of co-authors**

Poznań, 07/07/2025

M.Sc. Michał Kołodziejcki  
Laboratory of Functional Nanostructures  
Center for Advanced Technologies  
Adam Mickiewicz University in Poznań  
e-mail: mic.kolodziejcki1@gmail.com

#### DECLARATION

I hereby declare that in the following publications:

**A1. Michał Kołodziejcki, Anna Walczak, Zbigniew Hnatejko, Jack Harrowfield, Artur R. Stefankiewicz\***

*Unsymmetrical bidentate ligands as a basis for construction of ambidentate ligands for functional materials: Properties of 4,4-dimethyl-1-phenylpentane-1,3-dione*

*Polyhedron*, **2017**, Volume 137, 270-277; DOI: 10.1016/j.poly.2017.08.022

**A2. Michał Kołodziejcki, Aidan J. Brock, Gracjan Kurpiak, Anna Walczak, Feng Li, Jack K. Clegg\*, Artur R. Stefankiewicz\***

*Charge Neutral [Cu<sub>2</sub>L<sub>2</sub>] and [Pd<sub>2</sub>L<sub>2</sub>] Metallocycles: Self-Assembly, Aggregation, and Catalysts*

*Inorganic Chemistry*, **2021**, 60, 9673-9679; DOI: 10.1021/acs.inorgchem.1c00967

**A3. Michał Kołodziejcki, Artur R. Stefankiewicz\*, Jean-Marie Lehn\***

*Dynamic polyimine macrobicyclic cryptands – self-sorting with component selection*

*Chemical Science*, **2019**, 10, 1836-1843; DOI: 10.1039/C8SC04598D

my substantive contribution as a co-author include:


- in A1:
  - creation of the study concept;
  - synthesis of the ligand **bmpH** and its Al<sup>III</sup>, Co<sup>III</sup>, Ni<sup>II</sup>, Cu<sup>II</sup>, Zn<sup>II</sup> and Pd<sup>II</sup> complexes;
  - characterization of the complexes using NMR spectroscopy, mass spectrometry and elemental analysis;
  - obtaining crystals of the complexes with Cu<sup>II</sup> and Pd<sup>II</sup> for diffraction measurements;
  - carrying out of electronic absorption and luminescence measurements;
  - interpretation of experimental data and discussion of the research results;
  - creation of figures, schemes and tables for the manuscript and supplementary materials;
  - preparation of supplementary materials for the manuscript;
  - authoring of the manuscript text.
- in A2:
  - creation of the study concept;
  - synthesis of the tritopic ligand **H<sub>3</sub>L**;
  - characterization of the ligand using NMR spectroscopy, mass spectrometry, IR measurements and elemental analysis;
  - obtaining crystals of the ligand for diffraction measurements;
  - synthesis of Pd<sup>II</sup> complexes with different stoichiometry – metallacycle, polymer;



- characterization of the Pd<sup>II</sup> complexes using NMR spectroscopy, mass spectrometry, IR measurements and elemental analysis;
  - preparation of metal-ion induced conversion experiments and conducting of the designed experiments;
  - conducting thermogravimetric analysis;
  - co-preparation of the experiments for Suzuki-Miyaura Cross-Coupling reactions;
  - interpretation of experimental data and discussion of the research results;
  - creation of figures, schemes and tables for the manuscript and supplementary materials;
  - preparation of supplementary materials for the manuscript;
  - authoring of the manuscript text.
- in A3:
- co-creation of the study concept;
  - synthesis and isolation of the dynamic polyimine macrobicyclic cryptands A<sub>3</sub>T<sub>2</sub>-H<sub>3</sub>T<sub>2</sub>;
  - characterization of the synthesized dynamic polyimine macrobicyclic cryptands using NMR spectroscopy, mass spectrometry and elemental analysis;
  - obtaining crystals of the synthesized dynamic polyimine macrobicyclic cryptands – successfully for E<sub>3</sub>T<sub>2</sub> and F<sub>3</sub>T<sub>2</sub>;
  - XRD data co-analysis for E<sub>3</sub>T<sub>2</sub> and F<sub>3</sub>T<sub>2</sub>;
  - design and conduct of component self-sorting experiments taking into account the influence of various structural factors in simple dynamic libraries (2 aldehydes + triamine) (effect of the presence of a heteroatom, effect of the structural flexibility, effect of the number of aromatic rings and rigidity of the dialdehyde component, effect of the type of heteroatom);
  - design and conduct of component self-sorting experiments leading to a mixture of two cages;
  - design and conduct of component self-sorting experiments according to selectivity in a mixture of a six dialdehyde components;
  - design and conduct of component exchange experiments – acid/base assisted equilibration and cage-to-cage transformation;
  - interpretation of experimental data and discussion of the research results;
  - creation of all figures, schemes and tables for the manuscript and supplementary materials;
  - preparation of supplementary materials for the manuscript;
  - authoring of the manuscript text.

  
 M.Sc. Michał Kołodziejski

I hereby certify the contribution of M.Sc. Michał Kołodziejski to the aforementioned publications, as described above.

  
 Prof. dr hab. Artur R. Stefankiewicz

Poznań, 09/07/2025

Prof. dr hab. Artur R. Stefankiewicz  
Laboratory of Functional Nanostructures  
Center for Advanced Technologies  
Adam Mickiewicz University in Poznań  
e-mail: ars@amu.edu.pl

#### DECLARATION

I hereby declare that in the following publications:

**A1.** Michał Kołodziejcki, Anna Walczak, Zbigniew Hnatejko, Jack Harrowfield, Artur R. Stefankiewicz\*

*Unsymmetrical bidentate ligands as a basis for construction of ambidentate ligands for functional materials: Properties of 4,4-dimethyl-1-phenylpentane-1,3-dionate*

Polyhedron, **2017**, Volume 137, 270-277; DOI: 10.1016/j.poly.2017.08.022

**A2.** Michał Kołodziejcki, Aidan J. Brock, Gracjan Kurpik, Anna Walczak, Feng Li, Jack K. Clegg\*, Artur R. Stefankiewicz\*

*Charge Neutral [Cu<sub>2</sub>L<sub>2</sub>] and [Pd<sub>2</sub>L<sub>2</sub>] Metallocycles: Self-Assembly, Aggregation, and Catalysis*

Inorganic Chemistry, **2021**, 60, 9673-9679; DOI: 10.1021/acs.inorgchem.1c00967

**A3.** Michał Kołodziejcki, Artur R. Stefankiewicz\*, Jean-Marie Lehn\*

*Dynamic polyimine macrobicyclic cryptands – self-sorting with component selection*

Chemical Science, **2019**, 10, 1836-1843; DOI: 10.1039/C8SC04598D

my substantive contributions as a co-author include:

- conceptualization, organization, and management of the work;
- co-interpretation of experimental data and discussion of the research results;
- co-authoring of the manuscript text;
- correspondence with editors and referees.



Prof. dr hab. Artur R. Stefankiewicz



Strasbourg, 10/07/2025

Prof. Jean-Marie Lehn  
Institute of Supramolecular Science and Engineering  
University of Strasbourg  
e-mail: lehn@unistra.fr

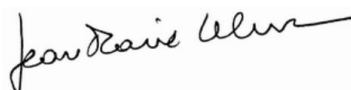
#### DECLARATION

I hereby declare that in the following publications:

**A3.** Michał Kołodziejcki, Artur R. Stefankiewicz\*, Jean-Marie Lehn\*  
*Dynamic polyimine macrobicyclic cryptands – self-sorting with component selection*  
Chemical Science, **2019**, 10, 1836-1843; DOI: 10.1039/C8SC04598D

my substantive contributions as a co-author include:

- conceptualization, organization, and management of the work;
- co-interpretation of experimental data and discussion of the research results;
- co-authoring of the manuscript text and supporting information;
- correspondence with editors and referees.



---

Prof. Jean-Marie Lehn

Queensland, 10/07/2025

Prof. Jack K. Clegg  
School of Chemistry and Molecular Biosciences  
The University of Queensland  
e-mail: j.clegg@uq.edu.au

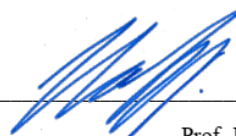
#### DECLARATION

I hereby declare that in the following publication:

A2. Michał Kołodziejwski, Aidan J. Brock, Gracjan Kurpik, Anna Walczak, Feng Li, Jack K. Clegg\*,  
Artur R. Stefankiewicz\*  
*Charge Neutral [Cu<sub>2</sub>L<sub>2</sub>] and [Pd<sub>2</sub>L<sub>2</sub>] Metallocycles: Self-Assembly, Aggregation, and Catalysis*  
Inorganic Chemistry, **2021**, 60, 9673-9679; DOI: 10.1021/acs.inorgchem.1c00967

my substantive contributions as a co-author include:

- co-conceptualization and management of the work;
- co-interpretation of experimental data and discussion of the research results;
- co-authoring of the manuscript text and supporting informations;
- correspondence with editors and referees.



Prof. Jack K. Clegg

Sydney, 10/07/2025

Dr. Feng Li  
School of Science  
Western Sydney University  
e-mail: Feng.Li@westernsydney.edu.au

#### DECLARATION

I hereby declare that in the following publication:

A2. Michał Kołodziejwski, Aidan J. Brock, Gracjan Kurpik, Anna Walczak, Feng Li, Jack K. Clegg\*,  
Artur R. Stefankiewicz\*  
*Charge Neutral [Cu<sub>2</sub>L<sub>2</sub>] and [Pd<sub>2</sub>L<sub>2</sub>] Metallocycles: Self-Assembly, Aggregation, and Catalysis*  
Inorganic Chemistry, **2021**, 60, 9673-9679; DOI: 10.1021/acs.inorgchem.1c00967

my substantive contributions as a co-author include:

- co-characterization of the Complex 2 using GC-MS and elemental analysis;
- X-ray analysis of Complex 2;
- co-interpretation of experimental data and discussion of the research results;
- co-authoring of the manuscript text and supporting informations.



---

Dr. Feng Li

Queensland, 11/07/2025

Dr. Aidan J. Brock  
School of Chemistry and Molecular Biosciences  
The University of Queensland  
e-mail: aidan.brock@qut.edu.au

#### DECLARATION

I hereby declare that in the following publication:

A2. Michał Kołodziejski, Aidan J. Brock, Gracjan Kurpik, Anna Walczak, Feng Li, Jack K. Clegg\*,  
Artur R. Stefankiewicz\*  
*Charge Neutral [Cu<sub>2</sub>L<sub>2</sub>] and [Pd<sub>2</sub>L<sub>2</sub>] Metallocycles: Self-Assembly, Aggregation, and Catalysis*  
Inorganic Chemistry, **2021**, 60, 9673-9679; DOI: 10.1021/acs.inorgchem.1c00967

my substantive contributions as a co-author include:

- synthesis of Complex 2;
- characterization of the Complex 2 using GC-MS and elemental analysis;
- crystal growth of Complex 2 for diffraction measurements;
- X-ray analysis of Complex 2;
- co-interpretation of experimental data and discussion of the research results;
- co-authoring of the manuscript text and supporting information.



Dr. Aidan J. Brock

Poznań, 10/07/2025

Prof. UAM dr hab. Zbigniew Hnatejko  
Department of Rare Earths  
Faculty of Chemistry  
Adam Mickiewicz University in Poznań  
Uniwersytetu Poznańskiego 8  
61-614 Poznań  
e-mail: zbychuh@amu.edu.pl

#### DECLARATION

I hereby declare that in the following publication:

**A1.** Michał Kołodziejcki, Anna Walczak, Zbigniew Hnatejko, Jack Harrowfield, Artur R. Stefankiewicz\*

*Unsymmetrical bidentate ligands as a basis for construction of ambidentate ligands for functional materials: Properties of 4,4-dimethyl-1-phenylpentane-1,3-dione*

*Polyhedron*, **2017**, Volume 137, 270-277; DOI: 10.1016/j.poly.2017.08.022

my substantive contributions as a co-author include:

- electronic absorption and luminescence measurements;
- co-interpretation of experimental data and discussion of the research results;
- co-authoring of the manuscript text.

Prof. UAM dr hab. Zbigniew Hnatejko

Poznań, 12/07/2025

Dr Anna Walczak  
Laboratory of Functional Nanostructures  
Center for Advanced Technologies  
Adam Mickiewicz University in Poznań  
e-mail: aj69161@amu.edu.pl

#### DECLARATION

I hereby declare that in the following publications:

**A1.** Michał Kołodziejcki, Anna Walczak, Zbigniew Hnatejko, Jack Harrowfield, Artur R. Stefankiewicz\*

*Unsymmetrical bidentate ligands as a basis for construction of ambidentate ligands for functional materials: Properties of 4,4-dimethyl-1-phenylpentane-1,3-dionate*

*Polyhedron*, **2017**, Volume 137, 270-277; DOI: 10.1016/j.poly.2017.08.022

**A2.** Michał Kołodziejcki, Aidan J. Brock, Gracjan Kurpik, Anna Walczak, Feng Li, Jack K. Clegg\*, Artur R. Stefankiewicz\*

*Charge Neutral [Cu<sub>2</sub>L<sub>2</sub>] and [Pd<sub>2</sub>L<sub>2</sub>] Metallocycles: Self-Assembly, Aggregation, and Catalysis*

*Inorganic Chemistry*, **2021**, 60, 9673-9679; DOI: 10.1021/acs.inorgchem.1c00967

my substantive contributions as a co-author include:

- in **A1**:
  - co-development of initial research concepts
  - XRD measurements, including the establishment and description of the structures of [Cu(bpm)<sub>2</sub>] and [Pd(bpm)<sub>2</sub>]
  - co-interpretation of experimental data and discussion of the research results;
  - co-authoring of the manuscript text;
  - co-authoring of the supplementary materials for the manuscript;
  - creation of figures and tables according to X-ray analysis.
- in **A2**:
  - XRD measurements, including the establishment and description of the structure of H<sub>3</sub>L
  - supervision of catalytic experiments, including reaction condition optimization, investigation of the scope and limitations of the catalytic system, and comparative studies between catalysts;
  - creation of figures and tables according to X-ray analysis and catalytic experiments;
  - co-interpretation of experimental data and discussion of the research results;
  - co-preparation of supplementary materials for the manuscript;
  - co-authoring of the manuscript text.



Dr Anna Walczak